Signal Transduction Systems in the *Myxococcus xanthus* Developmental Program

Dissertation

zur Erlangung des akademischen Grades
des Doktors der Naturwissenschaften
(Dr. rer. nat.)

dem Fachbereich Biologie
der Philipps-Universität Marburg
vorgelegt

von

Maike M. Glaser
aus Kassel

Marburg, November 2017

Die Untersuchungen zur vorliegenden Arbeit wurden von Oktober 2011 bis September 2013 am Max-Planck-Institut für terrestrische Mikrobiologie in Marburg sowie von Oktober 2013 bis September 2015 an der Wayne State University in Detroit, Michigan, USA unter der Leitung von Prof. Dr. Penelope I. Higgs durchgeführt.

Vom Fachbereich Biologie der Philipps Universität Marburg

als Dissertation angenommen am ___.___.___

Erstgutachter: Prof. Dr. Penelope I. Higgs

Zweitgutachter: Prof. Dr. Martin Thanbichler

Weitere Mitglieder der Prüfungskommission:

Prof. Dr. Lars-Oliver Essen

Prof. Dr. Victor Sourjik

Tag der mündlichen Prüfung: ___.___.___

Zum Zeitpunkt der Einreichung dieser Dissertation werden die folgenden Originalpublikationen vorbereitet, um die erzielten Ergebnisse zu veröffentlichen:

Glaser, M.M., Lee, B., McLaughlin, P.T., Mei, X. and Higgs, P.I., Coordination of the *Myxococcus xanthus* developmental program: multiple TCS and SPTK signaling systems converge on the transcriptional regulator MrpC. In preparation.

Glaser, M.M., Lee, B. and Higgs, P.I., Repression of the *Myxococcus xanthus* developmental program requires both kinase and phosphatase activities in TodK. In preparation.

Glaser, M.M. and Higgs, P.I., Characterization of the phosphoryl flow in the *Myxococcus xanthus* hybrid histidine kinase, Hpk30. In preparation.

Dedicated to my Family

Table of Contents

1. Zusammenfassung

Anhand des prokaryotischen Modellorganismus *Myxococcus xanthus* kann die Regulation von komplexen, sozialen Verhaltensweisen untersucht werden. In allen Lebenszyklus-Stadien zeigt *M. xanthus* multizelluläres Verhalten, einschließlich eines Entwicklungsstadiums, bei dem sich die Zellpopulation in mindestens drei unterschiedliche Zelltypen aufspaltet: Sporulation in vielzellige Fruchtkörper, *‚peripheral rods*‘ und lysierende Zellen. Dabei sind bisher weder der evolutionäre Vorteil dieser Differenzierung noch der Mechanismus, durch den die Separation einer Population in verschiedene Zelltypen induziert wird, vollständig verstanden. Ein potentieller Kandidat für die Regulation der Aufteilung in differenzierte Zelltypen ist allerdings MrpC, ein wichtiger Transkriptionsregulator im Entwicklungszyklus. Die MrpC-Akkumulation wird durch mehrere unterschiedliche Signaltransduktionssysteme gesteuert, einschließlich der (verwaisten) Histidin-Proteinkinasen (HPK) Esp, TodK, Red und Hpk30. In einem *M. xanthus* Stamm, dem drei der Systeme fehlen (Δ*esp* Δ*red* Δ*todK*) wird MrpC massiv überakkumuliert. Weiterhin zeigt dieser Stamm einen auffälligen Phänotyp, bei dem alle Zellen unangemessen schnell sporulieren und so einen Sporen-Teppich erzeugen.

In dieser Arbeit wird zunächst gezeigt, wie *M. xanthus* von der Sporenproduktion innerhalb von gut strukturierten Fruchtkörpern profitiert. Weiterhin wird thematisiert, wie Signaltransduktionsmechanismen die Fruchtkörperbildung und die Segregation in Zelltypen steuern können. Hierbei ist ausschlaggebend wie Red, TodK und Hpk30 die MrpC-Akkumulation kontrollieren könnten.

Ein Stamm, dem die Esp-, Red- und TodK-Signalsysteme fehlen, bildet keine organisierten Fruchtkörper. Dieser Phänotyp wurde sich in dieser Arbeit zu Nutzen gemacht, um die Rolle verschiedener Zelltypen bei der Verbreitung und der Ausbildung von Resistenz gegenüber Umwelteinflüssen von *M. xanthus* Fruchtkörpern zu studieren. Es konnte gezeigt werden, dass der Verlust der Fruchtkörpermorphologie zu einer verbesserten Verbreitung durch den Vektor *Drosophila melanogaster* führt. Dies geht jedoch auf Kosten der Umweltresistenz, wie durch den Einfluss von UV-Exposition auf Mutanten- und Wildtyp-Fruchtkörper sowie vereinzelte Wildtyp-Sporen gezeigt werden konnte.

Hinsichtlich der Frage, wie Signaltransduktionsmechanismen konvergieren können, um die MrpC-Akkumulation zu regulieren, wurde eine postulierte Verbindung zwischen dem Red-Signalsystem und einer Ser/Thr-Kinasen-Kaskade bestätigt. Von dieser Verbindung wird angenommen, dass sie die MrpC-Aktivität durch dessen Phosphorylierungsstatus kontrolliert. Um Mechanismen zu identifizieren, durch die TodK und Hpk30 die MrpC-Akkumulation beeinflussen könnten, wurde eine detaillierte Charakterisierung ihrer jeweiligen Signaltransduktionswege durchgeführt. TodK fungiert als eine bifunktionale Histidin-Proteinkinase/Phosphatase, deren Aktivität vermutlich durch die zwei N-terminalen PAS-Domänen moduliert wird. Die Charakterisierung von Hpk30 zeigte, dass Kinaseaktivität die zelluläre Antwort moduliert und dass diese Aktivität durch ihre zwei ‚*receiver*‘ Domänen sowie ein hypothetisches Protein, MXAN_4466, moduliert wird.

Zusammenfassend deuten die hier vorgestellten Daten darauf hin, dass unterschiedliche Signalsysteme konvergieren müssen, um die MrpC-Akkumulation in verschiedenen Zelltypen zu regulieren. Dies führt wiederum zur Segregation von Zellen in ‚*peripheral rods*' außerhalb oder Sporen innerhalb von Fruchtkörpern. Es wird postuliert, dass die Veränderung der räumlichen und/oder zeitlichen Akkumulation von MrpC in Zellen in der hungernden, sich entwickelnden Population dazu dient, die Morphologie des Fruchtkörpers an spezifische Umweltbedingungen anzupassen, in denen entweder die Verbreitung oder die Langzeitresistenz das Überleben von *M. xanthus* sichern kann.

2. Abstract

Myxococcus xanthus serves as a prokaryotic model organism for the regulation of complex social behaviors. During all aspects of its life cycle *M. xanthus* favors multicellular behavior, including a developmental program in which the population is segregated into at least three distinct cell fates (sporulation inside multicellular fruiting bodies, peripheral rods and cell lysis). Neither the evolutionary advantage of producing these distinct cell fates, nor the mechanism by which cell fate segregating is induced are fully understood. However, MrpC, a major developmental transcriptional regulator, is a good candidate for the regulation of cell fate segregation. MrpC accumulation is controlled by multiple distinct signaling systems including the (orphan) histidine protein kinases (HPKs) Esp, TodK, Red and Hpk30. A strain lacking three of the pathways (Δ*esp* Δ*red* Δ*todK*) massively over-accumulates MrpC and displays a striking phenotype in which all cells appear to sporulate inappropriately rapidly, producing lawns of spores. In this thesis research, I first report how *M. xanthus* benefits from production of spores inside of fruiting bodies. I next address how fruiting body formation and cell fate segregation can be controlled. To do so, I characterized the mechanisms by which Red, TodK and Hpk30 could control MrpC accumulation.

We have previously observed that a strain lacking Esp, Red and TodK signaling systems is deficient in the formation of organized fruiting bodies and essentially produces lawns of spores. By taking advantage of this mutant strain, I addressed the role of cell fate segregation in dispersal and environmental resistance of *M. xanthus* fruiting bodies. I showed that loss of fruiting body morphology leads to enhanced dispersal by the vector *Drosophila melanogaster*. However, this comes at the expense of environmental resistance as could be demonstrated by the impact of UV exposure on mutant and wild type fruiting bodies as well as wild type single spores.

To clarify how signaling systems may converge to regulate MrpC accumulation, I confirmed a putative connection between the Red signaling system and the Ser/Thr kinase cascade thought to control MrpC activity by phosphorylation. To start to identify possible mechanisms by which TodK and Hpk30 could affect MrpC accumulation, I carried out a detailed characterization of their respective signal flows. TodK functions as a bifunctional histidine protein kinase/phosphatase, whose activity is likely modulated by the two N-terminal PAS-domains. Hpk30 characterization revealed kinase activity as the signal output and that this activity is modulated by its two receiver domains as well as a hypothetical protein, MXAN_4466.

Together, these data suggest a model in which separate signaling systems converge to regulate MrpC accumulation in distinct cell types leading to segregation of cells into either peripheral rods outside or spores inside fruiting bodies. Altering the spatial and/or temporal accumulation of MrpC within cells in the developing population is used to adapt fruiting body morphology to specific environmental conditions in which either dispersal or long-term resistance might enhance *M. xanthus* survival.

3. Introduction

The transition from a unicellular to a multicellular lifestyle has been classified as a major evolutionary event and has been observed in all kingdoms of life (Claessen *et al.*, 2014, Cao *et al.*, 2015). Multicellularity can be observed in various prokaryotes and in versatile forms. Despite their simple morphology and relatively low number of differentiated cell types, these prokaryotic lifestyles in general resemble multicellular organisms (Munoz-Dorado *et al.*, 2016). One group which has made a very sophisticated leap into multicellularity, despite retaining a unicellular lifeform, is the myxobacteria. They exhibit multifarious social behaviors including coordinated group movement, cooperative predation, and a multicellular developmental program which involves segregation into distinct cell fates (recently reviewed in (Munoz-Dorado *et al.*, 2016)).

The complex behavior exhibited by the myxobacteria is directed and coordinated by signaling systems (Stock *et al.*, 2000, Kirby & Zusman, 2003, Galperin, 2005, Munoz-Dorado *et al.*, 2016). The myxobacteria have one of the largest number of histidine-aspartate signaling genes of all organisms (Whitworth & Cock, 2008). High abundance of signaling systems has been described as 'bacterial IQ' and their number as well as complexity can be linked to the lifestyle of an organism (Galperin, 2005). Over 40 of these histidine-aspartate signaling proteins have been identified to modulate social behaviors such as motility and/or development in the best characterized species of the myxobacteria, *Myxococcus xanthus* (Whitworth & Cock, 2008). The abundance, genetic organization, and atypical domain architectures of the *M. xanthus* signaling proteins*,* indicate that these signaling proteins are organized into complex networks of highly integrated signaling proteins (Shi *et al.*, 2008, Munoz-Dorado *et al.*, 2014) Thus, *M. xanthus* is an attractive model organism in which to study how signaling systems have evolved to coordinate multicellular behaviors.

3.1. Microbial signal transduction – how bacteria make decisions

All living cells are able to sense extracellular stimuli, enabling them to adjust to environmental conditions appropriately. A variety of signal transduction systems are used to rapidly respond to environmental stimuli including second messenger signals (e.g. cyclic-AMP or cyclic-di-GMP), methyl-accepting chemotaxis proteins, one component systems, histidine-aspartate (His-Asp) phosphorelay systems (also known as two-component systems) and serine/threonine kinases (also known as eukaryote like kinases) (Galperin *et al.*, 2010). In general, all kingdoms of life use signal transduction for environmental adaptation, yet, different preferences have become apparent. In eukaryotes, serine/threonine phosphorylation cascades play the most important role, whereas in bacteria and Archaea signaling primarily takes place via His-Asp phosphorelay systems (reviewed in (Stock *et al.*, 2000, West & Stock, 2001).

His-Asp phosphorelay systems are present in both Gram negative and Gram positive bacteria, in Archaea and eukaryotes, but seem so far to be absent from mammals (West & Stock, 2001, Wolanin *et al.*, 2002, Wuichet *et al.*, 2010). His-Asp phosphorelay systems often regulate bacterial virulence, and their absence from mammals make them a promising target novel antimicrobial drugs (Gooderham & Hancock, 2009, Moon & Gottesman, 2009, Schreiber *et al.*, 2009). In addition to virulence, His-Asp phosphorelay systems modulate many bacterial behaviors in response to environmental changes including locomotion, aerobic/anaerobic transitions, cell differentiation, to name only a few (Stock *et al.*, 2000). While His-Asp phosphorelay systems are broadly distributed in different bacteria, it has been proposed that the abundance of the systems correlates with the ecological niche(s) in which the organism resides (Galperin, 2005, Alm *et al.*, 2006). In other words, organisms living in a non-changing, static environment tend to encode fewer signaling systems than organisms living in environments that rapidly flux; also, these signaling systems are often isolated and linear. However, organisms displaying complex lifestyles tend to have more genes encoding His-Asp phosphorelay systems, which often involve multistep phosphorelay, branched or integrated systems (see section 3.1.1; (Appleby *et al.*, 1996)). In summary, the complexity of signaling systems correlates with the complexity of the organisms lifestyle and environmental challenges it encounters and is often referred to as ‘bacterial IQ’ (Galperin, 2005).

3.1.1. Histidine-Aspartate phosphorelay signal transduction systems in bacteria

‘Two-component systems’ - the paradigm of His-Asp phosphorelay signaling

The prototypical His-Asp phosphorelay system consists of a histidine protein kinase (HPK) and a cognate response regulator (RR) (Figure 1, A; (Stock *et al.*, 2000)). Upon sensing a stimulus with a variable sensing domain (= input), the HPK hydrolyzes ATP and autophosphorylates on a conserved histidine (His) residue in the kinase domain. The cognate RR subsequently catalyzes the phosphotransfer from HPK~P to a conserved aspartate (Asp) residue in its receiver domain. Phosphorylation of this residue leads to a global conformational change in the receiver which activates the associated effector domain and thereby mediates an appropriate output of the “two-component-system” (West & Stock, 2001). Intrinsic dephosphorylation activity of the receiver domain can lead to rapid loss of the active state thus terminate the signal. In summary, this pathway includes three steps of phosphotransfer: autophosphorylation of HPK, phosphotransfer to RR and dephosphorylation of RR to terminate the signal (Stock *et al.*, 2000).

‘Multistep phosphorelay systems’ - including additional proteins

A more complex version of this form of signal transduction is the multistep His-Asp phosphorelay system (Figure 1, B). These systems include more than one phosphor-transfer step and may involve additional proteins, including hybrid histidine kinases (in which the HPK is fused to a receiver domain) and a histidine phosphortransferase

(HPt) (Appleby *et al.*, 1996, West & Stock, 2001). These systems often function with a terminal RR which mediates the output of the system (Wolanin *et al.*, 2002).

'Multicomponent His-Asp phosphorelay systems' - adding more complexity

Multicomponent His-Asp phosphorelay systems can be highly modular and build very complex regulatory machineries. In these systems (Hy)HPKs and RRs can be organized in branched and sophisticated systems (Figure 1, C). By integrating several proteins into one system they can function in one-to-many mechanisms (one HPK is able to deliver a phosphoryl group to many RRs) as well as in many-to-one mechanisms (one RR receives a phosphoryl group from more than one HPK) (Stock *et al.*, 2000, Laub & Goulian, 2007).

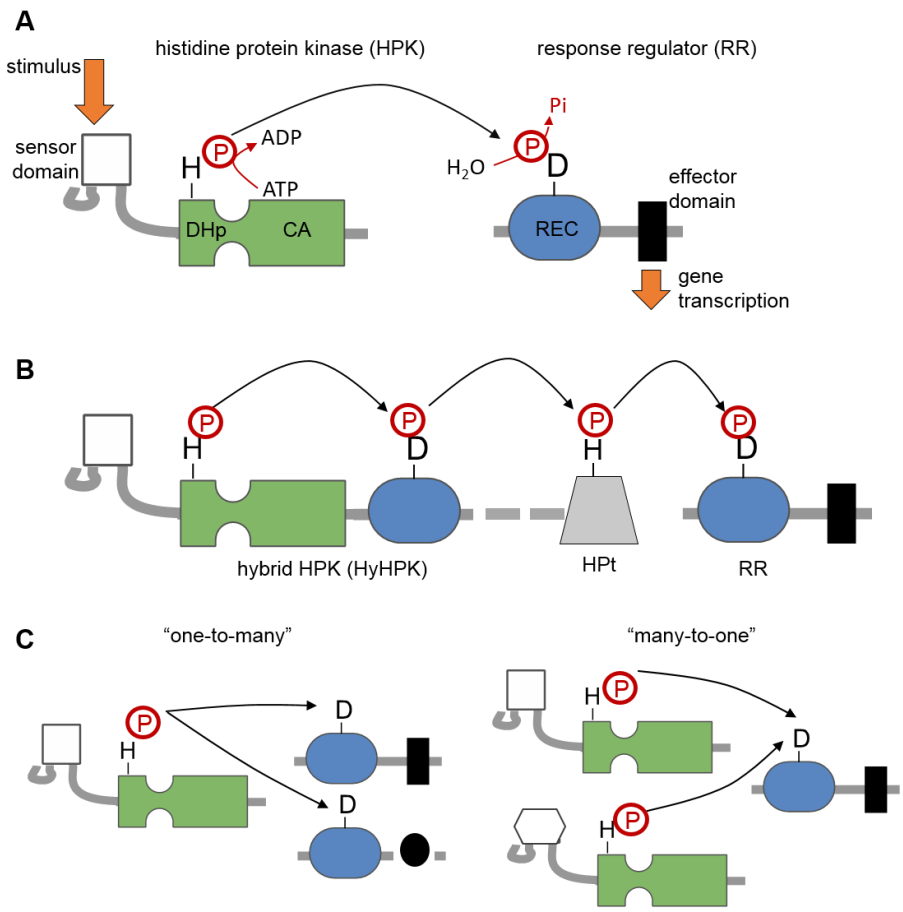

Figure 1: Schematic of His-Asp phosphorelay systems. (A) The paradigm of His-Asp phosphorelay signaling system. This system is composed of a histidine protein kinase (HPK) which, upon sensing a stimulus with its N-terminal sensing domain, autophosphorylates on a conserved histidine residue (H). The phosphoryl group (P) is subsequently transferred to the invariant aspartate (D) in the receiver (REC) domain of a cognate response regulator (RR). Phosphorylation of the receiver domain leads to activation of the downstream effector domain and generates the output of the system (generally regulating gene transcription). **(B) Multistep His-Asp-phosphorelay system.** These more complex signaling systems include more than one phosphotransfer step and often involve hybrid histidine protein kinases (HyHPK) as well as His-containing phosphotransfer proteins (HPt). **(C) Multicomponent His-Asp phosphorelay systems**. The integration of a multitude of proteins allows branching of signaling pathways in both 'one-to-many' and 'many-to-one' mechanisms.

Multistep and multicomponent His-Asp phosphorelay systems provide a greater number of regulation sites and are therefore thought to enable cells to integrate a multitude of signals and fine tune the cellular response in a sophisticated way (Appleby *et al.*, 1996, Hoch, 2000, Stock *et al.*, 2000, West & Stock, 2001, Goulian, 2010). Hence, it is not surprising that several complex cell adaptations are described to be regulated by multistep phosphorelays. These include sporulation of *Bacillus subtilis* (Burbulys *et al.*, 1991), regulation of virulence factors of *Bordetella pertussis* (Uhl & Miller, 1996), control of cell cycle progression in *Caulobacter crescentus* (Chen *et al.*, 2009) and developmental progression in *M. xanthus* (Rasmussen *et al.*, 2005, Jagadeesan *et al.*, 2009, Schramm *et al.*, 2012).

3.1.1.1 Histidine kinases

The prototypical HPK is membrane bound by its N-terminal integral membrane sensing domain with a C-terminal cytoplasmatic signal transmission domain (West & Stock, 2001). All HPKs share a highly conserved kinase core domain, which is comprised of a dimerization and histidine phosphotransfer domain (DHp domain a.k.a. His-KA) as well as a catalytic and ATP binding domain (CA domain a.k.a. HATPase_c) (West & Stock, 2001, Wolanin *et al.*, 2002). HPKs are homodimers mediated by their DHp domains (Hidaka *et al.*, 1997, Marina *et al.*, 2005). Interestingly, heterodimers have also been reported in *Pseudomonas aeruginosa* (RetS and GacS, (Goodman *et al.*, 2009)) and for *Arabidopsis thaliana* (Etr1 and Etr2, (Gao *et al.*, 2008, Grefen *et al.*, 2008)).

HPKs are defined by their ability to catalyze autophosphorylation by transferring the γ-phosphate of ATP to the conserved histidine residue in the DHp domain (Wolanin *et al.*, 2002). The autophosphorylation reaction is catalyzed by the CA-domain can occur *in cis* or *in trans*, depending on the HPK (Casino *et al.*, 2010). While trans-phosphorylation is more universal, cis phosphorylation has also been reported for HK853 in *Thermotoga maritima* and PhoR in *Staphylococcus aureus* (Casino *et al.*, 2009). The CA-domain includes conserved sequence regions, termed the N, G1, F and G2 boxes (Gao & Stock, 2009). Crystal structures of several HPKs (Casino *et al.*, 2009, Gao & Stock, 2009, Casino *et al.*, 2010) revealed the highly conserved ATP-binding pocket is defined by several residues of the N, G1, F and G2 boxes (Gao & Stock, 2009). A flexible region between F and G2 box comprises the ATP-lid which closes the cavity (Gao & Stock, 2009, Stewart, 2010). The phosphotransfer reaction is mostly Mg^{2+}-dependent, however, other ions have been reported to be essential for kinase activity in some specific cases (Gamble *et al.*, 1998, Psakis *et al.*, 2011). The co-factor is necessary for stabilization of the HPK-ATP complex. The hydrolysis of ATP is coupled to the release of Mg^{2+} and conformational changes in the HPK (Wolanin *et al.*, 2002).

Since chemical bonds of both phosphor-histidine (His~P) and phosphor-aspartate (Asp~P) residues are chemically labile, the need for dedicated phosphatases for signal termination was not obvious (Pereira *et al.*, 2011). However, several bifunctional HPKs have been reported which also display phosphatase activity

(Kenney, 2010). It is now assumed that most HPKs are bifunctional (Gao & Stock, 2009). RR dephosphorylation is important to limit the concentration of phosphorylated (activated) RR in order to control or reset the system output (Kenney, 2010). The first described bifunctional HPK was *Escherichia coli* NtrB (Ninfa & Magasanik, 1986). Over 30 years of research later, many advancements have been made to understand regulation and activity of histidine phosphatases and to identify them based on protein sequence motifs. The mechanisms found to regulate phosphatase activity in bifunctional HPKs are extremely versatile. Based on a comparative sequence analysis of the H-box sequence motif, conserved phosphatase motifs could be proposed for both the HisKA_3 as well as the HisKA subfamilies of HPKs (Figure 2), (Huynh *et al.*, 2010)). Both motifs are directly adjacent to the conserved histidine.

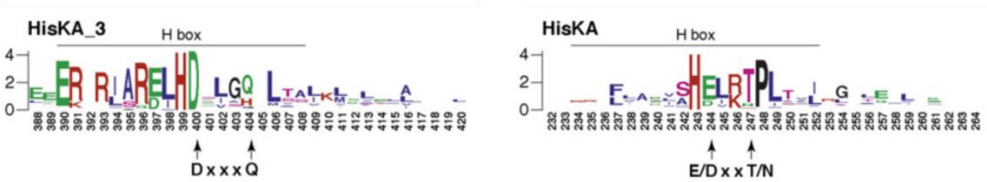

Figure 2: Sequence conservation of the H-box motif of histidine protein kinase classes HisKA_3 and HisKA. The motif analysis was modified from (Huynh *et al.*, 2010). Motifs are further described in the text.

Interestingly, the conserved histidine itself seems to have variable effects on phosphatase activity in different proteins, because was shown that amino acid substitutions of the invariant histidine can increase, decrease or not alter phosphatase activity (Dutta & Inouye, 1996, Haldimann *et al.*, 1997, Hsing & Silhavy, 1997, Zhu *et al.*, 2000, Chen *et al.*, 2009, Huynh *et al.*, 2010, Willett & Kirby, 2012). *C. crescentus* CckA phosphatase activity is not altered by a histidine to alanine substitution (Chen *et al.*, 2009), while *M. xanthus* CrdS and *E. coli* EnvZ phosphatase actively are reduced (Dutta & Inouye, 1996, Hsing & Silhavy, 1997, Zhu *et al.*, 2000, Willett & Kirby, 2012). Surprisingly, *E. coli* NarX (Huynh *et al.*, 2010) and *Enterococcus faecium* VanS (Haldimann *et al.*, 1997) phosphatase activities were even elevated by substituting the histidine with a glutamine. While phosphatase activity clearly originates in the DHp (HisKA) domain of HPKs, the CA (HATPase_c) domain seems also to be involved (Jiang *et al.*, 2000, Zhu *et al.*, 2000). However, the detailed mechanism remains to be experimentally elucidated.

3.1.1.2 Input domains

Most HPK proteins additionally include a sensing domain which regulates HPK activity. In contrast to the highly conserved signal transmission domains, sensing domains are very diverse and can sense variety of specific environmental stimuli. Sensing domains can either be located external to the cytoplasmic membrane, membrane embedded, or cytoplasmic (Cheung & Hendrickson, 2010) presumably corresponding to the location of the signal sensed.

Many HPKs contain a transmembrane segment(s), or are somehow membrane associated (Galperin, 2005). The signal transmission domains must be located in the

cytoplasm (the sole compartment containing ATP), but sensing domains can be entirely extracytoplamsmic, contained as a loop between two transmembrane domains, or may even be comprised of the transmembrane segment(s) itself. However, in some cases the transmembrane domain only serves to anchor the kinase at the membrane, with an additional cytoplasmic sensing domain to sense internal signals (Hoch, 2000, Mascher *et al.*, 2006). Nevertheless, HPKs can also be entirely cytoplasmic, including their sensing domains (Cheung & Hendrickson, 2010).

Sensing domains are as versatile as the environmental signals they detect. Stimuli include pH, light, O2, small molecules, or even protein-protein interactions (summarized in (Mascher *et al.*, 2006)). I will address only Per-ARNT-Sim (PAS) domains here as they are directly relevant to this study. PAS domains were first identified in the fruit fly *D. melanogaster*, but are also highly abundant in bacteria (Henry & Crosson, 2011). PAS domains are associated with a wide variety of signaling proteins including histidine kinases, serine/threonine kinases, transcription factors, guanylate cyclases, phosphodiesterases and even ion channels (Moglich *et al.*, 2009b). These domains are highly divergent at the amino acid sequence level, but share a conserved three dimensional fold of about 100 amino acids which compose a single anti-parallel, five-stranded β-sheet with intervening α-helices (Moglich *et al.*, 2009b). The helices together with the β-sheet create a pocket within which ligand binding often occurs. The signals detected by PAS domains show immense diversity. They range from dissolved gases, redox potential and visible light to ions, small molecules and proteins (Taylor & Zhulin, 1999, Henry & Crosson, 2011). Due to the low sequence homology amongst PAS domains, the prediction of ligands is very challenging. It was established that PAS domains form dimers or even higher order oligomers, which are in prokaryotes favorably homo-oligomers (Moglich *et al.*, 2009b). It is currently proposed that upon signal perception, conformational changes are induced in the oligomers and thus the output of the module is modulated (for greater detail on structure and ligand binding of PAS domains see (Moglich *et al.*, 2009b, Henry & Crosson, 2011)).

3.1.1.3 Response regulators

Response regulators (RR) usually function as phosphorylation-activated switches that mediate the adaptive response of the system (Stock *et al.*, 2000). The prototypical RR consists of a conserved amino-terminal receiver (REC) domain, which includes the invariant aspartate, and a variable carboxy-terminal effector domain (Gao & Stock, 2009). The REC domain of an RR has three distinct functions: it interacts with its cognate HPK and catalyzes the phosphotransfer to its aspartate residue; it regulates the activity of the effector domain in a phosphorylation-dependent manner, and it catalyzes its own dephosphorylation (West & Stock, 2001). Using small molecule phosphodonors (such as acetyl phosphate, carbamoyl phosphate, imidazole phosphate or phosphoamidate), it could be demonstrated that the transfer of the phosphoryl group from a HPK to a receiver domain is catalyzed by the RR itself (Stock *et al.*, 2000).

A REC domain can be found as part of a multi domain RR, in hybrid HPKs, or as a stand-alone domain (West & Stock, 2001). The receiver domain contains about 120 amino acids and has a globular structure of a doubly wound α/β-fold (Gao & Stock, 2009). One representative model of the receiver domain of RRs is the *E. coli* protein, CheY (Stock *et al.*, 2000, West & Stock, 2001). The conserved residues corresponding to Asp12, Asp13 and Asp57 in CheY are responsible for coordinating an Mg^{2+} ion which is required for stabilization of the transition state and therefore for phosphoryl transfer to Asp57 (West & Stock, 2001). The cluster of conserved residues that surround the active site of the regulatory domain is completed by two further highly conserved residues: Thr87 and Lys109 (Stock *et al.*, 2000). These two are not directly required for the phosphorylation/dephosphorylation reaction, but seem to be involved in the phosphorylation-dependent conformational changes (Stock *et al.*, 2000). The aspartyl-phosphate is the highest-energy phosphorylation which can exist in any protein (Stock & Da Re, 2000). Its high standard free energy of hydrolysis enables the RR to undergo large, energetically convenient conformational changes (Lewis *et al.*, 1999). The interactions between the REC domain and the effector domain are rather weak and are destroyed by introducing this much energy into the protein such that the REC domain modulates activity the effector domain (Stock & Da Re, 2000). The effects mediated by REC~P include dimerization, higher-order polymerization, interactions with other proteins or a combination of these effects (Stock *et al.*, 2000).

The stability (defined by the half-life) of phosphorylated RR is regulated by the intrinsic phosphatase activity of REC domains and can span of six orders of magnitude (West & Stock, 2001, Bourret *et al.*, 2010). It has been shown that the autodephosphorylation rate is greatly influenced by two variable amino acid residues corresponding to CheY amino acids at position 59 and 89 (Thomas *et al.*, 2008a). This work showed that 20 different pairs of residues at these positions resulted in 100-fold rages of autodephosphorylation in CheY (Thomas *et al.*, 2008a). Additionally, in many cases, the dephosphorylation of the receiver can be catalyzed by the HPK, where the conserved His is not necessarily required (see section 3.1.1.1 and (Casino *et al.*, 2010)).

3.1.1.4 Output domains

Effector domains associated with REC domains are very diverse both in structure and in function (West & Stock, 2001). Most often (63% of RRs) the effector domains comprise DNA-binding element which functions to regulate gene transcription (Gao & Stock, 2009). 13 % of RRs contain enzymatic effector domains, which are mostly involved in c-di-GMP regulation. 3 % of diverse effector domains mediate system output via interaction with other proteins or ligands (Gao & Stock, 2009). Finally, 17 % of receiver domains can function as stand-alone-module (Galperin, 2006, Gao & Stock, 2009). In Archaea as much as ~ 50 % of all RRs are single domain RRs (Bourret, 2010). The distribution of the output domains over bacterial phyla and Archaea shows that in α-proteobacteria, winged-helix DNA-binding domains as well as stand-alone RR are dominant, while in δ-proteobacteria stand-alone-RR and Fis-

DNA binding domains are the most abundant (Galperin, 2010). How exactly single domain response regulators mediate signal outputs is not currently understood. They have been shown to participate in multistep phosphorelay system (e.g. *Bacillus subtilis* Spo0F (Burbulys *et al.*, 1991)), be an allosteric effector of kinases (like DivK affects PleC in *C. crescentus* (Paul *et al.*, 2008)) or modulate an effector protein by direct interaction. The best characterized output modulated by protein-protein interaction of a stand-alone RR is the regulation of direction of flagella rotation. The phosphorylation-dependent interaction of CheY~P with the flagellar switch protein FliM has been first demonstrated in *E. coli* and later in other organisms such as *B. subtilis* and *Salmonella typhimorium* (Barak *et al.*, 1992, Roman *et al.*, 1992, Welch *et al.*, 1993, Welch *et al.*, 1994, Bren & Eisenbach, 1998, Szurmant *et al.*, 2003, Dyer & Dahlquist, 2006).

3.1.2. Serine/Threonine kinases and phosphatases in bacteria

While His-Asp phosphorelay systems are most commonly used in bacteria for signal transmission, serine/threonine protein kinases (STPK) and their counterpart phosphatases also function in bacteria. Bacterial STPK share sequence homology and structure with eukaryotic serine/threonine protein kinases, but cluster in bacterial specific clades and are therefore termed ‘eukaryotic-like serine/threonine kinases’ (eSTK) (Pereira *et al.*, 2011). Briefly, STPKs fold into a characteristic two-lobed catalytic lobe structure where the catalytic core lies in between the two lobes (Hanks & Hunter, 1995, Kornev & Taylor, 2010). The N-terminal lobe is usually involved in binding and positioning an ATP molecule as phosphodonor, while the C-terminal lobe facilitates binding of protein substrates and initiates the transfer of a phosphate group. STPKs are present in the cell either in their inactive (‘off’) or active (‘on’) state and act as “biological switches” (Huse & Kuriyan, 2002). They can be activated by diverse mechanisms such as subcellular localization or the binding of allosteric effectors (Pereira *et al.*, 2011). Probably the most important regulatory part of a STPKs is its activation segment including the activation loop. Either by autophosphorylation or by phosphorylation by another kinase on at least one residue (serine or threonine) the activation loop is stabilized in a conformation that allows substrate binding and catalysis of phosphotransfer (Huse & Kuriyan, 2002, Nolen *et al.*, 2004).

The very first STPK characterized in bacteria was Pkn1 of *M. xanthus* (Munoz-Dorado *et al.*, 1991). Pkn1 is required for proper *M. xanthus* development, as are several other STPKs which were subsequently described (Nariya & Inouye, 2002, Nariya & Inouye, 2005c, Nariya & Inouye, 2005b, Nariya & Inouye, 2006). The first crystal structure of bacterial STPK was obtained from PknB of *Mycobacterium tuberculosis* (Ortiz-Lombardia *et al.*, 2003, Young *et al.*, 2003). PknB was found to be very similar to the eukaryotic kinase PKA, a long studied model kinase, regarded as a prototype of STPKs (Madhusudan *et al.*, 2002, Taylor *et al.*, 2004). The number of STPKs identified in bacteria rapidly increases based on sequence and structural homologies. To date, a variety of physiological roles of STPKs have been described for cell division and cell wall synthesis (in *Corynebacterium glutamicum, Staphylococcus aureus*,

Enterococcus faecalis, *Streptococcus mutans* and *M. tuberculosis*); secondary metabolism (in *Streptomyces coelicolor*), virulence and central metabolism (in *M. tuberculosis*, *B. subtilis*, *S. coelicolor*, *Yersinia pseudotuberculosis*, *S. aureus* and *E. faecalis*) as well as developmental processes (in *B. subtilis*, *Streptomyces collinus* and *M. xanthus*) (summarized and reviewed in detail in (Pereira *et al.*, 2011)).

Since Ser/Thr phosphor-esters are in general rather stable, dedicated phosphatases are required to terminate signaling cascades. Eukaryote-like serine/threonine phosphatases (eSTPs) have been identified in both Gram-positive and Gram-negative bacteria (Pereira *et al.*, 2011). eSTPs compose a subfamily among the metal-dependent phosphatases and share a conserved catalytic domain with eukaryotic PP2C including 11 – 13 signature motifs and eight conserved residues (Pereira *et al.*, 2011). While in eukaryotes typically each STPK has a dedicated, cognate phosphatase, this seems not to be the case in bacteria (Pereira *et al.*, 2011). For example, *M. tuberculosis* encodes 11 STPKs and only one phosphatase (Av-Gay & Everett, 2000). In total less abundant and less well studied than STPKs so far, phosphatases seem to play similar physiological roles. They are described to be involved in cell division and peptidoglycan synthesis (in *B. subtilis* and *S. mutans*), virulence (in *Listeria monocytogenes*, *Bacillus antracis* and *S. aureus*) and developmental processes (in *B. subtilis* and *M. xanthus*) (summarized and reviewed in detail in (Pereira *et al.*, 2011)).

3.2. Multicellularity and cell differentiation – the social life of bacteria

For decades, bacteria have been viewed as unicellular organisms colonizing many diverse habitats. The highly coordinated and complex multicellular developmental cycles of for instance *Myxococcus xanthus* and *Streptomyces* spp. had been regarded as exotic exceptions to this. It is now apparent that most bacteria at live in (multispecies) biofilms, often composed of differentiated cells or even multiple species (van Gestel *et al.*, 2015, Tan *et al.*, 2017). The paradigm shift to viewing bacteria as multicellular organisms rather than free-living unicellular individuals was initiated by James Shapiro, who reviewed the variety multicellular lifestyles known at that time: cyst formation under nitrogen limitation in *Anabaena*, root infection and colonization of *Rhizobium*, cell differentiation of *Pseudomonas putida* as well as *Proteus mirabilis* (Shapiro, 1988). Also, three interesting features were already described for *M. xanthus*: directed group movement towards prey, formation of predatory spheres in water as well as the formation of fruiting bodies upon starvation.

Today it is widely accepted that bacteria predominantly exist as multicellular communities and differentiate into distinct cell types. Bacterial populations can benefit from multicellularity with respect to defense (persistence against antagonists by collective secretion of substances), offense (increase in virulence, colonization of new niches) and facilitation of viability (better accessibility of food resources and efficient

proliferation) (Shapiro, 1998, West *et al.*, 2007). Appearances of multicellularity are highly diverse (recently reviewed in (West *et al.*, 2007, Claessen *et al.*, 2014)); prominent and well-studied forms include:

i) Production of 'public goods' e.g. extracellular DNA, antibiotics, membrane vesicles, quorum sensing molecules and siderophores,

ii) Transient biofilm formation of *Bacillus subtilis*, *S. aureus*, *Pseudomonas aeruiginosa* and *E. coli*;

iii) Developmental programs culminating in resistant cell forms in *Streptomyces* spp., *Anabaena* spp., *M. xanthus* and *B. subtilis*.

Multicellularity is almost always accompanied by cell differentiation and population heterogeneity. Population heterogeneity is thought to benefit the entire population by creating specialized cells able to survive sudden changes in the environment (Lopez *et al.*, 2009b). Phenotypic heterogeneity is often created in pathogen species as an attempt to escape the immune response of the host (Lewis, 2007). This strategy is often termed as 'bet-hedging' and ensures the survival of the species.

An interesting cell fate is 'lysis', which was observed in starving populations of both *B. subtilis* and *M. xanthus* (Wireman & Dworkin, 1977, Lopez *et al.*, 2009b). Lysing cells are thought to provide the starving population with nutrients (Wireman & Dworkin, 1977, Gonzalez-Pastor, 2011). However, if this is an altruistic event or if cell lysis is forced by other cells remains an open discussion. For *B. subtilis*, it was found that some cells release a toxin to which they themselves are immune but which kills cells nearby (Lopez *et al.*, 2009a). On the other hand, cell death in *M. xanthus* has been frequently described as 'suicide' and would thus be regarded as altruism. However, experimental evidence for this hypothesis is lacking so far.

Variance in phenotypes has also been speculated to be utilized in order to explore and colonize new terrain and niches. Some species, such as *Caulobacter crescentus*, produces both motile and sessile cells (Skerker & Laub, 2004). While the sessile cells ensure population survival in the existing niche, motile swarmer cells can reach out to explore new feeding grounds (Dubnau & Losick, 2006). By differentiation into the sessile form, new niches can be colonized and acquired. Combining all the benefits from phenotypic heterogeneity in terms of motility, 'public goods' production, DNA uptake and environmentally resistant spore formation, *B. subtilis* is currently one of the best studied model organisms of multicellularity and cell differentiation among prokaryotes (Lopez *et al.*, 2009b, Lopez *et al.*, 2009a, Shank & Kolter, 2011, Vlamakis *et al.*, 2013, Tan & Ramamurthi, 2014). *B. subtilis* can differentiate into at least eight distinct cell fates. All these differentiation events are controlled by the three master regulators Spo0A, DegU and ComA, which regulate gene expression (Lopez *et al.*, 2009b). Briefly, activation of DegU by phosphorylation (DegU~P) leads to the production and secretion of proteases (subpopulation 'minors', Figure 3). Phosphorylation of ComA (ComA~P) leads to a surfactin producing subpopulation which can undergo a second differentiation event generating competent cells (subpopulations 'surfactin producers' and 'competent', Figure 3). Activated Spo0A (Spo0A~P) leads to the generation cells capable of biofilm matrix production,

cannibalism (toxin production and secretion) and endospore formation (subpopulations ‘matrix producers’, ‘cannibal’ and ‘spore’, Figure 3). Hereby, the concentration of Spo0A~P in the cell is crucial, as low concentrations lead to the formation of matric producers and cannibals, while high Spo0A concentrations induce sporulation genes.

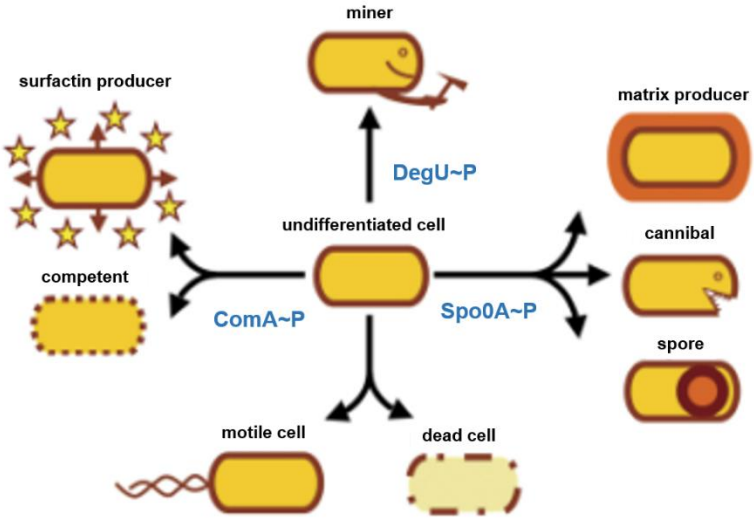

Figure 3: Three master regulators define cell fate segregation of a genetically identical population in *B. subtilis.* Master regulators are written in blue. Figure was adopted from (Lopez & Kolter, 2010)

Similarly, cell differentiation has been observed in *M. xanthus* both during vegetative growth and within the starvation induced developmental program. In a vegetative swarm, ‘cell clusters’ can be isolated which are distinctively different from the other vegetative cells (Lee *et al.*, 2012). During the complex developmental cycle three cell fates have been identified: formation of environmentally resistant spores (Dworkin, 1966, Zusman *et al.*, 2007), persister-like cells termed ‘peripheral rods’ (O'Connor & Zusman, 1991a) as well as programmed cell death (Wireman & Dworkin, 1977, Nariya & Inouye, 2008, Lee *et al.*, 2012). *M. xanthus* was used as the model organism in this study and will be described in more detail in the next sections.

3.3. *Myxococcus xanthus* as a model organism for cooperative behavior in bacteria

Originally isolated from rabbit dung (Beebe, 1941), Myxobacteria are ubiquitous in soil and rotten wood, as well as aquatic habitats preferentially in warm areas (Shimkets *et al.*, 2006). The best studied member of this group of δ-proteobacteria is *Myxococcus xanthus*, which has become a prokaryotic model organism for multicellular development and cell differentiation (Lee et al., 2010). With the fully annotated genome, which became available in 2006 (Goldman *et al.*, 2006), it is possible to generate specific mutants to study the role of genes and their protein products, or even the phenotypic effect of single amino acid substitutions *in vivo* (Lee *et al.*, 2010).

Both stages of the complex life cycle of *M. xanthus*, vegetative predation and multicellular development, are mediated by coordinated movement (Shimkets, 1999, Munoz-Dorado *et al.*, 2016). During vegetative growth, *M. xanthus* forms multicellular swarms which move in a coordinated fashion using two independent gliding motility systems termed adventurous (A-) and social (S-) motility (recently reviewed in (Nan & Zusman, 2011, Schumacher & Sogaard-Andersen, 2017)). When encountering prey microorganisms, the *M. xanthus* swarm secretes antibiotics and enzymes which paralyze and eventually digest their prey (recently reviewed in (Keane & Berleman, 2016)). Upon starvation, a developmental program is triggered in which cells move into aggregation centers, eventually forming mature fruiting bodies filled with environmentally resistant spores (recently reviewed in (Bretl & Kirby, 2016, Kroos, 2017)). During all these processes *M. xanthus* cells communicate via cell-cell communication, self-secreted extracellular matrix as well as exchange of outer membrane vesicles (Velicer & Vos, 2009, Pathak *et al.*, 2012, Cao *et al.*, 2015, Munoz-Dorado *et al.*, 2016).

3.3.1. Benefits of cooperative behaviors in *Myxococcus xanthus*

For half a century, *M. xanthus* has been a model organism to study social behaviors in bacteria (Cao *et al.*, 2015). Living in groups is an obligate situation for many bacteria as a consequence of the requirements of various traits. Interestingly, this is not the case for *M. xanthus* as it is capable of a solitary lifestyle (Velicer & Vos, 2009). Cells can move in isolation by A-motility and thus migrate away from groups. Nonetheless, it has been observed in most natural isolates that most cells do return to the group or are even hindered from wandering off by slime trails or adhesive surface components (Velicer & Vos, 2009). Individual *M. xanthus* cells are proposed to struggle to survive (Reichenbach, 1999), yet, as a collective are very successful predators (Cao *et al.*, 2015). Their great abundance in a wide range of water and soil habitats suggests they might even be a dominant species as a collective (Singh, 1947, Reichenbach, 1999, Li *et al.*, 2012, Cao *et al.*, 2015). While little is understood about the precise benefits resulting from cooperate behavior of *M. xanthus*, it is clear that there is a fitness advantage associated with social traits (Velicer *et al.*, 1998). In a physiologically

structured environment, cooperative behaviors seem to be favored, while in physiologically unstructured environments, the benefits and rewards of such are mute. In the past, social evolution was studied in a laboratory experimental setup of asocial conditions (Velicer & Stredwick, 2002). By conducting an evolution experiment in an asocial, nutrient rich environment, changes in the social interactions of *M. xanthus* could be quantified (Velicer *et al.*, 1998). Of 12 derived lines, only three were able to form fruiting bodies at all, but they were irregularly shaped and small (Velicer *et al.*, 1998). The majority of strains showed reduced potential to sporulate or even lost this ability completely. The study could also show that more than half of the derived lines lost S-motility while maintaining A-motility (Velicer *et al.*, 1998). The authors suggest that natural populations which frequently encounter physiologically unstructured environments may exhibit lower levels of social cooperative behaviors. Indeed, a large natural variation of both gliding motility and development could be experimentally confirmed (Vos & Velicer, 2008, Kraemer *et al.*, 2010).

Another study found that the predatory behavior of *M. xanthus* can evolve in less than 300 generations based on the availability of prey bacteria (Hillesland *et al.*, 2009). It was determined that populations that evolved on low prey density exhibited faster search rates than those evolved on high prey density plates. Whereas the populations allowed to evolve on high prey density showed more improvement in handling prey than the ones evolved on low prey densities. Interestingly, all evolved populations suffer losses in their ability to produce fruiting bodies upon starvation (Hillesland *et al.*, 2009). The authors concluded that social microorganisms can evolve their predatory and other social behaviors depending on the requirements thereof (Velicer *et al.*, 1998, Velicer *et al.*, 2002, Hillesland *et al.*, 2009).

The benefit of the formation of spore filled fruiting bodies for *M. xanthus* remains unclear to date. The vegetative lifestyle of *M. xanthus* swarms (prey on other microorganisms) raised the idea that multicellular fruiting bodies could be dispersed by animals to new feeding grounds. There, a multitude of cells could germinate in a group and immediately form a new swarm benefiting from cooperative feeding (Kaiser, 2001). Not necessarily a contradictory hypothesis was claiming spores inside of fruiting bodies might be better protected from environmental insults (Velicer & Hillesland, 2008, Dahl *et al.*, 2011). However, experimental evidence for either hypothesis is so far lacking.

3.3.2. The developmental program of *Myxococcus xanthus* is controlled by complex gene regulation networks

Upon nutrient limitation, *M. xanthus* enters a complex, highly organized developmental program (Figure 4), which culminates in the production of heat and sonication resistant spores (Sudo & Dworkin, 1969) inside multicellular fruiting bodies. During this program, the swarm divides into at least three distinct developmental cell fates (Wireman & Dworkin, 1977, O'Connor & Zusman, 1991a, Lee *et al.*, 2012). Approximately 80 % of the starting population lyse likely due to programmed cell death, while only 15 % aggregate to build up mounds of approximately 10^5 cells.

Within these, cells eventually differentiate into environmentally resistant spores generating mature fruiting bodies. The remaining 5 % of the starting population stay outside the fruiting bodies in a persister-like state termed peripheral rods. Once nutrient-rich conditions are sensed again, spores are able to germinate and to reenter the vegetative growth state.

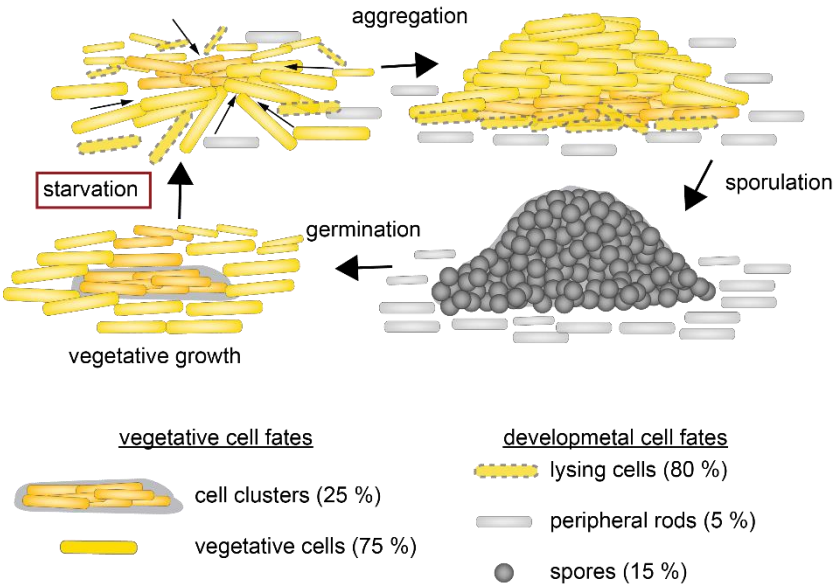

Figure 4: The multicellular life cycle of *M. xanthus*. When a vegetatively growing swarm encounters nutrient limitation, it induces a complex developmental program. During this program the isogenetic swarm differentiates into at least three distinct cell fates. Starving cells form mounds (aggregation centers), which will mature to fruiting bodies. Exclusively inside fruiting bodies, cells differentiate into environmentally-resistant spores. The majority of the starting population lyses, while a minority remains outside of fruiting bodies and are termed peripheral rods.

Of the three developmental cell fates, fruiting body formation and sporulation are the best understood to date. Fruiting body formation is tightly regulated by production and response to extracellular cues as well as a large gene regulatory network (Bretl & Kirby, 2016, Kroos, 2017). The gene regulatory network is composed of His-Asp phosphorelay systems and transcription factors which themselves comprise sequential and combinatorial cascades (Kroos, 2017). Consequently, more than 10 % of all genes of *M. xanthus* were found to be subject to developmental gene regulation (Huntley *et al.*, 2011). The complex developmental gene regulatory network has been is composed of four key modules: the Mrp-, FruA-, Nla24- and enhancer-binding-protein (EBP) cascade modules (see Figure 5; (Kroos, 2017)). The high abundance of transcription regulating proteins as well as the complex regulation and connectivity of signaling systems suggests that *M. xanthus* displays an unusually highly evolved signaling mechanism to orchestrate the temporal and spatial formation of fruiting bodies (Bretl & Kirby, 2016, Kroos, 2017).

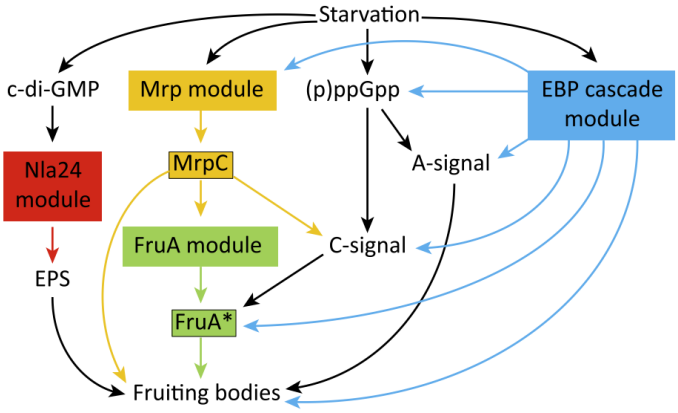

Figure 5: The complex gene regulatory network orchestrating fruiting body formation during *M. xanthus* starvation. Starvation causes the second messengers (p)ppGpp and c-di-GMP to accumulate in the cells and induces the Mrp (orange) and enhancer-binding-protein (EBP, blue) cascade modules. Further, the FruA (green) and Nla24 (red) modules are activated. The four modules, together with extracellular signals (A- and C-signal), build a complex network of feedback loops to eventually regulate gene expression appropriately for formation of fruiting bodies. Here, only the Mrp-module will be considered in detail (see text). The entire network was recently reviewed in (Kroos, 2017). Figure was obtained from (Kroos, 2017)

Depletion of nutrients is sensed at the single cell level via the stringent response (Bretl & Kirby, 2016). Deficiency of energy, phosphate, carbon sources and (as a result of these) amino acids is sensed by a RelA-dependent accumulation of (p)ppGpp (Diodati et al., 2008). The accumulation of (p)ppGpp is both necessary and sufficient to trigger initiation of the developmental program (Harris et al., 1998). The stringent response is proposed to initiate the developmental program by inducing the A-signal as a response to accumulation of uncharged tRNAs (Singer & Kaiser, 1995). The A-signal consists of a set of six amino acids (Trp, Pro, Phe, Tyr, Leu, Ile), peptides consisting of those and proteases that are capable of releasing these from *M. xanthus* cells by extracellular proteolysis (Kaiser, 2004). The concentration of A-signal molecules is directly proportional to the *M. xanthus* cell density (Kaiser, 2004). The intracellular response to A-signal results in up-regulation of a set of genes which are A-signal and starvation dependent (Kaiser, 2004).

Among the genes up-regulated in response to starvation and A-signal is the *mrp* locus, which consists of the *mrpAB* operon and the following gene *mrpC* and is essential for both aggregation and sporulation during the development of *M. xanthus* (Sun & Shi, 2001b, Sun & Shi, 2001a). The locus encodes the proteins MrpA, a proposed cytoplasmic histidine protein kinase; MrpB, an NtrC-like response regulator with a putative sigma54-activator domain as well as MrpC, a transcription factor which belongs to the cyclic-AMP receptor protein family. Genetic evidence suggests MrpB~P induces aggregation (Sun & Shi, 2001b). However, MrpA is unlikely MrpB's cognate kinase because both Δ*mrpB* as well as $MrpB_{D58A}$ mutants are defective in aggregation and sporulation, a Δ*mrpA* mutant merely shows defects in sporulation (Sun & Shi, 2001b). Expression of *mrpC* is dependent on MrpB but interestingly not on MrpA (Sun & Shi, 2001b). MrpC in turn is a key transcription factor of developmental gene regulation. A ChiP-Seq study of a developing *M. xanthus* population revealed MrpC binding sites in the promotor regions of almost 300 genes (Robinson *et al.*, 2014). Hence, it is not surprising that MrpC itself is subject to very

tight regulation at transcriptional and post-translational levels. An auto-amplification loop was proposed for *mrpC*, which would lead to a sudden increase in MrpC accumulation upon first induction of expression of the gene (Sun & Shi, 2001b, Nariya & Inouye, 2006). However, recent data suggests MrpC instead negatively regulates its own expression by interfering with the MrpB dependent regulation of *mrpC* expression ((Bhardwaj, 2013) and P.T. McLaughlin and P.I. Higgs, unpublished data). On the post-translational level, MrpC was proposed to be activated by proteolytic processing in which the N-terminal ~25 amino acids removed to form MrpC2 (Nariya & Inouye, 2006). MrpC2 was found to bind target promotors with a higher affinity than full length MrpC and was thus suggested to compose another signal amplification stimulus towards aggregation and sporulation (Nariya & Inouye, 2006). However, recent data of both two independent laboratories suggest MrpC2 to be an artefact of sample preparation and thus will not be considered further in this work (individually found by the teams of P.I. Higgs and L. Kroos, unpublished data). MrpC was further proposed to be phosphorylated on a threonine residue by the Pkn8-Pkn14 serine/threonine kinase cascade (Nariya & Inouye, 2005c). Phosphorylation of MrpC was proposed to decrease the proteins activity and negatively regulate *mrpC* expression (Nariya & Inouye, 2005c). However, recent data suggests MrpC~P is necessary to induce both aggregation and sporulation (B.E. Feeley and P.I. Higgs, unpublished data).

MrpC is also subject to proteolytic turnover. First, MrpC turnover is regulated by the Esp His-Asp phosphorelay system (further described below, see section 3.4.3.1; (Schramm *et al.*, 2012)). Esp~P stimulate an unknown protease to control MrpC accumulation during the aggregation stage of development. In the *esp* mutants, MrpC accumulates rapidly, causing uncoordinated fruiting body formation and inappropriate cell fate segregation (Higgs *et al.*, 2008, Lee, 2009, Schramm *et al.*, 2012). Second, MrpC could be shown to be highly sensitive to nutrient-regulated proteolysis (Rajagopalan & Kroos, 2014). The commitment to development was studied by adding nutrients back to a starving population and it was determined if development continued or was abolished. Both before and during the critical period of commitment to sporulation, addition of nutrients resulted in a rapid turnover of MrpC (Rajagopalan & Kroos, 2014). Since completion of the developmental program comes at the expense of losing the majority of the swarm, the authors speculate that regulation of MrpC turnover is a strategy to escape commitment to this process (Rajagopalan & Kroos, 2014).

One of MrpCs target genes is the orphan response regulator *fruA* (Ueki & Inouye, 2003). Whether FruA is phosphorylated and how this potential phosphorylation affects its activity is still under debate (Mittal & Kroos, 2009b). It was proposed that FruA becomes activated in response to C-signal (Ellehauge et al., 1998). The C-signal is a proteolytic product (17 kDa) of the cell-surface protein CsgA (25 kDa) and proposed to amplify signaling cascades inside of aggregates due to enhanced cell-cell-contacts (Kim & Kaiser, 1990c, Kim & Kaiser, 1990b, Kim & Kaiser, 1990a, Lobedanz & Sogaard-Andersen, 2003). The receptor which senses C-signal molecules is not yet known, but upon sensing C-signal, CsgA protein expression up-regulated, which in turn leads to an amplification of the signal itself (Sogaard-Andersen, 2004). Active

FruA is thought to stimulate the methylation of the Frz chemotaxis pathway, which is then proposed to direct cells to aggregate into mounds (Zusman et al., 2007). The increase of cell-cell-contact in these mounds is proposed to further stimulate C-signal and thereby create a positive feedback-loop increasing FruA activation (Kaiser, 2004).

FruA has been shown to accumulate in a cell fate specific manner. Cells in aggregates accumulate both MrpC and FruA, while cells outside do not (Lee *et al.*, 2012). The completion of development is dominated by positive feedback loops, MrpC regulates *fruA*, FruA regulates *frzCD*, the Frz system directs cells into aggregation centers and therefore C-signal is enhanced by an increase of cell-cell-contacts and thus all of the above are further stimulated (Bretl & Kirby, 2016). Together, MrpC and FruA are thought to regulate genes which are important for completion of the developmental program and sporulation (Mittal & Kroos, 2009b, Mittal & Kroos, 2009a). They bind cooperatively to the *fmg* genes (FruA and MrpC regulated genes) as well as the *dev* promoter (Mittal & Kroos, 2009b, Mittal & Kroos, 2009a, Lee *et al.*, 2011b, Son *et al.*, 2011, Campbell *et al.*, 2015). Induction of the *dev* operon is required for sporulation (Thony-Meyer & Kaiser, 1993), as is expression of the *exo* and *nfs* loci (Muller *et al.*, 2010, Muller *et al.*, 2012). Taking advantage of chemically induced sporulation, which uncouples the developmental processes of aggregation and sporulation, the transcriptional regulation of genes required merely for pure sporulation was investigated (Muller *et al.*, 2010). Interestingly, it was found that while 60 of 67 genes previously reported to be important for developmental progression were unregulated under these conditions, both *mrpC* and *fruA* were up-regulated. These data together with the observation that a Δ*mrpC* mutant is unable to produce glycerol induced spores, suggests MrpC to be the key transcriptional regulator inducing essential genes for developmental progression as well as core sporulation genes (Muller *et al.*, 2010).

3.3.3. Population heterogeneity – cell differentiation in vegetative and developing *Myxococcus xanthus* swarms

In organisms living cooperatively, like *M. xanthus*, population heterogeneity is a widespread phenomenon and thought to contribute to environmental fitness and therefore ensuring survival of the population. Phenotypic heterogeneity refers to the division of a genetically identical population into subpopulations with distinctive specialization. During vegetative growth, two types of heterogeneity have been described (phase variation and cell clusters), while the developing population divides into at least three distinct cell fates (fruiting body formation and sporulation, cell lysis and peripheral rods) (Higgs *et al*., 2014).

Phase variation in *M. xanthus* arises through the production of the pigment DKxanthine and thus allows the distinction of ‘yellow’ and ‘tan’ cells (Meiser *et al.*, 2006). It is important to note that cells can switch from state to state and that all populations contain a mixture of the two and the persistence of both variants suggests them both to be essential for population survival (Burchard & Dworkin, 1966, Laue & Gill, 1995, Higgs *et al*., 2014).

Differential centrifugation was established as a tool to separate *M. xanthus* cells inside of aggregates from solitary cells (Lee *et al.*, 2011a, Lee *et al.*, 2012). During vegetative growth, 25 % of cells can be isolated as an 'aggregated' cell fraction which was termed cell clusters (Lee *et al.*, 2012). Cell clusters appear to be encased in extracellular polymeric substances (EPS) (Berleman *et al.*, 2011). Some proteins have been shown to be exclusively present in cell clusters, (e.g. FibA) (Lee *et al.*, 2011a), or are differentially modified (i.e. methylation status of FrzCD, (Higgs *et al.*, 2014)). Moreover, the analysis of several developmental markers suggested that cell clusters likely follow a different developmental program (Lee *et al.*, 2012, Higgs *et al.*, 2014). The biological relevance of cell clusters is not well understood. Several roles have been proposed, which include clusters might be the *M. xanthus* equivalent to more sophisticated 'stalks' of fruiting bodies in related species (Reichenbach, 1993), a platform to for fruiting body formation (Curtis *et al.*, 2007) or mediate appropriate spacing between fruiting bodies (Xie *et al.*, 2011).

During the starvation induces developmental program, three distinct cell fates can be observed. Approximately 15 % of a population entering the developmental program will differentiate into myxospores (O'Connor & Zusman, 1991a). Myxospores are produced in order to survive long term nutrient limitation and environmental insults. They have been shown to be resistant to heat, sonication, UV-irradiation, detergents and enzymatic digestion (Dworkin & Sadler, 1966, Sudo & Dworkin, 1969). Spores are generally formed within multicellular fruiting bodies; the proposed benefits of fruiting body formation were discussed above (section 3.3.1), as was genetic regulatory network controlling fruiting body formation (section 3.3.2). Myxospore differentiation involves a major reorganization from a rod shape into sphere, as well and the synthesis and maturation of a rigid spore coat on the surface of the outer membrane (Muller *et al.*, 2012, Higgs *et al.*, 2014, Holkenbrink *et al.*, 2014). Moreover, a massive reorganization of gene transcription accompanies sporulation (Muller *et al.*, 2010), and replication is altered (Tzeng & Singer, 2005, Tzeng *et al.*, 2006). Once nutrients are available again, spores can germinate into vegetative cells and thus create a new predatory swarm.

The majority of the starting population (80 %) lyses during the course of development. Cell lysis was proposed to provide nutrients to the remaining starving population in order to offer them enough energy to complete the sporulation program (Wireman & Dworkin, 1977). It is still under debate as to whether cell lysis is achieved though autolysis (suicide) and therefore could be considered an altruistic event, or whether other cells secrete toxins and thus induce cells to lyse. It was proposed that cell lysis is achieved through a programmed cell death event (Nariya & Inouye, 2008) mediated by a novel toxin-antitoxin mechanism comprised of MazF as toxin and MrpC as anti-toxin (Nariya & Inouye, 2008). However, more recent data suggested this phenotype is only observed in the strain DK101 and could not be reproduced in the two wild type strains DZ2 and DK1622 (Lee *et al.*, 2012). Furthermore, the phenotypic differences of *mazF* deletion observed in DK101 are due to the known *pilQ*1 mutant allele present in DK101 (Boynton *et al.*, 2013). Subsequent studies demonstrated that rather than the original proposal of MrpC as an anti-toxin for MazF endoribonuclease activity

(Nariya & Inouye, 2008), MrpC actually stimulates MazF activity as an RNA interferase (Boynton *et al.*, 2013).

The remaining 5 % of the starting population of cells remain outside of fruiting bodies in a persister-like state, termed peripheral rods (O'Connor & Zusman, 1991a). Peripheral rods are different from vegetative rods and fruiting body cells as they do not accumulate lipid bodies (Hoiczyk *et al.*, 2009), do not significantly accumulate EPS (Lee *et al.*, 2012), and contain a unique proteome (O'Connor & Zusman, 1991b) including differential accumulation of key developmental regulators (O'Connor & Zusman, 1991b, Lee *et al.*, 2011a, Lee *et al.*, 2012). It has been proposed that early in the developmental program, cells destined to sporulate replicate their genome to become 2N, while peripheral rods could be shown to only contain a 1N genome (Tzeng *et al.*, 2006). However, using an alternate approach, peripheral rods where also shown to be 2N (Bhardwaj, 2013). Peripheral rods are non-motile and do not divide, yet, both these features can be regained by addition of nutrients (O'Connor & Zusman, 1991c). The ability of peripheral rods to form fruiting bodies when plated on starvation media at a sufficiently high cell density was investigated in two studies, leading to contradictory results. While one study found peripheral rods retained the ability to form fruiting bodies (O'Connor & Zusman, 1991c), the other one did not observe fruiting body formation (Hoiczyk *et al.*, 2009). The divergent results might be explained by the use of different wild type strains as well as experimental conditions of the studies (Higgs *et al.*, 2014). Since cell density of peripheral rods is rather low, it has been suggested that C-signal is not induced in those cells and thus sporulation specific genes are not expressed (Julien *et al.*, 2000). The proportion of peripheral rods produced increases with the level of nutrients in the starvation media (O'Connor & Zusman, 1991c). The authors therefore proposed that peripheral rods serve to take advantage of low level of nutrients which sufficient to support growth of the entire population (O'Connor & Zusman, 1991c, Higgs *et al.*, 2014).

3.4. Signaling in *Myxococcus xanthus*

The abundance of signaling systems used by a microorganism is often referred to as ‘bacterial IQ’ (Galperin, 2005). Genome studies suggest that the δ-proteobacteria, to which *M. xanthus* belongs, have the greatest average proportion of their genomes dedicated to signaling genes and therefore generate a remarkable ‘bacterial IQ’ for sensing their environmental stimuli (Galperin, 2005, Galperin *et al.*, 2010). *M. xanthus* is subject to a variety of stresses and stimuli, both biotic and abiotic, in its complex native environment. These external signals must be sensed and integrated efficiently to appropriately adjust the communal behavior. Additionally, the coordinated behavior of a multitude of cells is essential for the sophisticated multicellular lifestyle of *M. xanthus* (Whitworth & Cock, 2008). Hence, it is not surprising that genes encoding signal transmission proteins are abundant in the *M. xanthus* genome (Table 1). Interestingly though, the number of DNA binding proteins (i.e. transcriptional regulators) is underrepresented ((Goldman *et al.*, 2006, Schneiker *et al.*, 2007) and

MiST database (Ulrich & Zhulin, 2010)). The high abundance of more complex signaling systems highlights the great signaling potential of this organism and makes it an ideal model organism to study diverse and novel signal transduction mechanisms.

Table 1: Signaling proteins encoded in several bacteria. Table was adapted from P.I. Higgs.

organism	genome size (Mbp)	# proteins*		
		His-Asp phosphorelay	STPK	DNA-binding
C. crescentus NA1000	4.0	105 (2.7%)	0	195 (5.0%)
B. subtilis subsp. subtilis str. 168	4.2	71 (1.7%)	3 (0.07%)	271 (5.8%)
E. coli MG1655	4.6	60 (1.3%)	0	266 (5.6%)
P. aeruginosa PAO1	6.3	127 (2.3%)	5 (0.08%)	422 (7.6%)
S. coelicolor A3(2)	9.1	227 (2.8%)	36 (0.4%)	728 (8.9%)
***M. xanthus* DK1622**	**9.1**	**263 (3.6%)**	**98 (1.3%)**	**258 (3.5%)**

* Proteins were identified utilizing the Microbial Signal Transduction Database 2.2 (MIST2.2; mistdb.com) (Ulrich & Zhulin, 2010).

3.4.1. Eukaryotic-like Serine/Threonine protein kinases and phosphatases in *Myxococcus xanthus*

The *M. xanthus* genome encodes 99 putative serine/threonine protein kinases (STPK), and 88 of these are predicted to contain all the conserved amino acids required for kinase function (Perez *et al.*, 2008). The remaining eleven of these proposed to be inactive for kinase activity, and may be either pseudogenes or have an alternate function. The majority of *M. xanthus* STPKs have not been thoroughly studied (reviewed in (Inouye *et al.*, 2008)), but some have shown to have important roles in developmental regulation and motility (Munoz-Dorado *et al.*, 1991, Inouye *et al.*, 2000, Udo *et al.*, 2000, Nariya & Inouye, 2002, Thomasson *et al.*, 2002, Nariya & Inouye, 2003, Nariya & Inouye, 2005b, Nariya & Inouye, 2005c, Nariya & Inouye, 2005a, Nariya & Inouye, 2006, Stein *et al.*, 2006, Inouye & Nariya, 2008). Arguably the best studied to date are Pkn8 and Pkn14 (Nariya & Inouye, 2005b, Nariya & Inouye, 2005c, Nariya & Inouye, 2005a, Nariya & Inouye, 2006, Inouye & Nariya, 2008). It is proposed for this pathway that Pkn8 phosphorylates Pkn14 under vegetative growth conditions. Activated Pkn14 is thought to phosphorylate the transcription factor MrpC, hindering its activation. Under starvation conditions, this cascade is proposed to be switched off, thus, allowing activation of MrpC. The Pkn8/Pkn14 cascade is supposed to be anchored and coordinated by (multi)kinase-

associated proteins KapA, KapB and KapC (Nariya & Inouye, 2005b, Nariya & Inouye, 2005a). It should be noted however, that this pathway was studied in the DZF1 background and many of the mutant phenotypes are not reproduced in the DZ2 or DK1622 backgrounds (B.E. Feeley, V. Bhardwaj, X. Mei and P.I. Higgs, unpublished data).

Due to the chemical stability of phosphoester bonds, signal termination for serine/threonine phosphorylation-dependent activation requires dedicated phosphatases. Only 14 protein phosphatases have been identified in the *M. xanthus* genome (Treuner-Lange, 2010) and most of them not coupled in operons with kinases (Treuner-Lange, 2010). Of these 14 predicted phosphatases, only three have been investigated so far (Treuner-Lange *et al.*, 2001, Garcia-Hernandez *et al.*, 2009, Kimura *et al.*, 2011). All three have been reported to be necessary for proper aggregation and sporulation, however, not in the same regulatory pathway. To date, no relationship between kinase (cascades) and phosphatases have been demonstrated in *M. xanthus* signal transduction (Munoz-Dorado *et al.*, 2014).

3.4.2. *Myxococcus xanthus* His-Asp phosphorelay systems

An analysis of the *M. xanthus* genome revealed 251 His-Asp phosphorelay signaling protein encoding genes (non-chemosensory), including 118 HPKs, 119 RRs and 14 HPK-like proteins (Shi *et al.*, 2008). Surprisingly, only 29 % of these genes (37 pairs) are encoded in the usual paired gene organization. Interestingly, 16 % (14 identified clusters) are encoded as complex gene arrangements which are defined as a gene locus encoding more than two His-Asp phosphorelay signaling genes). 55 % (154 genes) are orphans defined as a gene encoding a His-Asp phosphorelay signaling protein not flanked by another His-Asp phosphorelay signaling coding gene) (Shi *et al.*, 2008). In these orphan or complex gene clusters, atypical HPKs (either hybrid kinases or cytoplasmatically localized) as well as atypical RRs (lacking a DNA binding domain or single domain RR) are overrepresented (Shi *et al.*, 2008). These observations are consistent with the hypothesis that signal transmission in *M. xanthus* involves highly integrated branched signaling pathways rather than the simpler 1:1 signal transduction systems employed by many bacteria (Shi *et al.*, 2008, Whitworth & Cock, 2008).

3.4.3. Signal transduction systems constrain developmental progression in *Myxococcus xanthus*

Several mutants of *M. xanthus* have been described which show accelerated development and perturbed cell fate segregation upon starvation; these genes have collectively been termed negative regulators (NR) of developmental progression. Most of these genes were identified in a transposon mutagenesis screen (K. Cho, P.I. Higgs and D.R. Zusman, unpublished data; (Lee *et al.*, 2005)) and were subsequently mapped to orphan histidine protein kinase genes: *espA* (1 mutant), *espC* (1 mutant), *red* locus (5 mutants) (see section 3.4.3.2), and MXAN_4465 (2 mutants) (see section

3.4.3.4) (Lee *et al.*, 2005, Lee, 2009). An additional orphan kinase was placed in this NR group based on a previously described phenotype (Rasmussen & Sogaard-Andersen, 2003, Lee, 2009).

Each individual mutant produced fruiting bodies with perturbed in fruiting body organization and defects in cell fate segregation (spores could be identified amongst peripheral rods, outside of fruiting bodies) (Lee, 2009). Genetic epistasis experiments suggest these proteins function in three parallel signaling pathways comprised of EspAC, Red, and TodK (MXAN_4465 was not analyzed for epistasis). Double mutants of *esp*, *red* or *todK* display additive phenotypes in which fruiting body morphology is progressively more disorganized. In a mutant missing all three systems (DZ2 Δ*espA* Δ*espC* Δ*red(CDEF*) *todK*::*tet*, designated ΔNR) spores are produced so early that fruiting body morphology is completely destroyed (Lee, 2009). Interestingly, analysis of developmental subpopulations indicated the proportion of cells inside aggregates (fruiting bodies), remained relatively constant in all mutants observed (Figure 6, (Lee, 2009)). However, the number of inappropriately sporulating peripheral rods increased proportionally.

Consistent with a shared phenotype but three distinct signaling pathways, mutants in *esp*, *red* or *todK* each display distinct patterns of early MrpC accumulation (Lee, 2009). In addition, the ΔNR mutant accumulates MrpC extremely early and at very high levels correlating with the complete reprogramming of peripheral rods into spores. Together these data support the hypothesis that MrpC is a major factor regulating cell fate segregation in the *M. xanthus* developmental program. While Esp is known to affect MrpC turnover (see section 3.4.3.1), it is essential to determine how the remaining NR systems affect MrpC accumulation.

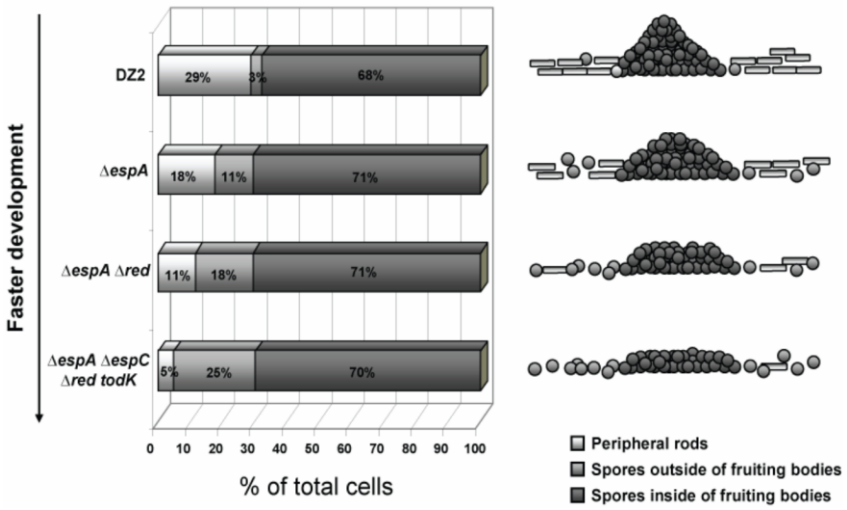

Figure 6: Peripheral rods are reprogrammed to sporulate inappropriately in mutants lacking negative regulator(s) of development. After 5 days of starvation, cell populations were separated by differential centrifugation, spores and cells were counted in the fractions and reported as percentage of the remaining population. Δ*red* = Δ*red(CDEF*). Figure was obtained from (Lee, 2009).

3.4.3.1 The Esp system

The Esp (early sporulation) system consists of two hybrid histidine protein kinases EspA (Cho & Zusman, 1999) and EspC (Lee *et al.*, 2005), two Ser/Thr kinases PktA5 and PktB8 (Stein *et al.*, 2006) as well as the putative transport protein EspB (Cho & Zusman, 1999) (current model see Figure 7). It could be shown that *espA* and *espB* are co-transcribed, yet have opposing effects on development (Cho & Zusman, 1999): the Δ*espA* mutant leads to early development, while the Δ*espB* mutant leads to delayed development (Cho & Zusman, 1999). EspB is thought to function in a module with PktA5 and PktB8 because mutants in any single gene as well as the triple mutant display the same phenotype (Cho & Zusman, 1999, Stein *et al.*, 2006). This EspB/PktB8/PktA5 module is thought to act upstream of EspA (Cho & Zusman, 1999, Stein *et al.*, 2006). Interaction between EspA and the two STPKs is likely mediated by a forkhead-associated (FHA) domain in EspA, consistent with the role FHA domains as a phosphor-threonine interaction module and the observation that PktA5 autophosphorylates on a threonine residue (Durocher *et al.*, 2000, Stein *et al.*, 2006).

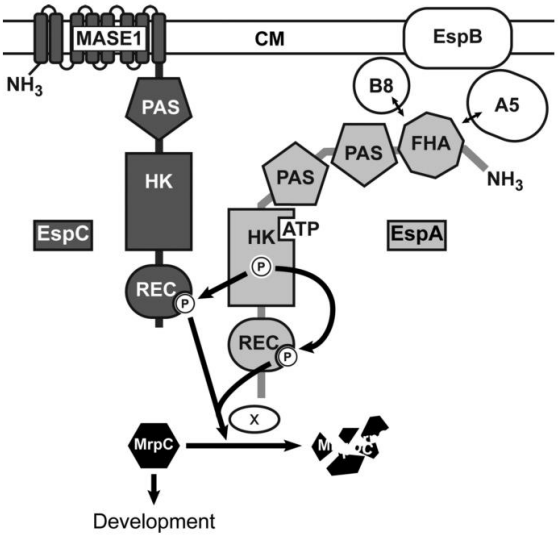

Figure 7: Current model of the Esp-signaling system. The complex system consists of the two hybrid histidine protein kinases EspC (dark gray) and EspA (light gray), which are likely modulated by two serine/threonine kinases, PktA5 (A5) and PktB8 (B8) as well as a putative transport protein (EspB). The histidine kinase domain (HK) of EspA autophosphorylates and donates a phosphoryl group to both its own and EspCs receiver domains. The system regulates the accumulation of the important developmental regulator, MrpC. The phosphorylation of both receiver domains (REC) at the same time activates a so far unknown protease (x) to stimulate MrpC proteolytic turnover. Figure was obtained from (Schramm et al., 2012). CM cytoplasmic membrane, MASE1 membrane associated sensor domain, FHA fork head associated domain, PAS per-arnt-sim domain.

Consistent with genetic epistasis analyses, EspA and EspC, both hybrid histidine kinases, function in a novel signaling module (Higgs *et al.*, 2008, Schramm *et al.*, 2012). While EspC can autophosphorylate *in vitro*, it cannot donate a phosphate group to its own receiver domain (Schramm *et al.*, 2012). EspC kinase is not important in regulation of development under laboratory conditions *in vivo*, because substitution of its conserved phosphoaccepting His residue, or deletion of its entire HPK catalytic domain, yields a wild type phenotype (Schramm *et al.*, 2012). Instead, both *in vitro*

and *in vivo* approaches indicate that EspA serves as the phosphodonor for both its own and EspCs receiver domains (Schramm *et al.*, 2012). Simultaneous phosphorylation of both EspA and EspC receiver domains is required for the system output, as alanine substitutions of either or both conserved aspartates leads to the same early developmental phenotype (Schramm *et al.*, 2012).

MrpC protein over-accumulates in a Δ*espA* strain, while levels of *mrpC* mRNA remained unaltered (Higgs *et al.*, 2008). Analysis of protein half-lives in both wild type cell lysates and lysates from a Δ*espA* Δ*espC* double mutant revealed that in wild type lysates MrpC has a half-life of 30min, but turnover could not be detected in the *espAC* mutant (Schramm *et al.*, 2012). Therefore, the Esp signaling system appears to stimulate an unidentified protease to degrade MrpC and delay developmental progression. The stimulus/stimuli the Esp signaling complex responds to and identity of the putative protease are currently unknown.

3.4.3.2 The four-component Red system

The Red system (regulation of early development) functions as a four-component His-Asp phosphorelay system consisting of a membrane bound HPK (RedC), a cytoplasmic kinase-like protein (RedE), a dual receiver domain protein (RedD) and a single domain response regulator (RedF) (Higgs *et al.*, 2005). The Red proteins are expressed under vegetative growth conditions and down-regulated after induction of development; the proteins, however, remain stable in the population until at least 24 h of starvation (Jagadeesan *et al.*, 2009, Lee, 2009). Interestingly, the Δ*red(CDEF*), Δ*redC* and Δ*redF* mutants each develop early, while the Δ*redD* and Δ*redE* mutants are each delayed (Higgs *et al.*, 2005, Jagadeesan *et al.*, 2009). *redC-F* are located in the seven gene redA-G operon. Deletions of *redA* (encoding a putative ribosome modulation protein), *redB* (encoding a hypothetical protein) and *redG* (encoding a putative metallopeptidase), however, did not result in significant developmental phenotypes and were not studied further (Higgs *et al.*, 2005).

The current model (Figure 8) was built on a combination of *in vitro* and *in vivo* data. Epistasis was determined by the creation of various combinations of deletion mutants. Signal flow within the system was elucidated by the analysis of non-functional substitution mutants and autophosphorylation/ phosphotransfer assays with purified proteins. In this model, repression of developmental progression is initiated by a stimulus sensed through the HPK RedC. RedC subsequently autophosphorylates on the conserved histidine residue of the kinase domain. This phosphoryl group is subsequently transferred onto RedF, which functions as the output of the system. Phosphorylated RedF (RedF~P) represses developmental progression. In later stages of development, upon sensing an unknown stimulus, RedC~P instead donates a phosphoryl group to the first REC domain of RedD. RedD transfers this group further onto RedE, a kinase like protein with a poorly conserved DHp domain which is incapable of autophosphorylation. RedE~P is able to act as a phosphatase on RedF~P which then releases the developmental block.

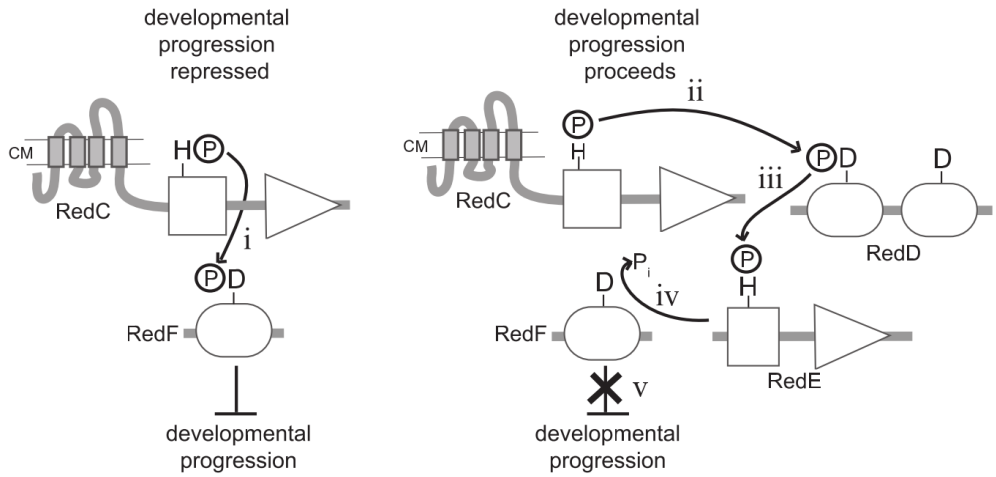

Figure 8: Current model of the Red-signaling system. The four-component system consists of an HPK RedC, an HPK-like protein RedE as well as the two response regulators RedD and RedF, both of which lack output domains. To repress developmental progression (left part), RedC senses a so far unknown signal, autophosphorylates and donates this phosphoryl group to the stand-alone response regulator RedF (i). Phosphorylated RedF (RedF~P) represses progression through the developmental program via a so far unknown mechanism. Upon sensing a different stimulus presumably in later stages of development, specificity of RedC~P shifts from RedF to RedD (right part). The phosphoryl group from RedC~P is now transferred to the first REC domain of RedD (ii). The phosphoryl group is further transferred to RedE (iii). Phosphorylated RedE (RedE~P) acts as a phosphatase on RedF~P. The phosphoryl group from RedF is removed (iv), and developmental repression is relieved (v). Figure was obtained from (Jagadeesan *et al.*, 2009). CM cytoplasmic membrane.

It could be shown that the Red-system regulates developmental progression by affecting accumulation of MrpC as well (Lee, 2009). The mechanism how RedF mediates the systems output and at which level MrpC is regulated by the system remains yet unknown.

In an effort to identify interaction partners, RedF was used as bait in a yeast-two hybrid genomic library resulting in identification of the KapC STPK-scaffolding protein as a putative candidate (X. Mei and P.I. Higgs, unpublished data). KapC is thought to interact with Pkn8 which has been proposed to influence MrpC phosphorylation. These data suggest that the Red system may modulate MrpC accumulation by altering the phosphorylation state of MrpC which may affect its activity and accumulation. However, this hypothesis requires verification.

3.4.3.3 The orphan histidine protein kinase TodK

The *todK* (timing of development kinase) gene was first analyzed in the alternate wild type strain DK1622 (Rasmussen & Sogaard-Andersen, 2003). In either generally used wild type strains (DZ2 and DK1622), a deletion or interruption of *todK* resulted in early aggregation and sporulation upon starvation (Rasmussen & Sogaard-Andersen, 2003, Lee, 2009). The *todK* mutant reacts appropriately to starvation and does not bypass the requirement for the known developmental regulators *csgA, fruA* and *devR* (Rasmussen & Sogaard-Andersen, 2003).

Surprisingly, differences in transcriptional regulation of *todK* have been reported in the two *M. xanthus* background strains. In DK1622, *todK* is transcriptionally downregulated 10-fold upon starvation (Rasmussen & Sogaard-Andersen, 2003), while in DZ2 *todK* expression remains mainly constant with a slight upregulation peaking at 12 h of starvation, being back to basal levels around 24 h of starvation (Lee, 2009).

Domain architecture prediction suggests TodK to be a cytoplasmic HPK, containing two N-terminal PAS domains and a C-terminal histidine kinase module. It is not known, if TodK constitutes an active HPK. However, the function of these domains in regulating TodK activity has not yet been addressed. Interruption of *todK* leads to miss-accumulation of MrpC (Lee, 2009), but the mechanism by which MrpC is affected is unknown. Elucidation of this mechanism would be facilitated by identification of the TodK signal output, which is currently unknown. DotR was considered as a candidate for a cognate response regulator for TodK. *dotR* (downstream of *todK* response regulator) is transcribed in the opposite direction from *todK*, and *todK* and *dotR* share overlapping stop codons (Rasmussen & Sogaard-Andersen, 2003). However, a Δ*dotR* mutant (generated in the DK1622 background) displayed a wild type phenotype, and it was concluded that DotR is not the TodK cognate response regulator (Rasmussen & Sogaard-Andersen, 2003).

3.4.3.4 The orphan histidine protein kinase Hpk30

MXAN_4465, encoding the orphan histidine kinase Hpk30 was designated a NR after its identification in a mutagenesis screen (K. Cho, P.I. Higgs, and D.R. Zusman, unpublished data) and a deletion mutant produced an early development phenotype in the DZ2 strain background (B. Lee, P. Mann and P.I. Higgs, unpublished data). MXAN_4465 (*hpk30*) was also found to be one of 25 orphan kinases which are transcriptionally upregulated upon starvation (Shi *et al.*, 2008). A DK1622 Δ*hpk30* mutant displayed normal developmental timing, but produced smaller, more numerous, and less condensed fruiting bodies compared to the wild type (Shi *et al.*, 2008).

Analysis of the Hpk30 domain architecture suggests it is cytoplasmic hybrid histidine kinase which lacks an input domain but contains two receiver domains following the kinase domain. All domains include the respective conserved active residues, but it has not been determined if all domains are required for *in vivo* function. Preliminary data suggest Hpk30 participates in a parallel signaling distinct pathway from the other NRs, because addition of the Δ*hpk30* mutation to the ΔNR strain produced an additively early phenotype (B. Lee and P.I. Higgs, unpublished data). We hypothesize Hpk30 is involved in the negative regulator network that controls *M. xanthus* developmental progression.

4. Scope of study

Myxococcus xanthus are bacteria that favor social behaviors throughout their complex life cycle, including a multicellular developmental program in which cells segregate into distinct fates. *M. xanthus* is enriched for signal transmission proteins (i.e. His-Asp phosphorelay proteins and Ser/Thr protein kinases), but is under-represented in DNA-binding proteins. This observation suggests *M. xanthus* may have evolved signaling networks involving hierarchical and branched signaling pathways that converge on a few hub transcriptional regulators - a hallmark of eukaryotic multicellular signaling networks. An excellent example of this are the Esp, Red, TodK, and Hpk30 signaling systems which constrain the developmental program. These systems converge on the MrpC hub protein; MrpC is a transcriptional regulator necessary for development.

In this study, I aimed to address how Red, TodK and Hpk30 signaling systems could coordinate MrpC accumulation. Since Hpk30 and TodK were primarily uncharacterized signaling proteins, the approach was to first define the signal flow within each protein to identify the signal output mechanisms. As the signal output of the Red system was already known, the approach was to confirm a putative link to regulation of MrpC accumulation. An additional aim was to understand the benefit of this signaling network to the *M. xanthus* life cycle. For this aim the approach was to compare dispersal and resistance of fruiting bodies between the wild type and a mutant lacking the signaling systems which constrain development.

5. Results

5.1. *Myxococcus xanthus* fruiting body morphology: environmental adaptation

Many mutants of *M. xanthus* have been identified over the years that present various phenotypes during the starvation induced developmental program. This phenotype includes inappropriate timing, perturbed cell fate segregation and irregular fruiting body morphologies. In a previous study (Lee, 2009), four of these mutants have been investigated and thorough genetic epistasis analysis suggested they function in three parallel signaling pathways. Intriguingly, all four genes map to orphan histidine kinases or complex His-Asp-phosphorelay systems. A strain lacking all three systems displays a strikingly additive phenotype since the formation of well-organized fruiting bodies is completely abolished. Here, I further investigated the fruiting body morphology of this strain. Moreover I wanted to elucidate the evolutionary advantage of the formation of well-structured fruiting bodies over the formation of a lawn of single spores.

5.1.1. Fruiting body morphology is drastically perturbed in the absence of constraining signaling systems

It has been previously shown that a mutant lacking three signaling systems that regulate developmental progression in *M. xanthus* displays very accelerated development. The morphology of fruiting bodies produced by this strain is severely affected (Lee, 2009). This phenotype was shown using a strain containing in-frame deletions of the *esp* and *red* systems and an insertion in the *todK* gene (Δ*espA* Δ*espC* Δ*red(CDEF) todK*::*tet*) termed 'delta negative regulator' (ΔNR) and under two established laboratory starvation conditions: CF-agar plates and in submerged culture (Lee, 2009).

For this study, a strain bearing in-frame deletions of all the negative regulator genes (Δ*espA* Δ*espC* Δ*red(CDEF)* Δ*todK*) was used. To examine fruiting body structure, cells were induced to develop under submerged culture starvation conditions. The mutant formed obvious aggregates at 19 h after induction of development, approximately 12 h earlier than the wild type (Figure 9). Both wild type and mutant aggregates produced darkened fruiting bodies which generally correlates with production of heat and sonication resistant spores. The mutant fruiting bodies were highly irregular and appeared flattened relative to the wild type (Figure 9). Since the observed phenotype of this new mutant (Δ*espA* Δ*espC* Δ*red(CDEF)* Δ*todK*) was indistinguishable from the previously studied mutant (Δ*espA* Δ*espC* Δ*red(CDEF) todK*::*tet*), they will both be termed 'delta negative regulator' (ΔNR) for the remainder of this document.

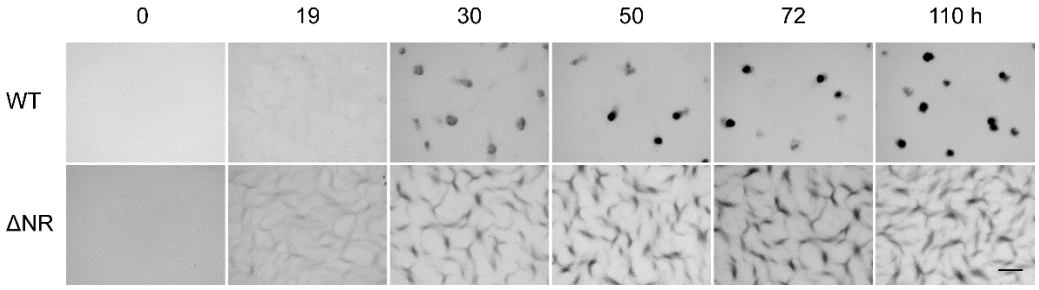

Figure 9: The ΔNR mutant aggregates earlier and produces disorganized fruiting bodies during starvation induced development. *Starvation assay.* WT (wild type, DZ2) and ΔNR mutant (Δ*espA* Δ*espC* Δ*red(CDEF)* Δ*todK*) strains were developed under submerged culture. Pictures were recorded at the indicated hours after initiation of starvation using a stereomicroscope. Pictures from two separate assays were combined to retrieve a complete developmental time course. Scale bar 500 µm.

To examine the relative heights of wild type and ΔNR mutant fruiting bodies, confocal laser scanning microscopy (CLSM) and fluorescein-conjugated concavalin A (FITC-ConA) was used to image unfixed cells grown under native, undisturbed submerged culture conditions as described previously (Lux *et al.*, 2004, Hu *et al.*, 2013). ConA binds to the ring structure of the carbohydrates α-D-glucose and α-D-mannose which are both present in in the exopolysaccharide (EPS) layer which surrounds *M. xanthus* fruiting bodies (Li *et al.*, 2003). After completion of the developmental program (120 h), cells were stained with FITC-ConA and examined by inverted CLSM. The wild type strain formed typical mound-shaped fruiting bodies. The top view (Figure 10, A and C) displayed a round base for fruiting bodies, with a dome-like structure that could be observed in the side view (Figure 10, E). The images of wild type fruiting bodies showed a previously observed volcano effect (Lux *et al.*, 2004, Smaldone *et al.*, 2014) that is likely due to the presence of optically dense myxospores in the center of the fruiting body which retards fluorescence collection. Measurement of wild type fruiting body height revealed an average height of 77 ±14 µm (Figure 10, G). However, very high fruiting bodies were also observed that peaked at ~260 µm. An earlier study in the alternative wild type strain DK1622 also reported some structures that were much higher than the average (Lux *et al.*, 2004). In contrast, the ΔNR mutant formed ridge like fruiting bodies that failed to separate (Figure 9), and that were also covered in EPS and nicely visible in the top views of CLSM images (Figure 10, B and D). Side view images indicated these fruiting bodies were flat (Figure 10, F), with an average height measured of 26 ±5 µm (Figure 10, G). No large variation in fruiting body height was observed.

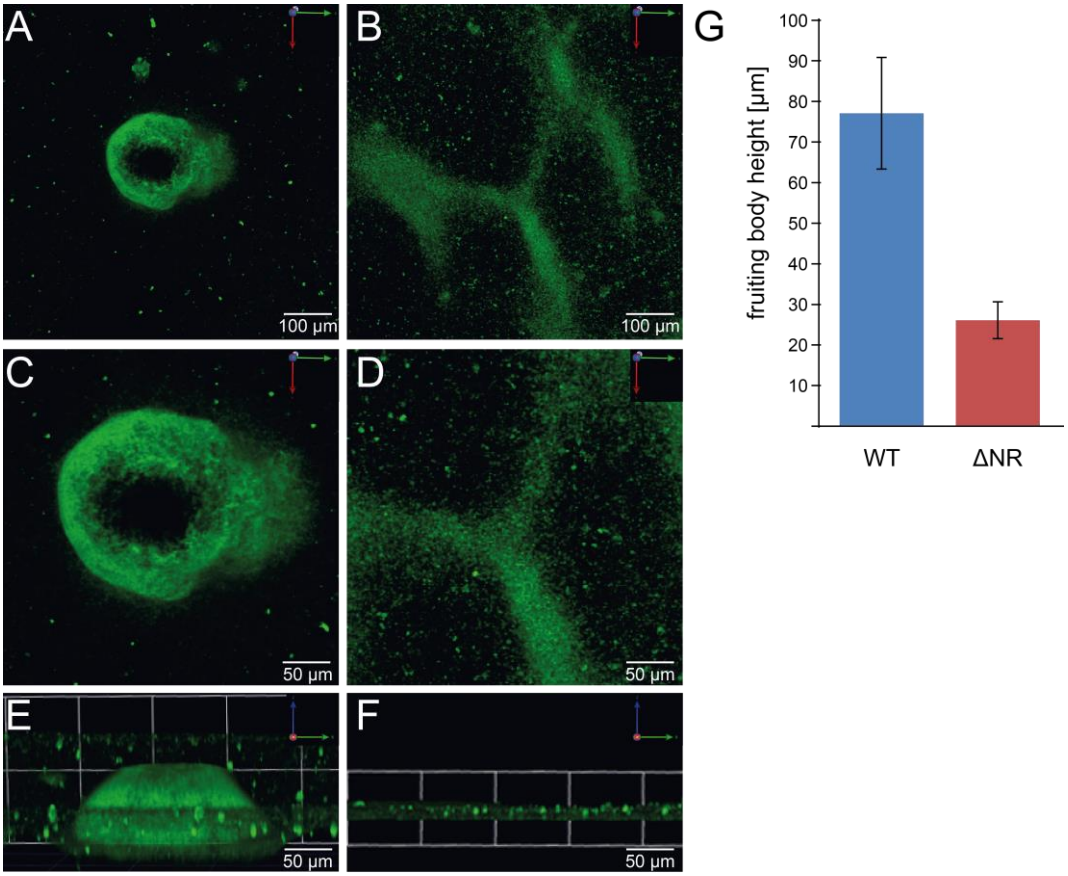

Figure 10: The ΔNR mutant produces flat fruiting bodies during starvation induced development in submerged culture. *Confocal laserscanning microscopy*. **(A-F)** Wild type (WT) and ΔNR mutant strains were developed under submerged culture in 35 mm culture dishes for 120 h and extracellular matrix was stained with fluorescein-conjugated concavalin A (FITC-ConA). Images were recorded with an inverted CLSM and processed with Volocity imaging software. WT **(A, C and E)** and ΔNR mutant **(B, D, and F)** images were compiled for top **(A-D)** and side **(E-F)** views. **(G)** The average height of WT (n = 37) and ΔNR mutant (n = 34) fruiting bodies. Error bars represent associated standard deviations.

These results demonstrated that deletion of the three negative regulator signaling systems result in the production of poorly resolved, flat fruiting bodies of approximately one third the height of the wild type. I took advantage of this observation to examine the role of fruiting body morphology and negative regulator genes in the *M. xanthus* life cycle.

5.1.2. The ΔNR mutant produces more spores than the wild type but the percentage of viable spores is equal

To begin to examine if the wild type mound-shaped and compact fruiting bodies have fitness advantages over flat, loosely packed fruiting body structures, I first set out to examine if both strains (wild type and ΔNR mutant) produce equally viable spores. Spores were harvested from mature fruiting bodies (120 h), and treated with heat (50 °C for 60 min) and sonic disruption. These spores were enumerated with a counting chamber, and then induced to germinate on rich media (CYE). Colony

forming units (CFU) arising from germinating spores were counted after four days of incubation at 32 °C.

Interestingly, the ΔNR mutant was found to produce ~600 % of the WT spores after 120 h of starvation in submerged culture (Table 2). Germination efficiency of wild type spores was observed on average at 15 %, the ΔNR mutant germinated at averaged 10 % efficiency. A student T-test confirmed that these rates are not significantly different.

Table 2: Sporulation and germination efficiency of wild type (WT) and ΔNR mutant after 120 h of starvation.

strain	spores* (x10^6)	% of WT	% viability **
WT	7.8 ± 4.1	100	15.7 ± 11.8
ΔNR	46.1 ± 28.5	592	10 ± 5.6

* Heat and sonication resistant spores were enumerated after 120 h of starvation.
** Viable spores were scored as colony forming units (CFU) after four days incubation at 32 °C and reported as % of spores present.
The average data from three biological (three technical replicates each) are presented.

The majority of colonies arising from germinating ΔNR spores were tan, while the majority of wild type germinating spore colonies appeared yellow (Figure 11, A). Tan locked mutants produce miss-organized fruiting bodies that appear translucent and are described as soft, immature mounds (Furusawa *et al.*, 2011). To exclude the possibility that the developmental phenotype of the ΔNR mutant stems from a tan-locked phenotype, cells from yellow and a tan clone were induced for development under submerged culture. Both clones showed the characteristic formation of ridge like fruiting bodies (Figure 11, B). While the ΔNR mutant may more often appear in the tan state, phase variation back to yellow could occur and these mutants were therefore not considered tan-locked.

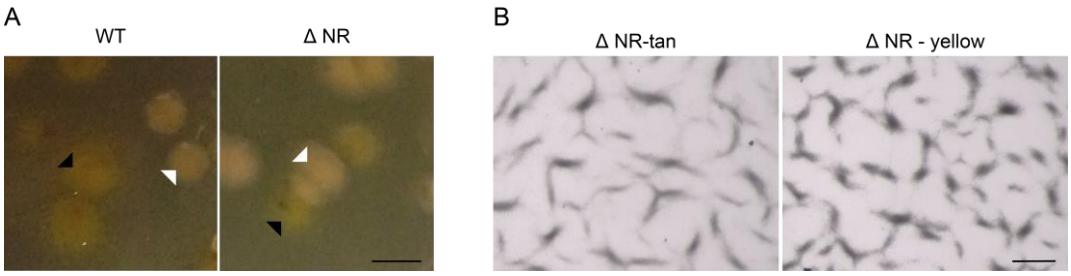

Figure 11: Phase variation can be observed in both wild type and ΔNR mutant. (A) Yellow (black arrows) and tan (white arrows) colonies of wild type *M. xanthus* (WT) and ΔNR mutant observed after single-colony isolation. Scale bar 0.5 cm. **(B)** A yellow and a tan clone of the ΔNR mutant displayed the characteristic ΔNR fruiting body morphology after 120 h of starvation induced development in submerged culture. Scale bar 500 µm.

In conclusion, I found that the ΔNR mutant produced 6-fold more resistant spores than the wild type, with similar percent viability.

5.1.3. Design of a novel dispersal assay for *Myxococcus xanthus* fruiting bodies

Two non-competing hypotheses have been proposed to explain why myxobacteria have evolved to produce spores in compact fruiting bodies. One hypothesis is that because *M. xanthus* growth rate depends upon population density (Rosenberg *et al.*, 1977), it would be advantageous for groups of spores to be dispersed to new environments to facilitate group germination and cooperative feeding (Kaiser, 2001). A second hypothesis is that spores inside mounds are better protected from environmental stresses and predation (Velicer & Hillesland, 2008, Dahl *et al.*, 2011). I took advantage of the disrupted fruiting body morphology of the ΔNR mutant to address these hypotheses and to begin to explore the role of the negative regulators for the developmental program.

To test the “dispersal-hypothesis”, I used small animals as vectors. I chose to use the fruit fly *Drosophila melanogaster* as a vector which could represent any small insect. *D. melanogaster* is not usually found associated with soil in nature and, is unlikely to be a natural vector for *M. xanthus* spore dispersal. However, *D. melanogaster* represents a model arthropod that has previously been used as representative vector to examine dispersal of spores produced by the social amoeboid *Dictyostelium discoideum* (Smith *et al.*, 2014).

To test *D. melanogaster* as a carrier to transfer *M. xanthus* cells, *M. xanthus* fruiting body formation was induced in 60 mm petri dishes in submerged culture for 120 h. After the supernatant was removed, 10 male flies of the *Drosophila melanogaster* wild type strain w^{1118} were added per plate (male individuals were chosen to avoid deposition of eggs on the plates). Flies were added to petri dish lids, plates were inverted (*D. melanogaster* demonstrates negative geotaxis (Rhodenizer *et al.*, 2008)), and flies were allowed to crawl amongst fruiting bodies for four hours at room temperature. Flies were then transferred to inverted CYE rich media plates and allowed to crawl for additional 4 h. Finally, all *D. melanogaster* individuals were removed and the plates incubated at 32 °C to allow *M. xanthus* to germinate and grow into colonies. Colonies were scored after 3-4 days.

Initial results indicated CYE rich media plates showed considerable contamination after 4 days incubation (Figure 12, A), indicating that i) flies crawled over the entire agar plate and did not avoid the moist surface, ii) transfer of bacteria (and possibly fungi) cells from fly legs to CYE medium occurred, and iii) there was no difference in mobility over the entire plate between flies coming from wild type or ΔNR mutant fruiting bodies. (Figure 12, B). To avoid growth of contaminants, CYE plates were supplemented with 10 µg/ml gentamycin for future assays- an antibiotic to which *M. xanthus* is naturally resistant (Dahl *et al.*, 2011).

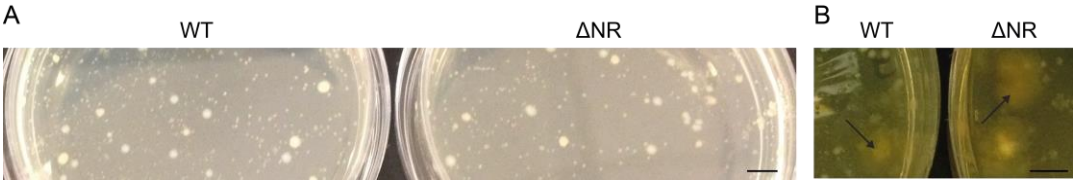

Figure 12: Dispersal of bacteria is possible by *D. melanogaster*. (A) Contamination on CYE medium after incubation with 10 male *D. melanogaster* flies which have previously crawled over *M. xanthus* fruiting bodies produced by wild type (WT) or ΔNR mutant, respectively. Scale bar 0.5 cm. **(B)** Transfer of *M. xanthus* by *D. melanogaster* was observed (arrows) for both wild type (WT) and ΔNR mutant. Scale bar 0.5 cm.

With this optimized dispersal assay for *M. xanthus* spores, using *D. melanogaster* as a model vector, I went on to address the question, if compact fruiting bodies (wild type) are dispersed more efficiently than miss-organized fruiting body structures (ΔNR mutant).

5.1.1. Redistribution of cell fates enhances dispersal by small animals

To assess transfer of fruiting bodies by *D. melanogaster*, wild type and ΔNR mutant strains were developed for five days (120 h) under submerged culture conditions and dispersal assays with *D. melanogaster* were performed as described above (section 5.1.3). Colonies formed by both strains were enumerated after three days (3 d) and seven or more days (≥ 7 d) (Figure 13, A) of germination in four biological replicates. Total colony number was determined and proportions of wild type (WT) and ΔNR mutant were calculated (Figure 13, B). After 3 d of germination, a clear trend emerged leading to the conclusion that transfer of ΔNR spores was more efficient than transfer of wild type spores, since 84 % of total colonies observed originated from this mutant, while only 16% originated from wild type spores. This trend was also observed after seven days of germination suggesting no artifact influence from differential germination rates. However, it needs to be considered that the ΔNR strain produced about 6-fold more spores than wild type did (section 5.1.2). Dispersal of ΔNR was about 5-fold more efficient over wild type. These two observations together indicate merely a minor advantage of ΔNR over wild type fruiting bodies/ spores when dispersed by *D. melanogaster*.

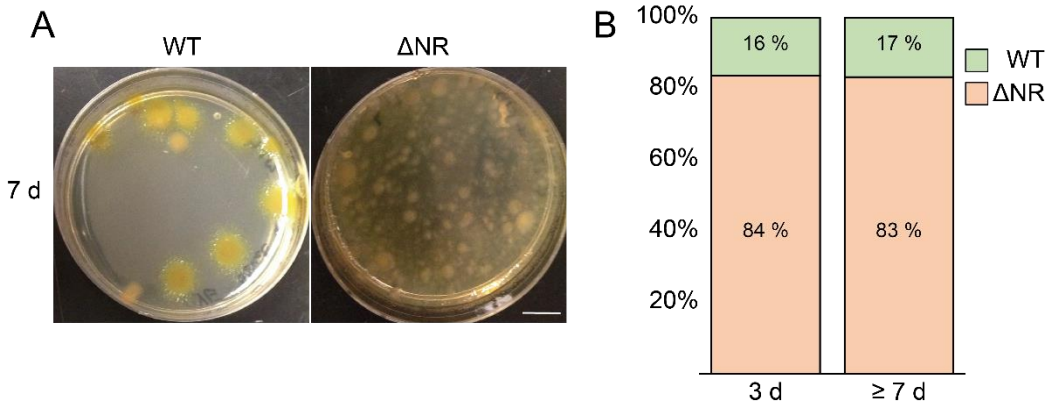

Figure 13: The ΔNR mutant is transferred more efficiently by *D. melanogaster* than the wild type. (A) *Representative plates showing M. xanthus growth on rich media after a dispersal assay. D. melanogaster* was allowed to interact with *M. xanthus* wild type (WT) or ΔNR mutant 120 h mature fruiting bodies and was then transferred to fresh CYE plates. Pictures were taken after seven days (7 d) of germination. Scale bar 1 cm. **(B)** *Quantification of transferred clones.* The majority of transferred colonies originated from ΔNR mutant spores. Colonies present after three (3d) or seven or more (≥7d) days of germination were enumerated to derive the total colony number. The percent arising from wild type (WT) or ΔNR mutant were subsequently calculated[1]. Four independent replicates were performed, 3d data consisted of four, ≥7d day data consisted of six independent biological replicates.

From this assay I was unable to distinguish whether germinating colonies originated from the transfer of fruiting bodies or from single spores / peripheral rods. Based on the sizes of *M. xanthus* fruiting bodies and *D. melanogaster* individuals it should be possible to observe whole fruiting bodies being transferred (Figure 14, A and B). To do so, the dispersal assay was conducted as described above with *M. xanthus* strains expressing mCherry under the control of the developmentally upregulated *nfsA* promoter. Fluorescence microscopy analysis of *D. melanogaster* bodies and severed legs was performed. No mCherry–labeled fruiting bodies could be observed attached to *D. melanogaster* bodies (data not shown) or legs (Figure 14, C). This suggested single spores/peripheral rods were instead dispersed by *D. melanogaster*. However, this could not definitely be shown, since microscopy at a magnification suitable for the detection of single *M. xanthus* spores was not possible due to the size of *D. melanogaster* and its autofluorescence in both mCherry and GFP channels.

[1] Strains bearing mCherry fusions exactly phenocopied their background strains and were pooled for this analysis. Hence, here "WT" refers to a pool of wild type (WT), WT *attB::*Pr_{pilA}*-mcherry* and WT *attB::*Pr_{nfsA}*-mcherry*; while ΔNR refers to a pool of ΔNR mutant, ΔNR *attB::*Pr_{pilA}*-mcherry* and ΔNR *attB::*Pr_{nfsA}*-mcherry*.

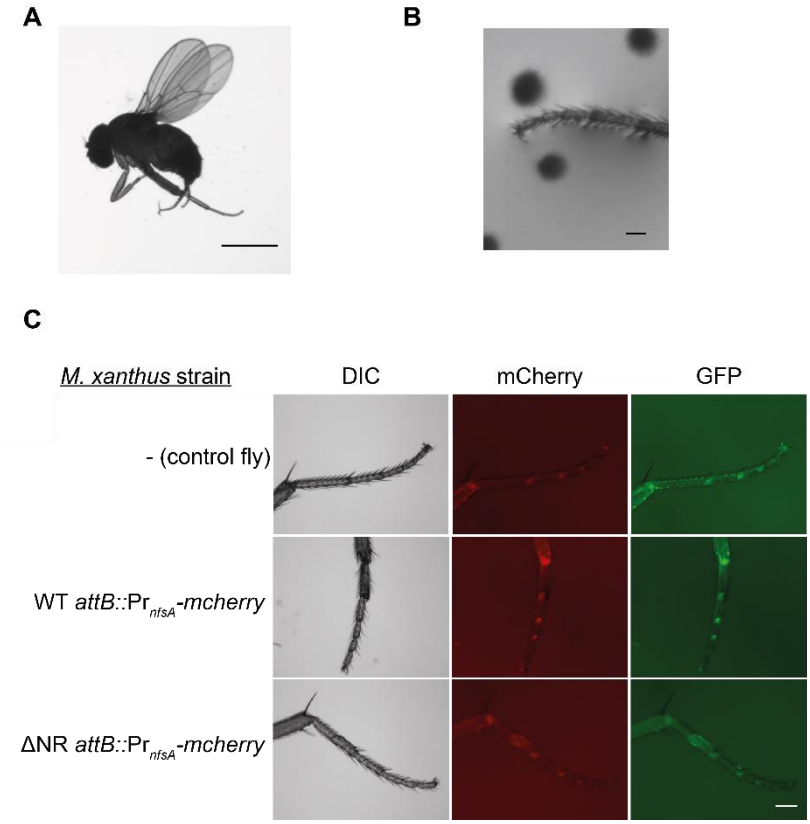

Figure 14: No *M. xanthus* fruiting bodies can be observed attached to *D. melanogaster* legs. (A) A *Drosophila melanogaster* fruit fly (w^{1118}), which was used for the dispersal assay. Scale bar 1 mm. **(B)** 120 h developed fruiting bodies of *M. xanthus* are captured next to the tip of a *D. melanogaster* leg for size reference. Scale bar 100 µm. **(C)** After a dispersal assay as described above, severed *D. melanogaster* legs were subjected to (fluorescence) microscopy. Wild type (WT) and ΔNR mutant expressing the fluorescent protein mCherry driven by the developmentally upregulated *nfsA* promoter were used. No specific fluorescence signals indicating the presence of *M. xanthus* fruiting bodies attached to *Drosophila* legs could be observed. Scale bar 100 µm.

My results indicate that formation of well-organized wild type fruiting bodies does not appreciably increase dispersal by small animals. Rather dispersal was equal to dispersal of disorganized fruiting bodies, taking into consideration that this strain produces a greater number of spores than wild type to begin with. However, taken together the production of more spores, spores outside of fruiting bodies and disorganized fruiting bodies, ΔNR mutant are 5-fold better dispersed in total numbers.

5.1.2. Well-organized fruiting bodies provide enhanced resistance to UV damage

A second hypothesis for the benefit of sporulation inside fruiting bodies is that spores are better protected from environmental insults when they are enclosed in well-organized fruiting bodies (Velicer & Hillesland, 2008). These insults could include biotic factors such as antibiotics produced by competitors and ingestion by predators, and/or abiotic factors such as UV exposure, dryness, prolonged starvation, pH extremes and heat. I tested this hypothesis using UV exposure as a representative environmental insult.

To address whether wild type *M. xanthus* fruiting body morphology was more resistant to UV stress, both wild type and ΔNR mutant were developed under submerged conditions for 120 h in 24-well plates. Fruiting bodies inside the wells were exposed to UV for 0 – 5 minutes. After UV exposure, cells from each well were harvested, aggregates were gently dispersed by mild sonication, serially diluted and 10 µl aliquots were spotted on rich CYE media. Colonies were enumerated after four days of germination.

Both wild type and ΔNR mutant formed a single dense swarm when they were not exposed to UV (0 min UV), indicating spores germinated efficiently under these harvesting conditions (Figure 15). After 0.5, 1, 2 or 5 min of UV exposure, wild type cells produced a confluent spreading colony of similar diameter. In contrast, after 0.5 and 1 min UV exposure, the ΔNR mutant produced a swarm of slightly reduced diameter, and after 2 and 5 min UV exposure very little swarm growth could be detected. This finding suggests, that spores inside a well-organized fruiting body produced by the wild type are better protected from UV insult than spores in the loosely organized flat fruiting bodies produced by the ΔNR mutant.

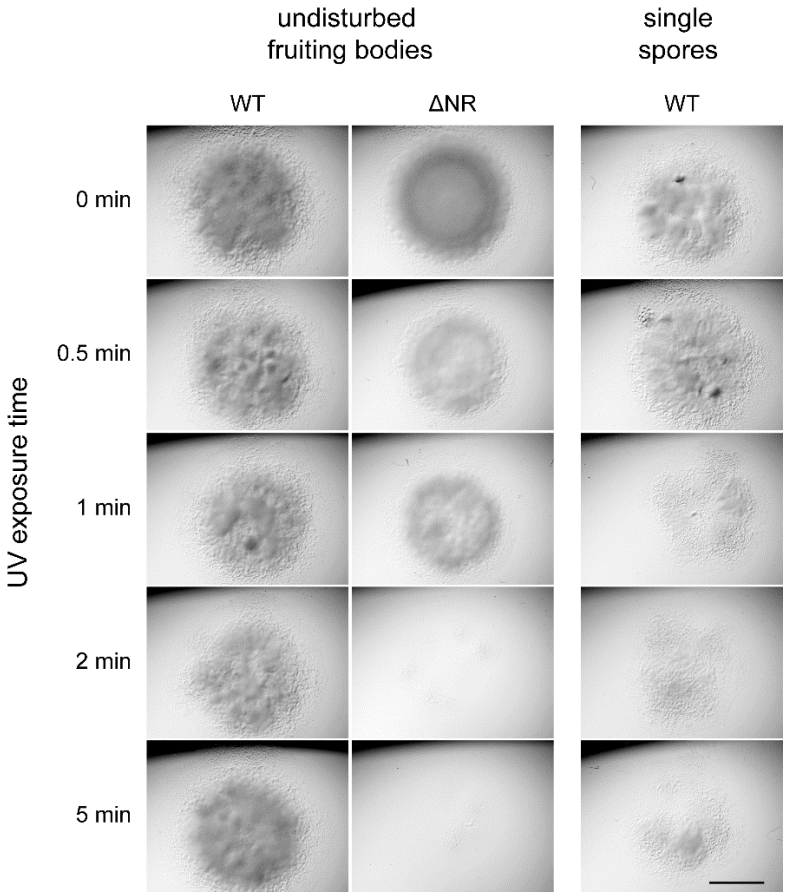

Figure 15: Well-organized fruiting bodies provide protection against UV-induced lethality. *UV resistance assay.* Wild type (WT) and ΔNR mutant were exposed to UV (254 nm, 4 Watt, 23 cm distance) for the indicated minutes, dispersed, spotted onto rich media, and incubated at 32 °C for four days to induce germination and swarm formation. Wild type fruiting bodies can survive up to 5 min UV irradiation with little reduction in swarm production. ΔNR mutant fruiting bodies are susceptible to UV-induced lethality after 2 min UV irradiation. Wild type spores which were dispersed before UV irradiation exhibited reduction in germination and failed to produce a swarming colony in WT size after 1 min of irradiation. Scale bar 5 mm.

To assess if this finding is indeed mediated by fruiting body morphology and is not accounted for by some unknown factor that gives the wild type additional UV resistance, wild type fruiting bodies were first gently dispersed by vigorous shaking in a cell homogenizer without beads (Lee *et al.*, 2011a), reseeded in liquid and exposed to UV as described above. Under these conditions, visible reduction of swarm density could be observed after 1 min or more of UV exposure. Interestingly, even after five minutes UV exposure wild type single spores were more UV resistant than spores from a ΔNR mutant fruiting body, since cell growth was observed. There might be an underlying effect of uncharacterized differences in spore coat maturation in the two strains used. Since development is severely accelerated in the ΔNR mutant, this might also affect spore coat maturation. Hence, it is possible that the wild type spore coat is more mature and provides more environmental resistance. Nevertheless, it can be concluded that packaging spores into a fruiting body gives wild type spores an increased resistance towards UV exposure.

Taken together, these results suggest that packaging of *M. xanthus* spores into well-organized fruiting bodies provides protection from environmental insults such as UV exposure, but impedes dispersal by small vectors. Since the negative regulator genes encode signaling systems, this raises the intriguing possibility that NR regulator systems may have evolved to allow *M. xanthus* to tune its spore packaging mechanism to environmental cues. The signals to which these systems respond are currently unknown, but it has been recently determined that each signaling system converges to affect accumulation of the major transcriptional regulator of development, MrpC. In a next step, I set out to investigate whether MrpC is crucial for the developmental phenotype of the ΔNR mutant. I also wanted to determine whether over-accumulation of MrpC is sufficient to induce ridge-like misshaped fruiting bodies.

5.2. MrpC accumulation is crucial for development of ΔNR mutant

MrpC is a key transcriptional regulator which is essential for both aggregation and sporulation during *M. xanthus* development (Sun & Shi, 2001b). We found this protein to be over-accumulated in the ΔNR mutant which develops in an accelerated manner into miss-shaped fruiting bodies, forming a larger number of spores than wild type ((Lee, 2009) and this study, section 5.1.2). In the past, several mutants that can (partially) bypass various developmental key genes have been reported, resulting in versatile developmental phenotypes (Rhie & Shimkets, 1989, Dunmire *et al.*, 1999, Hager *et al.*, 2001, Cusick *et al.*, 2002, Tse & Gill, 2002, Rasmussen *et al.*, 2005, Higgs *et al.*, 2008, Cusick *et al.*, 2015). To ensure that the developmental phenotype I observed in the ΔNR mutant is caused by the over-accumulation of MrpC and the strain is not able to bypass the MrpC regulatory pathway, I wanted to create an in-frame deletion mutant of *mrpC* in the ΔNR background and examine the developmental phenotype in submerged culture conditions. Due to technical difficulties, I was unable to delete *mrpC* from ΔNR. Hence, I made use of a previously described mutant Δ*esp* Δ*red todK::tet* (Lee, 2009), which differs from ΔNR only in

carrying a *todK* insertion mutant instead of an in-frame deletion. Phenotypes of this mutant and ΔNR are indistinguishable (data not shown). As previously published, deletion of *mrpC* from the wild type results in a non-developing phenotype ((Sun & Shi, 2001b) and Figure 16). Also deletion of *mrpC* in the Δ*esp* Δ*red todK::tet* background abolishes development completely, confirming that the MrpC pathway cannot be bypassed in this mutant.

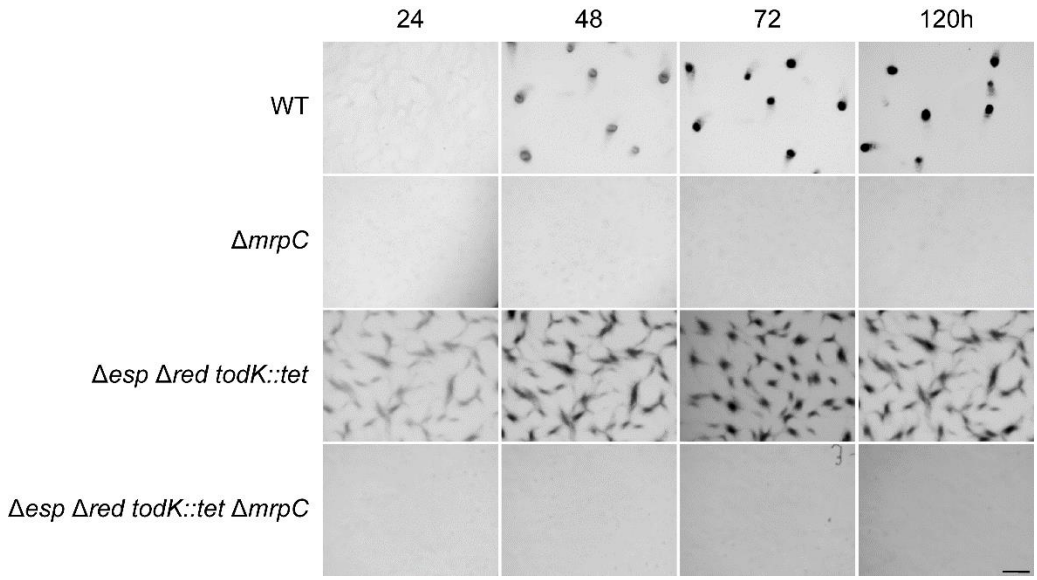

Figure 16: Deletion of *mrpC* abolishes development in ΔNR mutant. *Starvation assay.* Strains were starved under submerged conditions in a 24-well culture dish. Pictures were recorded at the indicated time points using a stereomicroscope. WT: wild type, Δ*red:* Δ*red(CDEF)*; Δ*esp:* Δ*espA* Δ*espC*; Scale bar 500 µm.

In a previous study, it was shown that deletion of *mrpC* and re-introduction at a secondary site in the genome under the control of the *pilA*-promoter does not lead to complementation of the Δ*mrpC* mutant phenotype (Bhardwaj, 2013). However, it could be shown in this non-developing strain that *mrpC* mRNA was produced (although at a lower level than in the wild type situation) while the MrpC protein did not accumulate in the population at 24 h of development (Bhardwaj, 2013). Interestingly, in an *espAC* deletion mutant (Δ*espA* Δ*espC*), deletion of *mrpC* and introduction of Pr_{pilA}-*mrpC* in the attachment site led to partial complementation of the non-developing phenotype and low levels of MrpC protein could be detected in immunoblot analysis (data not shown, P.T. McLaughlin, M.M. Glaser and P.I. Higgs; unpublished data).

In this study, I wanted to address whether total complementation of a Δ*mrpC* phenotype or a phenotype mimicking the ΔNR phenotype could be achieved when additional negative regulators were deleted and MrpC was re-introduced under the control of the constitutively active *pilA* promoter. I took advantage of this mutant to test our hypothesis that miss-accumulation of the developmental key transcriptional regulator MrpC is sufficient to induce a negative regulator deletion mutant-like developmental phenotype. To express *mrpC* artificially, I used the well-established promoter of the *pilA* gene, which codes for pilin, the structural key component of the *M. xanthus* type-four-pili machinery (Wu & Kaiser, 1995). The *pilA* promoter (Pr_{pilA}) has been shown in the alternative wild type strain DK1622 to be constitutively active

during vegetative growth and in the earlier stages of development, however expression from this promoter decreases slightly over the duration of a developmental time course (Wu & Kaiser, 1997).

Mutants lacking two (Δ*esp* Δ*red*) or three (Δ*esp* Δ*red todK*) negative regulator systems developed earlier than the wild type, as described previously (Lee, 2009). Cells formed aggregates before 24 h of starvation induced development (Figure 17, A). Deletion of the *mrpC* gene resulted complete abortion of development in all backgrounds (Figure 16 and data not shown). Introducing *mrpC* under the control of the *pilA* promoter at a secondary site of the genome led to partial complementation of the phenotype (Figure 17, A). A very faint image of the parental phenotypes could be observed in both strains: i) numerous faint mounds in Δ*esp* Δ*red* Δ*mrpC attB::* Pr_{pilA}-*mrpC* and ii) faint ridge-like structures in Δ*esp* Δ*red todK::tet* Δ*mrpC attB::* Pr_{pilA}-*mrpC*. Aggregation occurred between 24 and 48 h of development and aggregates of both strains did not mature into fruiting bodies but instead disintegrated during prolonged starvation until 120 h.

Investigation of MrpC protein accumulation by immunoblot analysis showed a low level of MrpC at the beginning of development in wild type cells and the known increase at 24 h (Figure 17, B). In the Δ*mrpC attB::* Pr_{pilA}-*mrpC* strain, a low level of MrpC was observed at 0 h of development while no MrpC could be detected by 24 h, consistent with previous reports (Figure 17, B; (Bhardwaj, 2013)). A strain with deletions of two negative regulator systems (Δ*esp* Δ*red*) showed MrpC highly accumulated at 24 h of development. A strain lacking *todK* in addition accumulated MrpC to even higher levels. Interestingly, when *mrpC* is merely expressed by the *pilA* promoter at a secondary site in the genome in both strains, only a minor accumulation of MrpC was observed. The level of MrpC accumulation was independent of the number of negative regulator systems that were missing.

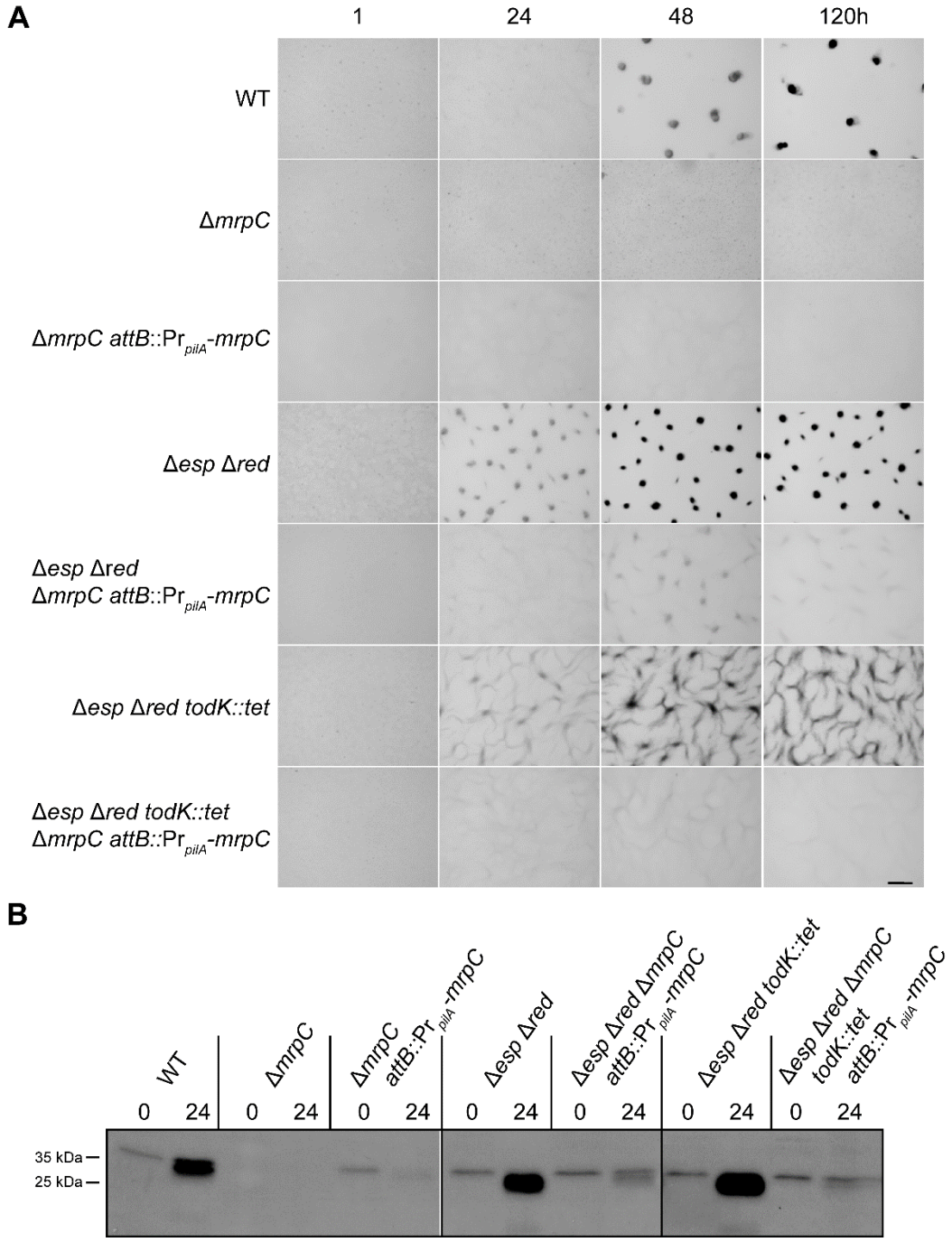

Figure 17: Deletion of combinations of negative regulators does not lead to complementation of a Δ*mrpC* phenotype by Pr*pilA*-*mrpC* in the *attB* site or high MrpC protein accumulation. (A) *Starvation assay.* Strains were subjected to starvation in submerged culture and developmental stages were recorded using a stereomicroscope at the indicated time points. At 120 h development was considered completed. Scale bar 500 µm. **(B)** *Immunoblot analysis of MrpC protein accumulation.* Development was induced as described above and the total population of cells was harvested at 0 and 24 h of starvation. Cells were lysed and 10 µg total protein per sample were analyzed in an immunoblot probed with α-MrpC polyclonal antibody. MrpC 27 kDa, WT: wild type, Δ*esp*: Δ*espA* Δ*espC*, Δ*red*: Δ*red(CDEF)*.

To gain further insight in how MrpC accumulation is regulated by the signaling modules investigated in this study, it is crucial to understand how they are connected to MrpC on a molecular level. In the following sections, I set out to examine how Red and TodK signaling systems could be connected to accumulation of MrpC.

5.3. The Red signaling system connects to an eukaryotic-like kinase cascade which leads to MrpC phosphorylation

The *esp*-signaling module affects MrpC accumulation via directed protein degradation (Schramm *et al.*, 2012), the link between the other signaling systems and MrpC protein accumulation remains unknown. A particularly interesting aspect is how RedF mediates the output of the Red signaling module. As a single domain response regulator, its mode of action is most likely regulation via protein-protein interactions that differ depending on phosphorylation induced conformational changes of the RedF protein. In an earlier study, a yeast two-hybrid screen was performed using RedF as bait protein (X. Mei and P.I. Higgs; unpublished data). Here, the kinase associated protein C (KapC) was found to be a potential interaction partner. Polyclonal antibodies were generated against KapC antigen and were shown to function well in immunoblot analysis (X. Mei, P. Mann and P.I. Higgs; unpublished data; Figure 18, left).

I set out to validate the possible interaction of KapC and RedF by performing *in vitro* pull-down experiments coupled with immunoblot analysis. Recombinant RedF was overexpressed and purified from *E. coli* (Jagadeesan *et al.*, 2009). Since RedF was expressed fused to a thioredoxin-hexa histidine-tag (Trx-His_6), this tag was expressed and purified itself in the same manner and used as a negative control in the pull-down-experiment. Genetic evidence indicated that RedF is phosphorylated in early development and likely in vegetative cells (Jagadeesan *et al.*, 2009). For this reason, RedF was autophosphorylated using acetyl-phosphate (Jagadeesan *et al.*, 2009). The control tag was treated in the same manner. Lysate of vegetative *M. xanthus* cells was used to capture prey proteins. I could show that Trx-His_6-RedF starts to elute from NiNTA beads at 50 mM imidazole (data not shown), so this concentration was used for the first elution step and concentration was increased in two steps to 150 mM and 300 mM, respectively. Immunoblot analysis probed with α-KapC-polyclonal antibodies was performed with the eluates retrieved from pull-downs using Trx-His_6-RedF as bait (Figure 18, middle panel) as well as Trx-His_6 tag alone as a negative control bait (Figure 18, right panel).

This analysis revealed that KapC could be pulled out of cell lysates from *M. xanthus* vegetative cells using Trx-His_6-RedF~P as bait but was not present in the negative control eluates. KapC was not found in its full length form, which was shown to run at 125 kDa (Figure 18, left) but was found in a dominant band running at 80 kDa. This band likely corresponded to a processed or degraded form of KapC. However, these degradation products did not result in a smear of degraded protein but appeared in three distinct bands that ran at the molecular masses of ~ 65 and 40-45 kDa (Figure 18, middle). Although protease inhibitor was present at all times during the experimental procedure, the degradation of KapC in the pull down analysis was likely due to left protease activity during the long but necessary incubation steps, and did not occur when lysates were quickly produced and denatured as during the regular sample preparation for wild type and Δ*kapC* lysates (Figure 18, left).

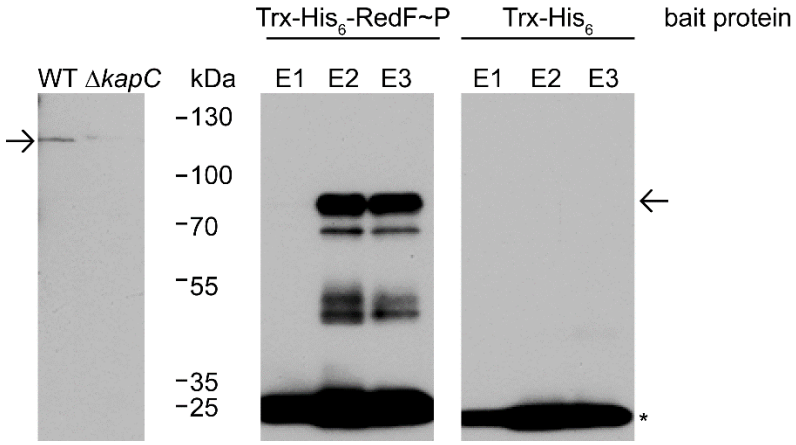

Figure 18: KapC can be pulled out of vegetative *M. xanthus* lysates using phosphorylated RedF (RedF~P) as bait. *In vitro Pull-down assay.* Cell lysate prepared from vegetative *M. xanthus* cells was incubated with autophosphorylated Trx-His$_6$-RedF~P and Trx-His$_6$ (as a negative control), respectively. Ni-NTA coated beads were used to extract formed bait-prey complexes from the lysate and complexes were eluted using a three step gradient of imidazole. Eluates were separated using SDS-PAGE, subjected to immunoblot analysis using an α-KapC-polyclonal antibody. Wild type (WT) and Δ*kapC* lysates were probed as controls. Full length KapC (calculated mass 124.4 kDa) is marked with a solid arrow. The asterisk marks a cross-reactive band present in all elution samples. E1: elution step one with 50 mM imidazole; E2: elution step two with 150 mM imidazole; E3: elution step three with 300 mM imidazole.

The finding that KapC protein can be captured using RedF~P as bait confirms the interactions suggested by a yeast two-hybrid-screen (X. Mei and P.I. Higgs, unpublished). With the RedF~P – KapC interaction, the Red system could be linked to the modulation of the phosphorylation state of MrpC via a serine/threonine kinase cascade (see section 3.4.3.2). However, this is just a starting point in understanding this network and further genetic and biochemical work is fundamentally needed to verify and proof the network proposed in earlier literature and this study.

5.4. TodK is a bifunctional histidine protein kinase that negatively regulates developmental progression in *Myxococcus xanthus*

Another negative regulator that appears to be necessary for appropriate MrpC accumulation is the putative histidine protein kinase TodK (Lee, 2009). To understand how the negative regulators may influence MrpC accumulation, it is necessary to identify the signaling output state of each system. We have previously been able to identify the output state of the Esp and Red systems by a systematic analysis of the signal flow and output state in each system (Jagadeesan *et al.*, 2009, Schramm *et al.*, 2012).

So far, only the developmental phenotype as well as the expression and protein accumulation pattern of some of the important developmental key genes in a *todK* minus strain were studied (Rasmussen & Sogaard-Andersen, 2003, Lee, 2009). The importance of TodK protein domains remained unknown. Here, I report on the genetic and biochemical characterization of this gene and its protein product *in vivo* and *in vitro*, as well as the investigation of two response regulators that had the potential to mediate the output of the TodK signaling module.

5.4.1. Investigation of *todK in vivo* at the native locus

5.4.1.1 Deletion of *todK* leads to accelerated development

TodK has been the subject of a previous study performed in the wild type strain DK1622 where it was found that deletion of *todK* led to accelerated development upon starvation (Rasmussen & Sogaard-Andersen, 2003). The wild type strain used in this study, DZ2, develops generally more slowly than DK1622, providing the advantage of more time resolution during the developmental process. Hence, I created a deletion mutant of *todK* (MXAN_6955) in DZ2, using the pAAR138 plasmid from Rasmussen *et al.* (Rasmussen & Sogaard-Andersen, 2003). This plasmid was used to delete the central part of *todK* (Figure 19) and the created mutant was investigated to study the phenotype upon starvation in detail.

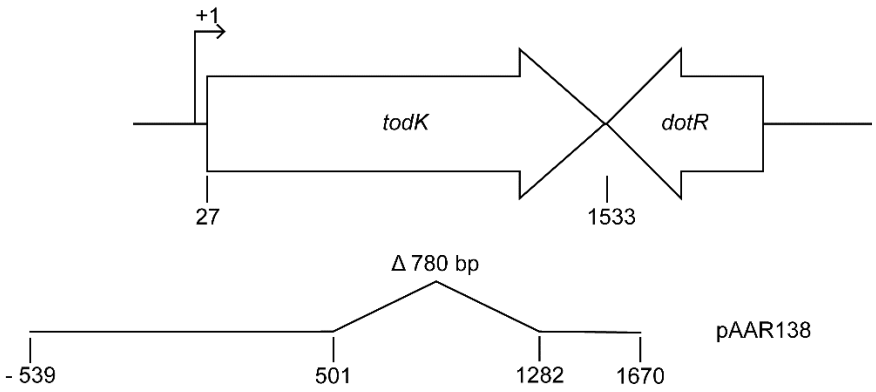

Figure 19: Schematic map of the *todK* genome region (top) and the plasmid used to generate Δ*todK* mutant (bottom). Figure modified from (Rasmussen & Sogaard-Andersen, 2003)**.**

Under starvation conditions (CF agar), a Δ*todK* strain aggregated at least 6 h earlier than the wild type (Figure 20, A). It could also be observed that a *todK* deletion mutant showed a very distinctive colony and fruiting body morphology. During the formation of mounds, it became apparent that the Δ*todK* strain formed a mound free ring near the periphery of the developing colony (Figure 20, A, closed arrow heads), followed by a dense ring of mounds/ fruiting bodies, creating a distinct colony border. When fruiting bodies were observed with a higher magnification, it could be noted that the Δ*todK* mutant formed aberrantly shaped fruiting bodies which did not form distinct borders, compared to the well-organized, round fruiting bodies like the wild type DZ2. Also, loosely packed accumulations of presumably spores could be found between fruiting bodies of the Δ*todK* mutant (Figure 20, A, open arrow heads).

Under alternate starvation conditions, in submerged culture, a Δ*todK* strain formed mounds at the same time as the wild type DZ2, between 24 and 30 h after onset of starvation (Figure 20, B). This phenotype has been reported previously for an insertion mutant of *todK* in DZ2 (Lee, 2009). In the earlier study, it was shown, that although aggregation timing was not affected in an insertion mutant of *todK*, at 48 h of starvation a *todK* mutant had produced twice the amount of spores as the wild type. This correlated with darkening of the obtained fruiting bodies. In this study, fruiting bodies produced by the Δ*todK* strain darkened at the same time (between 30 and 48 h), suggesting early sporulation took place as well. Lastly, it should be noted that the Δ*todK* strain produced more numerous and smaller fruiting bodies in submerged culture conditions than the wild type, DZ2. This phenomenon has been observed before in the *todK* insertion mutant (Lee, 2009)

To examine whether the MrpC accumulation was also premature in the Δ*todK* strain, I subjected this strain, and the wild type control, to α-MrpC immunoblot analysis (Figure 20, C). MrpC levels were low in both wild type and Δ*todK* under vegetative conditions (0 h), and remained low in early stages of development (0 – 18 h). In the Δ*todK* strain, MrpC accumulation peaked at 24 h of starvation, six hours earlier than in the corresponding wild type. The MrpC level remained this high in Δ*todK* at 30 h of development, which is when MrpC levels reached a maximum in the wild type population. In both strains studied here, MrpC levels decreased slightly after 30 h of starvation.

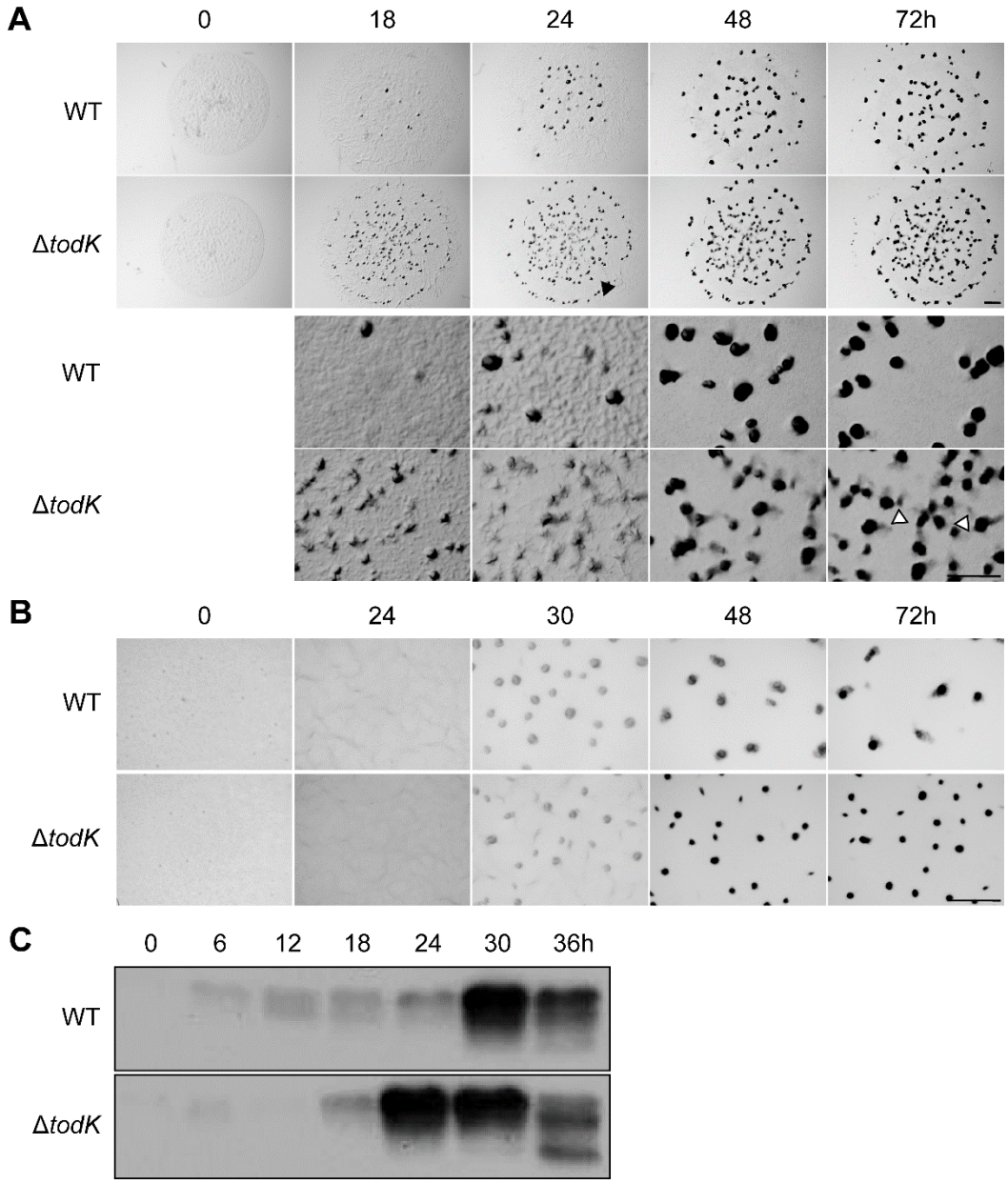

Figure 20: In-frame deletion of *todK* leads to early development and miss-accumulation of MrpC. (A) *Starvation assay on CF agar plates.* Strains were spotted on CF agar (10 µl at OD_{550nm} 7) and starvation induced development was observed for 72 h. Pictures were recorded at the indicated time points using a stereomicroscope. Colony as well as fruiting body morphology are depicted. Scale bars 1 mm. **(B)** *Starvation assay under submerged conditions.* Strains were subjected to starvation in submerged culture and developmental stages were recorded using a stereomicroscope at the indicated time points. Scale bar: 1 mm. **(C)** *Immunoblot analysis of MrpC protein accumulation.* Development was induced as described in B and the total population of cells was harvested at the indicated time points of starvation. Cells were lysed and 10 µg total protein per sample were analyzed in an immunoblot probed with α-MrpC polyclonal antibody. MrpC 27 kDa, WT: wild type.

These results showed that the newly generated deletion strain of the central part of the *todK* gene phenotypically mimics the formerly used insertion mutant of this gene. I therefore proceeded to analyze *todK*/TodK genetically and biochemically in an attempt to understand how it negatively regulates *M. xanthus* development.

5.4.1.2 TodK accumulates in vegetative and developing cell populations

In an earlier study, it has been shown by quantitative PCR that *todK* is expressed in vegetative cells and during development in the wild type strain DZ2 (Lee, 2009). To further understand the role of TodK during *M. xanthus* development, it was important to examine at which time the protein accumulated in the cells. To address this, custom antibodies were generated in rabbits (by Eurogentec; Seraign, Belgium), using Trx-His_6-TodK inclusion bodies as antigen (B. Lee and P.I. Higgs; unpublished data). Initial testing of the received antisera showed many non-specific bands and little specific TodK signal. Several measures were taken to improve signal specificity and target detection including i) purification of TodK antibodies from the sera via affinity purification using Trx-His_6-TodK as bait protein; ii) purified Trx-tag protein, as well as lysate from vegetative Δ*todK* cells was spiked into the antibody solution during incubation; iii) incubation was performed at 4 °C overnight, enhancing antibody stringency; and, iv) modification of SDS-PAGE conditions improved band separation (data not shown). All these measures improved immunoblot quality greatly, however, elimination of one strong cross-reactive band very close in size to TodK protein was not successful (Figure 21). It could be shown repeatedly that TodK accumulated in the cell population under vegetative conditions and up to 24 h of development under submerged culture conditions (Figure 21). From 30 h of development on TodK protein was no longer detectable.

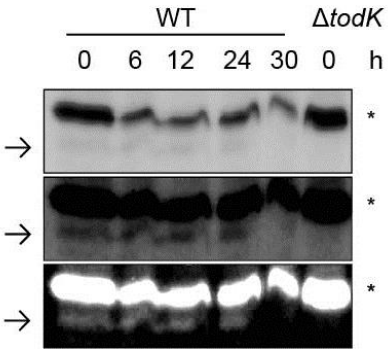

Figure 21: TodK protein accumulates in vegetative and developing cells up to 24 h. *Immunoblot analysis.* Total cell populations of developing wild type (DZ2) cells were starved in submerged culture and harvested at the indicated time points. Cells were lysed and 10 ug total protein was analyzed by immunoblot probed with α-TodK polyclonal antibody. In the top panel, a strong cross reactive band is marked with an asterisk (*) and the fainter band of specific TodK signal is marked with an arrow (→). The TodK specific band was visually amplified by changing contrast and levels in the lower two panels. TodK 57 kDa.

The very low detection of TodK by immunoblot had two possible causes, a) the antibodies detected TodK with very low specificity or b) TodK is present at low levels in the total population. A specificity test was performed using a dilution series of Trx-His_6-TodK protein. It could be shown that the antibody detects TodK protein to a concentration of 32 pg (data not shown), which indicated a very high affinity of this antibody to its antigen. Hence, I hypothesize that TodK was either present at a very low level in every cell of the starving population, or only accumulated in a small subpopulation (e.g. one specific cell fate). Attempts to discriminate between these two possibilities by tracing *todK* gene expression with a reporter protein using fluorescent microscopy were not successful to date but remain a very intriguing aspect for further

investigation. It could further be attempted to separate cell populations (described in (O'Connor & Zusman, 1991a, Lee *et al.*, 2012)) and probe them with α-TodK antibodies. By loading equal proportion of proteins, the peripheral rod population would be enriched in this assay and TodK could potentially be better detected than in total population, if the hypothesis was correct.

5.4.1.3 TodK might be a bifunctional histidine protein kinase and phosphatase

To gain further insight in how TodK regulates developmental progression, I needed to understand how it functions in cell signaling. SMART (Schultz *et al.*, 1998, Letunic *et al.*, 2015) analysis indicated that TodK consists of two PAS domains and a histidine kinase domain (Figure 22, A). This domain design resembled the paradigm domain architecture of a histidine protein kinase whose activity is modulated by one or both input domain(s).

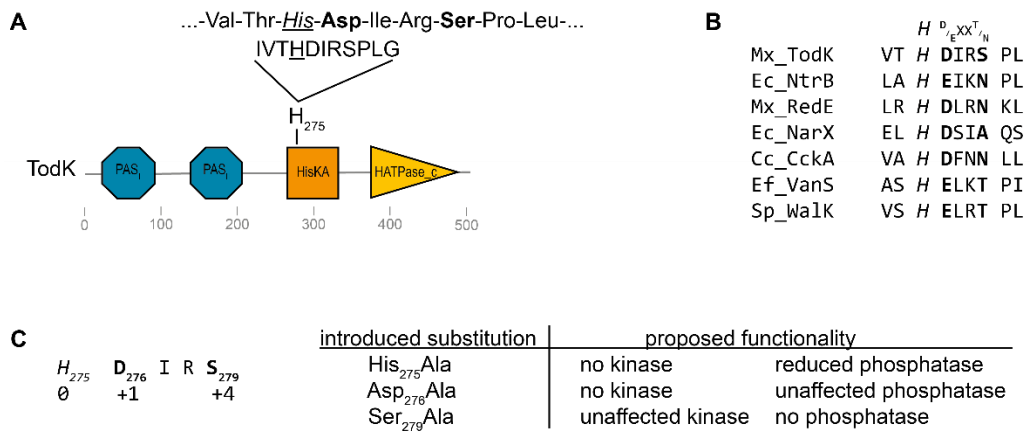

Figure 22: Schematic visualization of TodK domain structure as well as kinase motif analysis. (A) TodK is a 501 aa protein, consisting of two PAS domains followed by the typical motifs of a histidine protein kinase: a HisKA and a HATPase_c domain (SMART (Schultz *et al.*, 1998, Letunic *et al.*, 2015)). The potential site of phosphorylation is the invariant histidine at position 275. **(B)** Sequence alignment of the TodK kinase motif. The proposed motif of a bifunctional kinase/phosphatase protein is depicted at the top. TodK (Mx_TodK) was aligned with known bifunctional HPKs. This alignment indicated TodK might be either bifunctional or a dedicated phosphatase. Mx: *M. xanthus*, Ec: *E. coli*, Cc: *C. crescentus*, Ef: *Enterococcus faecium,* Sp: *Streptococcus pneumonia.* **(C)** TodK kinase/phosphatase motif and generated single amino acid substitutions *in vivo* with their proposed protein functionality.

Close examination of the kinase motif in TodK by sequence alignments with well characterized histidine protein kinases (Figure 22, B), led me to hypothesize that TodK might have phosphatase activity in addition to kinase activity. For both HPK subfamilies (HisKA and HisKA_3), phosphatase activity has been described as additional function (Huynh *et al.*, 2010). The sequence motif of TodK (HDIRS) did not resemble the exact proposed motif of a bifunctional protein, yet was similar enough to be a promising candidate. Based on this motif, TodK can be grouped within the HisKA subfamily of histidine protein kinases. It has been published that mutations in the invariant histidine abolished kinase function completely (K^-), while phosphatase activity can be affected to some extent as well ($P^{\pm}$) (Hsing & Silhavy, 1997, Huynh *et al.*, 2010, Willett & Kirby, 2012). To abolish only kinase activity and leave phosphatase

activity unaffected, mutations in the histidine +1 position have been made resulting in a K^-/P^+ phenotype (Willett & Kirby, 2012). For the reverse effect creating a protein with unaffected kinase functionality but no phosphatase activity (K^+/P^-), mutations at position histidine +4 were previously made (Huynh *et al.*, 2010, Willett & Kirby, 2012). To elucidate if TodK possessed kinase and/or phosphatase activity *in vivo*, several single amino acid substitutions in these proposed activity-critical residues were generated (Figure 22, C).

To analyze *in vivo* if TodK possessed kinase and/or phosphatase activity, single amino acid substitutions were introduced at the native locus. The codon for this substitution was chosen based on the most frequently used codon encoding this amino acid in *M. xanthus* (Nakamura *et al.*, 2000). Development was studied using two established starvation assays: on CF agar surface (Figure 23) and under submerged culture conditions (Figure 24). On CF agar plates a mutant with the disrupted kinase motif ($TodK_{H275A}$) showed early aggregation, yet not as early as the deletion mutant. Also, the characteristic fruiting body free ring around the developed colony was not as distinct as it was in the Δ*todK* strain (Figure 23). Fruiting body morphology was affected in the same way as with Δ*todK*. It was reported previously that amino acid substitutions of the invariant histidine sometimes not only affect kinase activity of a bifunctional protein but also reduces phosphatase activity (Huynh *et al.*, 2010, Willett & Kirby, 2012). This could potentially lead to a mixed phenotype. To better distinguish between the two potential activities of TodK, additional mutants were generated in amino acid positions reported to solely disrupt kinase ($TodK_{D276A}$) or phosphatase activity ($TodK_{S279A}$), respectively (see Figure 22). Surprisingly, both substitutions led to the same phenotype on CF starvation plates: early aggregation (as early as the deletion); a clear, fruiting body free ring around the developed colony and small, miss-shaped fruiting bodies (Figure 23). This was a first indication for a model in which both kinase and phosphatase activity of TodK were equally important to negatively regulate developmental progression in the wild type situation. Another possible explanation for these phenotypes was that the mutant versions of TodK were not stable in the cell and became degraded, leading to a deletion situation on protein level and the corresponding phenotype. Due to the low concentration of native TodK in the population (see section 5.4.1.2), examination of protein levels was not possible here. However, experiments with TodK mutant proteins expressed from a different promoter indicated that the mutant versions of TodK were stable in the cell (see section 5.4.2.2).

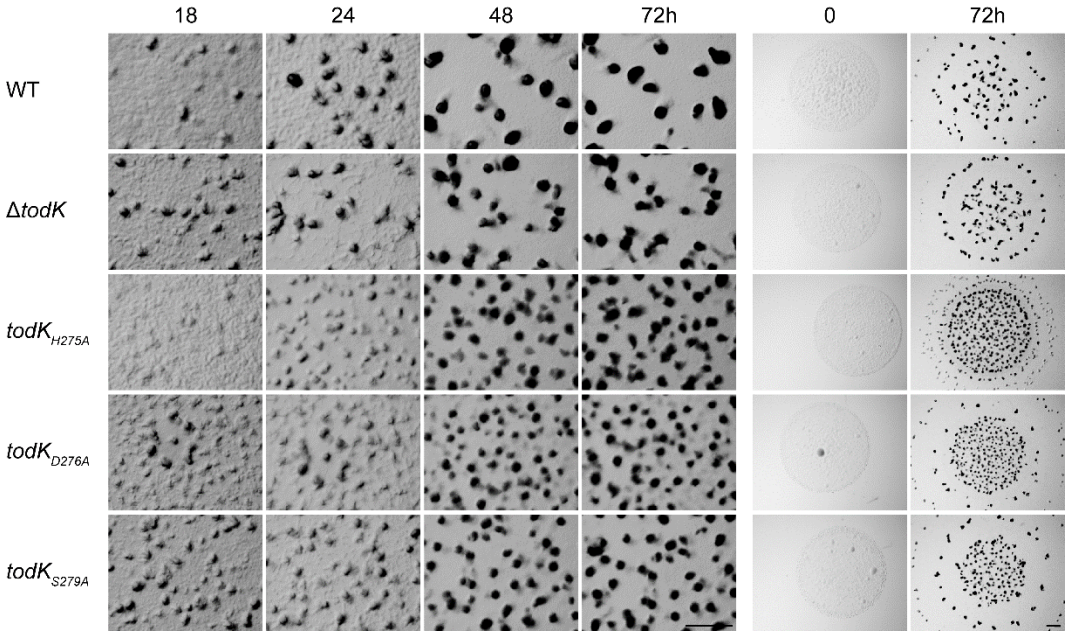

Figure 23: All strains carrying a TodK point mutation develop early on CF agar plates. *Starvation assay.* Logarithmically growing cells were spotted at $OD_{550\,nm}$ 7 on nutrient limited (CF) agar plates. Pictures were recorded at the indicated time points using a stereomicroscope. Left panel shows fruiting body morphology over the time course, right panel shows colony morphology of spotted (0 h) and developed (72 h) colony. WT: wild type, $TodK_{XnnnA}$: TodK with a single amino acid substitution of amino acid X at position nnn to alanine (A) at the native locus. Scale bars 1 mm.

When the strains described above were developed under submerged culture (Figure 24), cells expressing *todK*$_{H275A}$ showed aggregates after 18 h, at the same time as wild type and Δ*todK* mutant. However, the fruiting bodies of this mutant did not darken at the same speed as observed in the deletion mutant, suggesting sporulation might not happen as rapidly. Interestingly, this mutant strain exhibits more numerous fruiting bodies than both wild type and deletion mutant. Nevertheless, the fruiting body population consists of regular size and smaller fruiting bodies as observed for the *todK* deletion mutant. As described above in detail, a mutation at this position might, in addition to abolished kinase functionality, also have reduced phosphatase activity (given that the native version of the protein possessed both these functions). To distinguish between the roles of putative kinase and phosphatase activity of TodK, two additional mutant strains have been investigated: $TodK_{D276A}$ (predicted to abolish only kinase activity, K^-/P^+) and $TodK_{S279A}$ (predicted to only eliminate phosphatase activity, K^+/P^-; as per Figure 22). Under submerged culture conditions, both mutants exhibited the same aggregation timing as the wild type. Both strains produced regular sized and small fruiting bodies roughly at the same frequency as the deletion strain. However, $TodK_{S279A}$ produced less fruiting bodies overall.

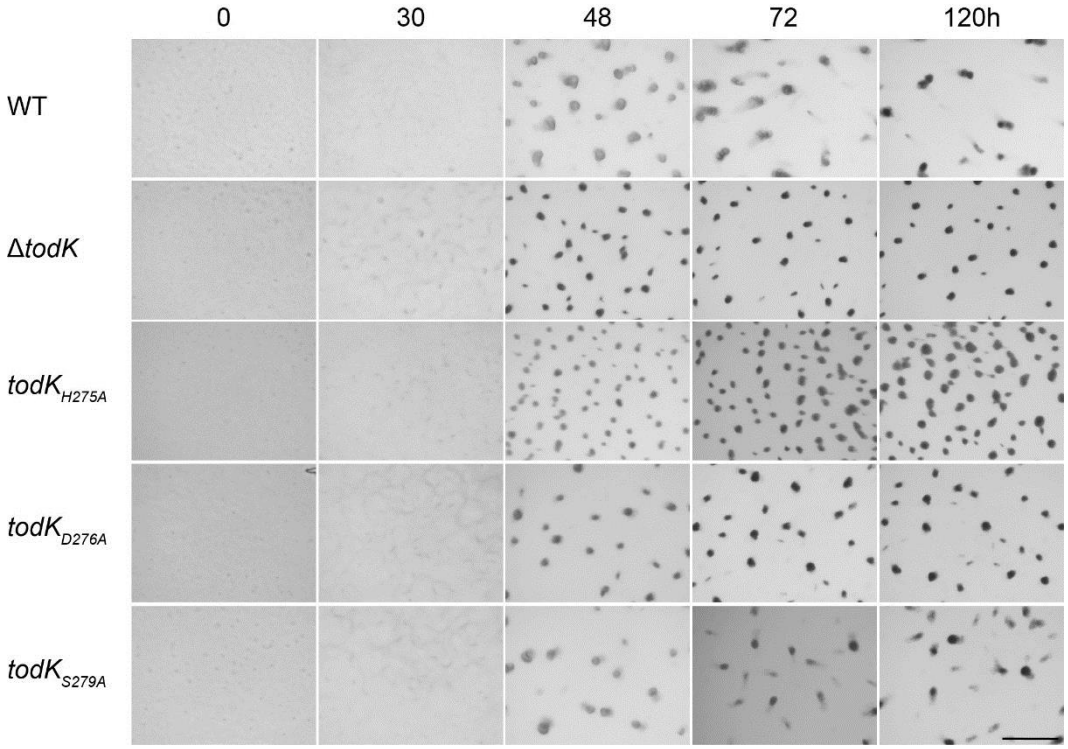

Figure 24: TodK point mutants aggregate at wild type timing under submerged culture conditions. *Starvation assay.* Strains were starved under submerged culture conditions and pictures were taken at the indicated time points after onset of starvation using a stereomicroscope. WT: wild type, $TodK_{XnnnA}$: TodK with a single amino acid substitution of amino acid X at position nnn to alanine (A) integrated at the native locus, scale bar 1 mm.

These findings suggested that TodK had both kinase and phosphatase activity *in vivo* and both activities seemed to be necessary to negatively regulate development. To investigate the effect of TodK and its various mutant versions on development when TodK expression is forced by a promoter to be presumably higher and in every cell fate, I set out to introduce all constructs under the control of the *pilA* promoter at a secondary genome site.

5.4.2. *todK* expression forced from the *pilA* promoter

As described previously (section 5.2), the strong and presumably constitutively active *pilA* promoter is a powerful tool to express proteins independently from developmental timing or cell fate. I took advantage of this promoter to express all previously described (section 5.4.1.3) versions of TodK: the native form as well as the three proteins with expected altered kinase or phosphatase activity based on single amino acid exchanges H275A, D276A and S279A (for details see Figure 22). The generated constructs were introduced into the phage attachment site Mx8 to complement the *todK* deletion strain.

5.4.2.1 Developmental progression is severely altered when *todK* is expressed from the *pilA* promoter

Cells of the generated strains were starved on CF nutrient limiting agar plates (Figure 25). The two control strains (wild type and Δ*todK*) developed as previously observed and described. The strain expressing $todK_{WT}$ driven by the *pilA* promoter formed aggregates at 48 h after onset of starvation. This was 24 h later than the wild type and 30 h later than the Δ*todK* strain (Figure 25, A).

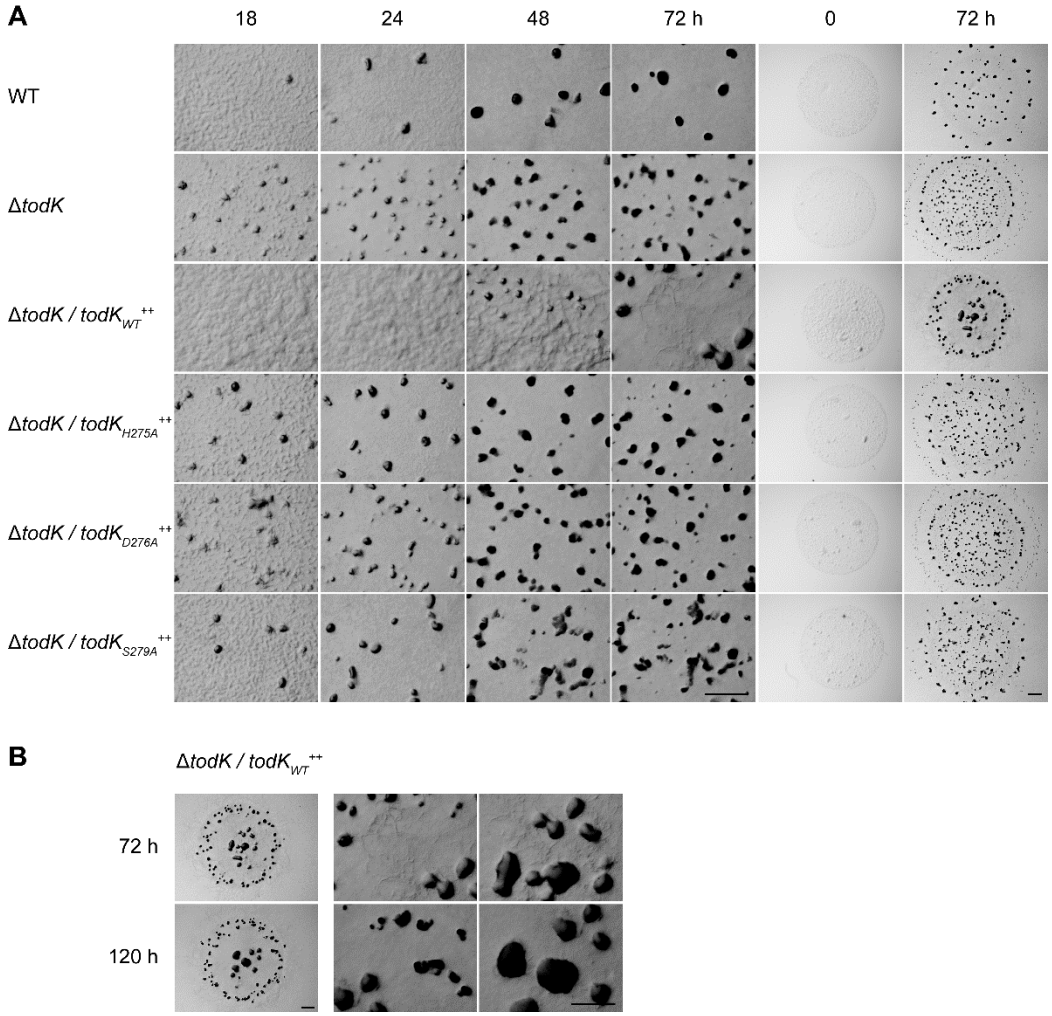

Figure 25: Development of strains expressing versions of *todK* from the *pilA*-promoter is analyzed on CF starvation plates. *Starvation assay.* **(A)** Vegetatively growing strains were harvested, 10 µl spots of $OD_{550\ nm}$ 7 were placed on CF nutrient limiting agar plates and were incubated at 32 °C. Pictures were taken at the indicated time points. **(B)** Fruiting bodies produced by Δ*todK*/$todK_{WT}^{++}$ after prolonged starvation (72 and 120 h). Complemented strains, expressing versions of *todK* under the control of the *pilA* promoter (Pr_{pilA}) from the Mx8 phage attachment site (*attB*) in the *M. xanthus* genome, were given the following designations: Δ*todK*/$todK_{WT}^{++}$ (Δ*todK attB*::Pr_{pilA}-$todK_{WT}$), Δ*todK*/$todK_{H275A}^{++}$ (Δ*todK attB*::Pr_{pilA}-$todK_{H275A}^{++}$), Δ*todK*/$todK_{D276A}^{++}$ (Δ*todK attB*::Pr_{pilA}-$todKD_{276A}$), Δ*todK*/$todK_{S279A}^{++}$ (Δ*todK attB*::Pr_{pilA}-$todK_{S279A}$); $^{++}$ indicates the proteins were not present at native levels but were over-produced driven by the strong *pilA* promoter. WT: wild type, Scale bars 1mm.

Interestingly, with prolonged starvation, the mounds in the center of the developing colony appeared to fuse together, generating very large fruiting bodies by 120 h of starvation (Figure 25, B). In contrast, all strains carrying a mutant form of TodK,

independent of the predicted activity of the mutant proteins, proceeded through development in an accelerated manner, like the Δ*todK* strain.

To investigate, if the Δ*todK*/*todK*$_{WT}^{++}$ (Δ*todK attB*::Pr$_{pilA}$-*todK*$_{WT}$) phenotype could be augmented by increasing TodK levels in the cells even further, the construct was introduced into the wild type background (WT/*todK*$_{WT}^{++}$) and the developmental phenotype was investigated. Indeed, developmental progression was even further delayed in this strain expressing *todK* both from the native and a secondary site (Figure 26, A). At 72 h of development, this strain showed only very shallow mounds. This was 48 h later than multiple mounds being formed in the wild type. When starvation was observed even longer it could be shown that development was never completed and sporulation appeared to be abolished in this strain (Figure 26, B).

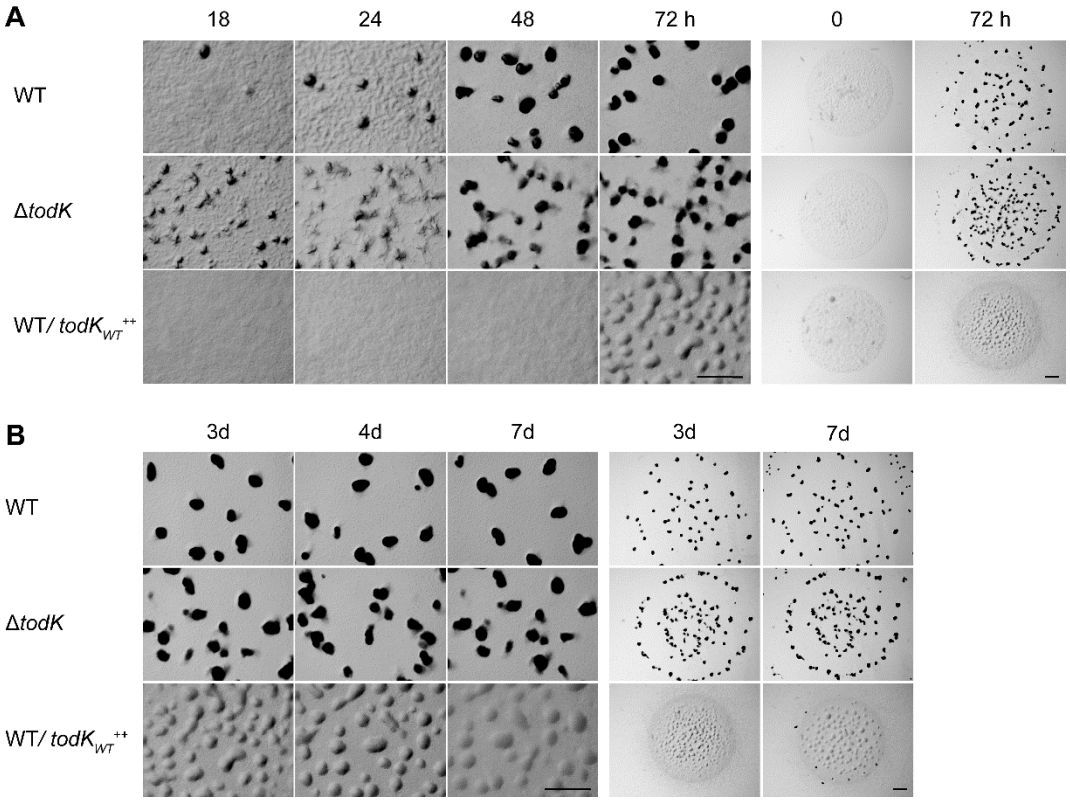

Figure 26: Development is severely delayed in a strain expressing *todK*$_{WT}$ driven by the *pilA* promoter from a secondary site in the genome in the wild type background. *Starvation assay on CF starvation agar plates.* Strains were grown in rich media to mid logarythmic phase, harvested and concentrated to $OD_{550\ nm}$ 7. 10 µl were spotted onto plates, dried and incubated at 32 °C. At the indicated time points pictures were taken using a stereomicroscope. **(A)** The strain WT/*todK*$_{WT}^{++}$ expressing Pr$_{pilA}$-*todK*$_{WT}$ from the *attB* site in the genome in wild type background (WT *attB*::Pr$_{pilA}$-*todK*$_{WT}$) formed shallow mounds after 72 h (= three days) of starvation. Left panel shows fruiting body morphology over the time course, right panel shows colony morphology of spotted (0 h) and developed (72 h) colony. **(B)** Starvation of the strains in A) was prolonged until seven days. Left panel shows fruiting body morphology over the extended time course, right panel shows colony morphology of developed (3 and 7 d) colony. WT: wild type, scale bars 1mm.

When starvation was induced under submerged culture conditions, both strains over-expressing *todK* in the native form (WT/*todK*$_{WT}^{++}$ and Δ*todK*/*todK*$_{WT}^{++}$) completely failed to develop (Figure 27). It was observed repeatedly that after 48-72 h of starvation, a white film occurred in both cultures. This film likely consisted of detaching and possibly dying starving *M. xanthus* cells. Timing of aggregate formation of strains

accumulating TodK mutant proteins in the Δ*todK* background were indistinguishable from wild type and Δ*todK* strains (Figure 27). However, they showed slight differences in fruiting body size and number. For instance, Δ*todK*/*todK*$_{D276A}^{++}$ produced more numerous but smaller fruiting bodies. The number and size of fruiting bodies were similar in Δ*todK*/*todKH*$_{275A}^{++}$ and Δ*todK*/*todK*$_{S279A}^{++}$, with slightly more disorganized fruiting bodies produced by Δ*todK*/*todK*$_{S279A}^{++}$. Also, darkening of fruiting bodies appeared to be accelerated in all three strains, similar to the Δ*todK* strain.

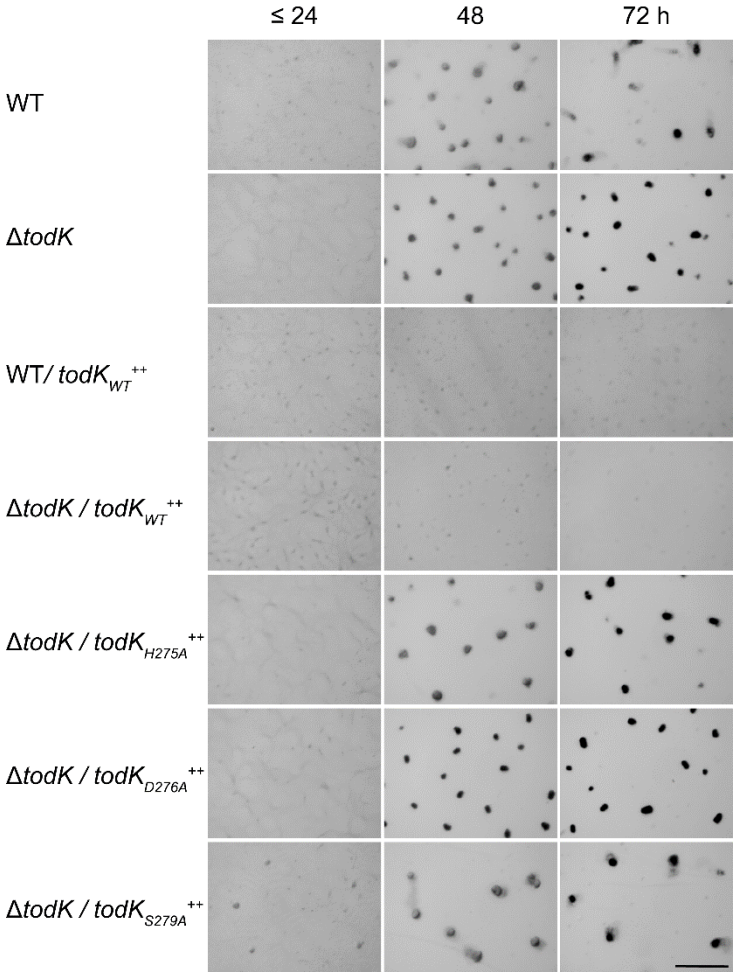

Figure 27: Development of strains expressing versions of *todK* from the *pilA*-promoter is analyzed under submerged conditions. *Starvation assay.* Strains were grown to mid exponential phase and seeded to develop under submerged conditions. Incubation took place at 32 °C and pictures were recorded at the indicated time points using a stereomicroscope. Strains were given the following designations: WT/*todK*$_{WT}^{++}$ (WT *attB*::Pr$_{pilA}$-*todK*$_{WT}$), Δ*todK*/*todK*$_{WT}^{++}$ (Δ*todK attB*::Pr$_{pilA}$-*todK*$_{WT}$), Δ*todK*/*todK*$_{H275A}^{++}$ (Δ*todK attB*::Pr$_{pilA}$-*todK*$_{H275A}^{++}$), Δ*todK*/*todK*$_{D276A}^{++}$ (Δ*todK attB*::Pr$_{pilA}$-*todKD*$_{276A}$), Δ*todK*/*todK*$_{S279A}^{++}$ (Δ*todK attB*::Pr$_{pilA}$-*todK*$_{S279A}$); $^{++}$ indicates the proteins were not present at native levels but were over-produced driven by the strong *pilA* promoter. WT: wild type, scale bar 1 mm.

Together, these results demonstrated that TodK is a negative regulator of development, since deletion leads to early aggregation, while forced over-production leads to delay in developmental progression. They also supported the hypothesis that TodK is acting both as a kinase and as a phosphatase on one or multiple output proteins, and that both functions are equally important or dependent upon each other to balance proper developmental progression. However, it was also a possibility that the mutant forms of TodK were instable or degraded in the cells and therefore I

observed a null phenotype. To further investigate this, immunoblot analysis of TodK in all the strains used in this section were performed.

5.4.2.2 TodK signaling mutants are produced as stable proteins

Two scenarios could cause early development in a TodK point-mutant strain: i) the protein lost its activity that allowed it to negatively regulate development in the wildtype strain and ii) the mutation rendered the mRNA or protein instable and it was degraded rapidly, resulting in a TodK deletion situation in terms of protein level. To be able to differentiate between these two possible causes for early development, western blot analysis of strains accumulating the mutant TodK proteins were performed. Expression of the constructs by the native promoter led to very low protein level, not detectable in immunoblot analysis (data not shown). This was in line with protein accumulation of native TodK in wild type populations (Figure 21 and Figure 28). However, the generation of strains expressing *todK* constructs (WT and single amino acid point mutants) driven by the *pilA* promoter from a secondary site in the genome gave me a great tool to test protein stability in immunoblot assays. At least 10 µg total protein of lysate were analyzed in western blots using α-TodK polyclonal antibodies. When X-ray films were exposed to these blots for more than 16 h, TodK protein was detected in lysates of the wild type but absent from the deletion mutant (Figure 28, A), always accompanied by the strong cross reactive band above the TodK signal. When analyzing lysates from strains expressing different *todK* versions from the *pilA* promoter in the Δ*todK* background, 1 µg lysate was sufficient to detect a strong TodK specific signal (Figure 28, A). I could detect all forms of TodK, both in vegetative cells (t=0h) and during (early) development[2]. Interestingly, when analyzing lysates of a strain expressing Pr_{pilA}-$todK_{WT}$ in the wild type background (WT/$todK_{WT}^{++}$), protein levels were strongly increased at all time points investigated (Figure 28, B). These increased TodK levels were unlikely to merely stem from *todK* expressed from the native site in addition to *todK* expressed from the *pilA* promoter at a secondary site, since native TodK levels were not detectable under these immunoblot conditions.

[2] Note: This serves exclusively to prove mutant forms of TodK are stable *in vivo.* Slight differences of TodK accumulation in the different strains are not addressed here (e.g. protein level appears lower in vegetative cells in native and D276A, higher in H275A and S279A; higher over the entire time course in S279A). To evaluate this, the assay needed to be repeated in a relevant number of biological and technical replicates and protein accumulation would need to be quantitated.

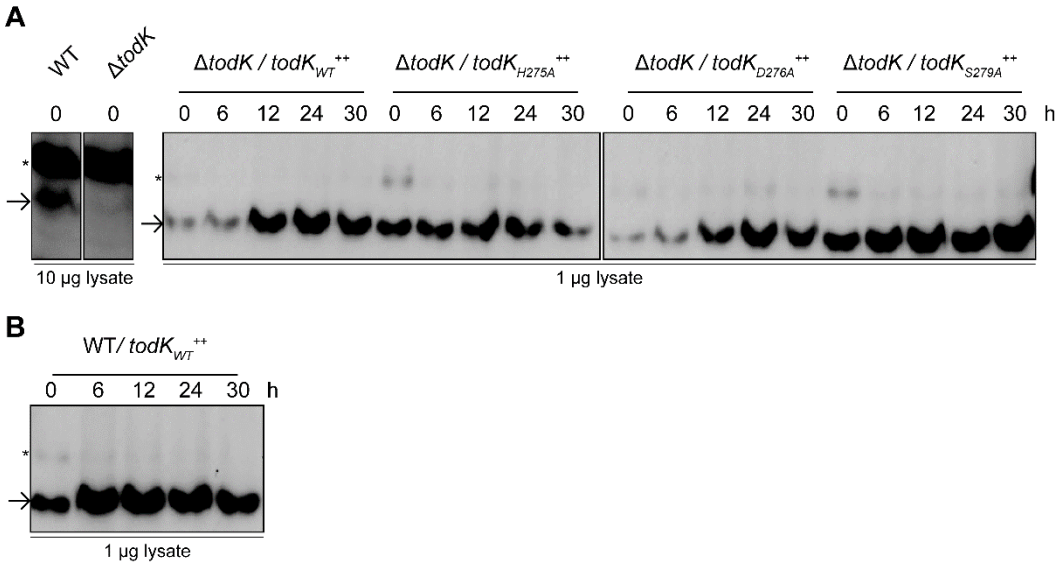

Figure 28: All TodK proteins are stable and over-accumulate when expressed from the *pilA*-promoter. *Immunoblot analysis.* Starvation was induced under submerged conditions and total cell populations were harvested at the indicated time points. Cells were lysed and analyzed in an immunoblot with α-TodK polyclonal antibody. A cross reactive band is marked with an asterisk (*) and the band of specific TodK signal is marked with an arrow (→). **(A)** For the controls (WT and Δ*todK*) 10 ug total protein was analyzed. The TodK (57 kDa) band is absent from the deletion strain while the cross reactive band is visible with comparable intensity as in the wild type. From strains expressing various versions of TodK under the control of the *pilA* promoter from a secondary site only 1 µg total protein was analyzed due to much more protein present. **(B)** WT/$todK_{WT}^{++}$ lysates were analyzed, 1 ug total protein was used for this analysis. Complemented strains, expressing versions of *todK* under the control of the *pilA* promoter (Pr_{pilA}) from the Mx8 phage attachment site (*attB*) in the *M. xanthus* genome, were given the following designations: Δ*todK*/$todK_{WT}^{++}$ (Δ*todK attB*::Pr_{pilA}-$todK_{WT}$), Δ*todK*/$todK_{H275A}^{++}$ (Δ*todK attB*::Pr_{pilA}-$todK_{H275A}^{++}$), Δ*todK*/$todK_{D276A}^{++}$ (Δ*todK attB*::Pr_{pilA}-$todKD_{276A}$), Δ*todK*/$todK_{S279A}^{++}$ (Δ*todK attB*::Pr_{pilA}-$todK_{S279A}$); WT/$todK_{WT}^{++}$ (WT *attB*::Pr_{pilA}-$todK_{WT}$), $^{++}$ indicates the proteins were not present at native levels but were over-produced driven by the strong *pilA* promoter. WT wild type.

I could show that all three single point mutants of TodK protein were expressed and stable in the cell population, therefore ruling out the possibility of early development being caused by lack of TodK protein in the cells. This further supports the hypothesis that TodK acts both as a kinase as well as a phosphatase on one or more downstream targets. Moreover, I could show that the observed delayed developmental phenotype of Δ*todK*/$todK_{WT}^{++}$ likely resulted from over-accumulation of TodK in the cell population. The even more dramatic delayed development of the strain WT/$todK_{WT}^{++}$ could also be convincingly explained by the observed even higher TodK protein levels over the investigated period of development.

5.4.2.3 TodK over-accumulation affects MrpC levels

My results strongly indicated that the delayed phenotypes of Δ*todK*/$todK_{WT}^{++}$ (Δ*todK attB*::Pr_{pilA}-$todK_{WT}$) and the even more severe phenotype of WT/$todK_{WT}^{++}$ (WT *attB*::Pr_{pilA}-$todK_{WT}$) resulted from over-accumulation of TodK. The early developmental phenotypes of all three substitution mutants (H275A, D276A and S279A) seemed to stem from loss of function rather than protein instability. In the next step, I set out to investigate the effect of over-accumulated TodK proteins on the presumed regulatory output of TodK: MrpC.

It has been shown previously that in a *todK* deletion strain, MrpC accumulates earlier and at higher levels than in the wild type when cells are starved under submerged conditions ((Lee, 2009) and (Figure 20 and Figure 29, top)). Consistent with the delayed phenotype observed under submerged culture conditions, starving Δ*todK/todK*$_{WT}^{++}$ cells produced much less MrpC, even at 30 h of development (Figure 29). This was the time point of maximum MrpC accumulation in the wild type. In line with the even more delayed developmental phenotype of WT/*todK*$_{WT}^{++}$ on CF starvation agar and no detectable development under submerged conditions also MrpC protein levels were even further reduced in this strain. In contrast to this, MrpC accumulated both earlier and at higher levels in all three TodK point mutant strains. Here, I detected MrpC six hours earlier than in wild type cells, consistent with when MrpC was detected in Δ*todK*. In all three strains expressing point mutants of *todK* MrpC accumulation was comparable, independent from the predicted loss of function of said mutant. Together, these results suggested that TodK acts both as a kinase and phosphatase to control its so far unknown output and negatively regulates developmental progression.

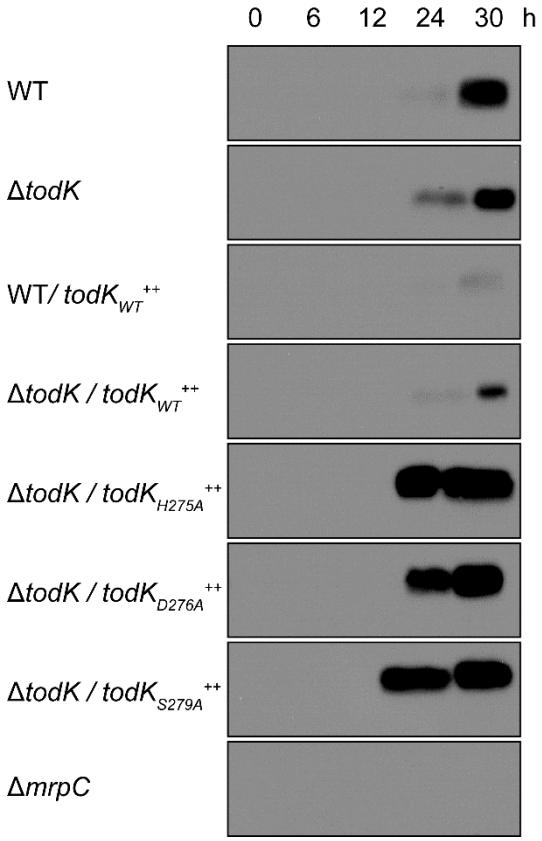

Figure 29: MrpC accumulation in strains expressing TodK protein versions from a secondary site is consistent with the developmental phenotypes. *Immunoblot analysis.* Strains were developed under submerged culture and harvested at the indicated time points. Lysates were prepared and 10 µg total protein was analyzed in an immunoblot assay using α-MrpC polyclonal antibody. Complemented strains, expressing versions of *todK* under the control of the *pilA* promoter (Pr$_{pilA}$) from the Mx8 phage attachment site (*attB*) in the *M. xanthus* genome, were given the following designations: Δ*todK*/*todK*$_{WT}^{++}$ (Δ*todK attB*::Pr$_{pilA}$-*todK*$_{WT}$), Δ*todK*/*todK*$_{H275A}^{++}$ (Δ*todK attB*::Pr$_{pilA}$-*todK*$_{H275A}^{++}$), Δ*todK*/*todK*$_{D276A}^{++}$ (Δ*todK attB*::Pr$_{pilA}$-*todKD*$_{276A}$), Δ*todK*/*todK*$_{S279A}^{++}$ (Δ*todK attB*::Pr$_{pilA}$-*todK*$_{S279A}$); WT/*todK*$_{WT}^{++}$ (WT *attB*::Pr$_{pilA}$-*todK*$_{WT}$), $^{++}$ indicates the proteins were over-produced driven by the strong *pilA* promoter. MrpC 27 kDa, WT: wild type.

5.4.3. Investigation of TodK phosphorylation status *in vitro* and *in vivo*

The *in vivo* data suggested TodK to be an active histidine protein kinase. I wanted to support this result and gain deeper knowledge in the proteins activity be studying it *in vitro*. To do so, I set out to overexpress and purify recombinant TodK from *E. coli* cells and perform radioactive kinase assays.

5.4.3.1 Overexpression and purification of recombinant Trx-His_6-TodK

In an earlier study, solubility screening of TodK expressed from several overexpression vectors was performed in *E. coli* cells and using pET32a (Invitrogen) was found to result in production of the biggest proportion of soluble TodK protein (roughly 50 % soluble, 50 % insoluble protein outcome, B. Lee and P.I. Higgs; unpublished data). Protein production from pET32a results in an N-terminally tagged protein of interest with the solubilizing fusion protein Thioredoxin (Trx) followed by a hexa-histidine (His_6) tag. For overexpression, *todK* was cloned into pET32a both in its native ($TodK_{WT}$) form as well as in the presumably kinase inactive form resulting from a single amino acid substitution mutagenesis ($TodK_{H275A}$). Expression conditions were optimized to using pLysS *E. coli* cells, growing them to midlogarithmic phase (OD_{600nm} 0.5) at 37 °C, cooling cultures to 18 °C and growing them further to late-mid logarithmic phase (OD_{600nm} 0.7). Expression of *todK* was induced with 0.5 mM IPTG and continued at 18 °C overnight. *E. coli* cells were lysed and the soluble fraction was separated from the insoluble fraction in two subsequent clarification centrifugation steps with increasing stringency (Figure 30, A $TodK_{WT}$ and B $TodK_{H275A}$). Purification of TodK was performed using Ni-NTA-affinity chromatography utilizing an ÄKTA purification system. The most important purification steps were analyzed on SDS-PAGE, where over-produced TodK protein migrated at approximately 70 kDa. This corresponded to the calculated molecular mass of TodK (55.7 kDa) plus Trx-His_6-fusion protein (16 kDa). The three purest elution fractions of each purification were pooled and subjected to dialysis (Figure 30, A and B, far right). Attempts to use Q Sepharose chromatography (HiTrap Q HP, GE Healthcare), a strong anion exchange anion column, to further purify TodK were not successful (data not shown).

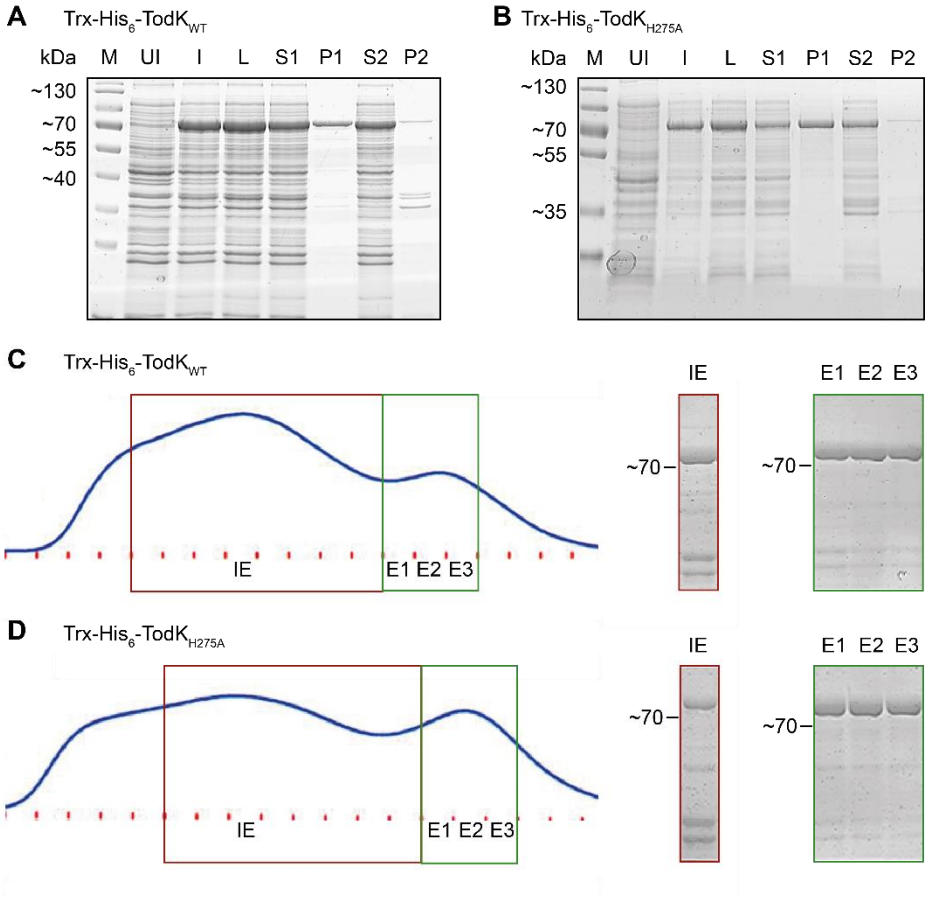

Figure 30: TodK can be soluble produced and purified from *E. coli*. *Purification of Trx-His$_6$-TodK$_{WT}$ and Trx-His$_6$-TodK$_{H275A}$ proteins via Ni-NTA column (Äkta).* Critical fractions during the purification of Trx-His$_6$-TodK$_{WT}$ **(A)** and Trx-His$_6$-TodK$_{H275A}$ **(B)**. Plasmids carrying the genes to overproduce Trx-His$_6$-TodK$_{WT}$ (pMG018) and Trx-His$_6$-TodK$_{H275A}$ (pMG019) were transformed into *E. coli* pLysS and induced for protein expression with 0.5 mM IPTG at 18°C overnight. Samples were taken during the entire process and equal proportions were subjected to SDS-PAGE (8 %). M Marker, UI un-induced; I induced; L lysate; S1 supernatant centrifugation 1; P1 pellet centrifugation 1; S2 supernatant centrifugation 2; P2 pellet centrifugation 2. Elution chromatograms and SDS-PAGE analysis of elution fractions of Trx-His$_6$-TodK$_{WT}$ **(C)** and Trx-His$_6$-TodK$_{H275A}$ **(D)**. Elution fractions were analyzed on SDS-PAGE (8 %) and the three purest were chosen for further analysis (green box), pooled and dialyzed. Eight fractions of lesser purity were pooled and used for a second purification step (red box). IE impure elution fraction representing the protein pattern of the eight fractions in the red box, E 1-3 three purest elution fractions. Molecular weight Trx-His$_6$-TodK ~70 kDa.

5.4.3.2 TodK is not an active kinase *in vitro*

To test if Trx-His$_6$-TodK was capable of autophosphorylation *in vitro*, the purified proteins (TodK$_{WT}$ and TodK$_{H275A}$) were incubated with radioactively labeled [γ^{32}P]-ATP (Figure 31). Even after 60 min of incubation, no autophosphorylation of 10 µM TodK$_{WT}$ could be detected under standard conditions containing 1 mM $MgCl_2$ in the reaction buffer (Figure 31, A). It is known that some proteins utilize different ions or need higher ion concentrations to function as an active kinase (Gamble *et al.*, 1998, Psakis *et al.*, 2011). In a next step, both proteins were incubated with reaction buffers supplemented with either $MnCl_2$ or $CaCl_2$ at 1 mM or 10 mM, respectively as well as

a high concentration of $MgCl_2$ of 10 mM (Figure 31, B). Under the described conditions no autophosphorylation could be observed.

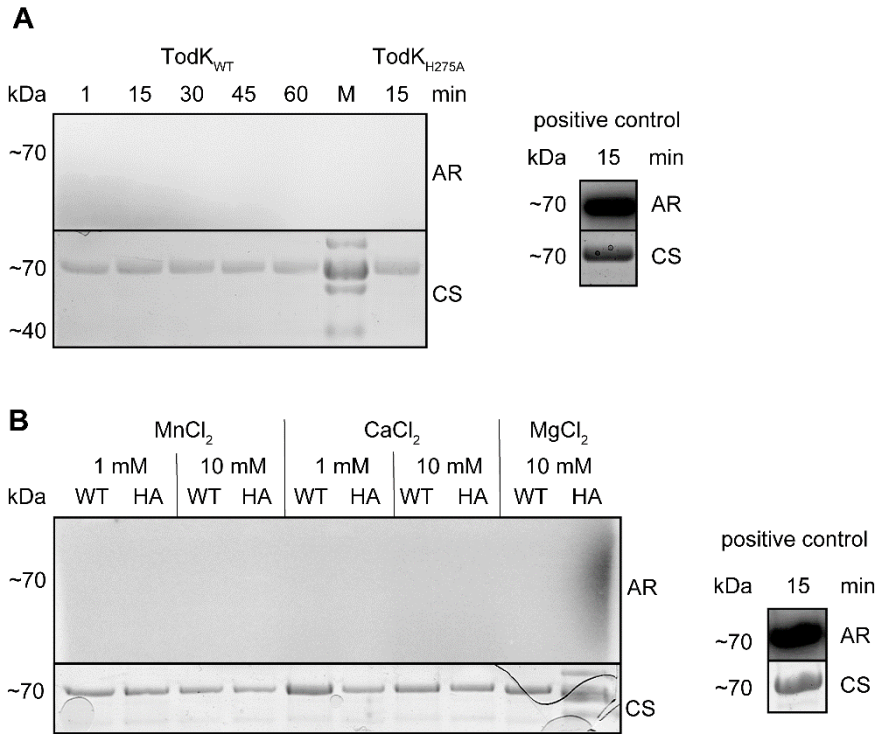

Figure 31: Trx-His6-TodK does not autophosphorylate *in vitro*. (A) *Radioactive phosphorylation assay using established standard conditions.* 10 µM purified protein were incubated for a total of 60 min with radioactively labeled [γ^{32}P]-ATP and 1 mM $MgCl_2$, aliquots were removed and quenched at the indicated time points. Proteins were resolved using SDS-PAGE and the radiolabel was detected by exposure to a storage Phospho Screen (autoradiogram, AR). Total loaded protein was visualized using Coomassie stain (CS) afterwards. Trx-His$_6$-TodK has a calculated molecular mass of around 70 kDa. A protein known to autophosphorylate was used as a positive control to ensure assay functionality. **(B)** *Assay variation of A.* Proteins were incubated with different ions and ion concentrations for 60 min in the presence of radioactively labeled [γ^{32}P]-ATP. M: Marker, WT: Trx-His$_6$-TodK$_{WT}$, HA: Trx-His$_6$-TodK$_{H275A}$.

Although the kinase inactive mutant had an accelerated developmental phenotype *in vivo* (section 5.4.1.3), the purified protein showed no activity *in vitro*. This might have different reasons: i) the PAS domains inhibited kinase activity and by binding a ligand release this repression, ii) another co-factor is required for kinase activity or iii) the tag on the N-terminus of the protein hindered activity and/or prohibits the correct and functional folding of all domains.

To investigate possibility one, single domain constructs of TodK were expressed and purified to analyze whether the kinase domain is capable of autophosphorylation without the PAS domain's inhibition (see section 5.4.4.1). Moreover, Phos-tag technology was established in the laboratory to study protein functionality and autophosphorylation *in vivo* (see section 5.4.3.3), to prevent the possible hindrances to protein activity listed as possibilities two and three.

5.4.3.3 TodK might become phosphorylated *in vivo*

In vitro activity of *M. xanthus* histidine protein kinases has been studied extensively, and it was very rare that the kinase domain alone would not autophosphorylate *in vitro* (section 5.4.4.1). In particular, since substitution of the invariant histidine (*todK*$_{H275A}$) showed impaired developmental progression, suggesting it to be an active histidine protein kinase *in vivo*. One elegant method to investigate the phosphorylation status of proteins *in vivo* is called Phos-tag technology (Kinoshita *et al.*, 2008). This method was initially developed to investigate phosphorylation of serine, threonine and tyrosine residues, but has also been used to study phosphorylation of aspartate (Barbieri & Stock, 2008) as well as histidine residues (Yamada *et al.*, 2007, Kinoshita-Kikuta *et al.*, 2016, Gajdiss *et al.*, 2017). Phos-tag-acrylamide SDS-PAGE has been successfully used to study aspartate phosphorylation in cell lysates of *M. xanthus* before (Kaimer & Zusman, 2013). Therefore, this method was a promising tool to investigate at which time point of development TodK was active, and subsequent studies of TodK activity in different cell fates were envisioned to gain insight in the role of TodK as well as its regulation.

<u>Theory of Phos-tag technology</u>

Phos-tag is a functional molecule that captures specifically phosphorylated residues, offering a variety of applications. One of these is the use of Phos-tag-acrylamide in a protocol of SDS-PAGE, in which proteins are not only separated by their size but also according to their phosphorylation status. By adding the Phos-tag substance as well as specific bivalent ions to the SDS-gel, phosphorylated proteins are captured by the compound and their migration through the gel matrix is delayed. Multiple phosphorylation states of a protein can be separated from each other and from the non-phosphorylated protein (Figure 32). A subsequent western blot allows specific detection of the separated forms of the protein of interest in a cell lysate sample.

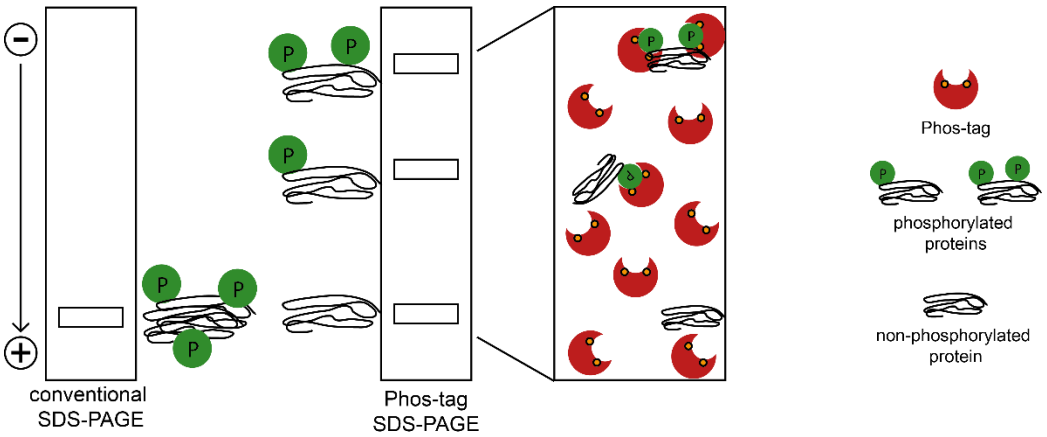

Figure 32: Principle of Phos-tag-acrylamide SDS-PAGE. In a conventional SDS-PAGE proteins run according to their molecular weight through the gel matrix. Non-phosphorylated proteins and their phosphorylated counterparts migrate at the same position, resulting in a singular band. In a Phos-tag SDS-PAGE, phosphorylated proteins are captured by the Phos-tag-compound which delays their migration. Proteins now also migrate corresponding to their degree of phosphorylation. This results in multiple bands, each corresponding to one specific phosphorylation status. Figure modified from Phos-tag protocol (available at http://www.wako-chem.co.jp/english/labchem/journals/phos-tag_GB2013/pdf/Phos-tag.pdf).

Phosphorylation of TodK might occur, but is independent from the invariant histidine

Due to the low concentration of TodK expressed from the native site in total cell population lysates, I decided to take advantage of the strains expressing TodK from the *pilA* promoter at a secondary site in the genome which contained higher TodK protein levels, as shown above (Figure 32). After conditions for Phos-tag-acrylamide SDS-PAGE were optimized (data not shown), total cell populations were harvested at various time points of starvation induced development and analyzed. Cells of the strain Δ*todK* were used as a control, to identify the cross-reactive band which in a regular SDS-PAGE runs at the size of 70 kDa (Figure 33, A). In lysates derived from the strain Δ*todK*/*todK*$_{WT}^{++}$ (Δ*todK attB*::Pr$_{pilA}$-*todK*$_{WT}$), next to the strong non-phosphorylated base line, two additional bands could be detected, indicating a phosphorylation induced band shift. However, both these bands were also present when a strain expressing a mutant form of TodK that was incapable of histidine autophosphorylation Δ*todK*/*todK*$_{H275A}^{++}$ (Δ*todK attB*::Pr$_{pilA}$-*todK*$_{H275A}$) was analyzed (Figure 33, B). Interestingly, all (mutant) versions of TodK investigated under these conditions resulted in these exact band shifts (data not shown).

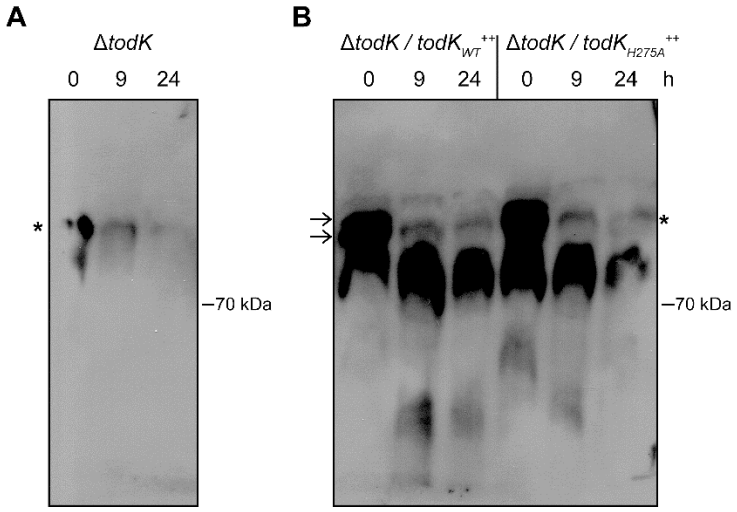

Figure 33: Phosphorylation induced band shift can be observed in Phos-tag SDS-PAGE, however this is not due to autophosphorylation of the invariant histidine H275. *Phostag SDS-PAGE.* Strains were developed under submerged culture conditions and total population was harvested at the indicated time points. Cells were lysed and 10 µg lysates were loaded to a Phos-tag SDS-PAGE, run and semi-dry blotted onto PVDF membrane. Immunoblots were probed with α-TodK polyclonal antibodies. Complemented strains, expressing versions of *todK* under the control of the *pilA* promoter (Pr$_{pilA}$) from the Mx8 phage attachment site (*attB*) in the *M. xanthus* genome, were given the following designations: Δ*todK*/*todK*$_{WT}^{++}$ (Δ*todK attB*::Pr$_{pilA}$-*todK*$_{WT}$), Δ*todK*/*todK*$_{H275A}^{++}$ (Δ*todK attB*::Pr$_{pilA}$-*todK*$_{H275A}^{++}$), $^{++}$ indicates the proteins were not present at native levels but were over-produced driven by the strong *pilA* promoter. **(A)** In a *todK* deletion strain, the cross-reactive band observed earlier is detected and marked with an asterisk. **(B)** Lysates of strains expressing either the native TodK protein (left) or a mutant predicted to be incapable of autophosphorylation of the conserved histidine TodK$_{H275A}$ (right) showed an indistinguishable band pattern. The cross-reactive band identified before is marked with an asterisk.

This raised the intriguing possibility that TodK indeed was phosphorylated, potentially regulating the activity of the protein, but histidine phosphorylation on H275 could not be shown under the conditions tested. One possible explanation for the band shift observed here was that TodK was phosphorylated on a serine or threonine residue, possibly to regulate the proteins activity. Interestingly, the shifted band was stronger

at the beginning of development and faded as development progressed. The phosphorylation status of TodK could be further investigated using mass spectrometry techniques to find the putative site(s) of phosphorylation. Additionally, it would be interesting to investigate the time-frame between zero and nine hours of development more closely, to determine if the putative phosphorylation of TodK decreases gradually over time or if there is a clear off switch at some developmental checkpoint. This information would be vital for understanding how TodK activity is regulated *in vivo*. The Phos-tag-approach could still be used to investigate histidine phosphorylation of TodK. However, the conditions would need to be optimized further. Several modifications of the protocol remained untested to this point, starting from acrylamide : bisacrylamide ratio variations, Phos-tag-acrylamide concentrations and ion concentrations, over testing different immunoblot techniques and conditions, to sample preparation including not freezing samples and variations in the cell lysis approach.

5.4.4. Signals and outputs of the TodK signaling module

When studying signaling systems, the most fundamental questions regarding signal transmission are: i) “What stimuli is the system reacting to and how does it sense it?” and ii) “What is the signal regulating and how is the output mediated?”. To address these questions, I set out to investigate the two PAS domains located at the N-terminus of TodK to assess if they are sensing the signal input and if they affect kinase activity (section 5.4.4.1). Since TodK is encoded in the *M. xanthus* genome as an orphan gene, it is challenging to determine the cognate response regulator that mediates the signal output of the system. Using bioinformatics tools and investigating the genomic region of *todK*, I identified two response regulators which had the potential to be the cognate partner of TodK and initiated basic phenotypic studies *in vivo* (section 5.4.4.2).

5.4.4.1 The PAS domains of TodK likely sense input stimuli and activate kinase function

Per Ant Sim (PAS) domains are frequently found at the amino terminus of histidine protein kinases, where they act as sensing domains to recognize the input stimuli to activate the system. I set out to investigate the PAS domains of TodK *in vivo* and assay if kinase activity depends on the PAS domains of the protein *in vitro*. The domain architecture of TodK has been described in detail before (section 5.4.1.3), so here I just briefly illustrate what portion of TodK protein is deleted in the domain deletion mutant as well as overexpression constructs used in this study (Figure 34).

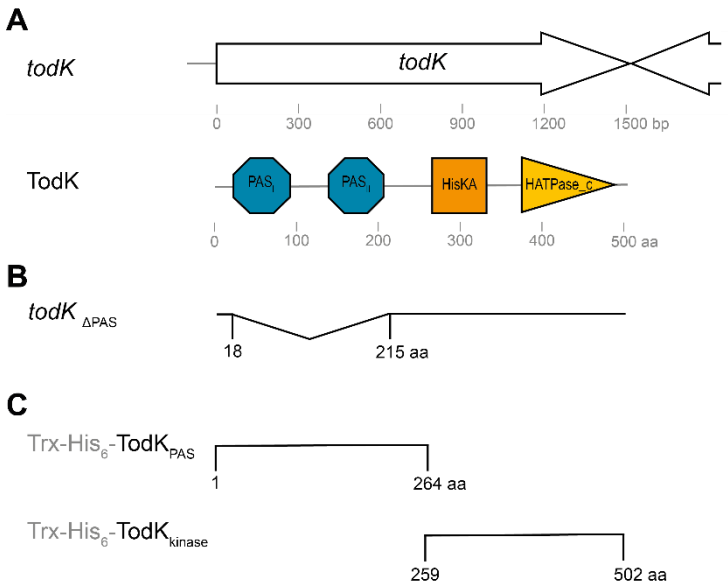

Figure 34: Schematic of domain deletion and single domain overexpression constructs of TodK. (A) Gene locus (top) and protein domain structure (bottom) of TodK. Domain assignment according to SMART (Schultz *et al.*, 1998, Letunic *et al.*, 2015). **(B)** The construct deleting both PAS domains (*todK*$_{\Delta PAS}$) deletes amino acids 19 – 214 from the native locus. **(C)** Overexpression constructs to express the TodK PAS domains and kinase domain separately in *E. coli*. Both were cloned into pET32a, generating Trx-His$_6$-tagged versions of the domains, tags are not depicted.

Deletion of TodK PAS domains leads to early development

In-frame deletion of the PAS domains was generated in *M. xanthus* and the resulting strains were assayed to develop on CF-starvation agar plates. The construct keep some distance to the kinase domain to not disturb its folding and therefore potentially activity (Figure 34, B). When cells of the resulting strains were starved, and allowed to develop on CF-nutrient limiting agar plates, *todK*$_{\Delta PAS}$ constructs resulted in a Δ*todK* phenotype with the hallmarks of early aggregation (more than six hours earlier than wild type), a fruiting body free ring near the colony periphery and disturbed fruiting body morphology (Figure 35).

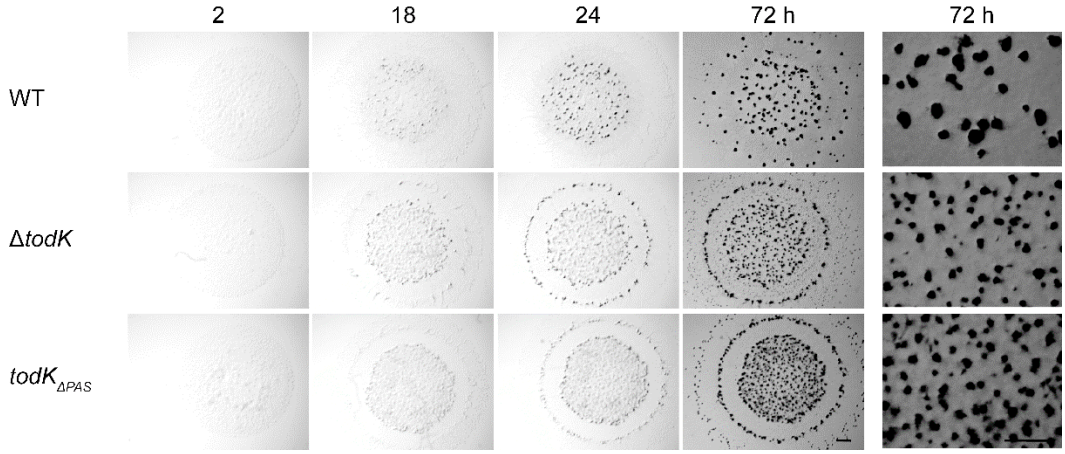

Figure 35: Deletion of PAS domains of TodK leads to phenocopy of *todK* deletion hallmarks. *Starvation assay on CF-nutrient limiting agar plates.* Aliquots of 10 µl OD $_{A550nm}$ 7 of all strains were spotted onto plates, dried and incubated at 32 °C. Pictures were recorded at the indicated time points using a stereomicroscope. Left panel shows colony morphology over the time course, right panel shows fruiting body morphology at 72 h of starvation. WT: wild type, *todK*$_{\Delta PAS}$: Δaa18-214; scale bars 1 mm.

Unfortunately, attempts to detect the remaining TodK protein by immunoblot failed, likely due to the earlier described low abundance of the protein and further reduced epitopes in the truncated versions. This leaves the possibility that truncating TodK, leaving only the kinase domain in the cells, results in lower protein levels or even complete degradation of the protein which would result in a Δ*todK* like protein situation in the cells and therefore a Δ*todK* like phenotype. However, I found during *in vitro* studies that it is possible to overexpress only the kinase domain soluble in *E. coli* (Figure 36), raising the optimistic anticipation this might also be the case *in vivo*. Assuming that the truncated forms of TodK are stable in the cell and present at similar levels as the full length protein, the developmental phenotype of both *todK*$_{\Delta PAS}$ suggested that the PAS domains are needed to activate kinase function rather than release an inhibition upon signal sensing. To further test this hypothesis, I overexpressed and purified recombinant single domain constructs of TodK and analyzed kinase activity in a radioactive kinase assay.

The kinase domain of TodK alone does not autophosphorylate *in vitro*

To investigate the activity of the TodK kinase domain without potential inactivation by the PAS domains, the separate domains were cloned, overexpressed and purified from *E. coli* using the same strategies as applied for the full length protein (section 5.4.3.1). Soluble expression from both constructs (Trx-His$_6$-*todK*$_{PAS}$ and Trx-His$_6$-*todK*$_{kinase}$, Figure 34 C) was possible (Figure 36). Although almost all of the PAS domain construct was found in the soluble fraction, only approximately 50 % of the kinase domain construct was found to be soluble whereas the other 50 % were found to be in the pellet fraction, likely in inclusion bodies. Also, induction of the PAS domain construct was stronger compared to the kinase domain. Protein purification was performed via NiNTA-affinity-chromatography using an ÄKTA machine. After elution (Figure 36, proteins were dialyzed against storage buffer and frozen at – 20 °C until further usage.

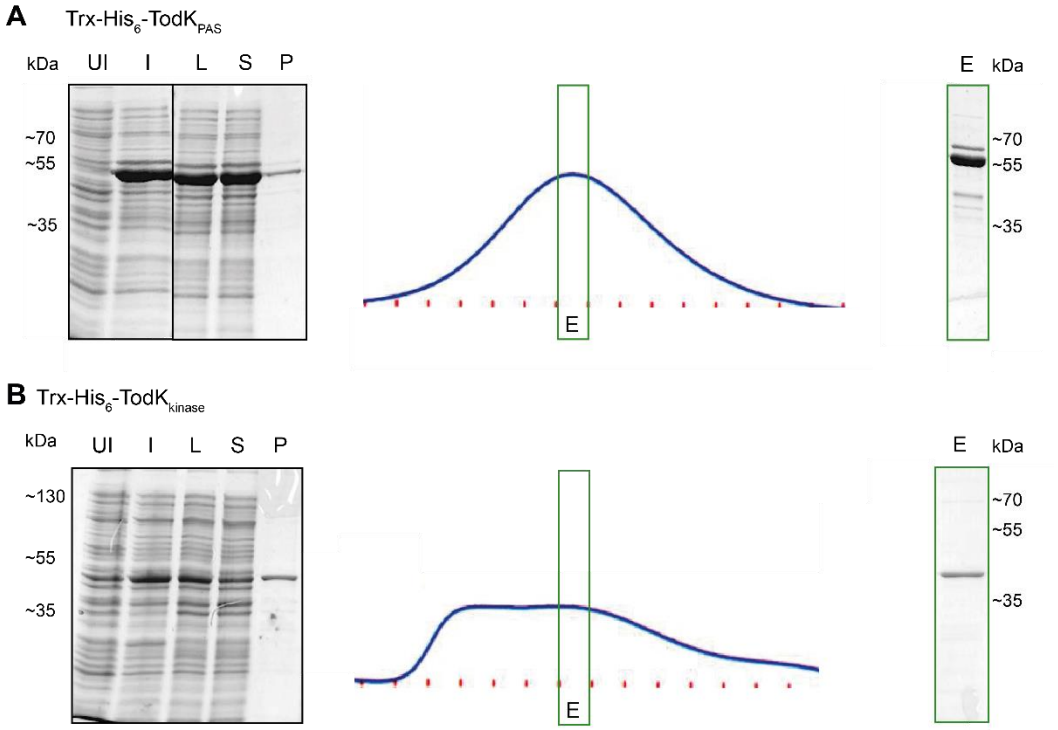

Figure 36: Soluble overexpression of TodK domain constructs is possible in *E. coli*. *SDS-PAGE of critical steps in protein overexpression and purification.* Trx-His$_6$-TodK$_{PAS}$ **(A)** and Trx-His$_6$-TodK$_{kinase}$ **(B)** constructs were induced to express the proteins of interest in pLysS *E. coli* cells with 0.5 mM IPTG at 18 °C. Purification was carried out via NiNTA-affinity chromatography (ÄKTA technology). Purest elution fractions were pooled, dialyzed and stored at -20 °C until further use. UI un-induced; I induced; L lysate; S supernatant; P pellet; E representative elution fraction.

In a radioactive assay the ability of Trx-His$_6$-TodK$_{kinase}$ to autophosphorylate was examined. The assay was performed under standard conditions, but even after 45 minutes of incubation, no autophosphorylation signal was detectable on Trx-His$_6$-TodK$_{kinase}$ (Figure 37). Also, the two single domain constructs Trx-His6-TodK$_{PAS}$ and Trx-His6-TodK$_{kinase}$ were mixed at an equimolar ratio to test if the presence of the PAS domains had an influence on kinase activity; this was not the case. Together with the data from domain deletion strains *in vivo*, this result suggested that the mechanism to

activate the TodK kinase includes the PAS domain(s) sensing a signal and actively stimulating kinase activity, rather than releasing kinase inhibition.

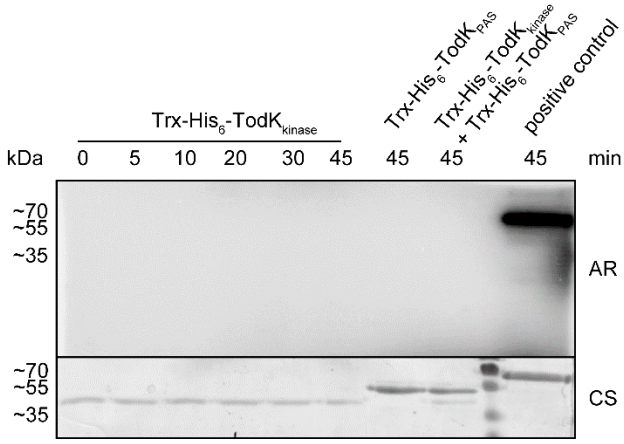

Figure 37: No phosphorylation signal can be detected on the kinase domain of TodK. *Radioactive kinase assay.* Autophosphorylation was analyzed in a standard radioactive phosphorylation assay, where 10 µM of the purified indicated protein was incubated for a total of 45 min with radioactively labeled [γ^{32}P]-ATP and 1 mM $MgCl_2$, aliquots were removed and quenched at the indicated time points. Proteins were subsequently resolved using SDS-PAGE and the exposed to a storage Phospho Screen to detect any radiolabel (autoradiogram, AR). Afterwards, total protein was visualized using Coomassie stain (CS). Trx-His_6-$TodK_{PAS}$ was used as a negative control at 45 min. A known active histidine kinase was used as a positive control to ensure assay functionality.

5.4.4.2 What is the output of TodK?

TodK is encoded in the genome as an orphan kinase, meaning it is not in an operon with its cognate response regulator. This makes it challenging to identify the associated response regulator of TodK. There are various strategies to identify cognate partners of orphan signaling proteins ranging from analysis of the genome region, subsequent gene disruption of all respective genes and classification of phenotypes to group potential signaling partners (for instance done for *E. coli* (Zhou *et al.*, 2003) and was planned for *Streptomyces* (Hutchings *et al.*, 2004)) to various bioinformatics based predictions. Here I applied two of these approaches which suggested two potential response regulators as signaling partner for TodK: *dotR* and MXAN_5052.

<u>DotR is unlikely to be part of the TodK signaling module</u>

dotR is encoded adjacent to *todK* in the *M. xanthus* genome, yet on the alternate DNA strand, resulting in an overlap of the stop codons of both genes. This close proximity and potential common regulation suggested DotR to be the cognate partner and signal output of TodK. This was previously suggested and found to be not the case in the alternate wild type DK1622 (Rasmussen & Sogaard-Andersen, 2003). However, as discussed before, the wild type strain DZ2 used in this study provides more resolution of timing during development, which led me to investigate the phenotype of a *dotR* deletion strain in more detail again. An in-frame deletion of *dotR* was generated using the pAAR140 plasmid generated by Rasmussen *et al.* and the developmental

phenotype was analyzed (Figure 38). While a Δ*todK* strain developed early on CF agar and exhibited perturbed fruiting body morphology, a Δ*dotR* strain showed a wild type like developmental progression and properly shaped fruiting bodies, a minimal delay in fruiting body formation could be observed. A double in-frame deletion mutant of both genes (Δ*todK* Δ*dotR*) phenocopied the Δ*todK* strain. These findings supported the data published earlier (Rasmussen & Sogaard-Andersen, 2003) and indicated that DotR is not the cognate response regulator of TodK.

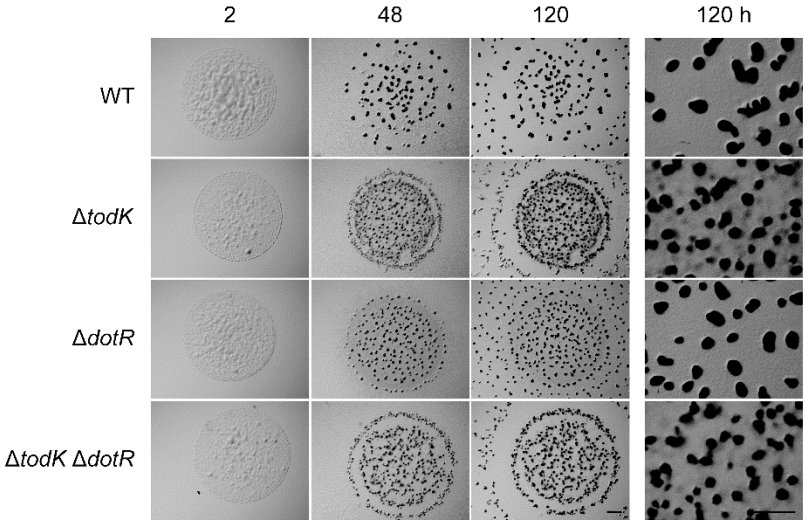

Figure 38: DotR is unlikely to be the cognate response regulator of TodK. *Starvation induced development assay on CF-nutrient limited agar plates.* Cells were spotted at OD_{550nm} 7, dried and incubated at 32 °C for a total of 5 days. Pictures were recorded at the indicated time points using a stereomicroscope. Left panel shows colony morphology over the time course, right panel shows fruiting body morphology at 120 h of starvation. WT wild type, scale bars 1mm.

MXAN_5052 is unlikely to be the cognate signaling partner of TodK

In a further attempt to identify potential signaling partners of TodK, I took advantage of a prediction software (http://www.swissregulon.unibas.ch/cgi-bin/TCS.pl) which used an algorithm that models known kinase/response regulator pairs based on amino acid sequence to predict interacting pairs specifically of orphan genes (Burger & van Nimwegen, 2008). The authors claimed to be most confident in predicting partners for kinases of the largest histidine kinase family, HisKA, in which TodK was included. The software predicted the orphan response regulator MXAN_5052 to be the cognate partner of TodK with a probability of 0.77; for perspective, the second hit (MXAN_6012) had a 10-fold lower likelihood of 0.073, which was followed by MXAN_2516 with a score of 0.053. No other orphan kinase tested (including Hpk30, EspA and EspC) revealed a possible partner with such a high probability. MXAN_5052 codes for a RR containing a REC domain followed by a domain of unknown function and an unstructured region (based on SMART analysis (Schultz *et al.*, 1998, Letunic *et al.*, 2015)). In-frame deletion strains of MXAN_5052 as well as a double deletion strains (Δ*todK* ΔMXAN_5052) were generated and their developmental phenotype was investigated on CF starvation agar plates (Figure 39). The creation of in-frame deletions of MXAN_5052 resulted in a low number of clones

and by the end of this study only one clone of a confirmed in-frame deletion could be acquired. For a double deletion strain missing *todK* and MXAN_5052, only two PCR confirmed clones could be created by the end of this study. It should be noted here that to strengthen the conclusion that MXAN_5052 has no impact on development and is therefore highly unlikely to be the cognate partner of TodK, more clones of both strains should be obtained and examined.

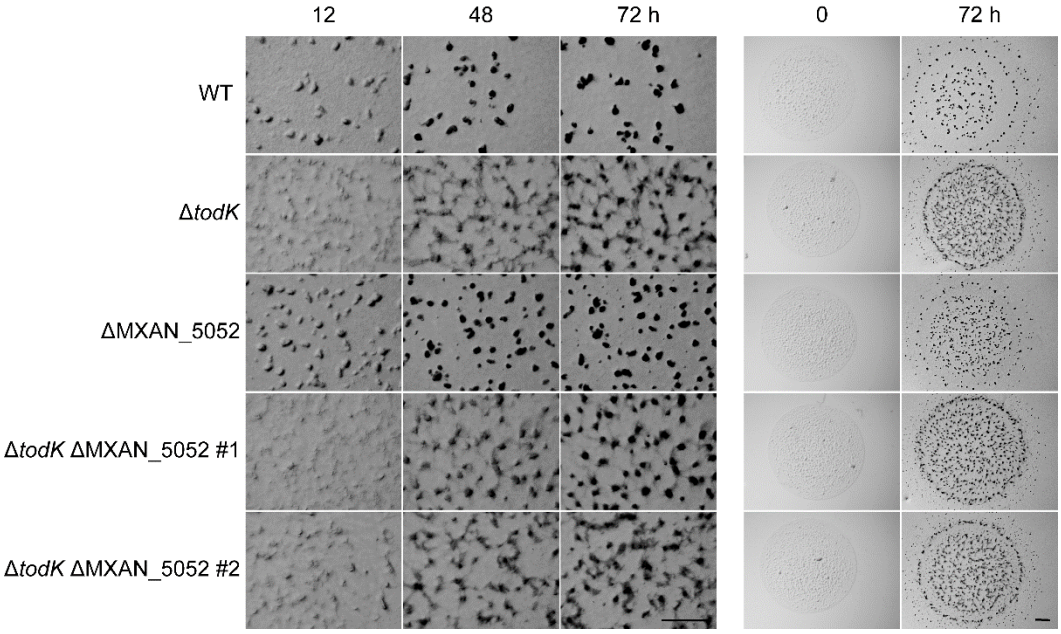

Figure 39: MXAN_5052 seems to have no impact on developmental progression and fruiting body morphology. *Starvation assay on CF agar.* Strains were grown to mid logarythmic phase, concentrated to $OD_{550\ nm}$ 7 and 10 µl aliquots were spotted. Dried plates were incubated at 32 °C. Pictures were taken at the indicated time points using a stereomicroscope. Left panel shows fruiting body morphology over the time course, right panel shows colony morphology of spotted (0 h) and developed (72 h) colony. WT wild type, scale bars 1 mm.

5.5. Hpk30 serves as a signal integration module that regulates *Myxococcus xanthus* developmental progression

An additional negative regulator involved in the appropriate regulation of *M. xanthus* development is the orphan putative histidine protein kinase Hpk30. We had the hypothesis that this kinase also is involved in appropriate MrpC accumulation. To further address how this might be facilitated, it was crucial to first understand the functionality and signal flow of this protein. Here I report the basic characterization of Hpk30 by combining *in vivo* and *in vitro* approaches.

5.5.1. Investigation of Hpk30 *in vivo*

5.5.1.1 Deletion of *hpk30* leads to early development and miss-accumulation of MrpC

In the genetic screen that identified Hpk30, two separate insertions in the gene MXAN_4465 were identified (K. Cho, P.I. Higgs, and D.R. Zusman; unpublished data). To confirm the phenotype, an in-frame-deletion strain of *hpk30* (Δ*hpk30*) was generated and the mutant phenotype investigated in detail in this study.

Under starvation conditions on nutrient limited CF agar plates, the Δ*hpk30* mutant produced aggregates after 18 h of starvation. This was 6-12 h earlier than observed for the wild type DZ2, which reached this point of developmental progression around 24-30 h (Figure 40, A). Interestingly, the exact timing of this mutant was variable to some degree: in most cases Δ*hpk30* developed as shown here (Figure 40), but occasionally it developed less quickly or (rarely) was indistinguishable from wild type cells. This variable phenotype did not depend on cell density when the strains were spotted onto CF agar (tested densities included $OD_{550\ nm}$ 1.75, 3.5, 7, 14 and 28) (data not shown). Also, a starvation assay on alternate solid medium (TPM) was performed, to investigate if media composition could have an effect on its developmental timing. Again, no correlation could be observed (data not shown). Hence, I decided to use the established assay on CF agar plates for further analysis.

When Δ*hpk30* development was investigated under submerged culture conditions, early aggregation was not observed: both wild type and Δ*hpk30* strains formed aggregates around 30 h of starvation which darkened between 48 and 72 h of development (Figure 40, B). While the wild type formed relatively regular and uniform fruiting bodies with respect to size and shape, the Δ*hpk30* mutant formed both big and very small fruiting bodies.

It has been shown previously that mutants aggregating earlier than wild type also had perturbed accumulation of the key transcriptional regulator, MrpC. To determine whether this was the case for the Δ*hpk30* mutant, lysates from cells developing in submerged culture harvested and analyzed by immunoblot. I could show that MrpC accumulated 6 h sooner in the Δ*hpk30* strain compared to wild type DZ2 (Figure 40, C). Also, similar to deletion strains of *todK* (this study and (Lee, 2009)) as well as *espA* and *espC* (Higgs *et al.*, 2008, Lee, 2009), MrpC over-accumulated in the Δ*hpk30* mutant at time of peak accumulation.

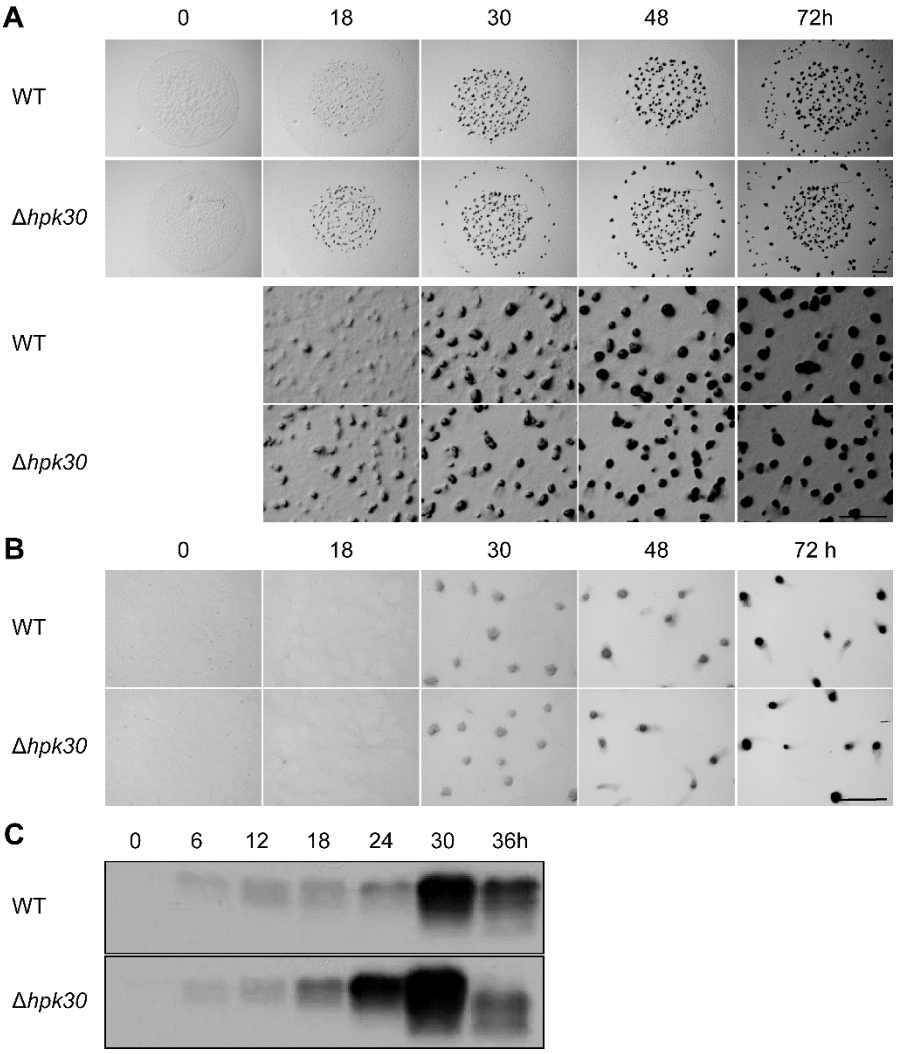

Figure 40: In-frame deletion of *hpk30* leads to accelerated development.
(A) *Developmental phenotype analysis on CF agar plates.* Strains were grown to mid exponential growth phase, harvested and 10 µl of concentrated cell suspension (OD_{550nm} 7) were spotted onto CF nutrient limited agar plates. Plates were incubated at 32 °C and starvation was observed for 72 h. Pictures were recorded at the indicated time points using a stereomicroscope. Colony as well as fruiting body morphology are depicted. Scale bars 1 mm. **(B)** *Developmental phenotype analysis under submerged conditions.* Strains were subjected to starvation in submerged culture at 32 °C and developmental stages were recorded using a stereomicroscope at the indicated time points. Scale bar 1 mm. **(C)** *Immunoblot analysis.* Development was induced under submerged starvation conditions and cell populations harvested at the indicated time points. Cells were lysed and 10 µg total protein were subjected to SDS-PAGE and analyzed by α-MrpC immunoblot. MrpC 27 kDa, WT: wild type.

Data presented in this section confirmed Hpk30 to be a negative regulator of development in *M. xanthus* which was demonstrated by early aggregation on CF agar plates, miss- and diversely shaped fruiting bodies as well as early and over-accumulation of MrpC. Using both genetic and biochemical techniques, I therefore set out to characterize the Hpk30 signaling module. This approach is an essential first step in elucidation of the mechanism by which Hpk30 effects MrpC accumulation.

5.5.1.2 *hpk30* is expressed and accumulated constantly during all life cycle stages

An earlier study reported gene expression of MXAN_4465 (*hpk30*) went up 2.1-fold between four and six hours of development in the alternate wild type strain DK1622, measured in a microarray approach (Shi *et al.*, 2008), but expression of this particular gene was not validated by quantitative real time PCR (qRT-PCR). For two reasons qRT-PCR was performed on this gene in this study: i) to validate the microarray results of Shi *et al.* and ii) to test whether the results obtained from the alternate wild type strain DK1622 are true for the wild type DZ2 (used in this study). DZ2 generally develops more slowly upon starvation, providing the advantage of more detailed time resolution. Quantitative real-time PCR revealed that *hpk30* mRNA levels indeed were upregulated upon induction of starvation and mRNA levels peaked at four hours of starvation (5.3 fold induction; normalized to vegetative expression levels at t = 0 h of development, Figure 41). Therefore, verifying the results of Shi *et al.* for the wild type strain DZ2.

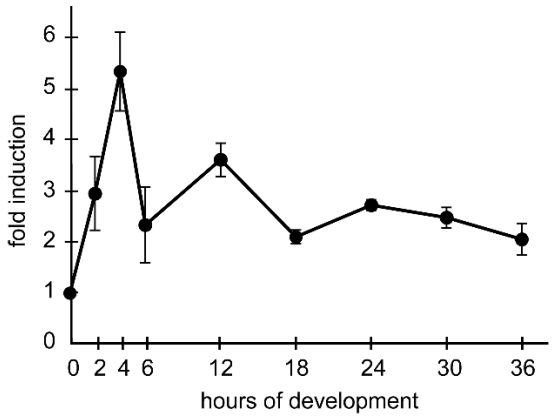

Figure 41: *hpk30* expression in vegetative and developing cells. *Quantitative real-time PCR of hpk30 mRNA.* Total RNA was isolated from wild type DZ2 cells at the indicated time points of starvation and transcribed into cDNA using random primers. Transcripts of *hpk30* were amplified with specific primers and detected by qRT-PCR. Signals were normalized to time point 0 h.

An important tool to address when Hpk30 could be active in the *M. xanthus* life cycle, is to first characterize the Hpk30 accumulation pattern. I therefore set out to generate customized α-Hpk30 antibodies. Purified recombinant Trx-His$_6$-Hpk30 protein was used as antigen for commercial antibody production by immunization of two rabbits. Initial testing of the resulting antisera with cell lysates prepared of wild type and Δ*hpk30* cells did not detect an Hpk30-specific signal by immunoblot analysis (data not shown and Figure 42, far left panel). This was due to many cross-reactive bands and is a commonly known complication. Therefore, specific α-Hpk30 antibodies were purified by incubating the sera with immobilized antigen, washing away non-specific antibodies (wash fraction), and then eluting the specific antibodies from the antigen (elution fraction). These antibody fractions were then assayed by immunoblot analysis of wild type and Δ*hpk30* cell lysates harvested from six hours of development, as well as the purified antigen (Figure 42). The wash antibody fraction showed the same cross reactive bands as the unpurified serum, indicating that the non-specific antibodies did not bind to the Hpk30 antigen. However, the purified antigen could still be detected in this fraction, suggesting that the amount of antigen used for capture

could have been increased. The elution antibody fraction were used at 1:500 (proportionally equivalent to unpurified sera) showed a strong signal for the purified target protein and very faint detection of band of 57 kDa, the calculated molecular mass of Hpk30, in the wild type but not *Δhpk30* lysate. If two-fold less dilute antibody was used, this specific Hpk30 signal was stronger.

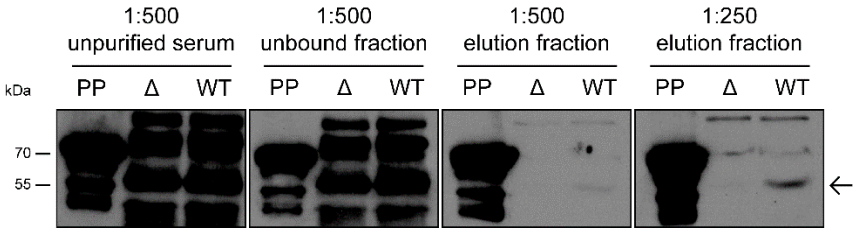

Figure 42: Purification of Polyclonal α-Hpk30 antibodies for immunoblot analysis of *M. xanthus* cell lysates. *Immunoblot analysis.* Cell lysates (10 µg total protein) of six hours developed *M. xanthus* strains (wild type WT and Δ*hpk30*) as well as purified protein (PP, Trx-His$_6$-Hpk30) were subjected to SDS-PAGE (9 %) and semi-dry immunoblotting. → marks Hpk30 (57 kDa) band, which was barely visible at 1: 500 dilution of purified antibody but well detectable at 1:250 dilution. It should be noted that antibody purifications lead to varying results regarding intensity of the Hpk30 specific band as well as number and intensity of cross reactive bands.

To investigate whether Hpk30 protein accumulation matched the mRNA expression pattern, immunoblot analysis using the custom generated and optimized α-Hpk30 antibodies was performed. Hpk30 protein accumulation in a wild type (DZ2) population was examined over a time course of development (Figure 43). Hpk30 could be detected in vegetative cells and did not disappear until 36 h of development (calculated molecular mass of Hpk30 57 kDa). In Δ*hpk30* cell lysates, a cross reactive band appeared at 24 and 30 h of development. This band could not be separated from Hpk30 under any assay modifications tested. Moreover, this band appeared at varying intensities in different assays and batches of purified antibody (data not shown). Therefore, I consider the increase of signal intensity observed in wild type lysates at 24 and 30 h of development not specific to Hpk30 and propose that Hpk30 is constitutively produced from 0 (vegetative cells) to at least 30-36 h of development.

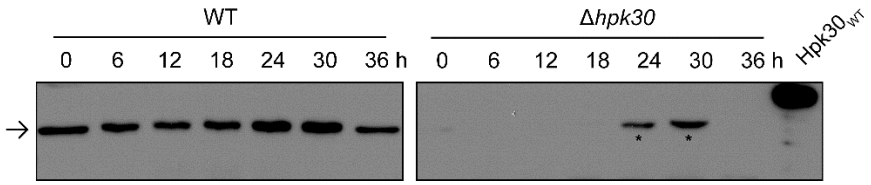

Figure 43: Hpk30 accumulates in vegetative and developing cells. *Immunoblot analysis.* Developing cell populations of wild type (WT) and Δ*hpk30* were harvested and cell lysates (10 µg total protein) were subjected to SDS-PAGE (9 %) and blotted onto PVDF membrane in a semi-dry procedure. Membranes were probed with affinity purified α-Hpk30 polyclonal antibodies. Purified protein (Hpk30$_{WT}$: Trx-His$_6$-Hpk30$_{WT}$) serves as a positive control and was detected at a higher molecular weight due to the attached Trx-His$_6$-tag used for protein purification (calculated mass of Trx-His$_6$-Hpk30 76 kDa). → marks Hpk30, * marks a cross reactive band, which appears at 24 and 30 h of starvation

5.5.1.3 Constitutive *hpk30* expression leads to delayed development

Deletion of *hpk30* led to an early developmental phenotype under different starvation conditions (Figure 40). I next wanted to investigate whether the developmental repression by Hpk30 could be forced by over expression of the protein. Therefore, I fused *hpk30* to the *pilA* promoter and integrated this Pr_{pilA}-*hpk30* construct into the Mx8 phage attachment site in the wild type and the Δ*hpk30* background strains. Strains were then developed on CF nutrient limiting agar plates and developmental progression was recorded.

Strains carrying the Pr_{pilA}-*hpk30* construct exhibited delayed development relative to the background strains (Figure 44). The mutant Δ*hpk30*/*hpk30*$^{++}$ (Δ*hpk30 attB*::Pr_{pilA}-*hpk30*) started to form aggregates after 30 h of starvation; 6 and 12 h later than was observed for the wild type and Δ*hpk30* strains, respectively. This delayed developmental phenotype was even more augmented in the strain WT/*hpk30*$^{++}$ (DZ2 *attB*::Pr_{pilA}-*hpk30*) which carries two copies of the *hpk30* gene. In this background, aggregation was only apparent after 48 h of development: an additional 12 and 24 h later than in Δ*hpk30*/*hpk30*$^{++}$ and wild type strains, respectively.

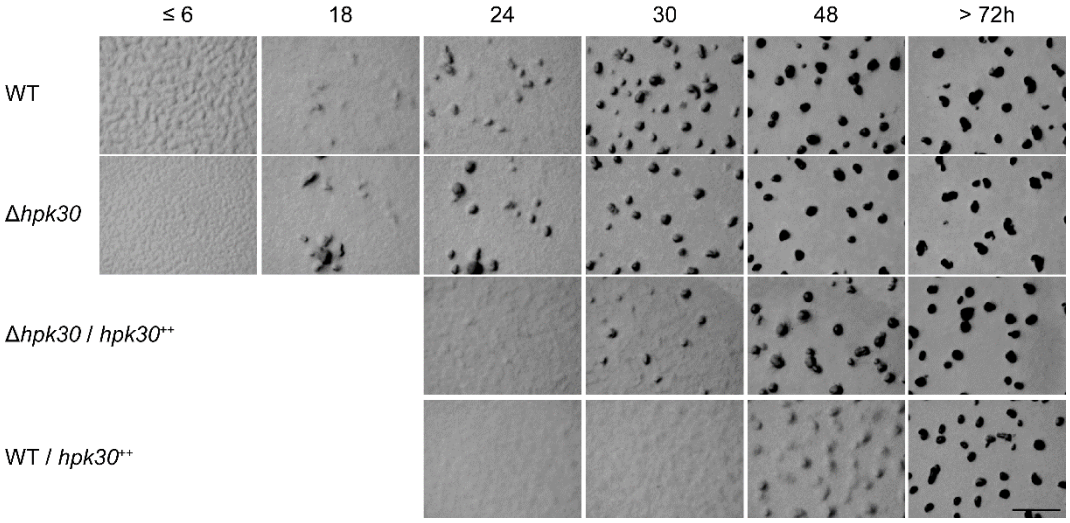

Figure 44: Expression of *hpk30* under the control of the *pilA*-promoter leads to delayed development. *Starvation assay on CF agar plates.* Vegetatively growing strains were harvested and 10 µl spots of $OD_{550\ nm}$ 7 were placed on CF nutrient limiting agar plates. Inverted plates were incubated at 32 °C and pictures were taken at the indicated time points. Complemented strains, expressing *hpk30* under the control of the *pilA* promoter (Pr_{pilA}) from the Mx8 phage attachment site (*attB*) in the *M. xanthus* genome, were given the following designations: Δ*hpk30*/*hpk30*$^{++}$ (Δ*hpk30 attB*::Pr_{pilA}-*hpk30*), WT/*hpk30*$^{++}$ (WT *attB*::Pr_{pilA}-*hpk30*). WT: wild type, scale bar 1 mm.

Interestingly, when the Pr_{pilA}-*hpk30* strains were analyzed under submerged culture developmental conditions, in which the early aggregation phenotype of the Δ*hpk30* is suppressed, the delay in aggregation was also not observed. (Figure 45). However, fruiting bodies failed to darken suggesting sporulation was likely delayed. Consistently, darkening of fruiting bodies was even further delayed in WT/*hpk30*$^{++}$ than in Δ*hpk30*/*hpk30*$^{++}$ at 120 h of starvation.

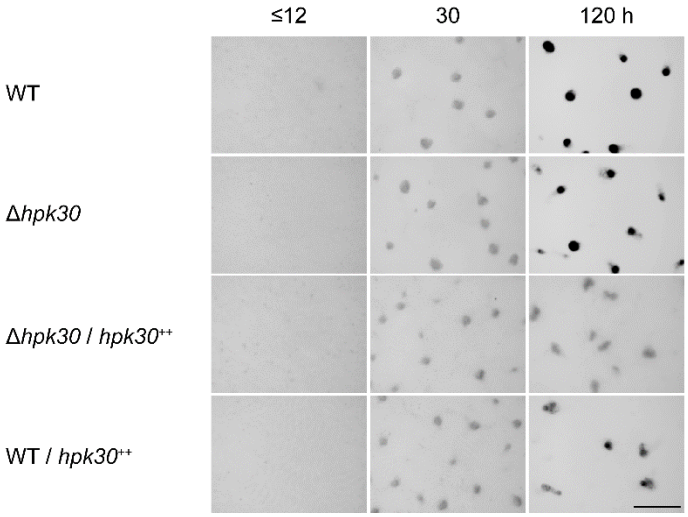

Figure 45: Expression of Hpk30 driven by the *pilA* promoter may cause delayed sporulation. *Starvation assay under submerged culture conditions.* Strains were grown to mid exponential phase and seeded to develop under submerged conditions. Incubation took place at 32 °C and pictures were recorded at the indicated time points using a stereomicroscope. Complemented strains, expressing *hpk30* under the control of the *pilA* promoter (Pr_{pilA}) from the Mx8 phage attachment site (*attB*) in the *M. xanthus* genome, were given the following designations: Δ*hpk30*/*hpk30*$^{++}$ (Δ*hpk30 attB*::Pr_{pilA}-*hpk30*), WT/*hpk30*$^{++}$ (WT *attB*::Pr_{pilA}-*hpk30*). WT: wild type, scale bar 1 mm.

To determine whether Hpk30 was indeed overproduced when expressed from the *pilA* promoter, total cell lysates from each strain developed for 0 and 24 h were harvested, lysed and equal concentration of total protein was subjected to immunoblot analysis utilizing purified α-Hpk30 polyclonal antibody (Figure 46). Hpk30 was barely detectable in the wild type strain, and absent from the Δ*hpk30* lysates. However, a very strong signal could be detected in both WT/*hpk30*$^{++}$ (WT *attB*::Pr_{pilA}-*hpk30*) and Δ*hpk30*/*hpk30*$^{++}$ (Δ*hpk30 attB*::Pr_{pilA}-*hpk30*) strains. Suggesting the delayed developmental phenotype to be caused by over-accumulation of Hpk30 protein and confirmed Hpk30 to be a negative regulator of *M. xanthus* development.

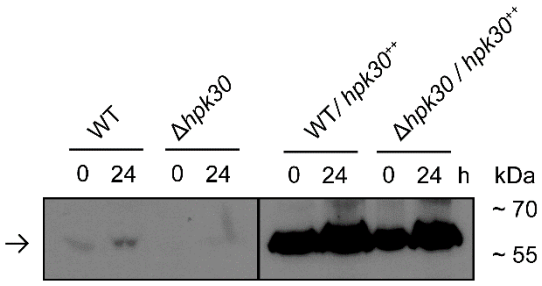

Figure 46: Hpk30 is overproduced and accumulates at high levels when expressed from the *pilA*-promoter. *Immunoblot analysis.* Development was induced under submerged culture conditions and total cell populations were harvested at 0 and 24 h of starvation. 10 ug total protein was analyzed in an immunoblot probed with affinity purified α-Hpk30 polyclonal antibodies. Both immunoblot panels were exposed for 5 min. Complemented strains expressing *hpk30* under the control of the *pilA* promoter (Pr_{pilA}) from the Mx8 phage attachment site (*attB*) in the *M. xanthus* genome, were given the following designations: WT/*hpk30*$^{++}$ (WT *attB*::Pr_{pilA}-*hpk30*); Δ*hpk30*/*hpk30*$^{++}$ (Δ*hpk30 attB*::Pr_{pilA}-*hpk30*). Hpk30 57 kDa, WT: wild type.

5.5.2. Characterization of the Hpk30 signaling domains *in vivo*

The data obtained so far suggested Hpk30 negatively regulated developmental progression upon starvation in *M. xanthus*. According to domain prediction programs, Hpk30 consists of a histidine kinase domain and two receiver domains. These three domains raised the question how this protein functions as a signaling module. Variable models were possible including autophosphorylation on the invariant histidine in the histidine kinase domain, phosphor transfer to one or both aspartates in the receiver domains or even the integration of two or three independent signals in a “many-to-one”-signal integration pathway. To investigate these possibilities, I started with generating single amino acid point mutants in the *M. xanthus* wild type background and investigated the obtained phenotypes under starvation conditions.

5.5.2.1 Substitution of the invariant histidine in Hpk30 kinase domain leads to early development

The first point mutant investigated was a mutation abolishing autophosphorylation. The putative site of autophosphorylation was determined to be H45 by sequence alignments. A putative kinase inactive mutant was obtained by mutating the H45 CAC codon to the GCG alanine codon (Figure 47, A). The codon was chosen based on the most frequently used codon encoding this amino acid in *M. xanthus* (Nakamura *et al.*, 2000). The mutation was introduced by homologous recombination into the native *hpk30* gene and confirmed by sequencing. The generated mutant strain was subjected to starvation on CF nutrient agar plates and developmental progression was monitored. While the wild type and Δ*hpk30* strains developed as described before, the $hpk30_{H45A}$ mutant developed with an early aggregation phenotype (Figure 47, B). This mutant formed aggregates around the same time as Δ*hpk30*, yet the resulting fruiting bodies formed by $hpk30_{H45A}$ were more disorganized than the ones formed by the deletion mutant. Also, darkening of the fruiting bodies appeared to be delayed, suggesting delayed sporulation or more spores produces outside of the fruiting body.

To test if the mutated version of the produced protein was stable, cell lysates were generated and analyzed by α-Hpk30 immunoblot (Figure 47, C). The entire cell population was harvested from submerged culture at 0 h of starvation (= vegetative growth). Signal intensities obtained from wild type and point mutant protein ($Hpk30_{H45A}$) were comparable, while the signal was absent from the deletion mutant. Suggesting that the protein was produced at wild type levels and stable in the cell. Hence, the starvation phenotype observed in this mutant likely resulted from disruption of function. In return this meant that Hpk30 likely acted as an active histidine protein kinase to negatively regulate developmental progression.

In the paradigm model of a hybrid histidine kinase, the signal would be transferred from the histidine over to a receiver domain to generate a signal output (Stock *et al.*, 2000, Jenal & Galperin, 2009). To investigate if this model was applicable to Hpk30,

I next generated alanine substitutions of the conserved aspartates in both the receiver domains of this protein.

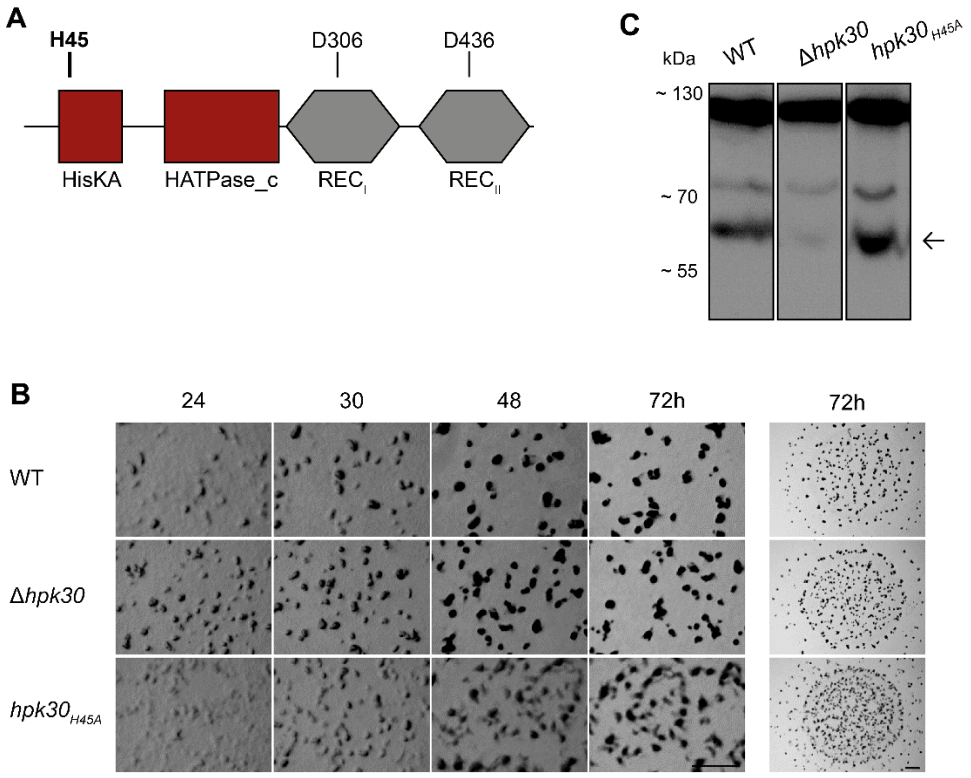

Figure 47: Substitution of the putative site of autophosphorylation leads to an early development phenotype. (A) *Schematic of the Hpk30 protein domain architecture and conserved histidine residue.* The histidine at amino acid position 45 was substituted by an alanine to generate and mimic a non-phosphorylated state. **(B)** *Developmental phenotype assay on CF agar.* Vegetatively growing strains were harvested and 10 µl spots of $OD_{550\ nm}$ 7 were placed on CF nutrient limiting agar plates. Inverted plates were incubated at 32 °C and pictures were taken at the indicated time points. Scale bars 1 mm. **(C)** *Immunoblot analysis.* Strains were harvested at 0 h of development from 16 ml submerged culture, lysed and 10 µg total protein were subjected to SDS-PAGE and immunoblot procedure using α-Hpk30 antibody. The arrow highlights the specific Hpk30 (57 kDa) band. WT: wild type.

5.5.2.2 Substitution of the conserved aspartate of the first receiver domain of Hpk30 causes delayed development

The first annotated receiver domain of Hpk30 was hypothesized to use the phosphorylated histidine kinase domain as phosphor donor and therefore be a signal output of this protein. Therefore, a mutant with this domain rendered inactive would have the same developmental effect during starvation as observed in the kinase inactive *hpk30$_{H45A}$* mutant strain. The conserved aspartate of the first receiver domain was determined by sequence alignments to be at amino acid position 306. To mutate this amino acid into an alanine, incapable of being phosphorylated, the codon GAC was mutated to GCG by overlap PCR and integrated into the genome by homologous recombination at the native site (Figure 48, A). Obtained mutants were confirmed by sequencing.

The generated mutant strain *hpk30*$_{D306A}$ was spotted onto CF starvation plates and developmental progression was monitored (Figure 48, B). Compared to the control strains, the *hpk30*$_{D306A}$ strain was delayed in aggregation. Mature aggregates were formed between 30 and 48 h of starvation, more than 12 h later than in the Δ*hpk30* mutant. Immunoblot analysis indicated that wild type and mutant Hpk30 levels were similar at the onset of development (Figure 48, C). This finding suggested that phosphorylation of Hpk30 REC$_I$ is necessary to induce efficient aggregation. It also suggests that the Hpk30 REC$_I$ phosphodonor is unlikely Hpk30 kinase activity, because the kinase inactive mutant has an opposing phenotype (Figure 47).

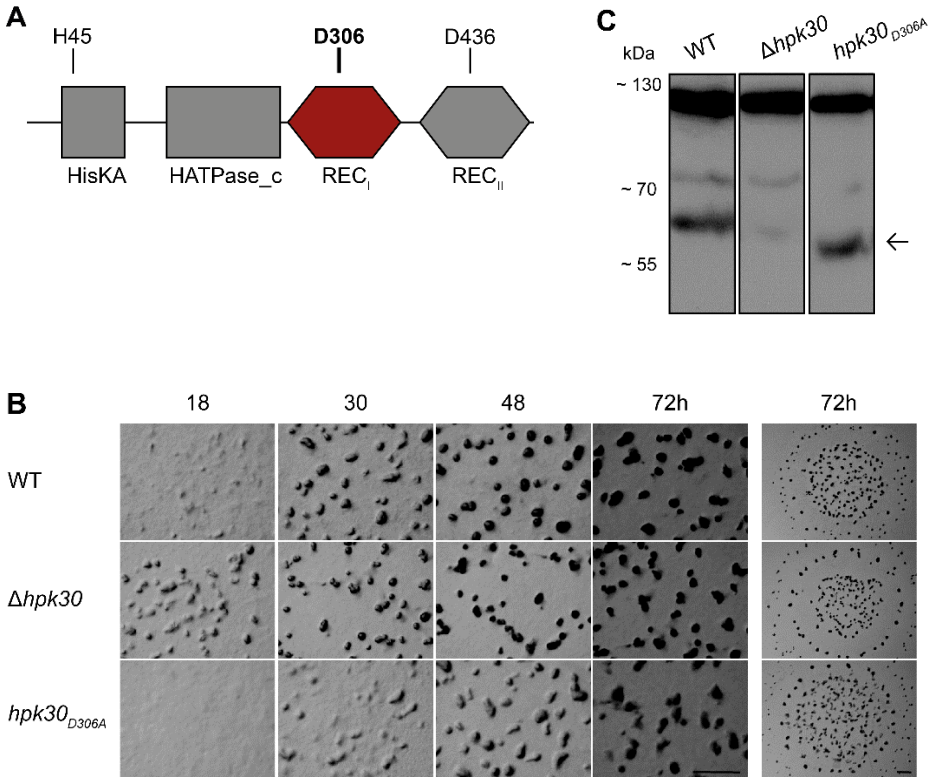

Figure 48: Substitution of the putative site of phosphorylation in the first receiver domain leads to delayed developmental progression. (A) *Schematic of the Hpk30 protein domain architecture and conserved aspartate residue in REC$_I$.* The aspartate at amino acid position 306 was substituted by an alanine, mimicking the non-phosphorylated state of this domain. **(B)** *Developmental phenotype assay on CF agar.* Vegetatively growing strains were harvested and 10 µl spots of $OD_{550\ nm}$ 7 were placed on CF nutrient limiting agar plates. Inverted plates were incubated at 32 °C and pictures were taken at the indicated time points. Scale bars 1 mm. **(C)** *Immunoblot analysis.* Strains were harvested at 0 h of development from 16 ml submerged culture, lysed and 10 µg total protein were subjected to SDS-PAGE and immunoblot procedure using α-Hpk30 antibody. The arrow highlights the specific Hpk30 (57 kDa) band. WT: wild type.

5.5.2.3 Substitution of the conserved aspartate in the second receiver domain of Hpk30 causes non-robust delayed development

I next examined whether Hpk30 Rec$_{II}$ was necessary for Hpk30 function by mutating the conserved aspartate at position 436 (Figure 49, A) from the native GAC codon to a GCG codon (encoding alanine). This mutation was generated in the native locus and confirmed by sequencing. Analysis of the developmental phenotype compared to

wild type and Δ*hpk30* cells indicated (Figure 49, B). The *hpk30*$_{D436A}$ mutant showed delayed aggregation. However, the degree of aggregation delay was not robust. Observed most frequently was that aggregates were formed 12 h later than in the wild type and 24 h later than in the Δ*hpk30* mutant (Figure 49, B). α-Hpk30 immunoblot analysis (Figure 49, C) showed that Hpk30$_{D436A}$ accumulated at levels comparable to the native version. Since this phenotype is also dissimilar to the one observed from *hpk30*$_{H45A}$ (kinase inactive mutant) (Figure 47), it is unlikely that phosphor transfer from the kinase occurred to the second receiver domain. Taken together, the results of these *in vivo* studies suggested a model in which Hpk30 acts as a signaling module integrating many input signals to modulate an output of the system.

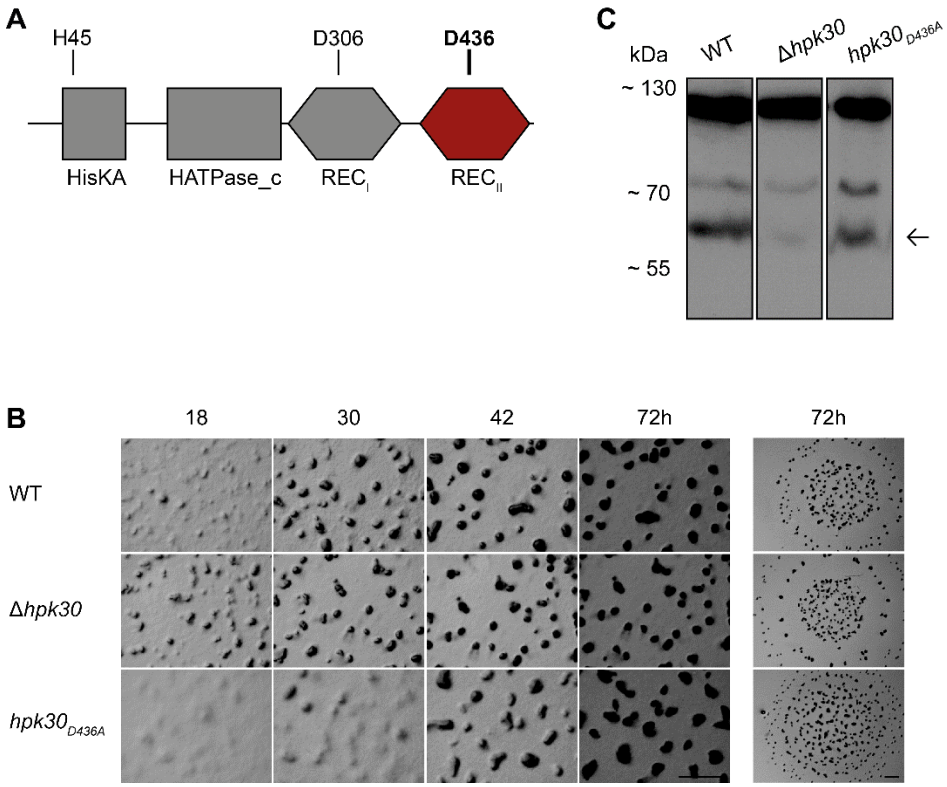

Figure 49: Substitution of the putative site of phosphorylation in the second receiver domain of Hpk30 leads to delayed developmental progression. (A) *Schematic of the Hpk30 protein domain architecture and conserved aspartate residue in REC$_I$.* The aspartate at amino acid position 436 was substituted by an alanine, resulting in a mutant form of the protein that mimics the non-phosphorylated state of this domain. **(B)** *Developmental phenotype assay on CF agar.* Vegetatively growing strains were harvested and 10 µl spots of $OD_{550\ nm}$ 7 were placed on CF nutrient limiting agar plates. Plates were incubated at 32 °C and pictures were taken at the indicated time points. Scale bars 1 mm. **(C)** *Immunoblot analysis.* Strains were harvested at 0 h of development from 16 ml submerged culture, lysed and 10 µg total protein were subjected to immunoblot procedure using α-Hpk30 antibody. The arrow highlights the specific Hpk30 (57 kDa) band. WT: wild type.

5.5.3. Investigation of Hpk30 *in vitro*

My genetic analyses suggested Hpk30 is an active histidine protein kinase *in vivo*, based on the early developmental phenotype of a mutant incapable of autophosphorylation (*hpk30*$_{H45A}$). To support this hypothesis and to gain deeper knowledge in the activity of this protein, *in vitro* analysis were performed. His$_6$-tagged recombinant Hpk30 was overexpressed in *E. coli* and purified via affinity tag chromatography to perform radioactive kinase assays. To better understand if Hpk30 transferred a phosphate from its histidine to either or both receiver domains, a chemical stability test supplemented this investigation.

5.5.3.1 Recombinant overexpression and purification of Hpk30

The *hpk30* gene (WT and H45A, kinase inactive mutant) were cloned into pET32a (Invitrogen) vectors, generating plasmids producing Trx-His$_6$-Hpk30$_{WT/H45A}$ upon induction via the T7 promoter. Out of a variety of induction and expression conditions, the following procedure resulted in the highest amount of soluble expressed protein of interest. Plasmids were transformed into the salt inducible *E. coli* strain GJ1158 (malP::(proUp-T7 RNAP)) and cells were grown to early mid-logarithmic phase (OD_{600nm} 0.5) at 37 °C. Cultures were transferred to 18 °C and continued to grow until late-mid logarithmic phase (OD_{600nm} 0.7). Induction of protein expression took place by addition of 300 mM NaCl and was continued over night at 18 °C, to ensure slow protein overexpression avoiding formation of inclusion bodies. Cells were lysed by French press and centrifugation was performed to separate soluble proteins from un-lysed cells and insoluble fractions. Successful induction and solubility of overexpressed proteins was shown using SDS-PAGE (Figure 50, A Trx-His$_6$-Hpk30$_{WT}$; expression of Trx-His$_6$-Hpk30$_{H45A}$ was performed accordingly, data not shown). Purification of Hpk30 proteins from the respective soluble fractions was performed via Ni-NTA-affinity chromatography on an ÄKTA system (Figure 50, B and C; elution chromatogram and SDS-PAGE of elution fractions; B Trx-His$_6$-Hpk30$_{WT}$ and C Trx-His$_6$-Hpk30$_{H45A}$). The four elution fractions of highest protein content and purity were pooled for each protein and dialyzed into storage buffer and used for further analysis.

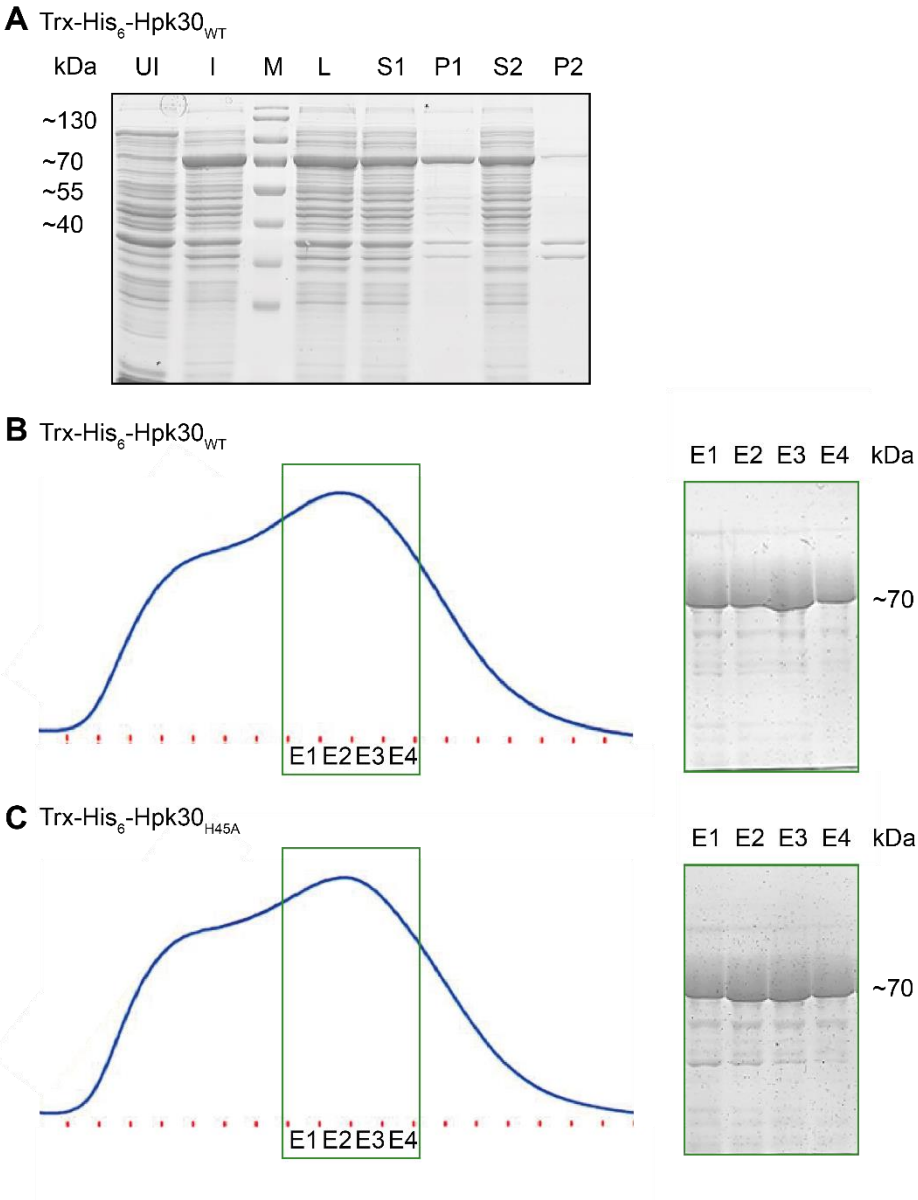

Figure 50: Soluble overexpression and affinity purification of Trx-His$_6$-Hpk30$_{WT}$ and Trx-His$_6$-Hpk30$_{H45A}$ from *E. coli* culture. (A) *SDS-PAGE of critical fractions obtained during expression and purification of Trx-His$_6$-Hpk30$_{WT}$.* The plasmid carrying the gene to overexpress Trx-His$_6$-Hpk30$_{WT}$ (pMG022) was transformed into the salt inducible *E. coli* strain GJ1158 (malP::(proUp-T7 RNAP)) and grown to early exponential phase at 37 °C. Protein overexpression was induced with 300 mM NaCl at 18 °C over night. Samples were taken during the entire process and equal proportions were subjected to SDS-PAGE (8 %). UI un-induced; I induced; L lysate; S1 supernatant fraction 1; P1 pellet fraction 1; S2 supernatant centrifugation 2; P2 pellet centrifugation Marker 2. Expression of Trx-His$_6$-Hpk30$_{H45A}$ was performed using plasmid pMG023 and looked similar (data not shown). *Elution chromatograms and SDS-PAGE analysis of elution fractions of Trx-His$_6$-Hpk30$_{WT}$* ***(B)*** *and Trx-His$_6$-Hpk30$_{H45A}$* ***(C)****. Protein purification was performed via Ni-NTA affinity chromatography (ÄKTA).* Elution fractions were analyzed on SDS-PAGE (8 %) and the four purest were chosen for further analysis (green box), pooled and dialyzed. E 1-4 four purest elution fractions. Calculated molecular weight Trx-His$_6$-Hpk30 ~70 kDa.

5.5.3.2 Hpk30 is an active histidine protein kinase *in vitro*

The early developmental phenotype of an Hpk30 mutant incapable of autophosphorylation (*hpk30$_{H45A}$*) suggested that phosphorylation of Hpk30 was needed for the protein to negatively regulate developmental progression (section 5.5.2). To test if Hpk30 is an active HPK *in vitro*, radioactive kinase activity assays were performed. Purified Trx-His$_6$-Hpk30$_{WT}$ protein was incubated with radioactively labeled ATP ([γ^{32}P]-ATP) and incubated at 32 °C. By 10 minutes, the radioactive label was detected on the wild type Hpk30 protein (Figure 51). The signal continued to further increase until 25 min. In contrast, no signal could be detected using the mutant protein where the potential phosphor-accepting residue histidine 45 was substituted with an alanine (Trx-His$_6$-Hpk30$_{H45A}$), even after prolonged incubation until 45 min. I concluded that Hpk30 is in fact an active histidine protein kinase which can autophosphorylate on the conserved histidine residue at amino acid position 45.

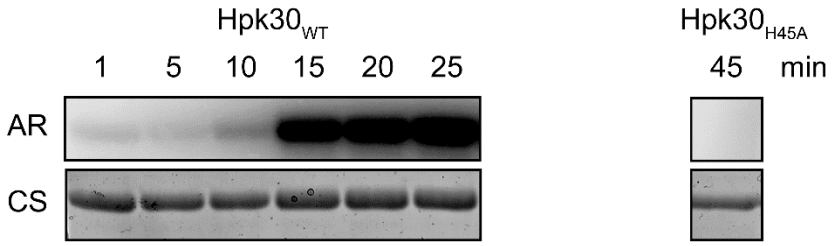

Figure 51: Trx-His$_6$-Hpk30$_{WT}$ autophosphorylates *in vitro*. *Radioactive phosphorylation assay.* 10 µM purified protein were incubated for a total of 45 min with radioactively labeled [γ^{32}P]-ATP, aliquots were removed and quenched at the indicated time points. Proteins were resolved using SDS-PAGE and the radiolabel was detected by exposure to a storage Phospho Screen (autoradiogram, AR). Total loaded protein was visualized using Coomassie stain (CS) afterwards. Trx-His$_6$-Hpk30 has a calculated molecular mass of ~70 kDa. Trx-His$_6$-Hpk30$_{H45A}$ was used as a negative control and showed no incorporation of radioactively labeled ATP at the endpoint of this assay.

5.5.3.3 Phosphorylation likely solely occurs on the histidine and is not transferred to the receiver domains

Hpk30 is a multi-domain protein consisting of a histidine protein kinase domain followed by two receiver domains. *In vivo* data suggested that phosphorylation occurred on histidine 45 but was not transferred further to either receiver domain (Figure 47, Figure 48 and Figure 49). To test if phosphor-transfer from kinase to receiver domain(s) occurs *in vitro*, a chemical stability test of the phosphoryl group on phosphorylated Hpk30 was performed. The assay takes advantage of the differential stability of phosphor-histidine under acidic and alkaline media conditions: N-phosphates (phosphohistidine) are stable under alkaline conditions but labile in acidic environments; in contrast, acyl phosphates (phosphoaspartate) are labile under both conditions (Duclos *et al.*, 1991).

Purified Trx-His$_6$-Hpk30 was incubated with [γ^{32}P]-ATP as described above (section 5.5.3.2) to autophosphorylate. The phosphorylation reaction was quenched with SDS-sample buffer and divided into four aliquots: one was immediately frozen at – 20 °C as an assay control to show total radiolabel on the protein after 30 min

autophosphorylation time. The three remaining aliquots were treated with either 1 M HCl, H_2O, or 1 M NaOH, and incubated at 42 °C for one hour. Protein was subjected to SDS-PAGE and radiolabel was detected using a phosphor screen (Figure 52 A). Chemical stability assay was performed in four technical replicates and obtained radiolabel was quantified (Figure 52, B). The aliquot that was frozen as an assay control assured assay functionality. The recorded signal was set as 100 % for ratio quantification of the signal from the three chemical treatments. The aliquot treated with water gave a signal comparable to the untreated sample. Indicating that incubation of the phosphorylated protein at higher temperature for a longer time did not result in loss of signal. Acid treatment resulted in an 88 % signal reduction, while the signal remained similar to the water control and in alkaline conditions.

The finding suggested that accumulation of radiolabel occurred solely on the histidine. This was consistent with the observation *in vivo* (section 5.5.2) and supported the hypothesis that no phosphor transfer took place to both receiver domains. If there would be phosphate transmission onto an aspartate in either (or both) of the receivers, a decrease in the radiolabel recorded in the alkaline (NaOH) treated aliquot would occur. It should be noted that there also would be the slight possibility that phosphor transfer to the receiver domain(s) occurred but the obtained phosphorylation was very instable overall. Dephosphorylation would occur so quickly that it could not be monitored in this assay. To test this possibility, this assay could be complemented with an assay to monitor free phosphate generated in the solution to gain knowledge about rates of dephosphorylation in various chemical environments.

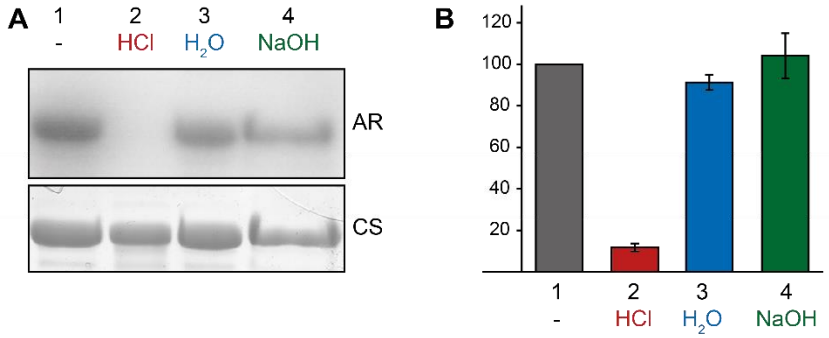

Figure 52: Phosphorylation of Trx-His$_6$-Hpk30$_{WT}$ is acid labile but base stabile. (A) *Radioactive phosphorylation assay.* One batch 10 µM purified protein was incubated at 32 °C for a total of 30 min with radioactively labeled [γ^{32}P]-ATP. Afterwards reaction was quenched with SDS-sample buffer and the batch was separated into four aliquots that were treated with different chemicals: 1) frozen at -20 °C immediately; 2) 1 M HCl; 3) pure water; 4) 1 M NaOH. Incubation was done for 60 min at 42 °C. Proteins were resolved using SDS-PAGE and the radiolabel was detected by exposure to a storage Phospho Screen (autoradiogram, AR). Total loaded protein was visualized using Coomassie stain (CS). **(B)** *Quantification of phosphorylation signal*. Four technical replicates of the assay described in A were performed and quantified using image J; the average and associated standard deviation are reported**.**

5.5.4. MXAN_4466 influences Hpk30 activity *in vivo*

In the paradigm two component system, the histidine protein kinase is encoded in one operon together with the response regulator that mediates the output of the signaling module (Stock *et al.*, 2000). Hpk30 was found to be encoded in the *M. xanthus* genome as an orphan gene (Shi *et al.*, 2008). By definition this means no potentially cognate response regulator is encoded next to the *hpk30* gene, neither as an operon nor in a complex gene cluster (Shi *et al.*, 2008). However, when investigating the genetic locus of *hpk30* (MXAN_4465), I found that it is encoded adjacent to another gene (MXAN_4466) predicted to be partially overlapping. Genes which overlap in part or even only on the stop/start codons are often transcriptionally coupled. Hence, I hypothesized a functional connection between these two genes and their resulting proteins and set out to further investigate the importance and potential function of MXAN_4466.

5.5.4.1 Comparative genomic analysis of *hpk30* and MXAN_4466

MXAN_4465 (*hpk30*) and MXAN_4466 were annotated to overlap by 80 base pairs at the starting time of this study (May 2011). In a comparative genomics approach, I could show comparing the annotations of both genes in the genomes of *M. xanthus* (Goldman *et al.*, 2006), *M. fulvus* (Li *et al.*, 2011) *M. stipitatus* (Huntley *et al.*, 2013) and *M. macrosporus* (unpublished data, kindly provided by Stuart Huntley and Lotte Søgaard-Andersen) that the annotation in *M. xanthus* was most likely incorrect and that the real start codon of MXAN_4466 overlapped with the stop codon of *hpk30*. MXAN_4466 was re-annotated to the same sequence I predicted in January 2014.

Comparative genomic analysis was also used to elucidate the evolutionary conservation of the two genes (Figure 53). Ortholog genes were identified in the published Myxococcales genomes (Goldman *et al.*, 2006, Huntley *et al.*, 2011, Li *et al.*, 2011, Huntley *et al.*, 2012, Huntley *et al.*, 2013) using a reciprocal BLASTp analysis and in the unpublished genomes (kindly provided by Stuart Huntley and Lotte Søgaard-Andersen) using the Artemis Comparison Tool (Wellcome Trust Sanger Institute). The second approach was also used to confirm genes identified with the reciprocal BALSTp method. By comparing published and non-published genomes of different *Myxococcales*, I could show that MXAN_4466 orthologs were only present in very closely related species: *M. xanthus* (Goldman *et al.*, 2006), *M. fulvus* (Li *et al.*, 2011), *M: macrosporus* (unpublished data, kindly provided by Stuart Huntley and Lotte Søgaard-Andersen) and *M. stipitatus* (Huntley *et al.*, 2013). In contrast, *hpk30* was also present in rather distantly related species like *C. coralloides* (Huntley *et al.*, 2012) and *S. aurantiaca* (Huntley *et al.*, 2011); whereas both genes were missing in *A. dehalogenans* (Thomas *et al.*, 2008b), *S. cellulosum* (Schneiker *et al.*, 2006) and *H. ochraceum* (Ivanova *et al.*, 2010). This led to the hypothesis that the gene MXAN_4466 is specific to the *Myxococcus* genus and was evolutionary rather recently acquired.

The co-occurrence of the two genes in the *Myxococcus* genus together with the overlap of a few base pairs raised the intriguing hypothesis that MXAN_4466 could be transcriptionally coupled with *hpk30* and had the potential to be the regulatory output of this signaling module.

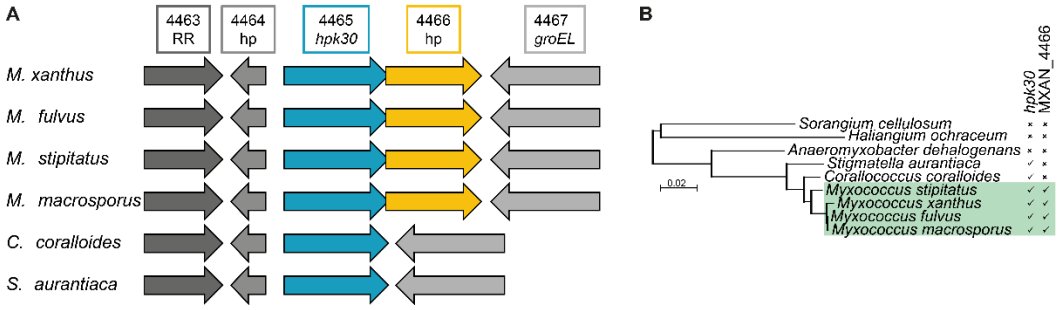

Figure 53: Comparison of the genetic context of *hpk30* in *M. xanthus* with related species. (A) *Genetic locus of hpk30.* Depicted are *hpk30* and neighboring genes with their orientation on the genome and according to their length. *hpk30* and MXAN_4466 overlap with their respective stop/ start codons. hp: hypothetical protein. **(B)** *Co-occurrence of hpk30 and MXAN_4466 orthologs in different species.* The dendrogram represents the relationship of members of the order *Myxococcales* based on their 16s rRNA (kindly provided by Stuart Huntley). √ gene present in analyzed genome, x gene absent from analyzed genome; marked in green is the genus *Myxococcus.*

5.5.4.2 *hpk30* and MXAN_4466 are co-transcribed

Since *hpk30* and MXAN_4466 overlap with their respective stop and start codon, I investigated if they were co-transcribed as an operon (Figure 54, A). For this purpose, cDNA was generated by reverse transcription of mRNA obtained from three hours starved *M. xanthus* DZ2 cells. Reverse transcription was performed using an oligonucleotide which binds mRNA of MXAN_4466, reading reverse in the direction of *hpk30* (Figure 54, A). Obtained cDNA was used for test PCRs to elucidate if cDNA of the transcript from *hpk30* was generated as well from this oligonucleotide binding in the gene MXAN_4466. One scenario would support the hypothesis that *hpk30* and MXAN_4466 are transcribed in a transcriptional unit. This means if both genes are transcriptionally coupled they are transcribed as one mRNA. If mRNA is reverse transcribed into cDNA from the gene MXAN_4466 backwards both genes are present in one fragment of cDNA. A second possibility would reflect the scenario that *hpk30* and MXAN_4466 are transcriptionally independent. This would show that reverse transcribing mRNA into cDNA from MXAN_4466 in the direction of *hpk30* leads only to cDNA of MXAN_4466 since *hpk30* would be an independent fragment of mRNA.

Three individual test PCRs were performed (Figure 54, B):

i) a control to ensure reverse transcription (cDNA generation) was successful using oligonucleotides binding in MXAN_4466 itself (Figure 54, B yellow), the same gene the oligonucleotide to generate cDNA bound in;

ii and iii) PCRs testing if *hpk30* cDNA could be obtained using an oligonucleotide binding on mRNA of the other gene (Figure 54, B blue and green).

In each PCR set (i, ii and iii) a positive control using genomic DNA (gDNA) was included to assure correct assay design (primer comparability, elongation times and temperatures). As a negative control total mRNA was included in each PCR set (i, ii and iii), to exclude the possibility of gDNA contamination in the reaction mix for cDNA generation. Both control PCRs worked correctly for all three PCR sets (i, ii and iii).

The PCR performed with a primer pair binding inside the gene MXAN_4466 (Figure 54, B yellow) confirmed cDNA generation was successful. PCR products on cDNA using primers binding inside *hpk30* (Figure 54, B blue) as well as over the gene junction (Figure 54, B green) confirmed that the two investigated genes were transcribed as one mRNA and therefore are transcriptionally coupled. This supported the intriguing hypothesis that MXAN_4466 could be the signaling output of Hpk30 in the *M. xanthus* developmental program.

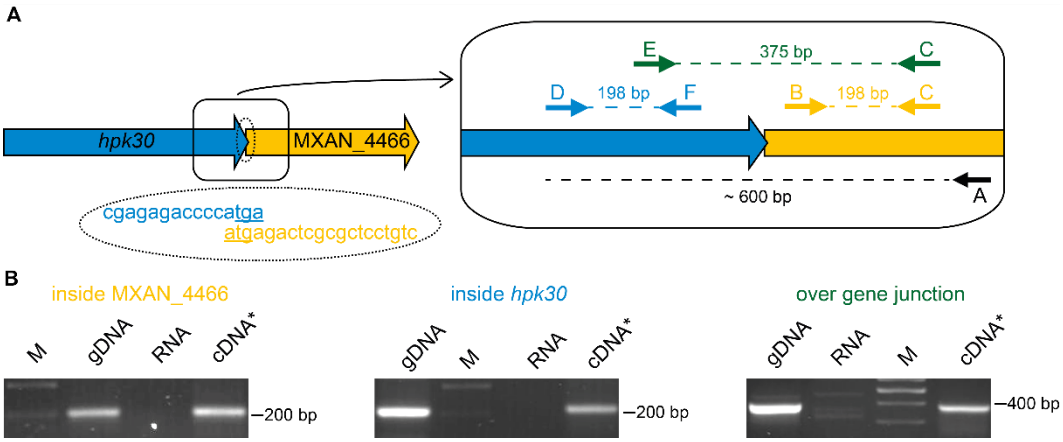

Figure 54: *hpk30* and the gene downstream MXAN_4466 are encoded in an operon. (A) *Schematic of the gene locus.* The neighboring genes *hpk30* (blue) and MXAN_4466 (yellow) overlap with their stop and start codons. To test if they are co-transcribed, primers were generated binding in various locations of both genes (for a detailed description see text and (B)). **(B)** *Operon mapping by PCR on cDNA.* cDNA was generated from wild type, developed for 3 h under submerged culture conditions using primer "A". Oligonucleotide primer pair "B and C" (yellow) were used to amplify a fragment inside the gene MXAN_4466, primer pair "D and F" (blue) from gene *hpk30*; primer pair "E and C" (green) spans over both genes with one oligonucleotide binding in each of them. Genomic DNA (gDNA) from wild type was used as a positive control, the same RNA used for cDNA generation was used as a negative control.

5.5.4.3 MXAN_4466 encodes a protein that positively regulates development

An insertion mutant in the gene MXAN_4466 was generated to investigate impact of this gene on *M. xanthus* developmental progression. All attempts at generating an in-frame deletion of this gene failed, which is why I continued to work with the insertion mutant. Several independent clones of this insertion mutant displayed comparable developmental phenotypes. When starved on nutrient limiting CF agar plates, the insertion mutant MXAN_4466::pMG011 started to form aggregates at 48 h of starvation; 24 h later than the wild type strain DZ2 (Figure 55). This was particularly interesting since it was the opposite phenotype displayed by Δ*hpk30*, which developed earlier than wild type under these conditions. The delayed phenotype of this insertion mutant suggested MXAN_4466 to either be a positive regulator of

development or to be needed to release developmental inhibition from a negative regulator.

The data suggested *hpk30* and MXAN_4466 to be transcribed into one mRNA and mutations of either gene resulted in opposite developmental phenotypes. However, the approach could not distinguish between two possible levels of MXAN_4466 functionality: i) on RNA level, or ii) on protein level. If MXAN_4466 would be operating on the RNA level, the possibility stands that the insertion mutant removed a structural feature of the mRNA with an impact on either *hpk30* translation or mRNA stability. Moreover, a small RNA regulatory element could be encoded in the 5' region of the annotated gene MXAN_4466. The second scenario would be that MXAN_4466 was translated into a protein and operated at this level to affect developmental progression. To differentiate between these possibilities, I inserted a single-base-pair near the 5' end of MXAN_4466 generating a premature stop codon. This mutation (designated MXAN_4466$_{stop}$) was expected to prevent translation of MXAN_4466 into a protein, yet have little to no impact on mRNA stability and structure. The observed phenotype of the mutant during starvation on nutrient limited CF agar plates was highly similar to the one of the MXAN_4466::pMG011 insertion mutant (Figure 55). This strongly suggested that MXAN_4466 needed to be translated into a protein to have a developmental impact, rather than acting on a RNA regulatory level.

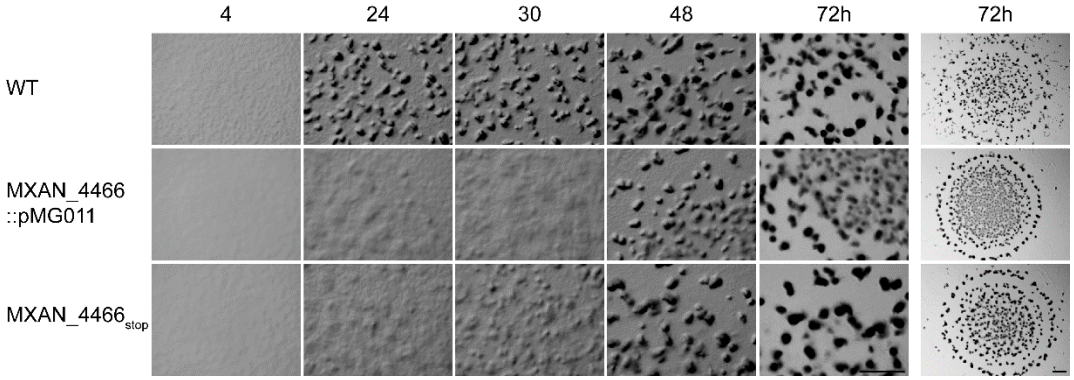

Figure 55: A gene disruption mutant of MXAN_4466 as well as an introduced premature stop codon in this gene cause developmental delay. *Developmental phenotype assay on CF agar plates.* Vegetatively growing strains were harvested and 10 µl spots of $OD_{550\ nm}$ 7 were placed on CF nutrient limiting agar plates. Inverted plates were incubated at 32 °C and pictures were recorded at the indicated time points. Left panel shows fruiting body morphology over the time course, right panel shows colony morphology of developed (72 h) colony. WT: wild type, scale bars 1 mm.

5.5.4.4 MXAN_4466 acts upstream of Hpk30

To investigate epistasis of the transcriptional unit *hpk30*- MXAN_4466, a double deletion mutant was created and tested under equivalent conditions. While strains wild type, Δ*hpk30* and MXAN_4466::pMG011 developed as previously described (section 5.5.4.3), the double deletion mutant showed a phenotype similar to Δ*hpk30*, yet not identical (Figure 56). The mutant Δ(*hpk30*-MXAN_4466) produced aggregates at 18 h that were slightly more prominent than the ones of wild type at the time but less far developed than Δ*hpk30*. During further developmental progression, the double mutant and Δ*hpk30* developed similarly. For instance, at 24 h of starvation

both exhibited more distinct aggregates than the wild type did. Also, the fruiting body morphology of the strains Δ*hpk30* and Δ(*hpk30*-MXAN_4466) looked alike. Both strains produced a higher proportion of small fruiting bodies than the wild type did. This result suggested the Δ*hpk30* phenotype to be the dominant one. Therefore, Hpk30 is likely to be the signaling output of the system, based on the hypothesis that the two proteins form a signaling module in general.

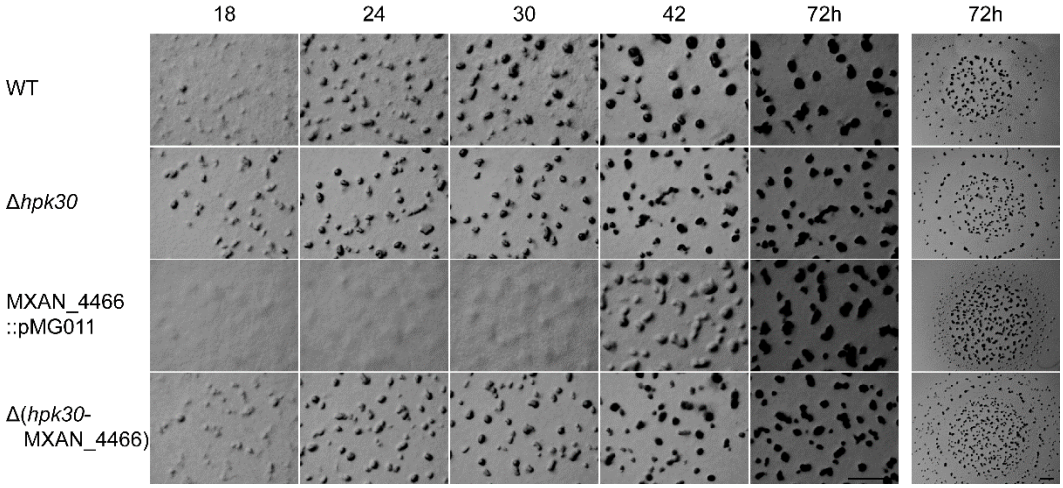

Figure 56: A double deletion mutant of *hpk30* and MXAN_4466 shows slightly accelerated development and small fruiting bodies. *Developmental phenotype assay on CF agar plates.* Vegetatively growing strains were harvested and 10 µl spots of $OD_{550\ nm}$ 7 were placed on CF nutrient limiting agar plates. Inverted plates were incubated at 32 °C and pictures were taken at the indicated time points. Left panel shows fruiting body morphology over the time course, right panel shows colony morphology of developed (72 h) colony. WT: wild type, scale bar 1 mm.

6. Discussion

Myxococcus xanthus has been a model to study bacterial multicellularity for decades. Amongst other interesting behaviors, the developmental cycle, which enables *M. xanthus* to survive during unfavorable environmental conditions, has been thoroughly investigated. Big advancements have been made in understanding the spatial and temporal regulation of cells during developmental progression, as well as how an isogenic bacterial population differentiates into distinct cell fates (recently reviewed in (Higgs *et al*., 2014, Bretl & Kirby, 2016, Kroos, 2017)).

Nevertheless, a lot is still unknown about the details of developmental regulation, functionality of signaling systems and one central question remains: “Why are fruiting bodies formed at all?”. In the study presented here, an attempt was made to answer this question by taking advantage of a mutant that was discovered to form very irregular fruiting bodies and impaired cell fate segregation upon starvation. This mutant lacks several negative regulators of development, which were previously found to affect MrpC accumulation via independent signaling pathways (Lee, 2009). Using genetic and biochemical tools, this study attempted to elucidate the mode of action and link to MrpC for two of them (TodK and the Red signaling system). Additionally, a putative histidine protein kinase, Hpk30, was investigated in detail genetically and biochemically, which functions in yet another negative regulator system of developmental progression in *M. xanthus*. Here, I present the emerging model for how several negative regulator signaling modules function and how they affect developmental progression. This leads to a proposed model on the topic of why *M. xanthus* forms fruiting bodies to survive or escape hostile environments.

6.1. *Myxococcus xanthus* signaling modules interlock to enable adaptation to different environmental insults

Upon starvation, *M. xanthus* initiates a complex developmental program which culminates in the formation of environmentally resistant spores (Figure 57, A). In the wildtype, sporulation exclusively takes place inside of well-organized, dome-shaped fruiting bodies. These fruiting bodies are surrounded by persister-like cells termed peripheral rods. Several regulators of this developmental program, both positive and negative, were identified over the years. A mutant lacking a set of negative regulators (ΔNR) was found develop rapidly into irregularly shaped fruiting bodies (Figure 57, B). These fruiting bodies are surrounded predominantly by single spores (inappropriately sporulating peripheral rods). In all single mutants, MrpC accumulated earlier and/or at higher levels than in the wildtype, while in double or multiple deletion mutants this effect was intensified synergistically (Lee, 2009).

Additive or even synergistic phenotypes indicate that the signaling systems are functioning in parallel pathways to coordinate cell behavior and cell fate segregation. By converging on the regulation of one hub protein, MrpC, each pathway could be

affecting a different aspect of MrpC regulation (e. g. transcriptional, translational or post-translational modification). I propose, cell fate coordination is modulated by the differential presence and activity of negative regulators within the population. With the signaling proteins repressing MrpC accumulation in at least the cells destined to become peripheral rods (potentially also in a timely manner in accumulating cells), the *M. xanthus* population gains sufficient time to form well organized fruiting bodies. These are in the wild type dome-shaped and surrounded by peripheral rods. In the ΔNR mutant, this regulation is lost and fruiting bodies are formed very quickly at the expense of organization. Also, peripheral rods sporulate inappropriately, resulting in flat, ridge like formed structures surrounded by singular spores. I hypothesize that signaling systems are used to evaluate the environmental conditions and to fine tune the kind of developmental program *M. xanthus* undergoes. This reaction would be based on an assessment if dispersal to a new niche seems reasonable or if survival in the current environment by persisting the insults as spores is preferred.

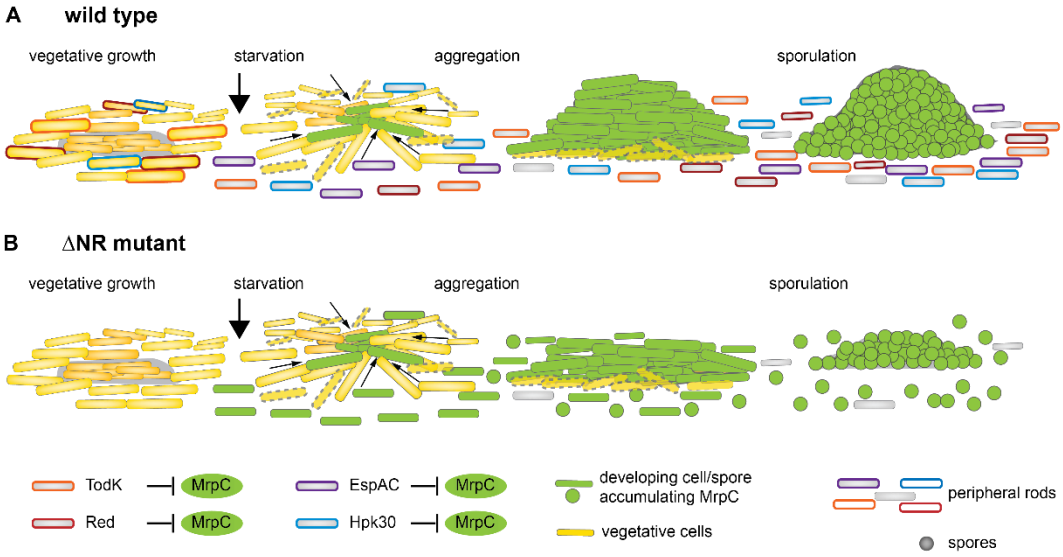

Figure 57: Proposed model of developmental regulation by negative regulator pathways. A) Depicted is the protein expression and cell fate regulation in the wild type. The cell fate "peripheral rods" is not comprised of identical cells but sub-populations exist. In these subpopulations, different negative regulators suppress the expression and/or accumulation of the key transcriptional regulator MrpC. The well-orchestrated developmental program leads to high, haystack formed fruiting bodies surrounded by peripheral rods. B) Development in ΔNR mutant, lacking four signaling pathways that coordinate cell fate determination. Absence of these signaling systems results in ridge like structures and single spores instead of peripheral rods.

To understand the proposed model (Figure 57) in detail, at first the suggested modes of actions of TodK and Hpk30 will be discussed (sections 6.2 and 6.3). In the following section, a potential link between MrpC and the negative regulator system Red is elucidated (section 6.4). Potential signal inputs of the negative regulator systems will be hypothesized afterwards (section 6.5). Furthermore, the regulation of MrpC (section 6.6) is followed by an analysis of the generation of fruiting bodies and cell fate segregation (section 6.7). Finally, the broader context of why fruiting bodies are formed at all and why a regulation by signaling systems might be beneficial will complete the discussion on the matter of regulation of fruiting body morphology and developmental timing in *M. xanthus* (section 6.8).

6.2. How TodK influences *Myxococcus xanthus* development: Proposed model of a bifunctional protein kinase / phosphatase

TodK was previously described as a putative histidine protein kinase which negatively regulates developmental progression in both the commonly used wild type strains of *M. xanthus* DK1622 and DZ2 (Rasmussen & Sogaard-Andersen, 2003, Lee, 2009). In my thesis research, I could show that the phenotypes of early aggregation as well as miss-accumulation of MrpC in a *todK* in-frame deletion mutant are indistinguishable from the previously studied *todK* insertion mutant indicating that the mutants can be used interchangeably. Moreover, the negative regulator function could be nicely demonstrated in a strain over accumulating TodK by expression from a secondary site forced from the essentially constitutively active *pilA* promoter (Figure 26, Figure 27 and Figure 28). In addition to the over-production of TodK from the *pilA* promoter, TodK was also likely expressed in every cell type. A future study could assess how this affects cell fate segregation (e.g. levels of peripheral rods and spores outside the fruiting bodies could be evaluated as well as cell death events).

Interestingly, the WT/ *todK*$^{++}$ strain aggregated even further delayed than the Δ*todK*/*todK*$^{++}$ strain. Consistently, the TodK protein accumulation was increased as well, as detected in immunoblot analysis. The augmented level of TodK in the population was particularly interesting because native levels of TodK were barely detectable under these assay conditions (Figure 28). This raises the intriguing possibility of TodK being involved in an auto-amplification loop, inducing additional *todK* expression from the native promoter in WT/*todK*$^{++}$.

Based on domain prediction tools, TodK was hypothesized to be a histidine protein kinase (Rasmussen & Sogaard-Andersen, 2003, Lee, 2009). Additionally, I performed sequence alignments and based on the motif following the conserved histidine, the proposed site of autophosphorylation, I hypothesized it to be a phosphatase as well (Figure 22). However, *in vitro* attempts to demonstrate kinase activity in a radioactive autophosphorylation assay failed. *In vitro* even the solitary kinase domain did not autophosphorylate. A plausible explanation would be that the kinase domain needs to be activated by one or both PAS domains upon sensing a stimulus, rather than an inhibition being released. While this would be an unusual regulation for a histidine kinase, it was previously described for the histidine phosphatase, WalK. Phosphatase activity of WalK on WalR~P in *Streptococcus pneumoniae* is unconditionally dependent on the presence of the PAS domain (Gutu *et al.*, 2010). Nevertheless, I can't exclude inactivity of the kinase domain *in vitro* to be caused by steric hindrance from the tag used for purification. A Trx-His$_6$-tag was utilized to overexpress soluble protein in my research. Recombinant expression using a different tag could be optimized or a cleavage site could be introduced between tag and TodK to proteolytically remove the tag after purification for the activity assay to rule out steric hindrance interfering with kinase activity.

My hypothesis of kinase activity being induced by PAS domain(s) sensing a signal was further strengthened by my observation that deletion of the TodK PAS domains (*todK*$_{\Delta PAS}$) produced the same early developmental phenotype observed by the strain

producing kinase inactive TodK (*todK*$_{H275A}$). If the PAS domains would merely release an inhibition of the kinase activity by sensing a stimulus, the opposite phenotype (delayed development) would be expected in a strain lacking the PAS domain(s) due to loss of inhibition and therefore constitutively active kinase domain of TodK. Nevertheless, it must be noted that protein stability of the kinase domain could not be shown *in vivo* (*todK*$_{\Delta PAS}$), due to very low TodK levels in total population cell lysates combined with and additional loss of potential antisera epitopes by deletion of the PAS domains. Although I assumed that the TodK$_{\Delta PAS}$ was stable in *M. xanthus* because it can be stably expressed as a recombinant protein in *E. coli*, definitive proof could be determined by expressing *todK*$_{\Delta PAS}$ from the *pilA* promoter in *M. xanthus*. Cell lysates could be used to detect the single domain via western blot and to determine its stability in *M. xanthus*. Finally, if my hypothesis is correct, a DZ2 *attB*::Pr$_{pilA}$*todK*$_{\Delta PAS}$ mutant would be expected to develop early, like the kinase inactive mutant *todK*$_{H275A}$.

The H-box motif of TodK suggested it might be a bifunctional protein, possessing histidine kinase as well as phosphatase activities. However, kinase activity could not be demonstrated *in vitro*. The putative TodK phosphatase activity could not be tested *in vitro* because a substrate / cognate response regulator has not been identified. *In vivo*, however, it could be shown using different strains accumulating specific point mutants of TodK that TodK likely possesses both kinase and phosphatase activity (Figure 23)[3]. Interestingly, all mutants exhibited early developmental phenotypes, suggesting that the usually opposing functions of kinase and phosphatase of TodK modulate the systems output(s) in the same manner. It has been generally assumed that most bifunctional kinases display opposing kinase and phosphatase phenotypes because they act to initiate and terminate (respectively) signaling on a single cognate effector protein. For example, in the chemotactic systems of *E. coli* and *Rhodobacter sphaeroides*, the histidine kinases CheA in *E. coli* and its homolog CheA$_3$ in *R. sphaeroides* not only activate their cognate response regulators (CheY in *E. coli* and its homolog CheY$_6$ in *R. sphaeroides*) by phosphorylation, but also terminate the signal by promoting its dephosphorylation within equal respective signal response times (Berg & Purcell, 1977, Segall *et al.*, 1982, Porter *et al.*, 2008b). Furthermore, it was described that depending on the availability of nitrogen, the *E. coli* kinase NtrB either autophosphorylates and serves as a phosphodonor for NtrC, its cognate response regulator, or stimulates the prompt dephosphorylation of NtrC~P (Weiss *et al.*, 2002). Finally, the cell envelope stress response of *Listeria monocytogenes* is modulated by the phosphatase activity of the bifunctional histidine kinase LiaS$_{Lm}$ (Fritsch *et al.*, 2011). This study suggests that the kinase activity of LiaS$_{Lm}$ and subsequent phosphotransfer to LiaR$_{Lm}$ is mediated as a reaction to exposure to cell wall active antibiotics. Signal termination is accomplished by activation of LiaS$_{Lm}$ phosphatase activity which is induced in the absence of envelop stress by the interaction with the cell wall associated protein LiaF$_{Lm}$ (Fritsch *et al.*, 2011). Many bifunctional kinase/phosphatase proteins share the feature that they

[3] The phenotypes observed are interpreted based on the assumption that the resulting mutant proteins display the predicted functions (see section 5.4.1.3, Figure 22).

regulate one output (response regulator) in the cell, causing opposing effects through phosphorylation and dephosphorylation.

For TodK, I propose a model of regulation in which TodK first needs to autophosphorylate to activate phosphatase activity on a cognate response regulator (Figure 58). In this scenario, TodK would sense a stimulus through the PAS domain(s) which induces kinase activity. Upon autophosphorylation, TodK acts as a phosphatase on an undefined receiver domain, terminating or delaying the signal to induce developmental progression. Upon loss of signal or sensing a secondary stimulus through the other PAS domain, TodK activity as kinase and phosphatase is lost. The cognate response regulator would remain phosphorylated and mediate its output to allow developmental progression to continue.

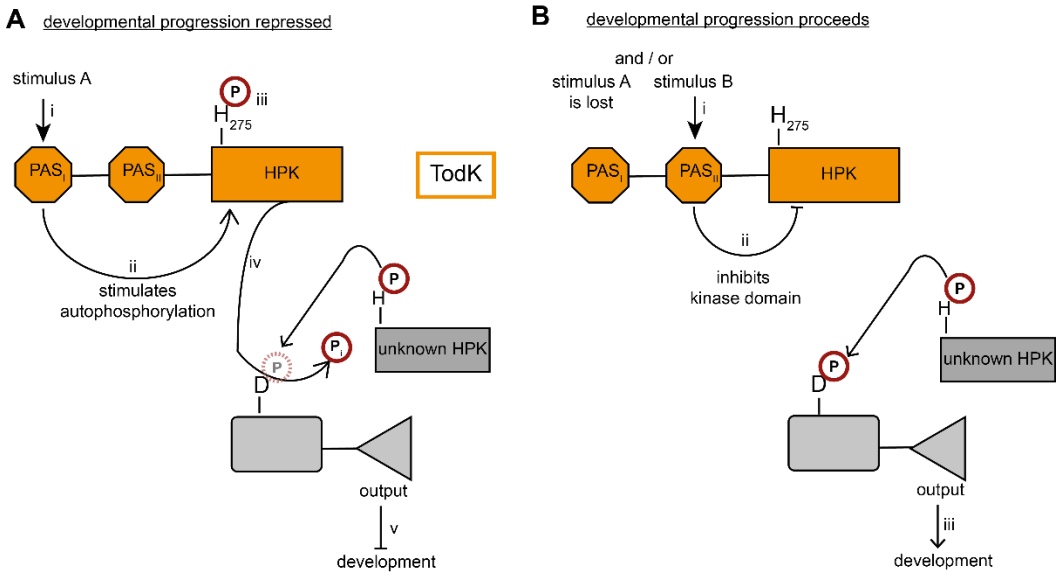

Figure 58: TodK acts as an autophosphorylation activated phosphatase to constrain developmental progression. A) *Developmental progression is repressed*. By sensing a so far unknown signal (stimulus A) with one or both PAS domains (i), TodK autophosphorylates (ii) on the conserved histidine H275 (iii). This phosphorylation activates TodK to become a phosphatase on a so far unknown cognate response regulator (RR) (iv). The dephosphorylated RR with the non-activated effector domain does not generate a development stimulating output. Hence, developmental progression is not supported (v). B) *Developmental progression proceeds*. Either stimulus A is lost or an alternative stimulus is sensed with the respective other PAS domain of TodK (i), leading to inactivation of the kinase activity (ii). Non-phosphorylated TodK also does not possess phosphatase activity. Therefore, the cognate response regulator remains phosphorylated and can generate its output to support developmental progression.
Alternatively, TodK is not present in cells inside of fruiting bodies (e.g. aggregating and sporulating cells) and therefore the system promoting these steps is not antagonized in those cells.
An intriguing observation from Phostag-SDS-PAGE is that additional regulation of TodK activity might be mediated by Ser/Thr phosphorylation. This putative connection to a STPK cascade is not depicted here.

Such a model would require: i) different sensing domains in a single kinase regulating different activities and ii) phosphorylation and dephosphorylation of a single receiver domain by two different kinases. Interestingly, however many of these features have been described previously. Evidence for feasibility of feature i) comes from a well-studied bifunctional kinase CckA (cell cycle kinase A, (Mann et al., 2016)). CckA is a bifunctional kinase with tandem sensory PAS domains, integrating cell fate cues in *Caulobacter crescentus*. During the cell cycle, CckA goes from diffuse localization to

densely packed at the cell poles. It could be shown *in vitro* that one PAS domain activates kinase activity of CckA in a CckA density dependent manner. Moreover, it was demonstrated that the second PAS domain sensed cyclic di-GMP, a second messenger which is asymmetrically partitioned and concentrated at the future stalked cell pole (Christen *et al.*, 2010). Stimulation of the PAS domain by interaction with cyclic di-GMP resulted in inactivation of CckAs kinase-, and stimulation of its phosphatase-, activities (Mann *et al.*, 2016). Thus, CckA could dephosphorylate the master regulator CtrA, which is known to be inactivated at the stalked cell pole (Chen *et al.*, 2009, Mann *et al.*, 2016).

Evidence for feature ii) comes from as from the chemosensory systems (reviewed in (Szurmant & Ordal, 2004, Wadhams & Armitage, 2004, Porter *et al.*, 2008a)) as well as from the four component Red system in *M. xanthus* (Jagadeesan *et al.*, 2009). In *E. coli* chemotaxis, chemoreceptors modulate the CheA activity, a dedicated kinase. Subsequently, phosphotransfer occurs to cognate response regulators, one of them being CheY. Although CheY~P auto-dephosphorylates, this hydrolysis reaction can be accelerated ~100-fold by CheZ, a dedicated phosphatase (Appleby & Bourret, 1998, Silversmith *et al.*, 2008). In the Red system, the sensor kinase RedC phosphorylates the response regulator RedF during early developmental stages. Dephosphorylation of RedF, however, is accomplished in later developmental stages through RedE. RedE needs to become phosphorylated through phosphor-transfer from RedD to act as a phosphatase on RedF (Jagadeesan *et al.*, 2009). Indeed, the kinase/phosphatase motif of RedE and TodK share an intriguing similarity: both possess an aspartate (D) at the +1 position after the conserved histidine. More commonly, histidine kinases have a glutamate (E) at this position, while D is only the second most common amino acid (Willett & Kirby, 2012).

To test whether TodK activity is modulated as proposed, it would be necessary to create a constitutively phosphorylated kinase *in vivo*. The predicted phenotype of such a mutant strain would be a delayed development due to constant activity of the autophosphorylation induced phosphatase activity of TodK. Unfortunately, there is no such system currently established to my knowledge. Since phosphor-transfer would not be required in this system, I would propose to create TodK mutants analogously to how a constitutively activated conformation in single domain response regulators is achieved (phosphorylation induced conformational change of receiver domains is reviewed in (Bourret, 2010)). Phosphorylation independent activation of the response regulators CheY, OmpR and NtrC has been previously observed when the phosphor accepting aspartate was mutated to the phosphor-mimetic amino acid glutamate (Klose *et al.*, 1993, Moore *et al.*, 1993, Lan & Igo, 1998, Smith *et al.*, 2004). However, whether such mutations result in the desired “phosphorylation induced active conformation” of a kinase needs to be experimentally tested. It has been reported that phosphatase activity was elevated by a histidine to glutamine substitution in the two histidine kinases *E. coli* NarX (Huynh *et al.*, 2010) and *Enterococcus faecium* VanS (Haldimann et al., 1997). Investigation of whether TodK phosphatase activity can be stimulated by this mutation could give more insight into the system, in case the generation of a phosphomimetic substitution of the histidine in TodK proves to be unsuccessful.

An alternative model of regulation would be that TodK is merely a dedicated phosphatase, but the conserved histidine is essential for this function. This phenomenon could be previously shown for the *E. coli* osmosensor EnvZ (Dutta & Inouye, 1996, Zhu *et al.*, 2000). The proposed model for this dephosphorylation mechanism is reverse phosphotransfer from the receiver domain to the kinase domain. Although in a different mechanism, reverse phosphorelay was also described in *Pseudomonas aeruginosa* (Hsu *et al.*, 2008). Here, a phosphate group is not only transferred from a sensor kinase to an HPt protein, but also the reverse transfer was observed *in vitro*.

In addition to TodK being regulated by inputs sensed through the PAS domain(s), it might be additionally regulated by a serine/threonine protein kinase (STPK). This is suggested by the histidine independent shift observed in Phos-Tag SDS-PAGE (Figure 33). Cross talk between STPK and TCS systems has been described several times (Rajagopal *et al.*, 2006, Chao *et al.*, 2010, Canova *et al.*, 2014, Horstmann *et al.*, 2014, Libby *et al.*, 2015). When analyzing TodK with the phosphorylation site prediction tool NetPhos 3.0 (Blom *et al.*, 1999), several serine and threonine positions were predicted to be phosphorylated with a high score. Three such sites are positioned within the first PAS domain. Although I couldn't identify an example for PAS domain phosphorylation yet, taking into consideration the board range of PAS domain stimuli, post-translational modifications are not unlikely. Phosphorylation can induce conformational changes in proteins (Greenstein *et al.*, 2005), and also PAS domains are known to transmit signals by changing conformation upon signal perception (Moglich *et al.*, 2009b). How the signal is transmitted from a PAS domain to modulate activity of the kinase domain is not fully understood to date. The linker domain connecting the two domains is a hot-spot for mutations and therefore is believed to be of major importance for the signal transmission (Weiss *et al.*, 2002). In this important region of TodK, a serine residue is predicted to be phosphorylated with a high likelihood (score of 0.997). Within the kinase domain, six more putative sites are predicted, one of them within the dimerization and histidine phosphorylation domain. This domain has been reported to be highly important for phosphatase activity (Russo & Silhavy, 1991, Jiang *et al.*, 2000, Zhu *et al.*, 2000, Porter *et al.*, 2008b). It is unlikely that TodK would be this heavily phosphorylated, yet there is high potential for a secondary regulation by STPK phosphorylation. This mechanism could be tested by introducing phosphorylation-mimicking substitutions of these residues *in vivo* to investigate the effect on the phenotype during starvation. Moreover, if TodK could be enriched (e.g. by identifying and separating the cell type it is accumulated in), the protein's Ser/Thr-phosphorylation status could be investigated by mass-spectrometry.

First attempts to identify cognate response regulators for TodK have failed. The two most likely candidates (DotR, based on genetic location and MXAN_5052 based on a prediction tool) did not show a developmental defect upon deletion (this study, section 5.4.4.2 and (Rasmussen & Sogaard-Andersen, 2003)). Redundancy of response regulators is still a possibility and would make both candidates cognate partners. In such a scenario, *M. xanthus* could compensate deletion of one by over-accumulating the other. To test if DotR and MXAN_5052 are redundant, a double

deletion mutant should be created and the developmental phenotype should be investigated. Also, expression and protein levels could be assessed in different mutants by RT-PCR and immunoblot analysis. Future approaches to identify the cognate effector protein of TodK could include pull down approaches combined with cross linking, however, for this to be successful it should first be determined in which cell type and at which developmental period active TodK can be expected, to narrow down spatial and temporal occurrence of the cognate effector protein.

In conclusion, this study provides new insights into the signal flow and activity modulation of TodK. Specifically, TodK needs to be activated to autophosphorylate, in order to serve as a phosphatase on a currently undefined cognate RR to repress developmental progression. These new aspects build a good foundation to further understand how TodK influences accumulation of MrpC and there with both developmental progression and cell fate segregation.

6.3. Hpk30: An unusual signaling module integrating different stimuli to fine-tune development in *Myxococcus xanthus*

My thesis research involved the characterization of an unusual hybrid histidine kinase, Hpk30, that is required for appropriate developmental progression in *M. xanthus*. A Δ*hpk30* mutant shows accelerated developmental progression on CF agar plates, suggesting Hpk30 functions as a negative regulator of starvation induced development. The opposite phenotype (delayed development) could be induced by introducing a copy of *hpk30* under the constitutive *pilA* promotor, forcing overexpression of Hpk30. Driven by the *pilA* promoter, Hpk30 was presumably produced in every cell type and at non-physiologically high levels. In a future study, it could be determined how cell fate segregation is affected by this inappropriate Hpk30 accumulation, e.g. if peripheral rods are produced at all in this strain or if cell death rates are affected in this strain.

Next, the functionality of the predicted protein domains as well as their phosphorylation status was assessed. Based on a genetic approach in which the phenotypic effect of mutating conserved phosphoaccepting residues was examined, I propose a model in which Hpk30 autophosphorylates on the histidine residue of its kinase domain and this activity is required for its function *in vivo*. Interestingly, however, genetic analyses suggested that Hpk30~P does not donate a phosphoryl group to either of its associated receiver domains. These data were supported by *in vitro* analysis, in which Hpk30 was shown to autophosphorylate in a radioactive kinase assay. A chemical stability test, based on known acid/base stability of phosphor-histidine and phosphor-aspartate residues (Duclos *et al.*, 1991), provided additional confirmation that no phosphotransfer occurs to the receiver domains. I cannot rule out, however, that phosphotransfer does occur but could not be monitored within the experimental setup. To finally prove the absence of phosphotransfer to either receiver domain, an experiment measuring free Pi could be performed. This

experiment would rule out the possibility that after phosphotransfer to one or both receiver domains instant dephosphorylation occurred, hence no phosphorylation on aspartate residues could be detected. To biochemically determine if the receiver domains have an impact on Hpk30 kinase activity, kinetic assays could be performed evaluating the autophosphorylation rates of Hpk30 full length protein in comparison to a kinase domain only construct. Also, kinetics could be compared to single or double point mutant constructs and single domain deletion constructs.

Based on phenotypic studies of currently available mutants, I propose a model in which the kinase domain functions as the signaling module output (Figure 59).

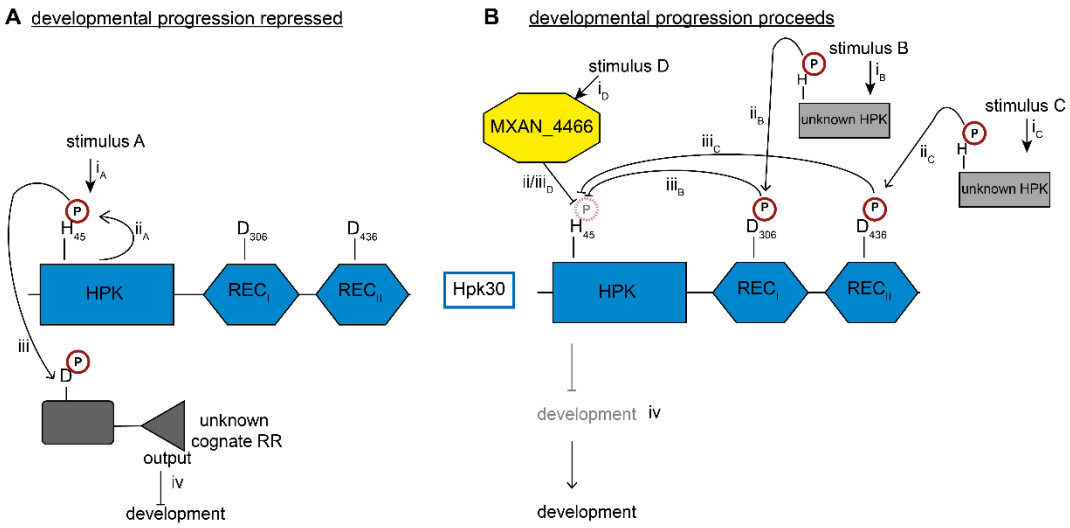

Figure 59: Hpk30 integrates multiple signals to regulate developmental progression. A) Developmental progression is repressed. Hpk30 is activated by stimulus A (i_A; potentially by protein-protein interaction, post-translational modifications or perhaps Hpk30 is constantly active until it is switched off (see B)) and autophosphorylates on the conserved histidine (H45, ii_A). This phosphoryl group is subsequently transferred to a currently unknown cognate receiver domain (iii), generating the signal output to repress developmental progression (iv). B) Developmental progression proceeds. Genetic evidence suggests Hpk30 kinase activity is repressed by three factors: phosphorylation of either receiver domain (on D306 and/or D436) and by the co-expressed hypothetical protein MXAN_4466. The stimuli B and C are proposed to activate two so far unknown HPKs (i_B and i_C) which autophosphorylate and phosphotransfer to the aspartates in Hpk30s receiver domains (D306 ii_B and D436 ii_C, respectively). Separately or cooperatively, the phosphorylated receiver domains inhibit autophosphorylation of the kinase domain and promote dephosphorylation thereof (iii_B and iii_C). Hence, developmental repression is relieved, MrpC can accumulate and development can proceed (iv). The other kinase activity modulating factor is MXAN_4466. By sensing a stimulus D (i_D), it becomes activated and either via direct interaction or with the help of an unknown mediating protein (ii/iii_D) inactivates Hpk30 kinase domain. Developmental repression is relieved as described above and developmental progression proceeds (iv).

In the model proposed here, Hpk30 acts as a signal integrator to mediate one output. To repress developmental progression, Hpk30 autophosphorylates on histidine 45 and thereby represses developmental progression. It has been previously reported that kinase domains can both be stimulated (Paul *et al.*, 2008) or inhibited (Inclan *et al.*, 2008) by their cognate receiver domains. In this model, both receiver domains repress the kinase activity and/or induce its dephosphorylation, lifting the developmental repression. Therefore, in a deletion mutant as well as in *hpk30*$_{H45A}$, repression is not established in the first place, allowing development to proceed inappropriately rapidly. In contrast, with Hpk30$_{D306A}$ as well as Hpk30$_{D436A}$,

dephosphorylation of the kinase domain is not achieved, leading to a delay in development due to inappropriately long repression by Hpk30~P.

It could be shown that Hpk30 protein accumulates in both vegetative cells and developmental cells up until 36 h of starvation. This observation raises the intriguing possibility of different functionalities at separate times during the *M. xanthus* life cycle. Although point mutations in either receiver domain led to a delayed developmental phenotype, these phenotypes differed both in severity and reproducibility. These differences gave additional reason to suggest two independent inputs (determined as stimulus B and C, Figure 59), modulating the kinase activity of Hpk30. Unfortunately, the generation of double point mutants has so far been unsuccessful. It is still unclear whether this is merely due to technical difficulties (several mutants in this particular locus have been challenging to generate), or if there is an underlying physiological reason. To separate between these possibilities, two strategies could be applied: a functional wildtype copy of *hpk30* could be introduced at a secondary site in the genome, either under the native promoter or under the control of the *pilA* promoter. In this newly generated background strain it could be attempted to generate a double point mutant at the native site (e.g. $hpk30_{H45A/D306A}$, $hpk30_{H45A/D436A}$ and/or $hpk30_{D306A/D436A}$). If the resulting mutant strains can still not be obtained, it is likely due to technical difficulties of the native locus since any physiologically challenging effects of the mutant protein should be outperformed by the active wild type protein produced from the secondary site. In an alternate approach, plasmids carrying the designed point substitution genes could be introduced at a secondary site in the deletion background (Δ*hpk30*). These constructs should be under the control the native promoter (ideally), or the *pilA* promoter. The native promoter area functionality should firstly be demonstrated by complementing with the wild type *hpk30* gene. If, in this scenario, the mutants could not be obtained, I would suspect these mutants produced physiologically challenging (lethal) effect. Obtaining all the point mutant combinations mentioned above is crucial to conclusively determine the epistasis of the three signaling domains of Hpk30.

In the *M. xanthus* developmental program such an unusual histidine protein kinase with multiple response regulators has been described before, designated RodK (Rasmussen *et al.*, 2005, Rasmussen *et al.*, 2006, Wegener-Feldbrugge & Sogaard-Andersen, 2009). This kinase, including its autophosphorylation activity is essential for both morphological events of development (Rasmussen *et al.*, 2005). The kinase domain, like Hpk30, was shown to be active *in vitro*, yet phosphotransfer could only be observed to the third receiver domain (Rasmussen *et al.*, 2006). An additional cognate response regulator, RokA, was identified later and was found to be preferentially phosphorylated by the kinase domain (Wegener-Feldbrugge & Sogaard-Andersen, 2009). Hpk30 and RodK share several similarities in their functions. They both contain multiple receiver domains. Two of them are not subject to phosphotransfer from the kinase domain *in vitro*, yet kinase activity is essential for the protein's functions *in vivo*. Hence, signal integration into the two receiver domains from other kinases is suggested, since mutations in the potential sites of phosphorylation results in loss of function *in vivo* (this study and (Rasmussen *et al.*, 2006)). Both hybrid kinases accumulate under vegetative growth conditions and

persist into the later stages of development, raising the opportunity to integrate different stimuli at different developmental stages (this study and (Rasmussen *et al.*, 2005)). Also, both proteins phosphorylate a receiver domain on a cognate response regulator protein (RokA for RodK (Wegener-Feldbrugge & Sogaard-Andersen, 2009), unidentified for Hpk30). However, the influences of the two kinases on developmental progression differ as they do not share the same aggregation phenotype (this study and (Rasmussen *et al.*, 2005)), suggesting that this complex signal integration might be a sophisticated way of assimilating the multiple signals occurring during development of *M. xanthus*.

MXAN_4466 can be added as yet another regulating element to modify Hpk30 activity. I could show that this gene is encoded in an operon with *hpk30* and that a functional protein is expressed from it. I could also show that MXAN_4466 is epistatic to Hpk30. Whether this is mediated by direct interaction or whether other proteins are involved remains unknown at this point. Both *in vitro* and *in vivo* studies could be applied to gain further insight in the putative interaction, including pull-down approaches (if needed combined with crosslinking), bacterial or yeast two hybrid systems (BACTH / Y2H) or immunoprecipitation.

So far, MXAN_4466 is classified as a hypothetical protein and domain prediction tools did not identify any known domain annotation. Further bioinformatic analyses led to two putative functionalities, which could nicely fit together with the regulation of Hpk30. When performing BLASTp and PSI-BLAST searches (Altschul *et al.*, 1997, Schaffer *et al.*, 2001) sequence similarity to several (putative) serine/threonine kinases was revealed. Since Hpk30 lacks input domains, regulation of its activity by serine/threonine phosphorylation is an intriguing possibility. A system in which activity of a two-component system (TCS) is regulated by a eukaryotic like serine/threonine protein kinase (STPK) has previously been described in *Bacillus subtilis* (Libby *et al.*, 2015). The study shows how the STPK PrkC phosphorylates the response regulator WalR on a threonine and thereby increases its activity. Threonine phosphorylation of a receiver domain has also been described to decrease activity of the effector domain. For instance, the Vancomycin-resistance-associated response regulator *Staphylococcus aureus* VraR has been shown to be phosphorylated on two Thr residues in the receiver domain of the protein by the Ser/Thr kinase Stk1 (Canova *et al.*, 2014). Converging regulation by STPK and TCS signaling systems has been demonstrated to be important for the regulation of dormancy in *Mycobacterium tuberculosis* as well (Chao *et al.*, 2010). Here it could be shown that PknH phosphorylates the response regulator DosR on two threonine residues which are important for activation and dimerization of DosR. A crosstalk pathway between STPK and TCS systems has also been proposed to fine-tune a cellular reaction for environmental adaptation in *Streptococcus* (Rajagopal *et al.*, 2006, Lin *et al.*, 2009, Horstmann *et al.*, 2014). These studies provide evidence that both in Group A and Group B *Streptococci* the response regulator CovR is phosphorylated on a threonine by Stk1. This phosphorylation results in a decrease of phosphorylation on the invariant aspartate (D53) in the same receiver domain, which results in altered output of the system and eventually affects virulence in a mouse model (Horstmann *et al.*, 2014).

When analyzing Hpk30 with the phosphorylation site prediction tool NetPhos 3.0 (Blom *et al.*, 1999), a remarkable number of potential phosphorylation sites were identified. These residues included T326, close to D306, the suggested site of phosphorylation in the first receiver. Also, seven serine residues were predicted, distributed over all signaling domains of Hpk30 (HisKA domain S92 and S93; inter-domain region between HisKA and HATPase_c S98, S122 and S125, Rec_I S287 and Rec_{II} S493). To test the hypotheses that i) Hpk30 is phosphorylated on a serine/threonine residue and ii) this phosphorylation is achieved through MXAN_4466 both, *in vitro* and *in vivo* analysis could be performed. To first test *if* Hpk30 is phosphorylated on Ser/Thr residues *in vivo*, Phostag technology could be optimized for this protein and *M. xanthus* lysates from different developmental stages and/or cell fates could be tested for phosphorylation induced band shifts. To further test if a band shift is dependent on the presence of MXAN_4466, lysates of a deletion/insertion or the early stop codon point mutant used in this study could be tested additionally in Phostag SDS-PAGE. As an *in vitro* confirmation, both proteins Hpk30 and MXAN_4466 could be overproduced in *E. coli*, purified and tested in a radioactive kinase assay. Since Hpk30 autophosphorylates efficiently in this assay, the inactive point mutant $Hpk30_{H45A}$ should be used for this phosphotransfer assay.

Another interesting possibility for how MXAN_4466 could potentially regulate Hpk30s activity arises from a bioinformatics approach concerning protein folding structure. When analyzing MXAN_4466 using Phyre² software (Kelley *et al.*, 2015), a high similarity to hydrolases was identified. However, most of the found structures stem from proteins which are not further characterized and therefore a definite prediction of function is not possible at this point. Nevertheless, the potential of MXAN_4466 to act as a hydrolase of some kind, for instance as a phosphatase, adds an interesting point to the Hpk30-model proposed here. Whether MXAN_4466 acts as a phosphatase on Hpk30 could also be tested using Phostag SDS-PAGE or the *in vitro* radioactive kinase assay, however, the latter assay would only show if MXAN_4466 dephosphorylates the autophosphorylated H45 of Hpk30. If a so far unknown serine/threonine kinase phosphorylated Hpk30 to regulate its activity and MXAN_4466 counter-acts this by de-phosphorylating the yet unknown residue, identification of the kinase would need to occur before testing phosphatase activity of MXAN_4466 *in vitro*. If MXAN_4466 acts neither as kinase nor as phosphatase of Hpk30, it could still have an impact on activity of Hpk30. To test this, autophosphorylation kinetics of Hpk30 could be measured in an *in vitro* radiolabeled assay and it could be assessed if these kinetics change upon addition of purified MXAN_4466.

In summary, my data suggests a model in which Hpk30 autophosphorylates on H45 during early development, inhibiting developmental progression. Three inhibitors of this autophosphorylation are proposed here: phosphorylation of D306 and D436 in the both receiver domains of Hpk30 as well as the protein MXAN_4466. These three mediate the relief of developmental repression, allowing *M. xanthus* to form fruiting bodies and spores. I hypothesize that Hpk30 is a signal integrating protein, whose activity is modulated by at least two so far unknown kinases phosphorylating the two aspartates in the receiver domains and a signal activating MXAN_4466 (Figure 59). As an ultimate output, Hpk30 influences accumulation of the developmental

transcription factor, MrpC. It is still unknown how this regulation is mediated. Identifying the signals Hpk30 responds to as well as the output to regulate MrpC should be the next major step of this project.

While identification of the signals seems impossible without identifying all modulating proteins of Hpk30 first, a semi *in vivo* approach could be applied to identify the cognate response regulator of Hpk30. Since Hpk30 autophosphorylates *in vitro*, purified kinase could be phosphorylated using an ATP analog, e.g. ATPγS or biotinylated ATP (Besant & Attwood, 2009, Carlson *et al.*, 2010, Wilke *et al.*, 2012, Senevirathne & Pflum, 2013, Garre *et al.*, 2014). It was previously shown that ATPγS can be generally used by histidine protein kinases for autophosphorylation as well as for phosphotransfer to cognate receiver domains (Kinoshita *et al.*, 2014). However, it needs to be experimentally determined if Hpk30 can utilize the analog(s) as well. Phosphorylation with ATPγS could have an additional positive effect which could be used to optimize Phostag technology for this protein. Thiophosphohistidines have been described to be more stable than regular phosphohistidines (Lasker *et al.*, 1999). Hence, *in vitro* autophosphorylated Hpk30~P* could be utilized to find optimal Phostag-PAGE conditions to study this protein also *in vivo* in lysates. *In vitro* prepared Hpk30~P* would be mixed with lysates of *M. xanthus* populations. Ideally, the time point of Hpk30 activity would be previously be determined using Phostag technology, but a lysate mixture from different stages of development could suffice as well. In the lysate, P*-transfer could occur from Hpk30 to the cognate receiver domain, which subsequently could be pulled out by using a specific antibody (i.e. according to (Allen *et al.*, 2007, Carlson *et al.*, 2010), a thiophosphate ester specific antibody is commercially available as monoclonal antibody 51-8 from Epitomics) or an iodacetyl-agarose (according to (Blethrow *et al.*, 2008), iodacetyl-agarose commercially available as SulfoLink® from Pierce). Recovered protein could be identified via mass-spectrometry. As a negative control, it is crucial to perform a side-by-side experiment with Hpk30 phosphorylated with regular ATP, to be able to subtract all non-specific proteins that might be captured with the antibody or agarose.

6.4. The Red four component system is connected to MrpC~P via the KapC Serine/Threonine protein kinase scaffold protein

A previous study demonstrated that the four-component Red signaling system also affects MrpC accumulation via a pathway independent from other negative regulators (Lee, 2009). While RedF was known to be the output of the Red system (Jagadeesan *et al.*, 2009), it remained unclear how RedF is connected to MrpC. Since RedF is a single domain response regulator, different scenarios were proposed to address how RedF could regulate the developmental program (Jagadeesan *et al.*, 2009):

i) RedF in its phosphorylated form could participate in another multi-step phosphorelay by interacting with a histidine phosphotransferase, similar to the described function of Spo0F during the initiation of sporulation of *B. subtilis* (Burbulys *et al.*, 1991).

ii) RedF might act as an allosteric activator of a so far unknown kinase, similar to the role of DivK on PleC in *Caulobacter crescentus* (Paul *et al.*, 2008).

iii) RedF could function via direct protein-protein interaction with an effector protein that modulates developmental progression. This mode of action has been studied in detail in motility systems regulated by chemotaxis in *E. coli* and *B. subtilis (Welch et al., 1993, Szurmant et al., 2003).* Here, the stand-alone response regulator, CheY, regulates direction of flagellar rotation by directly binding to a flagellar switch protein.

We first set out to investigate the most likely scenario that a direct interaction partner of RedF(~P) existed. In a yeast-two-hybrid screen, using RedF as bait protein, the kinase associated protein C (KapC) was identified as a putative interaction partner of RedF (X. Mei and P.I. Higgs; unpublished data). In this study, I could confirm this finding using an *in vitro* pull-down approach (Figure 18). KapC constitutes an intriguing candidate to interact with RedF, because several pleiotropic phenotypes associated with the deletion of *redF* [reduced EPS production (S. Jagadeesan and P.I. Higgs; unpublished data), reduced total cell numbers during development (Lee, 2009) and miss-accumulation of MrpC (Lee, 2009)] could be explained by this interaction (Figure 60). KapC has been identified to be a modulating factor of Pkn4, the kinase which activates 6-phosphofructokinase (PFK) (Nariya & Inouye, 2002, Nariya & Inouye, 2005b, Nariya & Inouye, 2005a). PFK regulates glycogen metabolism which is required for effective sporulation in *M. xanthus* (Nariya & Inouye, 2003). Pkn4 also interacts with KapB, which was also found to interact with Pkn8 (Nariya & Inouye, 2005a). An interaction between Pkn8 and FruD could be identified in a yeast-two-hybrid screen (Nariya & Inouye, 2005a), which could link the Red-system to cell division (Akiyama *et al.*, 2003). Experimental (re-)examination of all proposed interactions of this network is needed.

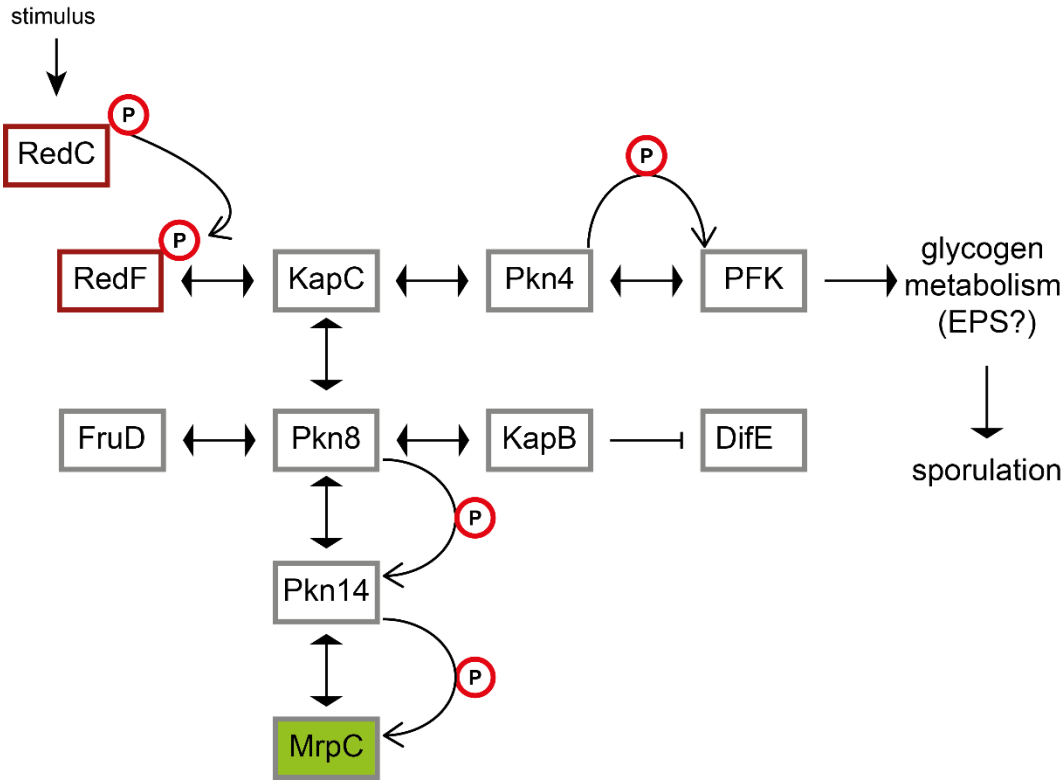

Figure 60: The four-component Red system might act on MrpC via a eukaryotic like kinase pathway. The interaction between RedF~P and KapC could be shown *in vitro*. Based on this connection, the phenotypes observed in a Δ*redF* mutant concerning developmental timing, MrpC accumulation, cell number during development, EPS production and sporulation could be explained. For details on assembly of this network see text.

Of highest interest within the scope of this study is the pathway linking RedF via interaction with KapC to MrpC. KapC has been suggested to interact with the serine/threonine kinase Pkn8 in *M. xanthus* (Nariya & Inouye, 2005a) and therefore was proposed to be linked to MrpC phosphorylation status via the published phosphorylation cascade of Pkn8 and Pkn14 (Nariya & Inouye, 2005c, Nariya & Inouye, 2006). I hypothesize a model in which KapC functions as a scaffold protein for at least RedF~P and Pkn8, although additional interacting proteins are possible. Utilizing *in vitro* binding studies, such as basic pull-down assays or more sophisticated approaches like Biacore technology (to also study binding kinetics) the interaction(s) between KapC, RedF and Pkn8 should be determined in more detail. Here, dependence of phosphor-status would be of special interest. Furthermore, it should be elucidated *in vivo*, at and until which time of development as well as in which cell type(s) this interaction is maintained. To achieve this, protein fusions with fluorescent marker proteins, cell type separation assays, and/or protein cross-linking techniques could be used in combination with microscopy and immunoblotting methods.

Recent data suggests the Pkn8-Pkn14 phosphorylation cascade to be more relevant for sporulation events than for aggregation (B.E. Feeley and P.I. Higgs; unpublished data). Based on this, Pkn8 could be rendered inactive by being bound to KapC and anchored there by the RedF~P induced conformation. Upon developmentally induced de-phosphorylation of RedF, the complex of RedF-KapC-Pkn8 could be released and Pkn8 would be activated. Active Pkn8 could autophosphorylate and induce the

phosphorylation cascade which eventually leads to phosphorylation of MrpC. It was previously suggested that phosphorylated MrpC (MrpC~P) binds with lesser affinity to its own promoter, thus inhibiting its proposed auto-activation (Nariya & Inouye, 2006). It has since been shown that the auto-activation model published by Nariya *et al.* is not the only way MrpC influences its own expression ((Bhardwaj, 2013) and P.T. McLaughlin and P.I. Higgs; unpublished data). The MrpC regulation and modulation model is currently under thorough re-investigation. Therefore, also the interaction of RedF~P with KapC influences on MrpC modulation thereof, need to be re-assessed and interpreted once the MrpC (auto-) regulation is newly established.

6.5. Which signals might the NRs respond to?

In this study as well as previously, it has been observed that mutants of certain negative regulator deletions behave differently under varying starvation conditions. More precisely, both *todK* and *red* deletion mutants show dissimilar aggregation timing in submerged culture compared to CF agar starvation assays (this study and (Lee, 2009)); a Δ*hpk30* occasionally shows variation in aggregation timing (this study). All these signaling systems regulate accumulation of MrpC. MrpC levels are crucial for developmental progression and are also suggested to determine cell fate segregation (Lee *et al.*, 2012). By fine tuning the negative regulator signaling systems, MrpC accumulation (and therefore tight regulation of developmental progression as well as defining proportions of sub-populations) could potentially be perfected to adapt to the ever-changing environment in the most appropriate manner. However, the precise stimuli the negative regulator systems respond to remain unidentified to date.

Histidine protein kinases can sense stimuli in different ways. Membrane bound kinases sense stimuli from the outside of the cell, signals can be perceived at the cytoplasmic membrane or stimuli are detected by soluble kinase in the cytoplasm (Mascher *et al.*, 2006). Although the majority of histidine kinases contain a membrane-spanning domain (Galperin, 2005), interestingly most of the negative regulator kinases (except EspC and RedC) are cytoplasmic proteins. The signals they respond to are yet unknown. The EspAC system has various sensing domains which were analyzed previously (Schramm *et al.*, 2012). Briefly, EspA contains two PAS domains and an FHA domain; EspC contains a MASE1 domain as well as a PAS domain. While PAS domains are suggested to bind various ligands as well as modulating protein interaction and localization (Henry & Crosson, 2011), FHA domains usually recognize phosphor-threonine containing proteins and facilitate protein interaction (Pallen *et al.*, 2002). The EspA FHA domain is thought to be involved in binding of two serine/threonine kinases, PktA5 and PktB8, which modulation EspA activity (Stein *et al.*, 2006). RedC, the sensor protein of the Red system, contains four transmembrane domains which likely sense two so far unknown different stimuli, regulating the proteins specificity towards RedF and RedD (Jagadeesan, 2008, Jagadeesan *et al.*, 2009). Hpk30 however, lacks any sensing domains. Based on my data, I propose Hpk30 to be a signal integrating module whose kinase activity (likely

the output of the system, phosphorylating a yet unknown cognate response regulator), is modulated by phosphorylation of the two receiver domains. Also a separate regulation through Ser/Thr phosphorylation is possible (see Section 6.2 for details). The signals Hpk30 responds to are not identified yet and it remains unsolved why Δ*hpk30* shows varying developmental timing in starvation assays. Therefore, it is likely that Hpk30's activity is modulated by proteins which sense signals that are not controlled in our assays (e.g. light exposure, humidity of the environment, temperature shifts from opening and closing incubators, number or genotype of strains spotted to the same CF plate) or react very sensitive to slight differences in culture conditions than it can be controlled for (e.g. pH, lot variations of media components, water quality and particles).

TodK on the other hand contains two PAS domains which are proposed to be sensing domains. Stimuli prediction of PAS domains is very complicated, since PAS domains have been reported to respond to factors from abiotic factors such as light, pH and redox potential to ligand binding from ions to small molecules and proteins (Moglich *et al.*, 2009b, Henry & Crosson, 2011). Similarities of PAS domains can rather be addressed by their folds, because they do not share much sequence similarity (Moglich *et al.*, 2009b). A subtype of PAS domains has been introduced as light-oxygen-voltage (LOV) domains (Crosson *et al.*, 2003). These domains always occur in tandems and are defined by their ability to be photosensors that bind Flavin nucleotides and display phototropin like photochemistry (Moglich *et al.*, 2009b). While there is so far no indication that TodK PAS domains should be defined as a LOV domain, light and oxygen are intriguing potential stimuli for this system. It was shown repeatedly that TodK mutants display different phenotypes under alternating starvation conditions (i.e. starvation on nutrient limited CF plates or under submerged culture) (this study and (Lee, 2009)). Speculations about what causes this phenomenon include differences in nutrient levels, differences in oxygen levels and repeated light exposure. By sensing oxygen and/or light, TodK could function to define the position of a cell within the population (i.e. inside an aggregation center, at the periphery or outside by oxygen sensing as well as lower to the ground or higher up by light sensing). Testing this hypothesis would be challenging, but designed PAS-kinase chimers have been reported previously (Moglich *et al.*, 2010). It could be tested, whether fusing the TodK kinase domain to known light and/or oxygen sensors results in a wild type like phenotype. Moreover, it should be tested if both PAS domains are required for signal reception. Single domain deletions should be obtained *in vivo* and their developmental phenotype should be observed. It was previously reported that PAS domains can have cooperative effects and that by the presence of one PAS domain modulated the signal response of the second (Moglich *et al.*, 2010). Also chimeric proteins were generated by fusing known blue-light-sensors to kinase domain which was regularly modulated by an oxygen sensor (Moglich *et al.*, 2009a). By subjecting cells to blue light, the kinase was artificially activated. Such an approach could be used to artificially induce activity of TodK in a population, to test if constantly active TodK leads to a delay in developmental progression in the same way an over accumulation of the protein does.

It is obvious that signal sensing within the negative regulation of developmental progression in *M. xanthus* is very complex. The eventual output of the systems is the regulation of MrpC, a transcription factor at the center of developmental gene regulation and involved developmental timing as well as in cell fate decisions (Sun & Shi, 2001b, Ueki & Inouye, 2003, Lee *et al.*, 2012). The central role in the developmental program justifies and requires modulation by such complex signaling systems which depend on multiple stimuli, integrating and fine adjusting the cellular response most appropriately to complex environmental conditions.

6.6. MrpC functions as a hub protein

The developmental program of *M. xanthus* is highly sophisticated and consists of a complex regulatory signaling network of STPK, TCS, and transcription factors. Many of these developmental regulators can be bypassed in mutant backgrounds of *M. xanthus*, leading to highly variable phenotypes (Rhie & Shimkets, 1989, Dunmire *et al.*, 1999, Hager *et al.*, 2001, Cusick *et al.*, 2002, Tse & Gill, 2002, Rasmussen *et al.*, 2005, Higgs *et al.*, 2008, Cusick *et al.*, 2015). To my knowledge, there no mutant that is able to bypass MrpC, suggesting MrpC is a central player in the regulatory network. I could show that a ΔNR mutant additionally lacking *mrpC* was incapable of starvation induced development, the same phenotype that was observed for all strains lacking MrpC investigated so far. This suggested that the phenotype observed in ΔNR was truly induced by MrpC miss-accumulation and not a result of an MrpC independent suppressor mutant. Next, I wanted to elucidate if early and high accumulation of MrpC was sufficient to induce the phenotype observed in ΔNR. Therefore, I set out to express MrpC from a secondary site driven by the promotor of the pilin subunit *pilA*. The *pilA* promoter has been reported to be constitutively active in vegetative cells and early development (Wu & Kaiser, 1997) and has been successfully used previously to complement several gene deletions in *M. xanthus* including *csgA* (Lobedanz & Sogaard-Andersen, 2003), *romR* (Leonardy *et al.*, 2007), *bacM* (Koch *et al.*, 2011), *pkn14* (Bhardwaj, 2013) and *crdS* (Willett & Kirby, 2012). With a different scope of study, the overexpression of *mrpC* through the *pilA* promoter was tried previously and failed (Bhardwaj, 2013). This result could be reproduced in this study (Figure 17).I hypothesized that the high level of regulation on MrpC in the wild type background prohibits overexpression of this protein. Hence, I further hypothesized that in a strain background lacking one or several MrpC regulators, MrpC overexpression could be feasible. And indeed, a Δ*espAC* Δ*mrpC* mutant did not develop (as was expected), while upon introduction of Pr_{pilA}-*mrpC* at a secondary site of the genome partial development was restored and low levels of MrpC could be detected in immunoblot analysis (P.T. McLaughlin, M.M. Glaser and P.I. Higgs, unpublished data). Surprisingly, it was not possible to gain more MrpC accumulation by introducing further deletions of negative regulators (*todK* and *red(CDEF)).* These findings suggested three conclusions, which will be further elaborated below:

i) The *pilA* promoter does not have the capacity to induce sufficient expression of MrpC.

ii) Usage of a non-native promoter uncouples all endogenous regulatory mechanisms.

iii) Other regulatory mechanisms prohibit a higher MrpC protein accumulation.

The *pilA* promotor is generally believed to be highly and constitutively active (Wu & Kaiser, 1997). Yet, it is possible that it does not possess the capacity to induce expression of *mrpC* at such high levels as seen in the ΔNR mutant or even at wild type levels which are necessary for *M. xanthus* to complete the developmental program. A tunable promoter might be used to try to induce *mrpC* at different levels, for *M. xanthus* there are currently three such promoters described in the literature (controlled by copper (Gomez-Santos *et al.*, 2012), vanillate or IPTG (Iniesta *et al.*, 2012)). Unfortunately, both the copper and vanillate-inducible promoters have been shown to be unsuitable for *mrpC* induction during development ((Bhardwaj, 2013) and P.T. McLaughlin and P.I. Higgs, unpublished data).

Despite the *pilA* promoter being potentially not strong enough to induce *mrpC* effectively, it is also a possibility that MrpC is involved in the regulation of this particular promoter. Recently, it has been shown that MrpC has two putative binding sites within the *pilA* promoter region (Robinson *et al.*, 2014). The expression profile of *pilA* showed the gene to be primarily up-regulated during early development but later down-regulated as development progresses (Wu & Kaiser, 1997). These two observations taken together suggest that there might be a connection between MrpC accumulation which increases during development and *pilA* expression being down-regulated. Both studies were performed in the alternate wild type strain DK1622 where MrpC accumulation was shown to peak between 15 and 24 h of starvation (Rajagopalan & Kroos, 2014), while transcription of *pilA* decreases between 12 and 18 h of starvation (Wu & Kaiser, 1997). This regulation could be achieved by regulating the *pilA* promoter itself or *pil*-regulating elements. Both these options could be tested by electrophoretic mobility shift assay (EMSA), in order to if and with what affinity MrpC binds to the promoter regions *in vitro.* The proposed binding sites by Robinson and co-workers could be verified by introducing mutations altering the potential MrpC binding sites within the *pilA* promoter.

MrpC is heavily regulated both at a transcriptional and post-translational level. Hence, the hypothesis that merely deletion of four negative regulators was not sufficient to allow overexpression and artificial over accumulation of MrpC arose. During vegetative growth, accumulation of MrpC is likely prohibited by nutrient dependent proteolysis (Rajagopalan & Kroos, 2014). The protease facilitating the vegetative degradation of MrpC is not defined yet but seemingly is an ATP-independent metalloprotease (Rajagopalan & Kroos, 2014). Recently, yet further negative regulators of MrpC accumulation were characterized (Rajagopalan & Kroos, 2017). These authors demonstrated that DevT as well DevI and DevS negatively regulate

MrpC accumulation, yet not necessarily within the same pathway (Rajagopalan & Kroos, 2017).

By using a non-native promoter, translational and post-translational regulation are uncoupled from transcriptional regulation. For the EspAC system it has been demonstrated that the system regulates MrpC accumulation by activating a yet uncharacterized protease (Schramm *et al.*, 2012). The amount of MrpC which was produced in Δ*espAC* Δ*mrpC attB*::Pr_{pilA}*mrpC* likely was the portion regulated by this system within the total cell population. It is probable that the EspAC regulated proteolytic turnover of MrpC only occurs in (a subset of) peripheral rods, more likely even only in a subset of those. It was established that EspAC system functions independently from both TodK and Red (Lee, 2009). I now propose that TodK controls MrpC accumulation on the transcriptional level and Red to affect MrpC activity based on Ser/Thr phosphorylation. I could show that in a Δ*todK* mutant MrpC is miss-accumulated and the strain develops early (Figure 20). Additionally, I could show that in a strain overproducing TodK, MrpC accumulation is decreased and development is severely delayed (Figure 26, Figure 27 and Figure 29). Transcript levels of *mrpC* could be investigated in these strains (Δ*todK*, WT/*todK*$^{++}$ and Δ*todK*/*todK*$^{++}$). If TodK has an impact on the *mrpC* feedback loop at the transcriptional level, *mrpC* mRNA would be expected to be elevated in Δ*todK* while decreased in WT/*todK*$^{++}$ and Δ*todK*/*todK*$^{++}$. Resulting in the altered MrpC accumulation as detected in immunoblot analysis (Figure 20 and Figure 29). It was previously shown that *mrpC* transcription is unaffected in Δ*espA* (Higgs *et al.*, 2008). The same methodological setup could be used to study *mrpC* transcript in Δ*todK* as well as in WT/*todK*$^{++}$ and Δ*todK*/*todK*$^{++}$.

The finding that MrpC overexpression could not be accomplished by stepwise deletion of negative regulators further supports the finding that the negative regulators modulate MrpC via different pathways, on different levels and potentially in different (subsets) of cell populations.

6.7. Cell fate segregation and the generation of fruiting bodies

It could be shown previously that deletion of negative regulators leads to an increase of spores surrounding mature fruiting bodies of *M. xanthus* (Lee, 2009), suggesting peripheral rods sporulate inappropriately in these strains. Also, it was shown in the same study that this was a stepwise effect by deleting three negative regulator systems (TodK, Esp and Red), indicating that the three systems are differentially expressed or activated in subpopulations of peripheral rods. In this study, an attempt was made to generate a system to track gene expression as well as protein accumulation of *todK*/TodK at the single cell level (data not shown), unfortunately without success so far. Such a tool is urgently needed to further study spatial and temporal gene expression and subsequently protein accumulation of developmental regulators during the uninterrupted developmental process of *M. xanthus in vivo*.

More evidence for the hypothesis that negative regulators are present/active in subsets of peripheral rods comes from an earlier observation on the cell fate specific accumulation of MrpC (Lee, 2009). The cell fate specific accumulation of MrpC in the developing population was reported previously (Lee *et al.*, 2012). It was shown that at 48 h of development MrpC was merely present in the aggregating fraction (i.e. fruiting bodies) and was cleared from the non-aggregating cells (i.e. peripheral rods). In both Δ*red(CDEF)* and Δ*todK* mutants however, MrpC accumulation within the investigated cell populations was altered compared to the wild type. MrpC accumulated at higher levels in the non-aggregating cells, suggesting MrpC repression by Red and TodK was missing in this cell (sub)population.

In this study as well as in a previous study (Lee, 2009) it was observed that mutants affecting TodK, Hpk30 and the Red system exhibit different phenotypes under alternate starvation conditions (i.e. on CF nutrient limiting agar and under submerged culture). I hypothesize that this effect is caused by differences in the proportion of peripheral rods within the population. The proportion of peripheral rods in a developing *M. xanthus* population increases with increasing nutrient concentrations in the starvation medium (O'Connor & Zusman, 1991c). Starvation under submerged conditions in MMC medium (which is merely a buffer containing salts, see section 8.2.1.5) is considered more stringent starvation compared to starvation on CF agar, which is described as nutrient limited medium (containing low amounts of nutrients, see section 8.2.1.5). Hence, if negative regulator signaling systems are specifically active within peripheral rods and the proportion of peripheral rods is increased during starvation on CF-agar, the effect of these proteins would be increased as well, resulting in a stronger and more pronounced phenotype. One way to test if negative regulators are enriched in peripheral rods would be to separate the developing population (O'Connor & Zusman, 1991a, Lee *et al.*, 2012) and perform western blots with specific antibodies. Since cell separation assays from CF agar are technically challenging, it could also be an option to modify the submerged culture medium to be more nutrient rich. By adding stepwise more nutrients to submerged culture, it could be tested if the phenotypes of mutants lacking TodK, Hpk30 or the Red system become more pronounced under submerged culture as well.

Using (bifunctional) histidine protein kinases modulate cell fate segregation is a well-known mechanism from other organisms. In *B. subtilis*, cell fates are determined by phosphorylation of the respective master regulators Spo0A, DegU and ComA (reviewed in (Lopez & Kolter, 2010)). In *Caulobacter crescentus*, the single domain response regulator DivK is modulated by two antagonistic players, PleC and DivJ, in its role to establish asymmetry by localization and phosphorylation status (Paul *et al.*, 2008). Also modulation of phosphorylation status of the master regulator CtrA is controlled by the bifunctional kinase CckA (Mann *et al.*, 2016). In total, the complexity of establishing asymmetry for cell division and differentiation in *Caulobacter crescentus* includes several more kinases to regulate this crucial step tightly (Childers & Shapiro, 2014, Childers *et al.*, 2014, Mann *et al.*, 2016).

If the negative regulators are (mostly) acting in peripheral rods, it remains an open question why early development occurs in these mutants as well as why fruiting body

morphology is severely altered in the ΔNR mutant. The currently favored hypothesis assumes that cell density is miss-sensed when peripheral rods inappropriately accumulate MrpC and eventually sporulate. It has been shown that at least in Δ*red(CDEF)* and Δ*todK* mutants MrpC is accumulated at incorrectly high levels in peripheral rods (Lee, 2009). When cell density is miss-sensed, suggesting to the cells to be present at a higher density than they actually are, developmental progression is accelerated, due to stimulation of positive feedback loops. One result of this is the higher accumulation of MrpC within aggregates (Lee *et al.*, 2012). In the ΔNR mutant, developmental progression is severely accelerated, thus, time is not sufficient to form well-structured fruiting bodies, until sporulation is triggered. Thereby, the loosely packed EPS covered, flat fruiting body structures could be explained. During the developmental process, *M. xanthus* cell movement is directed towards aggregation centers. With MrpC at inappropriately elevated levels in cells normally destined to become peripheral rods, direction of the closest aggregation center might be miss-sensed as well in the ΔNR population. Lack of a definite direction towards aggregation centers, likely results in ridge like structures as were observed in the ΔNR population.

6.8. Why form fruiting bodies after all?

Fruiting body formation is a common social, obligate multicellular behavior of myxobacteria and must be evolutionary beneficial, otherwise it would have been expected to be lost over time. It was even experimentally shown that if selection favoring development was relaxed, the ability to develop was lost in populations (Velicer *et al.*, 1998). Two hypotheses have been raised over the years what this benefit could be, yet to date no experimental evidence for one or the other was gained. One hypothesis was that spores inside of fruiting bodies are better protected from environmental insults and predation than single spores (Velicer & Hillesland, 2008, Dahl *et al.*, 2011). The non-competing other hypothesis is formed around the idea that spores are better dispersed by being grouped as fruiting bodies and the population can benefit from group predation upon germination (Kaiser, 2001). As part of this study, I attempted to test both these hypotheses.

By taking advantage of the ΔNR mutant and comparing it to the wild type I tested resistance of mature spores to UV light exposure. I could show that spores within wild type fruiting bodies were more resistant to UV light exposure than both separated wild type spores as well as ΔNR spores within undisturbed flat, ridge like fruiting bodies Figure 15). This observation suggests spores are better protected from damaging UV light within well structured, densely packed fruiting bodies. This is the first experimental support for the “protection-hypothesis”. However, there are various possibilities to test further environmental insults on wild type and ΔNR fruiting bodies including desiccation, reduced oxygen conditions and pH stress. The effect of high cell density on development under pH stress has been recently tested. It was determined that under acidic pH stress the ability to form fruiting body was increasingly dependent on high cell densities (unpublished data Peitz and Velicer,

mentioned in (Velicer *et al.*, 2014)). This experimental setup could be utilized to test the pH resistance of wild type and ΔNR mutant spores and fruiting bodies.

Additionally, formation of dense fruiting bodies could be beneficial to survive killing either by other microorganisms or predation by animals such as nematodes. It was found that the nematode *Caenorhabditis elegans* does prey on the vegetatively growing slime mold *Dictyostelium discoideum* (Kessin *et al.*, 1996). However, upon *D. discoideum* development of a slime sheath is formed that protects the developing population (Kessin *et al.*, 1996). Such a function would be plausible for *M. xanthus'* EPS as well and should be experimentally tested.

M. xanthus spores can survive the gut of insects such as *C. elegans* (Dahl *et al.*, 2011). Also, it was shown that fruiting bodies are more resistant to predation by the bacteriophagous nematode than were dispersed, vegetative cells (Dahl *et al.*, 2011). I hypothesize that single spores which are surrounding fruiting bodies of the NR mutant would survive ingestion by nematodes, which theoretically could be living in the same natural habitats as *M. xanthus*, than would peripheral rods which surround fruiting bodies of the wild type. This could be tested either on undisturbed fruiting bodies and surrounding cells, or populations could be harvested and separated for aggregated and non-aggregated cells. The latter ones would be subsequently fed to nematodes.

The "dispersal-hypothesis" was experimentally tested using both *C. elegans* nematodes and *D. melanogaster* as dispersal vectors. Surprisingly, more dispersal was observed for the ΔNR mutant than for the wild type (Figure 13). Unfortunately, attempts to detect *M. xanthus* single spores or fruiting bodies on fly bodies failed (Figure 14). I hypothesize that only single cells outside of fruiting bodies are dispersed by *D. melanogaster*: Flies were not sterile when added to this experiment, so the natural flora of bacteria and fungi was present on fly legs. Due to the predicted resistance of spores (i.e. single cells outside of ΔNR fruiting bodies) to stresses arising from competitive microorganisms, these cells may survive this transport rather than peripheral rods (i.e. single cells surrounding wild type fruiting bodies). A previous study reported the fruit fly *D. melanogaster* to be a vector of both bacteria and yeast through ingestion (Gilbert, 1980). Here, I would hypothesize that again single spores of the ΔNR mutant could survive this method of transportation, while peripheral rods might lyse within the insect gut environment. This could be tested as described above for ingestion of *M. xanthus* by nematodes. Another aspect to this is that *D. melanogaster* might not be big enough to transport whole fruiting bodies produced by *M. xanthus*. Bigger insects such as milkweed bugs (*Oncopeltus fasciatus*) were tried as vectors within this study, but the experimental setup for these needs more optimization.

Since dispersal was performed to pre-digested CYE media, there would be no advantage to dispersed groups over dispersed single cells. Growth rates of *M. xanthus* are dependent on cell density when growing on casitone media (Rosenberg *et al.*, 1977). It could be shown convincingly that populations grew faster on long peptides when cell density was increased, likely due to the benefit of high concentration of secreted extracellular digestive enzymes. Growth rate was found to

be unaffected when strains were grown in pre-digested peptide media (Rosenberg *et al.*, 1977). If the dispersal assay would be repeated using a media where social growth is beneficial, e.g. by using complex media in which secreted extracellular peptidases at high concentrations are needed (casitone, bacteria or yeast prey media), effects arising from social behavior might be intensified. *Drosophila* is likely not naturally found in the same environmental niches as *M. xanthus*. More work is needed to identify potential natural vectors for *M. xanthus* dispersal. A larger invertebrate could possibly transport entire fruiting bodies of the wild type as well as ingest spores or (partial) fruiting bodies. Spores are more likely to survive the gut passage than vegetative cells and peripheral rods. Moreover, ingestion would put spores (singular or in groups) near populations of prey bacteria of both the gut and dung of insects. Testing dispersal of wild type and ΔNR fruiting bodies by larger insects together with dispersal to more challenging habitats could add deeper insights into verifying or rejection of the dispersal-hypothesis.

Interestingly, a study on the social amoeba *D. discoideum* revealed that dispersal of spores is increased when spores were presented in fruiting bodies (Smith *et al.*, 2014). *D. discoideum* formed fruiting bodies on agar at the bottom of a conical tube. In some tubes, the fruiting bodes were physically disrupted by concussion and *D. melanogaster* fruit flies were introduced and interacted with either dislodged single spores or intact fruiting bodies. It was demonstrated that flies acquired spores more rapidly from intact fruiting bodies (Smith *et al.*, 2014). However, there are several differences between fruiting bodies produced by *D. discoideum* and *M. xanthus* that make both alternating observations plausible. First, *D. discoideum* fruiting bodies can be easily physically disrupted simply by banging the tubes to a solid surface (Smith *et al.*, 2014). This fragility is likely because the spore masses are produced at the end of a long stalk. It is likely that when *D. melanogaster* touched *D. discoideum,* fruiting bodies they disrupted and thus flies were exposed to multitude of single spores at once, spreading over wide parts of their bodies as was shown by fluorescence microscopy (Smith *et al.*, 2014). When fruiting bodies were dislodged prior to fruit fly exposure, spores were merely picked up one by one by fly legs. Therefore, it is likely that although fruiting body formation of *D. discoideum* increases spore transportation by fruit flies, spores seem to be dispersed as single spores. Since, during vegetative growth *D. discoideum* lives solitarily and does not exhibit social behaviors such as *M. xanthus* wolf pack like predation or social motility, this is likely of no disadvantage to the amoeba. Another aspect is that Dictyostelid species vary drastically in the length of the stalk on which spore masses are elevated above the soil ground (Romeralo *et al.*, 2013). In contrast, *M. xanthus* fruiting bodies are difficult to disperse without harsh physical methods (Lee *et al.*, 2012) likely because the non-stalked, dome-shaped fruiting bodies have greater contact with the surface. Thus, simple contact between flies and *M. xanthus* fruiting bodies was unlikely to either disrupt fruiting bodies or dislodge them from the surface. Thus, lawns of spores are more easily transferred by files. Interestingly fruiting body morphology of myxobacteria show a great diversity, from mounds close to the ground, (*M. xanthus*), to tree shaped, upstanding structures, formed by *Stigmatella aurantiaca* (reviewed in (Shimkets,

1990)). Hence, it is possible that distinct species evolve according to the exact needs of being dispersed or being sticky to stay in one spot even as developed fruiting body.

A study of the genetic population structure of *M. xanthus* at a centimeter scale found that long-distance dispersal seems not to occur frequently (Vos & Velicer, 2006). The authors base this on their finding of low proportion of distantly related clones. Another not necessarily contradictory possibility, would be that clones that arrive long-distance are mal-adapted to the new environment and thus decrease rapidly in frequency (Vos & Velicer, 2006). Hence, the authors claim *M. xanthus* evolution to be largely clonal. These observations are nicely consistent with my experimental finding that *M. xanthus* wild type fruiting bodies are poorly dispersed by *D. melanogaster* and suggests that it is more beneficial for *M. xanthus* to form densely packed fruiting bodies which have evolved to reduce dispersal by sticking to the surface they were formed on and enhance resistance to environmental insults. However, the observation that production spores inside fruiting bodies can be controlled by signaling systems, suggests that *M. xanthus* may be able to choose, in response to environmental cues, whether to favor dispersal (loosely connected spores) or favor resistance (compact fruiting bodies). The nature of these environmental cues is unknown, and identification of the stimuli to which each of the Esp, Red, TodK and Hpk30 respond would be important to clarify this process.

We can test experimentally, whether there is an evolutionary fitness advantage for one phenotype or the other (i.e. well-structured fruiting bodies surrounded by peripheral rods as produced by the wild type versus ridge like flat fruiting bodies surrounded by spores as produced by ΔNR mutant). In an asocial environment, such fitness determining experiments have been described before (Velicer *et al.*, 1998, Velicer *et al.*, 2002). Here, I propose to test evolutionary fitness in the natural habitat rather than under laboratory conditions. Both strains (wild type and ΔNR mutant, both carrying a fluorescent or antibiotic marker for later scoring) could be seeded into patches of soil and left to persist the natural environmental insults and microbial competition. After a period of time, bacteria inherent in the soil patches could be harvested, and surviving individuals of wild type and ΔNR mutant could be enumerated. The two *M. xanthus* strains could be seeded in separate patches or even in the same. The latter would also test for a dominating strain in direct competition.

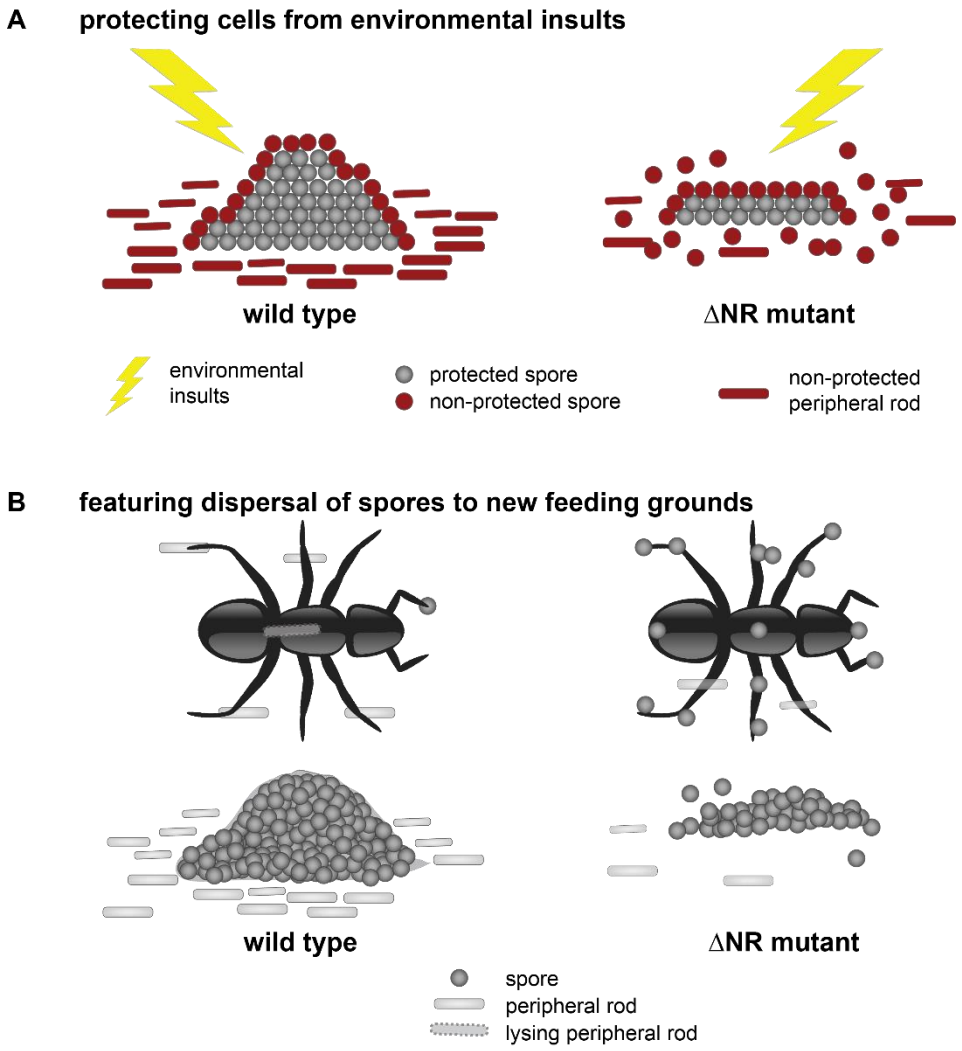

Figure 61: Current model: *M. xanthus* uses signaling systems to precisely tune cell fates to environmental conditions. (A) Well-structured fruiting bodies protect more efficiently. In a complex habitat, *M. xanthus* faces a multitude of environmental insults. Inside a tightly packed, well-structured fruiting body (wild type, left) spores are well protected from such stresses. Merely spores at the periphery of fruiting bodies and peripheral rods are affected. Alternatively, in loosely packaged, ridge like fruiting bodies (ΔNR mutant, right side), spores are less protected and more spores are suffering damage from environmental stresses. In conclusion, to resist environmental insults it is beneficial to form compact fruiting bodies by activating the 'negative regulator proteins'. **(B) Well-structured fruiting bodies are less well dispersed compared to loosely packaged ones surrounded by spores.** In an environment where it is beneficial to be dispersed to new feeding grounds, ΔNR seems to have an advantage. Hence, by switching off its 'negative regulator signaling systems', *M. xanthus* can adopt to this need and produce lawns of spores. Also, single spores likely have a selective advantage over peripheral rods when dispersal is carried out through ingestion by insects (illustrated as lysing peripheral rod inside the ant).

The finding that both observed phenotypes seem to have advantages to one environmental situation or another opens new, intriguing fields. It is a reasonable possibility that *M. xanthus* utilizes its signaling systems to adopt to individual environmental situations (Figure 61). Thereby assessing which phenotype would be more suitable for the population to survive the environmental insults present – form densely packaged fruiting bodies to stick to one habitat and sense when nutrients become available again utilizing peripheral rods, or form singular spores and loosely packed fruiting bodies to be dispersed to new feeding grounds.

7. Conclusion and future perspectives

This thesis research provides a scaffold for the thought that the systems regulating and achieving multicellularity in *Myxococcus xanthus* are structured in the same way as eukaryotic signaling systems. Multicellularity is controlled by converging several signaling systems on one major hub protein. In the case of *M. xanthus* development, this hub protein is the transcription factor MrpC. Hierarchical as well as parallel signaling systems control accumulation of MrpC in various ways (e.g. at the transcriptional level as well as via post-translational modifications and proteolytic turnover). These signaling systems of *M. xanthus* have diverse input domains and the systems are likely interconnected (e. g. phosphorylation of Hpk30s two receiver domains by yet unknown HPKs or the Red system being linked to a STPK cascade). In the *M. xanthus* genome DNA-binding elements are underrepresented compared to other (social) microorganisms, suggesting conversion of several signaling pathways on hub proteins might be occurring more often. The extreme complexity and modulation capacity of signaling systems regulating *M. xanthus'* developmental progression and cell fate segregation through MrpC seems reasonable, taking into consideration that completion of the process comes at the expense of lysis of the majority of a population.

Unraveling the signal flow and identification of the system output has been successful in the past to determine how a signaling system regulates MrpC accumulation. By verifying the proposed interaction between RedF and KapC, this research could show again that once the output of a system is defined, the appropriate questions can be asked to identify interaction partners and pathways. The basic characterization of the signal flow within the previously unstudied negative regulators of development, TodK and Hpk30, provides the basis for the definition of the absolute connection to MrpC accumulation. The output of TodK likely is phosphatase activity on a so far unknown cognate response regulator, regulated by one or both PAS domains of the protein. In the Hpk30 signaling module, kinase activity is expected to be controlled by at least three factors. Identification of the modulating factors and inputs of the two systems would gain additional insight in which environmental stimuli activate or repress these systems.

In conclusion, this work provides more evidence that a sophisticated social behavior relies on likewise special and complex regulating systems. By integrating multiple input domains and (hierarchic) signaling systems to regulate one hub protein *M. xanthus* gains the required flexibility to react appropriately to diverse environments.

8. Material and Methods

8.1. Materials

8.1.1. Chemicals and Reagents

All chemicals and media components used in this study were purchased from Sigma-Aldrich, Carl Roth, Merck and Difco at high purity. Oligonucleotides were synthesized by Sigma-Aldrich. Preparation of all solutions was performed using demineralized and where necessary autoclaved water. Recipes for media and buffer solutions are included in the relevant chapters.

Table 3: Chemicals and kits used in this study.

Pure chemicals	Carl Roth, Merck, Sigma-Aldrich
Media components, agar agar	Carl Roth, Difco
Protein (Page Ruler Prestained Protein Ladder Plus) and DNA (MassRuler DNA Ladder, Mix) size standards	Thermo Scientific
PCR purification and Gel extraction kit	Quiagen
Plasmid purification kit	Zymo Research
BCA™ Protein Assay Kit	Thermo Scientific
Bradford reagent	Thermo Scientific
DNA modifying enzymes (restriction endonucleases, polymerases, T4 DNA ligase, Antarctic phosphatase)	Thermo Scientific or New England Biolabs
DNA sequencing	Eurofins MWG Operon or Genewiz
goat- α-rabbit-HRP antibodies	Thermo Scientific
Custom made antibodies (*α*-TodK, *α*-Hpk30, *α*-KapC, *α*-MrpC) polyclonal rabbit antisera	Eurogentec (Belgium, Serain)
His-trap FF affinity columns	GE Healthcare
[γ^{32P}]-ATP	Hartmann analytic

8.1.2. Equipment and Software

Equipment used in this study is listed in Table 4. All system settings will be described in the respective sections. Software used in this study is listed in Table 5.

Table 4: Instruments used in this study.

Application	Program name	Manufacturer
PCR	Mastercycler personal	Eppendorf (Hamburg)
	Mastercycler gradient	
Real time PCR	7300 Real time PCR system	Applied Biosystems
Cell disintegration	French® pressure cell press	SLM instruments (Urbana, IL)
	FastPrep 24 cell and tissue homogenizer	MP Biomedicals
Ultrasound sonification	Branson sonifier 250	Heinemann
FPLC protein purification	Äkta™ Purifier	GE Healthcare
Protein electrophoresis	Mini-PROTEAN® 3 Cell	Bio-Rad
Western blotting	PerfectBlue Semi-Dry Elektroblotter	PEQLAB Biotechnologie
	TE42 Protein transfer tank	Amersham Bioscience
	TE62	Hoefer
Microscopy	MZ 8 stereomicroscope Eclipse E600	Leica microsystems Nikon
Phosphor autoradiography	StormTM 840 imager	GE Healthcare Life science
	Storage phosphor screen	
Electroporation	Gene pulser Xcell	Bio-Rad
UV lamp	UVG-11 Compact UV lamp (UL-3101-1, 1st edition, CSA C22.2 No.1010.1-92); P/N 95-0016-14; Properties: 254 nm UV, 4-Watt, 115 V ~ 60Hz, 0.16 Amps	Entela

Spectrometry	Ultrospec 2100 pro	Amersham Bioscience
	Nanodrop ND-1000 UV-Vis spec.	Nanodrop
DNA illumination and documentation	UVT 20 LE UV table	Herolab
	2 UV Transilluminator	UVP BioDoc-IT-System
Reaction incubation	Thermomixer comfort	Eppendorf
Incubation of cell cultures	Innova-4000® -44® orbital incubator	New Bronswick Scientific
	B6420 incubator	Heraeus (Langenselbold)

Table 5: Software used in this study.

Application	Program name	Manufacturer
Microscopy imaging	Leica Application Suite NIS-Elements Microscope Imaging Software	Leica microsystems (Nikon).
In silico cloning	Vector NTI AdvancedTM 11 Lasergene	Invitrogen DNA Star
Predicition of protein parameters	ProtParam (Web based)	SIB (Genève, Switzerland); http://web.expasy.org/protparam/
Sequence alignment	Clustal W	SFI
Äkta system management	UNICORN	GE Healthcare Life science
Phosphor autoradiography	Image Quant 3 and 5.2	GE Healthcare Life science
Quantification of 1D Gel	Image J	NIH
Statistical analysis	Excel 2007	Microsoft
Ortholog identification	ACT: Artemis Comparison Tool	Wellcome Trust Sanger Institute http://www.sanger.ac.uk/
	BLASTp and tBLASTn	NCBI, www.ncbi.nlm.nih.gov

8.2. Microbiological methods

8.2.1. Myxococcus xanthus

In this study, the wild type strain DZ2 (Campos & Zusman, 1975) was used as basis for all generated mutant strains.

8.2.1.1 Growth conditions

M. xanthus was grown on casitone yeast extract (CYE) media plates at 32 °C in the dark. When needed, plates were supplemented with kanamycin (100 µg/ml), oxytetracycline (10 µg/ml) or galactose (2.5 % w/v). For growth in liquid culture, Erlenmeyer flasks were filled with sterile CYE liquid media to 1/10th of their maximum volume and cells were inoculated using a sterile wooden stick. Flasks were incubated overnight on an orbital shaker at 220 rpm for optimal aeration of the culture. The density of a bacterial culture was determined by measuring the optical density at 550 nm (OD_{550nm}) using a spectrophotometer.

CYE	CYE plates	CYE top agar
0.1 % (w/v) Bacto™ Casitone 0.5 % (w/v) yeast extract 10 mM MOPS, pH 7.6 8 mM $MgSO_4$	CYE supplemented with 1.5 % (w/v) agar-agar	CYE supplemented with 0.75 % (w/v) agar-agar

8.2.1.2 Storage of *M. xanthus* strains

Plates carrying *M. xanthus* strains were kept at 32 °C for the maximum time of 7 days. Strains were re-streaked onto a fresh CYE plate only once. For long term storage, 25 ml of the respective strain was grown over night and DMSO was added to a final concentration of 0.5 M (900 µl from a 13.66 M stock solution). These chemically-induced sporulation and strains are more stable when deep frozen. After another overnight incubation at 32 °C in shaking culture, spores were harvested by centrifugation (4600 x g, 20 min, RT). The supernatant was discarded and the pellet was resuspended in 1-5 ml of fresh CYE. Cell aliquots of 1 ml were mixed with 250 µl DMSO in a 2 ml screw cap tube and stored at – 80 °C. Non-sporulating strains were frozen as vegetative cells without addition of DMSO and a second overnight incubation. Cells were harvested and frozen with DMSO as described above.

8.2.1.3 Preparation and transformation of electro competent *M. xanthus*

DNA was transformed into *M. xanthus* by electroporation. Desired strains were grown in 100 ml CYE culture overnight to a cell density of OD_{550nm} 0.35 - 0.7. Cells were pelleted (4600 x g, 15 min, RT) and the supernatant was removed. The cell pellet was washed twice with 25 ml sterile ddH_2O each and pellet again as above. Cells were

resuspended into 1 ml of ddH_2O and pelleted again (4000 x g, 5 min, RT). Supernatant was removed and cells were resuspended in approximately 150 µl ddH_2O. Aliquots of 50 µl were used per transformation reaction. Electro competent cells could be used fresh or be stored at – 80 °C until use.

For the electroporation, 1 µg of plasmid DNA or 5 µg of genomic DNA were mixed on ice with the thawed competent cells and transferred into a 0.1 µm electroporation cuvette (Biorad). Transformation took place at 0.65 kV, 25 µF and 400 Ω (BioRad Gene Pulser). Cells were immediately recovered in 1 ml fresh CYE and transferred into a 2 ml Eppendorf cup. Recovery took place for 4-6 h shaking at 32 °C. Subsequently, 100, 300 and 600 µl of cells were plated in CYE top agar (1.5 % agar in CYE) onto CYE plates, both containing the appropriate antibiotics. Dried plates were inverted and incubated at 32 °C for 5-7 days and checked frequently for growing clones.

8.2.1.4 Generation of insertion, in-frame deletion and substitution strains

Gene knock-out mutants of *M. xanthus* were generated by either interrupting the target gene (insertion mutant) or by deletion of the entire gene (in-frame deletion mutant). Site specific substitution mutants were generated by replacing the codon coding for the targeted amino acid by the codon most used in *M. xanthus* to code for the desired amino acid (selected based on (Nakamura *et al.*, 2000)).

For the generation of insertion mutants, a 500 bp internal fragment of the target gene was cloned into the suicide plasmid pBJ114 and transformed into *M. xanthus*. Positive integrants were selected by plating transformants on CYE plates supplemented with kanamycin.

In-frame deletion mutants in *M. xanthus* were generated as described before in detail in (Lee et al., 2010). Briefly, ~500 bp fragments up- and downstream of the target gene were amplified by PCR from genomic DNA (primers used for the up-stream fragment are designated A and B; primers used for the down-stream fragment are designated C and D). Primers B and C include an overlap region, allowing to fuse AB and CD fragments together in a following PCR using primers A and D. For this overlap PCR, fragments AB and CD were PCR purified or gel excised and purified and 40 ng of each fragment were used as template. Primers A and D included restriction sites. After gel extraction of the generated fusion fragments, they were digested with the appropriate enzymes and inserted into the suicide plasmid pBJ114 (Julien *et al.*, 2000). After ensuring that the generated plasmid (insert) was error-free by sequencing, it was transformed into *M. xanthus*. The vector includes a kan^R cassette in addition to the *galK* gene of *E. coli*. Via a homologous recombination event, the plasmid can integrate into the *M. xanthus* genome. Positive integrants were selected on CYE plates containing kanamycin. Single clones of integrants were inoculated into CYE broth and cultivated to mid logarhythmic phase over night. During this incubation without kanamycin selection pressure, some integrants will undergo a second spontaneous homologous recombination event and ‘loop-out’ the vector. For *galK*-

mediated counter selection, selecting for clones which lost the vector, cells were plated onto CYE plates containing 2.5 % (w/v) galactose (Ueki et al., 1996). Incubation on galactose containing medium is toxic for cells who still have the vector incorporated in their genome. These cells produce galactokinase from the *galK* gene, leading to the accumulation of galactose phosphate. Since *M. xanthus* is unable to metabolize galactose phosphate, it accumulates to toxic levels in the cells and is eventually lethal.

Resulting kanamycin sensitive galactose resistant clones were screened by colony PCR for strains lacking the target gene using primers outside of AB and CD fragments, designated primers E and F.

Site-specific amino acid substitutions were generated using the same method. The codon substitution was included in the overlapping sequence parts of primers B and C for the first PCR reaction. Resulting kanamycin sensitive galactose resistant clones were screened by colony PCR using E and F primers as described before. However, in this special case, the E primer ended exactly on the altered codon. To screen for point-mutant strains, an E primer ending on the substituted sequence was used (E_{mut}), to screen for wild type strains, an E primer ending on the native sequence was used (E_{WT}). All identified substitution mutants were subsequently confirmed by sequencing of the DNA region.

Strains expressing a gene from a secondary site under the control of the *pilA* promotor were integrated via site specific recombination at the MX8-attachment site. The base plasmid used was pVG126 (Bhardwaj, 2013). The target gene was exchanged in this vector by using the same restriction sites to remove the present insert and replacing it with another one. The vector backbone was gel excised and purified in between. Insertion of a plasmid at the *attB*-site was confirmed using three established PCRs, performed on isolated crude genomic DNA. A correct integration could be determined from the length of the PCR products obtained in the three PCR reactions: PCR I (700-800 bp), PCR II (840 bp) and PCR III (no product). An empty, non-altered *attB* site, would result in the following pattern: a PCR product of ~500 bp in PCR III, the absence of a product in PCR I and II. To ensure the phenotype observed was specific and reproducible, at least three independent clones of each generated mutant was tested initially.

Strains used in this study are listed below (Table 6). Plasmids used for strain generation and primers used for construction of plasmids as well as testing of proper integration or in frame deletions can be found in section 8.3.8 (Table 8 and Table 9, respectively).

Table 6: *M. xanthus* strains used in this study.

strain	genotype	reference
DZ2	wild type	(Campos & Zusman, 1975)
Insertion mutants *M. xanthus*		
PH1054	DZ2 Δ*espA* Δ*espC* Δ*red(CDEF)* *todK*::miniTTn5 (tet)8846	(Lee, 2009)
PH2017	DZ2 Δ*espA* ΔespC Δ*red(CDEF)* Δ*mrpC* *todK*::miniTTn5 (tet)8846	this study
PH2018	DZ2 MXAN_4466::pMG011	this study
attB-site insertion mutants *M. xanthus*		
PH2019	DZ2 *attB*::pGL1	this study*
PH2020	PH2002 *attB*::pGL1	this study*
PH2021	DZ2 *attB*::pAL4	this study*
PH2022	PH2002 *attB*::pAL4	this study*
PH2023	PH2003 *attB*::pVG111	this study
PH2024	PH2017 *attB*::pVG111	this study
PH2025	PH1025 *attB*::pVG111	this study**
PH2026	DZ2 *attB*::pMG013	this study
PH2027	DZ2 *attB*::pMG014	this study
PH2028	DZ2 *attB*::pMG015	this study
PH2029	DZ2 *attB*::pMG016	this study
PH2030	PH1045 *attB*::pMG013	this study
PH2031	PH1045 *attB*::pMG014	this study
PH2032	PH1045 *attB*::pMG015	this study
PH2033	PH1045 *attB*::pMG016	this study
PH2034	DZ2 *attB*::pMG017	this study
PH2035	PH2000 *attB*::pMG017	this study

strain	genotype	reference
In-frame deletion mutants *M. xanthus*		
PH1045	DZ2 Δ*todK*	(Lee, 2009)
PH2000	DZ2 Δ*hpk30*	P. Mann and P.I. Higgs
PH1103	DZ2 Δ*redF*	(Jagadeesan *et al.*, 2009)
PH1025	DZ2 Δ*mrpC*	(Lee *et al.*, 2012)
PH1047	DZ2 Δ*espA* Δ*espC*	(Lee, 2009)
PH2001	DZ2 Δ*kapC*	X. Mei, P. Mann and P.I. Higgs
PH1053	DZ2 Δ*espA* Δ*espC* Δ*red*(*CDEF*)	(Lee, 2009)
PH2002	DZ2 Δ*espA* Δ*espC* Δ*red*(*CDEF*) Δ*todK*	B. Lee and P.I. Higgs
PH2003	DZ2 Δ*espA* Δ*espC* Δ*red*(*CDEF*) Δ*mrpC*	this study
PH2004	DZ2 Δ*todK*Δ*dotR*	this study
PH2005	DZ2 $todK_{\Delta Pas}$	this study
PH2007	DZ2 ΔMXAN_5052	this study
PH2008	DZ2 Δ*todK* ΔMXAN_5052	this study
PH2009	DZ2 Δ*hpk30*-MXAN_4466	this study
Substitution mutants *M. xanthus*		
PH2010	DZ2 $todK_{H275A}$	this study
PH2011	DZ2 $todK_{D276A}$	this study
PH2012	DZ2 $todK_{S279A}$	this study
PH2013	DZ2 $hpk30_{H45A}$	this study
PH2014	DZ2 $hpk30_{D306A}$	this study
PH2015	DZ2 $hpk30_{D436A}$	this study
PH2016	DZ2 $MXAN\_4466_{stop}$	this study

* constructed by G. Leung under my supervision

** remade to reconstruct PH1116, previously made in (Bhardwaj, 2013)

8.2.1.5 Developmental assays

Starvation on CF-nutrient limiting agar plates

Clone fruiting (CF) nutrient limiting agar plates were prepared by adding 25 ml molten CF-agar to a petri dish. Plates were solidified overnight at room temperature. Cell density was determined by measuring the absorbance at 550 nm (A_{550}). 1 ml of each culture was harvested (4600 x g, 10 min, RT), washed with 1 ml MMC and pelleted again. Cells were concentrated to OD_{550nm} 7 and 10 µl were spotted to pre-warmed (32 °C) CF plates. A maximum of 5 strains were spotted to one plate, a wildtype reference was taken along on each plate. After drying, plates were inverted and incubated at 32 °C. Pictures were recorded using a Leica MZ8 stereomicroscope and a Leica DFC320 camera.

CF agar

0.015 % Bacto™ Casitone
10 mM MOPS pH 7.6
8 mM $MgSO_4$
1 mM KH_2PO_4
0.2 % $C_6H_5Na_3O_7$*$2H_2O$
0.02 % $H_8N_2O_4S$
1.5 % Difco™ agar
Solution was autoclaved and cooled to 60 °C.

Prior to use 0.1 % sodium pyruvate was added.

MMC

10 mM MOPS, pH 7.0
4 mM $MgSO_4$
2 mM $CaCl_2$

Starvation in submerged culture

Overnight M .xanthus cultures in exponential phase were diluted to OD_{550nm} 0.035 in fresh CYE medium and either 16 ml or 0.5 ml were seeded into 90 mm petri dishes each well of a 24 well plate tissue culture plate, respectively. After incubation for 24 h at 32 °C, CYE was replaced with the same volume of MMC and plates incubated at 32 °C. Pictures of developing cells were recorded using a Leica MZ8 stereomicroscope and a Leica DFC320 camera.

Determination of heat- and sonication resistant spores

Cells were starved under submerged culture conditions as described above in 24 well plates. Three wells were used per strain and per time point. Cells were harvested from the wells in the remaining MMC media, transferred to an Eppendorf tube and pelleted (4600 x g, 10 min, RT). Pellets were resuspended in 500 µl H_2O and heated at 50 °C for one hour. Cells were then sonicated at output 3, 30 % duty cycle, 2x 20 pulses (Branson Sonifer 250). Phase-bright spores were counted under a light microscope using a Helber bacterial counting chamber (Hawksley, UK). Sporulation efficiency was determined as percentage of wild type spores.

Germination assay

To determine viability of heat- and sonication resistant spores, germination assays were performed. Spores heated and sonicated as above were serial diluted (100 fold steps) in autoclaved H_2O, mixed with molten CYE top agar and poured over CYE agar plates. After solidifying, these were inverted and incubated at 32 °C for 3-7 days. Colonies were enumerated and germination efficiency was determined as percentage of wild type.

8.2.1.6 Dispersal assay

Starvation was induced under submerged culture conditions in small Petri dishes (35 mm, bidi, Martinsried) and strains were developed for five days at 32 °C. Supernatant was taken off and plates were kept inverted. Male individuals of wild type *Drosophila melanogaster* (strain w^{1118}) were added to lids of plates (10 per plate) an co-incubated with mature fruiting bodies for 4 h at RT. Flies were narcotized and transferred to inverted CYE agar plates supplemented with 10 µg/ml gentamycin and incubated for another 4 h at RT. Flies were removed and agar plates were incubated at 32 °C. Germinating colonies of *M. xanthus* were counted and pictures were recorded after 3-4 days.

8.2.1.7 UV resistance assay

Strains of interest were developed under submerged conditions for five days. Development was performed in 24-well plates, where one plate was prepared per planned UV treatment. After 120 h of development, one well of wild type fruiting bodies per plate was harvested in 500 µl autoclaved ddH_2O and transferred to a screw cap tube which was additionally sealed with parafilm. Fruiting bodies were disrupted into single spores using the FastPrep® 24 cell and tissue homogenizer by shaking twice at 5 m/s for 45 sec each. Resulting single spores were re-seeded in the plate. Remaining MMC media of other wells was replaced with 500 µl autoclaved ddH_2O. UV treatment was carried out one plate at a time for the desired time (0, 0.5, 1, 2, 5 and 10 minutes) using the UV lamp (Compact UV lamp, Entela, 254 nm UV, 4-Watt) set up horizontally at 23 cm above plate ground. The plates currently not under the UV lamp were kept closed in the same room for the duration of the UV treatment of all plates. Afterwards well contents were harvested into 2 ml reaction tubes and sonicated (10 %, 5 pulses of 0.5 sec each) to separate into single cells. Samples were diluted 1:10 stepwise in autoclaved ddH_2O, spotted onto CYE plates and allowed to germinate at 32 °C. Pictures were taken and germinated clones were counted after three, four and five days.

8.2.2. Escherichia coli

8.2.2.1 Growth conditions

E. coli strains were cultivated at 37 °C on Luria Bertani (LB) agar plates. For cultivation in liquid culture, a single colony was picked and inoculated in LB media. Incubation took place at 37 °C over night on an orbital shaker at 220 rpm. When applicable both broth and solid plates were supplemented with appropriate antibiotics (50 µg/ml kanamycin or 100 µg/ml ampicillin). *E. coli* strains used as hosts for cloning and protein overproduction are listed below (Table 7).

LB media	LB agar
1% (w/v) tryptone 0.5% (w/v) yeast extract 1% (w/v) NaCl	LB media supplemented with 1 % (w/v) agar-agar

Table 7: *E. coli* strains used in this study.

strain	genotype	reference
Host for cloning		
Top10	F⁻ endA1 recA1 galE15 galK16 nupG rpsL ΔlacX74 Φ80lacZ ΔM15 araD139 Δ(ara, leu)7697 mcrA Δ(mrr-hsdRMSmcrBC) λ-	Novagen
Host for protein overproduction		
BL21λDE3/pLysS	F- ompT gal dcm lon hsdSB(rB- mB-) λ(DE3) pLysS(cmR)	Novagen
GJ1158	ompT hsdS gal dcm ΔmalAp510 malP::(proUp-T7 RNAP) malQ::lacZhyb11 Δ(zhf-900::Tn10dTet)	(Bhandari & Gowrishankar, 1997)

8.2.2.2 Storage of *E. coli* strains

After overnight incubation at 37 °C, colonies were visibly grown on LB agar plates. These plates were sealed with Parafilm and stored in the fridge at 4 °C for a maximum of four weeks. For longer term storage, cryo stocks were generated. Strains were grown in liquid culture overnight and 680 µl of cell suspension was mixed with 320 µl of sterile 50 % (v/v) glycerol solution. Screw cap tubes were stored at – 80 °C.

8.2.2.3 Preparation and transformation of electro competent *E. coli*

Electro competent *E. coli* cells were used to transform relaxed plasmids (i.e. after a ligation). Competent cells were generated based on a protocol from Inoue *et al.* (Inoue *et al.*, 1990). *E. coli* TOP10 cells were grown over night in a 5 ml culture and subsequently sub-cultured in 1 l LB. Cultures were grown at 37 °C with shaking until the optical density reached OD_{550nm} 0.7. Cells were harvested (4600 x g, 30 min, 4 °C) and washed with decreasing volumes of 10 % sterile glycerol solution (1000 ml, 500 ml, 250 ml, 40 ml) with in between centrifugation steps as above. The last obtained pellet was resuspended in 2 ml ice cold 10 % glycerol solution and aliquots of 50 µl were frozen at – 80 °C after shock freezing.

Per transformation reaction, 2 – 5 µl ligation reaction was added to a tube of cells, which were thawed on ice before. The solution was transferred into a 0.1 µm electroporation cuvette (BioRad) and electroporation was performed at 1.25 kV, 25 µF and 200 Ω. Cells were recovered in 1 ml LB and incubated at 37 °C for 40 – 60 min. Of the cell suspension, 100 µl and 900 µl were plated onto LB plates containing the appropriate antibiotics.

8.2.2.4 Preparation and transformation of $CaCl_2$ chemical competent *E. coli*

$CaCl_2$ competent cells were prepared according to (Seidman *et al.*, 2001). Minor adjustments to the published protocol included: step 1, pre-cultures were grown in 5 ml LB in culture tubes at 37 °C with shaking; step 4, cells were harvested in 50 ml aliquots; step 8, cells were stored in 100 µl aliquots at – 80°C. Transformation was performed according to protocol, except competent cells were not transferred to new tubes but DNA was directly added to thawed cell aliquots. Also, heat shock was performed in a heating block instead of a water bath.

<u>$CaCl_2$ solution</u>

60 mM $CaCl_2$
15 % v/v glycerol
10 mM PIPES
pH 7

8.2.2.5 Preparation and transformation of TSS chemical competent *E. coli*

For preparation of TSS competent *E. coli* cells (Chung *et al.*, 1989), the desired strains were grown overnight in 5 ml cultures at 37 °C. Cells were subcultured into 1:100 into fresh 5 ml of LB and grown to the optical density of OD_{550nm} 0.7. Aliquots of 1 ml were harvested (4600 x g, 5 min, 4 °C). Each cell pellet was resuspended in 50µl TSS solution. TSS competent cells were either shock frozen and stored at – 80 °, or used fresh to transform supercoiled plasmid DNA. Per reaction 1 – 5 µl cold plasmid DNA was added to competent cells on ice and incubated on ice for 30 min. Heat shock transformation was performed at 37 °C for 2 min and cells were recovered in 1 ml LB for 40 – 60 min with shaking. Afterwards, 100 and 900 µl of the reaction were plated to LB plates containing appropriate selection antibiotics. Plates were incubated at 37 °C over night.

TSS solution

1 % (w/v) trypton
0.5 % (w/v) yeast extract
1 % (w/v) NaCl
10 % (w/v) PEG 3350
5 % (v/v) DMSO
50 mM $MgCl_2$
pH 6.5

8.2.3. Microscopy

8.2.3.1 Confocal laserscanning Microscopy

Strains were starved in submerged culture until completion of development. For this assay, special petri dishes were used (uncoated µ-dishes, 35 mm, Ibidi, Martinsried) and 2.1 ml of bacterial culture were used to start development. MMC was removed and 2 ml staining mix was added. Staining solution was composed of MMC supplemented with 2 mM $MnCl_2$ and 15 µl of Fluorescein conjugated concanvalin A (ConA) (5 mg ml -1; solubilized in 0.1 M $NaHCO_3$ pH 8.3, Invitrogen, Karlsruhe, Germany). ConA binds to a-mannopyranosyl and a-glucopyranosyl residues, which were reported to be present in *M. xanthus* fruiting body EPS (Li *et al.*, 2003). Incubation was performed for 30 min at RT in the dark. Stain solution was removed and fruiting bodies were washed twice with each 1 ml MMC plus 2 mM $MnCl_2$. For microscopy, 2 ml of MMC were added back to the cells. Fluorescein signal was recorded at an excitation wavelength of 494 nm and an emission wavelength of 518 nm. Pictures were taken with an inverted TCS-SP5 confocal microscope (Leica, Bensheim, Germany). Image data were processed by using IMARIS Software package (Bitplane AG, Zurich, Switzerland) or Volocity Software (Perkin Elmer).

8.2.3.2 Fluorescence microscopy of *D. melanogaster* legs

Legs of *D. melanogaster* were severed by manual manipulation under a dissecting microscope (performed by A. Chaubal). Detached legs were placed on a microscopy slide and the cover slide was fixated with clear nailpolish at the edges. Microscopy was performed using a Nikon Eclipse E600 microscope equipped with a QImaging Retiga 1300 camera. Pictures were analyzed and prepared using NIS-Elements Microscope Imaging Software (Nikon).

8.3. Molecular biology methods

8.3.1. Isolation of genomic DNA from *M. xanthus*

To isolate genomic DNA, respective *M. xanthus* strains were grown in a 25 ml culture overnight at 32 °C. Cells were harvested by centrifugation (4600 x g, 10 min, RT) and concentrated to OD_{550nm} 7 in TE buffer. Of this cell suspension, 1.3 ml were taken into a fresh tube and mixed well with 5 % (w/v) SDS, 100 µg/ml proteinase K and 50 µg/ml RNase A and incubated for 60 min at 37 °C. Subsequently, 0.167 volumes of 5 M NaCl and 0.114 volumes of 12.15 % (w/v) CTAB/NaCl solution were added and solution was incubated at 65 °C for 10 min. Afterwards, the solution was supplemented by 975 µl of a phenol:chlorophorm: isoamyl alcohol solution at a ratio of 25:24:1 and centrifuged (17000 x g, 2 min, RT). The aqueous layer was transferred into a fresh tube and mixed with an equivalent volume of a chlorophorm:isoamyl alcohol solution at an 24:1 ratio. After an additional centrifugation step as above, again the aqueous layer was taken to a fresh tube. Finally, 0.6 volumes of isopropanol were added and the solution gently inverted until the genomic DNA precipitated as a white string. The DNA precipitate was taken with a wooden stick to a fresh tube containing 1 ml of 70 % (v/v) ethanol. After centrifugation (17000 x g, 5 min, RT), the supernatant was removed and the pellet was washed once again with 1 ml of 70 % (v/v) ethanol. Finally, the pellet was dried and reconstituted in 50 µl ddH_2O. Concentration was determined using nanodrop technology.

TE buffer

10 mM Tris pH 8.0
1 mM EDTA

CTAB/NaCl
275 mM cetyl trimethyl ammonium bromide
700 mM NaCl

8.3.2. Isolation of crude DNA from *M. xanthus*

Crude genomic DNA was isolated from *M. xanthus* colonies by scraping off some cells from a CYE plate using a wooden stick. Cells were transferred into an Eppendorf tube containing 20 µl sterile ddH_2O. Cell disruption was achieved by boiling at 99 °C for 5 min. Released DNA (and other cytoplasmic cell components) were separated from whole cells and cell debris by centrifugation (4700 x g, 5 min, RT). Tubes were subsequently placed on ice and the supernatant containing the crude genomic DNA was used as a template for screening PCR reactions.

8.3.3. Isolation of plasmid DNA from *E. coli*

Plasmid DNA from *E. coli* was isolated from overnight liquid cultures using the Zyppy plasmid purification kit classic (Zymo Research, Freiburg, Germany) according to the manufacturers manual. The kit technology is based off of the alkaline lysis method described in (Birnboim & Doly, 1979).

8.3.4. Amplification of DNA fragments by PCR

DNA fragments were amplified using polymerase chain reaction. For the amplification, Pfu DNA polymerase was used when proof reading was required, Taq DNA polymerase was used when absolute sequence accuracy was not immediately required. Both were used along with Buffer J (Bioline). One reaction was generally composed of 10 – 100 ng template DNA, 0.5 µM of each primer and 0.2 – 0.5 µl DNA polymerase (dNTPs are provided in Buffer J). PCR programs were designed according to primer properties, length of the desired fragment and DNA polymerase used. Generally, 25 to 35 amplification cycles were performed. All PCR fragments were purified either from agarose gel fragments or from the PCR reaction by QIAquick Gel Extraction Kit or the QIAquick PCR purification kit, respectively, according to manufacturer's instructions.

8.3.5. Restriction digestion, de-phosphorylation and ligation of DNA

Plasmid DNA (~ 1 µg) and PCR products (200- 500 ng) were digested with 0.5 – 1 µl of FastDigest endonucleases (NEB) or regular restriction endonucleases (NEB) in a total reaction volume of 20 µl 1x FastDigest reaction buffer or the appropriate NEB reaction buffer. Incubation took place for 30 min to 2 h at 37 °C. If needed, digested plasmid DNA was additionally de-phosphorylated to minimize re-ligation. Therefore, 1-2 µl Antarctic phosphatase (NEB) was added to the reaction. Additional 5 – 10 µl reaction buffer and the appropriate adjusting amount of ddH_2O were added to the mix to a final volume of 50 µl and incubation at 37 °C was continued for 30 min. DNA fragments were purified either from agarose gel fragments or from the PCR reaction by QIAquick Gel Extraction Kit or the QIAquick PCR purification kit, respectively, following manufacturer's instructions. For ligation, generally 30 fmol insert DNA was mixed with 10 fmol plasmid DNA, these amounts were adjusted if necessary. In a total reaction volume of 20µl 1 µl T4-DNA ligase was used in 1 x T4-DNA ligase buffer. Ligation took place at 16 °C over night. From this ligation reaction 5 – 10 µl were directly transformed into electro competent *E. coli* cells.

8.3.6. DNA gel electrophoresis

Gel electrophoresis was performed using 0.5 – 2 % (w/v) TAE agarose gels in 0.5 x TAE buffer. To visualize DNA fragments, gels were supplemented with 0.01 % (v/v) ethidium bromide. *BstEII* digested λ phage size standard (Thermo Scientific) was used to determine both fragment size and estimate concentration. For DNA visualization and documentation, gels were exposed to a 2UV-Transilluminator at a wavelength of 365 nm and images were recorded using a thermo video printer. If desired, DNA fragments were gel excised and purified with the QIAquick Gel Extraction Kit according to supplier's recommendations.

TAE buffer

40 mM Tris pH 8.0
1 mM EDTA

6x Loading Dye

0.2 % (w/v) bromophenolblue
0.2 % (w/v) xylencyanol
50 % (v/v) glycerol

8.3.7. Sequencing of DNA

DNA analyzed at MPI Marburg: Samples were sent for sequencing to MWG Operon and the sequencing data was analyzed using VectorNTI™ express (Invitrogen).

DNA analyzed at WSU, Detroit: Samples were sent for sequencing to Genewiz and resulting sequencing files were analyzed using DNA star Lasergene software.

8.3.8. Construction of Plasmids

All plasmids used in this study were generated by amplification of a target gene (insert), restriction digest of insert and vector backbone and ligation of both. Resulting plasmids were shown to be of correct sequence by sequencing analysis, prior to use. Plasmids used in this study are listed below (Table 8). The relevant data for the construction of the plasmids constructed in this study can be found below (Table 9).

Table 8: Plasmids used in this study.

plasmid	vector	Insert/genotype	reference
Vector backbones			
pVG126	pFM18*	P_{pilA}-*pkn14*	(Bhardwaj, 2013)
pET32a	T7-Promotor, His_6-Tag (N- and C-terminal), Thioredoxin-Tag and S-tag (Nterminal), *Amp* ^{R}		Novagene
pBJ114	pUC119 with *Km*^{r} and *galK*; derived from pKG2		(Julien *et al.*, 2000)
pPH164	pBJ114	Δ*mrpC*	(Lee *et al.*, 2012)
pAAR140	pBJ113	Δ*dotR*	(Rasmussen & Sogaard-Andersen, 2003)
Insertion mutants *M. xanthus*			
pMG011	pBJ114	MXAN_4466	this study
Att-site insertion mutants *M. xanthus*			
pAL4	pSL8	P_{nfsA}-*mcherry*	(Muller *et al.*, 2010)
pGL1	pSL8	P_{pilA}-*mcherry*	G. Leung and P.I. Higgs
pMG013	pVG126**	P_{pilA}-*todK*$_{WT}$	this study
pMG014	pVG126**	P_{pilA}-*todK*$_{H275A}$	this study
pMG015	pVG126**	P_{pilA}-*todK*$_{D276A}$	this study
pMG016	pVG126**	P_{pilA}-*todK*$_{S279A}$	this study
pMG017	pVG126**	P_{pilA}-*hpk30*$_{WT}$	this study

plasmid	vector	Insert/genotype	reference
In-frame deletion mutants *M. xanthus*			
pMG001	pBJ114	*todK*$_{\Delta Pas}$	this study
pMG024	pBJ114	Δ*todK* Δ*dotR*	this study
pMG003	pBJ114	ΔMXAN_5052	this study
pMG004	pBJ114	Δ*hpk30*-MXAN_4466	this study
Substitution mutants *M. xanthus*			
pMG005	pBJ114	*todK*$_{H275A}$	this study
pMG006	pBJ114	*todK*$_{D276A}$	this study
pMG007	pBJ114	*todK*$_{S279A}$	this study
pMG008	pBJ114	*hpk30*$_{H45A}$	this study
pMG009	pBJ114	*hpk30*$_{D306A}$	this study
pMG010	pBJ114	*hpk30*$_{D436A}$	this study
pMG012	pBJ114	MXAN_4466$_{stop}$	this study
plasmid	**vector**	**Insert/genotype**	**reference**
Protein overproduction			
pSJ019	pET32a	*redF*	(Jagadeesan, 2008)
pMG018	pET32a	*todK*	this study
pMG019	pET32a	*todK*$_{H275A}$	this study
pMG020	pET32a	*todK*$_{kinase}$	this study
pMG021	pET32a	*todK*$_{PAS}$	this study
pMG022	pET32a	*hpk30*	this study
pMG023	pET32a	*hpk30*$_{H45A}$	this study

* (Muller *et al.*, 2010)

** (Bhardwaj, 2013)

Table 9: Primers used in this study. Restriction sites are in bold, codon substitutions are underlined**.**

Plasmid / used for	Primer name	designation	Sequence	Restriction site	Template DNA	Target plasmid
pMG001	oPH1571	A	GAC**GAATTC**CCCACCTCACCTTGTTCG	EcoR1	DZ2	pBJ114
	oPH1593	B	CGGCTGCGCGGCGGAAGGCTCGGCCAGG			
	oPH1594	C	CCTTCCGCCGCGCAGCCGGGCGTGGACG			
	oPH1597	D	GAC**GGATCC**GGTGCCTTCCGCCTCATCG	BamH1		
	oPH1620	E	CAGCCAGGTCTTCTACGGAGACG			
	oPH994	F	CACCGTCTTGTTGCTCCAGCG			
pMG024	oPH1571	A	GAC**GAATTC**CCCACCTCACCTTGTTCG	EcoR1	DZ2	pBJ114
	oPH1615	B	AAGAAGGTCGGCGGGGGTGGGGGGCATG			
	oPH1616	C	ACCCCCGCCGACCTTCTTGCGCCTCGG			
	oPH1617	D	GAC**GGATCC**CATCGCATCCTCTACAGC	BamH1		
	oPH1618	E	CGCGCCAAGCGCATCGGC			
	oPH1619	F	CCGCGTCGGTGCGTGCATC			
pMG003	oPH1740	A	CG**GAATTC**GCGCGTATCTGAGAACGC	EcoRI	DZ2	pBJ114
	oPH1741	B	GTCCGGAAACATCGTGTAGGGCGAGGC			
	oPH1742	C	TACACGATGTTTCCGGACCGGGGCCAC			
	oPH1743	D	CA**GGATCC**ACGAGGTGGACCTGCTCC	BamHI		
	oPH1783	E	ACCCGGTGAAGGCGATGC			
	oPH1784	F	GCGAGGACTTCGACGAGC			
pMG004	oPH1156	A	CG**GAATTC**ACGGCTACCGGCGCAGGC	EcoR1	DZ2	pBJ114
	oPH1157	B	TCAGGGCACGCTTGTACGCAACGCACC			
	oPH1158	C	CGTACAAGCGTGCCCTGACCGCCAGGC			
	oPH1159	D	CG**AAGCTT**CCTACCTCCGCGCGCTGC	BamH1		
	oPH1160	E	GCGGAACGTCGTCTACATGGC			
	oPH1161	F	CCACCGAGACGGAGATGAAGG			
pMG005	oPH972	A	CG**GAATTC**CTGGTGCACTGCCGTGAC	EcoRI	DZ2	pBJ114
	oPH973	B	GTC<u>CGC</u>GGTGACGATGCCCATGAGCTG			
	oPH974	C	ACC<u>GCG</u>GACATCCGCAGCCCGCTGGGC			
	oPH975	D	CA**GGATCC**GAAGGGCTCGAAGAGGTG	BamHI		
	oPH992	E_{wt}	GCTCATGGGCATCGTCACC**C**			
	oPH993	E_{mut}	GCTCATGGGCATCGTCACC**G**			
	oPH994	F	CACCGTCTTGTTGCTCCAGCG			

Plasmid / used for	Primer name	designation	Sequence	Restriction site	Template DNA	Target plasmid
pMG006	oPH972	A	CG**GAATTC**CTGGTGCACTGCCGTGAC	EcoRI	DZ2	pBJ114
	oPH1634	B	GCGGATCGCATGGGTGACGATGCCCATG			
	oPH1635	C	CACCCATGCGATCCGCAGCCCGCTGGGC			
	oPH975	D	CA**GGATCC**GAAGGGCTCGAAGAGGTG	BamHI		
	oPH1636	E_{wt}	TGGGCATCGTCACCCATGAC			
	oPH1637	E_{mut}	TGGGCATCGTCACCCATGCG			
	oPH994	F	CACCGTCTTGTTGCTCCAGCG			
pMG007	oPH972	A	CG**GAATTC**CTGGTGCACTGCCGTGAC	EcoRI	DZ2	pBJ114
	oPH1638	B	CAGCGGCGCGCGGATGTCATGGGTGAC			
	oPH1639	C	ATCCGCGCGCCGCTGGGCGCCATCATG			
	oPH975	D	CA**GGATCC**GAAGGGCTCGAAGAGGTG	BamHI		
	oPH1640	E_{wt}	GTCACCCATGACATCCGCAGC			
	oPH1641	E_{mut}	GTCACCCATGACATCCGCGCG			
	oPH994	F	CACCGTCTTGTTGCTCCAGCG			
pMG008	oPH1002	A	CG**GAATTC**GCGTGCTCGCGCTCCTCG	EcoRI	DZ2	pBJ114
	oPH1003	B	CAGCTCCGCCAGCACCTCCGCCGCCAG			
	oPH1004	C	GTGCTGGCGGAGCTGCGACAACCGCTG			
	oPH1005	D	CA**GGATCC**CACCGACAAGCCCAGTCC	BamHI		
	oPH1136	E_{wt}	CTGGCGGCGGAGGTGCTGCAC			
	oPH1137	E_{mut}	CTGGCGGCGGAGGTGCTGGCG			
	oPH1007	F	GTTCTTCGCGGTGACGATGAGGTCCAC			
pMG009	oPH1006	A	CG**GAATTC**CGCGCCTCATTGAACAGC	EcoRI	DZ2	pBJ114
	oPH1007	B	GTTCTTCGCGGTGACGATGAGGTCCAC			
	oPH1133	C	GTCACCGCGAAGAACCTGCCCGGCATG			
	oPH1009	D	CA**GGATCC**CCATGGTGAGGTGCTCGG	BamHI		
	oPH1138	E_{wt}	GGTGGACCTCATCGTCACCGAC			
	oPH1139	E_{mut}	GGTGGACCTCATCGTCACCGCG			
	oPH1015	F	CAGGATCCGCTGCTGCGGATTCAGGG			
pMG010	oPH1012	A	CG**GAATTC**TGATGGGCAAGGAGTGCG	EcoRI	DZ2	pBJ114
	oPH1013	B	CGTGAACGCCCAGCTCACCACCACGCC			
	oPH1014	C	AGCTGGGCGTTCACGCCCGCCTACGGG			
	oPH1015	D	CA**GGATCC**GCTGCTGCGGATTCAGGG	BamHI		
	oPH1141	E_{wt}	GGCGTGGTGGTGAGCTGGGAC			
	oPH1142	E_{mut}	GGCGTGGTGGTGAGCTGGGCG			
	oPH1143	F	ATCGTCTAGACTTGTCCACCCGCCACAGC			

Plasmid / used for	Primer name	designation	Sequence	Restriction site	Template DNA	Target plasmid
pMG011	oPH1000	for	CG**GAATTC**GGCACCCCACTGCTCACC	EcoRI	DZ2	pBJ114
	oPH1001	rev	CA**GGATCC**CACACGTCCTGGCCCACC	BamHI		
	oPH1141	E	GGCGTGGTGGTGAGCTGGGAC			
	oPH1145	F	GGCCTACCTCCGCGCGCTGCC			
pMG012	oPH1699	A	CG**GAATTC**GAGCTGGCGCAGCAGGCG	EcoRI	DZ2	pBJ114
	oPH1700	B	TCGGAGGAGTCAAGCAACACCCAACAGC			
	oPH1701	C	TGTTGCTTGACTCCTCCGACAAGCCGCC			
	oPH1702	D	CA**GGATCC**CGGGCTCCCCGCACCTGC	BamHI		
	oPH1141	E*	GGCGTGGTGGTGAGCTGGGAC			
	oPH1145	F	GGCCTACCTCCGCGCGCTGCC			
pMG013	oPH 944	A	AT**GGATCC**GCTGATCGACAGTTATCGTC	BamHI	DZ2	pVG126
	oPH1670	B	GGTGGGGGGCATGGGGGTCCTCAGAGAAGG			
	oPH1671	C	ACCCCCATGCCCCCCACCCCCGCCAAGAAGC			
	oPH1672	D	CAT**AAGCTT**TTAGTCGCGCGGGCTTCC	HindIII		
pMG014	oPH944	A	AT**GGATCC**GCTGATCGACAGTTATCGTC	BamHI	PH2010	pVG126
	oPH1670	B	GGTGGGGGGCATGGGGGTCCTCAGAGAAGG			
	oPH1671	C	ACCCCCATGCCCCCCACCCCCGCCAAGAAGC			
	oPH1672	D	CAT**AAGCTT**TTAGTCGCGCGGGCTTCC	HindIII		
pMG015	oPH944	A	AT**GGATCC**GCTGATCGACAGTTATCGTC	BamHI	PH2011	pVG126
	oPH1670	B	GGTGGGGGGCATGGGGGTCCTCAGAGAAGG			
	oPH1671	C	ACCCCCATGCCCCCCACCCCCGCCAAGAAGC			
	oPH1672	D	CAT**AAGCTT**TTAGTCGCGCGGGCTTCC	HindIII		
pMG016	oPH 944	A	AT**GGATCC**GCTGATCGACAGTTATCGTC	BamHI	PH2012	pVG126
	oPH1670	B	GGTGGGGGGCATGGGGGTCCTCAGAGAAGG			
	oPH1671	C	ACCCCCATGCCCCCCACCCCCGCCAAGAAGC			
	oPH1672	D	CAT**AAGCTT**TTAGTCGCGCGGGCTTCC	HindIII		
pMG017	oPH 944	A	ATGGATCCGCTGATCGACAGTTATCGTC	BamHI	DZ2	pVG126
	oPH1673	B	GGGTGTTTCCATGGGGGTCCTCAGAGAAGG			
	oPH1674	C	ACCCCCATGGAAACACCCGTGCCGCTC			
	oPH1675	D	CAT**AAGCTT**TCATGGGGTCTCTCGTTTG	HindIII		
pMG018	oPH601	for	GAC**GAATTC**ATGCCCCCCACCCCCGCC	EcoRI	DZ2	pET32a
	oPH604	rev	GCG**GTCGAC**TTAGTCGCGCGGGTTCC	SalI		
pMG019	oPH601	for	GAC**GAATTC**ATGCCCCCCACCCCCGCC	EcoRI	PH2010	pET32a
	oPH604	rev	GCG**GTCGAC**TTAGTCGCGCGGGTTCC	SalI		
pMG020	oPH1107	for	GAC**GAATTC**ACCCGGCGGCACTCCGAG	EcoRI	DZ2	pET32a
	oPH1108	rev	GCG**GTCGAC**TTAGTCGCGCGGGCTTC	SalI		
pMG021	oPH1105	for	GAC**GAATTC**ATGCCCCCCACCCCCGCC	EcoRI	DZ2	pET32a
	oPH1106	rev	GCG**GTCGAC**CTCGGAGTGCCGCCGGG	SalI		

Plasmid / used for	Primer name	designation	Sequence	Restriction site	Template DNA	Target plasmid
pMG022	oPH1109	for	GAC**GAATTC**ATGGAAACACCCG	EcoRI	DZ2	pET32a
	oPH1110	rev	GCG**GTCGAC**TCATGGGGTCTCTCG	SalI		
pMG023	oPH1109	for	GAC**GAATTC**ATGGAAACACCCG	EcoRI	PH2013	pET32a
	oPH1110	rev	GCG**GTCGAC**TCATGGGGTCTCTCG	SalI		
sequencing primers	oph 553	m 13 For	TTCGCTATTACGCCAGCTGG			
	oph 554	m 13 Rev	TTAGCTCACTCATTAGGCACC			
attB PCR**	oPH 477	*attB* left	CGGCACACTGAGGCCACATA			
	oPH 478	*attB* right	GGAATGATCGGACCAGCTGAA			
	oPH 479	attP left	GGGAAGCTCTGGGTACGAA			
	oPH 480	attP right	GCTTTCGCGACATGGAGGA			
qRT-PCR	oPH1432	*hpk30,*for	TGACGAAATCATCATCCGCATG			
	oPH1433	*hpk30,* rev	TGTCGGTGACGATGAGGTCCAC			
operon mapping ***	oPH1025	A, cDNA generation, rev	AGAGGTCCGTTTCGTCCGCCG			
	oPH1027	B	GACGCCTCGGCGCTCAGC			
	oPH1028	C	TGCCCGCATCGTCTGTCC			
	oPH996	D	ATGCGCCGGGTGGACGTG			
	oPH997	E	CAGCGCCTTGCCCAGCTC			
	oPH1026	F	GCGGGCGTGGTGGTGAGC			

* For this mutant no E_{WT} and E_{mut} test-PCR was performed but the DNA fragment surrounding the insertion was amplified from crude DNA with primers E and F and sequenced to ensure proper distinction of wild type from mutant clones.

** Primer combinations for *attB* site PCR:
PCR I: oPH477/oPH480; PCRII: oPH478/oPH479; PCR III: oPH477/oPH478.

*** Primer combinations for operon mapping:
inside MXAN_4466: oPH1027/1028;
inside *hpk30*: oPH996/oPH997;
over gene junction: oPH1026/oPH1028

8.3.9. RNA isolation, cDNA synthesis and quantitative real time PCR

Total RNA from *M. xanthus* cells was isolated using the hot-phenol method. Strains were grown under vegetative conditions or developed in submerged culture (16 ml dishes) format as described previously. Cells were harvested by centrifugation 4600 x g, 10 min, at 4 °C) and the supernatant was discarded. The cell pellet was resuspended in 1 ml of ice-cold solution 1 and transferred into a 15 ml Falcon tube containing 1 ml of solution 2 at 65 °C. The solution was gently homogenized by inverting the tubes 5 times. Subsequently, 2 ml of hot (65 °C) phenol was added to the sample, gently homogenized by inversion and the incubated for 5 min at 65 °C. The solution was then quick-chilled using liquid nitrogen (sample was not frozen!) and centrifuged (4600 x g, 5 min, 4 °C). The aqueous layer was transferred to a fresh 15 ml falcon tube (containing 2 ml of hot phenol), chilled and centrifuged as described above. The aqueous layer was again transferred to a fresh tube containing 2 ml of a phenol: chloroform: isoamyl alcohol (25:24:1) mixture, homogenized by inversion and centrifuged as above. The aqueous layer was transferred to a tube containing 2 ml of a chloroform: isoamyl alcohol (24:1) mixture and centrifuged as above. RNA was precipitated by transfer of the aqueous layer (~1 ml) to a fresh Eppendorf tube containing 100 µl of 3 M sodium acetate (pH 4.5) and 2.5 ml of 96 % EtOH. Incubation was performed – 80 °C for at least 30 min or overnight. After this incubation, the sample was centrifuged (4600 x g, 30 min, 4 °C) and the supernatant was removed carefully. RNA was washed with 5 ml of ice-cold 75 % EtOH and pelleted as above. The wash step was repeated once more. Finally, the supernatant was removed and the pellet was air dried. Purified RNA was dissolved in 100 µl of RNase-free water. Concentration and purity of RNA was measured by NanoDrop. 10 µg of the total extracted RNA was incubated in the presence of 10 µl RNase-free DNase I (EN0521, 1000 U, Thermo Scientific) in a 100 µl 1x reaction buffer solution (1 h, 37 °C). Afterwards, 1 µl of 25 mM EDTA was added and the reaction was incubated further at 65 °C for 10 min to inactivate the enzyme. Finally, the RNA was purified using by precipitation as described above.

For cDNA synthesis, 1 µg of DNA-free RNA was used as a template for reverse transcription using the Superscript III kit (Invitrogen). The manufacturer's protocol was followed. A 13 µl reaction mixture containing RNA (1 µg, <10 µl), random hexamers or specific cDNA synthesis primer (2 µl, 100 ng/µl), DNTPs (1 µl, 10 mM) was prepared in RNase-free water in a thin wall PCR tube which was incubated at 65 °C for 5 min and snap cooled on ice. To this solution, 4 µl of 5x RT-buffer, 1 µl of RNasin (RNase inhibitor), 1 µl of Superscript III RT enzyme and 1 µl of 0.1 M DTT (prepared as a master mix, 7 µl per reaction) was added. This reaction mix was incubated in a PCR machine programmed at 25 °C for the first 5 min; at 55 °C for the following 50 min and at 70 °C for the final 15 min.

The quantitative real time PCR (qRT-PCR) was performed using the SYBR® Green PCR master mix kit (Applied Biosystems). Each reaction containing cDNA (2 µl, diluted appropriately), 2X PCR-solution (13 µl), specific qPCR primer-mix (2 µl, 5 µM each primer) and water (9 µl) in a total volume of 26 µl was performed in triplicates. Control reactions contained no cDNA (no reverse transcriptase) and H_2O (no

template) as negative controls and gDNA as positive control. The following protocol was applied:

Initial denaturation:	95 °C – 10 min	
Denaturation:	95 °C – 10 min	
Primer annealing and elongation:	60 °C – 15 sec	⎤ 40 cycles
Denaturation:	95 °C – 1 min	
Recording of dissociation curve:	60 °C – 30 sec	

95 °C – 15 sec

hold: 4 °C

solution 1	solution 2
0.3 M sucrose 0.01 M sodium acetate pH 4.5	2% (w/v) SDS 0.01 M Na Ac pH 4.5

8.4. Biochemical methods

8.4.1. Recombinant protein overexpression in *E. coli*

Protein production from pET32a results in an N-terminally tagged protein of interest with the solubilizing fusion protein Thioredoxin (Trx) followed by a hexa-histidine (His_6) tag. Genes coding for the proteins of interest were cloned into pET32a and overproduced as described below.

8.4.1.1 RedF

RedF was purified as previously described (Jagadeesan, 2008, Jagadeesan *et al.*, 2009). Briefly, pET32a-*redF* was transformed into TSS competent *E. coli* GJ1158 cells. Logarithmically growing cultures were induced to overproduce the protein by addition of 300 mM NaCl (final concentration). After continued to incubation at 37 °C for 2 h, cells were harvested and stored at -20 °C.

8.4.1.2 TodK

For *in vitro* analysis, *todK* in its native ($TodK_{WT}$) form as well as in the presumably kinase inactive form resulting from a single amino acid substitution ($TodK_{H275A}$) were used. Optimization of expression conditions resulted in transformation of pET32a-$todK_{WT/H275A}$ into TSS competent pLysS *E. coli* cells and growing them to mid-logarithmic phase (OD_{600nm} 0.5) at 37 °C. Cultures were transferred and cooled to 18 °C and growing continued until late-mid logarithmic phase (OD_{600nm} 0.7). Expression of *todK* was induced with 0.5 mM IPTG and incubation continued at 18 °C overnight. Cultures were harvested and stored at -20 °C.

8.4.1.3 Hpk30

pET32a plasmids carrying $hpk30_{WT}$ as well as $hpk30_{H45A}$ were transformed into TSS competent cells of the salt inducible *E. coli* strain GJ1158. Cultures were grown to early mid-logarithmic phase (OD_{600nm} 0.5) at 37 °C. Subsequently, cultures were transferred to 18 °C and continued to grow until late-mid logarithmic phase (OD_{600nm} 0.7). Induction of protein expression took place by addition of 300 mM NaCl (final concentration) and was continued over night at 18 °C. Cultures were harvested and stored at -20 °C.

8.4.2. Affinity protein purification

All proteins were purified using affinity chromatography on ÄKTA technology. Cell pellets were either used fresh or thawed on ice. Pellets were resuspended in the respective binding buffer, supplemented with 1:150 SMPI. Cells were disrupted through French Press (18000 PSI) in three cycles. For TodK and Hpk30 constructs potential inclusion bodies and un-lysed cells were pelleted by a low speed centrifugation (3500 x g, 15 min, 4 °C), for RedF constructs this step was not performed. In a second clarification centrifugation, cell debris was pelleted (20000 x g, 30 min, 4 °C). Proteins of the remaining supernatant were purified by affinity chromatography via FPLC equipment (ÄKTA technology, GE Healthcare) using a 1 ml HisFF1 trap nickel affinity column (GE Healthcare). The column was equilibrated with 5 column bed volumes of binding buffer and supernatant was loaded onto the chromatography column with a flow rate of 1 ml/min at 4 °C. The column was washed with 15-25 column volumes of binding buffer to remove unbound proteins. Fusion proteins were eluted by a gradient from 20- 500 mM imidazole in 20-30 ml of elution buffer. Fractions were collected in 1 ml increments and subjected to SDS-PAGE for analysis of purity and concentration. Purest and highest concentrated fractions were pooled and dialyzed over night with storage buffer.

Binding buffer RedF

10 mM HEPES, pH 7.4
500 mM NaCl
20 mM Imidazole

Elution buffer RedF

10 mM HEPES, pH 7.4
500 mM NaCl
500 mM Imidazole

Binding buffer TodK and Hpk30

50 mM Tris, pH 7.6
300 mM NaCl
20 mM Imidazole

Elution buffer TodK and Hpk30

50 mM Tris, pH 7.6
300 mM NaCl
500 mM Imidazole

Storage buffer (all proteins)

50 mM Tris, pH 8
10% (v/v)glycerol
150 mM NaCl
1 mM DTT

8.4.3. SDS-PAGE

Proteins were analyzed under denaturing conditions in sodium dodecyl sulfate polyacrylamide gel electrophoresis (SDS-PAGE, (Laemmli, 1970)). Resolving gels consisted of x % Rotiphorese® Acrylamide/Bisacrylamide (29:1) solution (percentages used see Table 10), 0.35 mM ammoniumperoxodisulfat (APS) and 0.06 % (v/v) N,N,N,N-Tetramethylethyleneediamine (TEMED) in 1x resolving buffer. The stacking gel was composed of 5 % Rotiphorese® NR-Acrylamide/Bisacrylamide (29:1) solution, 0.44 mM APS and 0.076 % (v/v) TEMED in 1x stacking buffer. Samples were mixed with 2 or 5 x Laemmli sample buffer (LSB) and loaded into the

gel pockets. Electrophoresis was performed in BioRad electrophoresis chambers in Tris-Glycine-SDS buffer at a constant voltage of 100 – 150 V. For evaluation of molecular masses, a size standard (PageRulerTM Prestained Protein Ladder, Thermo Scientific) was applied to every gel. After electrophoretic separation of proteins, SDS-PAGES were either stained with Coomassie blue or used for immunoblot analysis. Coomassie blue staining was performed for 30 min to over night at RT with agitation. Gels were de-stained for 1 h to overnight and subsequently relaxed in water. SDS-gels were either dried or scanned for result documentation.

4x resolving buffer

1.5 M Tris-HCl pH 8.8
0.4 % (w/v) SDS

4x stacking buffer

500 mM Tris-HCl pH 6.8
0.4 % (w/v) SDS

TGS

2.5 mM Tris
19.2 mM glycine
0.1% (w/v) SDS

LSB

125 mM Tris-HCl pH 6.8
20 % (v/v) glycerol
4 % (w/v) SDS
10 % (v/v) β-mercaptoethanol
0.02 % (w/v) bromphenolblue

Coomassie blue staining solution

0.2 % (w/v) Coomassie Brilliant Blue R250
50 % (v/v) methanol
7 % (v/v) glacial acidic acid

De-staining solution

50 % (v/v) methanol
7 % (v/v) glacial acidic acid

8.4.4. Phostag

For Phostag analysis, *M. xanthus* strains were starved under submerged conditions and harvested at pre-sporulation time points. Cells were detached from the plates using a cell scraper, transferred with all starvation Media (MMC) present (16 ml) into a 50 ml falcon tube and harvested by centrifugation (4600 x g, 10 min, 4 °C). The supernatant was discarded and pellets were frozen at -20 °C until lysis. Pellets were thawed on ice and resuspended by pipetting in 300 µl clear LSB supplemented with 1:20 SMPI and transferred to Eppendorf tubes. Tubes were briefly vortexed and incubated on ice for 10 min, this was repeated once. Potentially non-lysed cells were pelleted by centrifugation (2000 x g, 5 min, 4 °C) and the supernatant was transferred to a fresh Eppendorf tube. Protein content was determined using BCA assay and samples were diluted to 1 mg/ml protein concentration with regular LSB. Samples were heated at 50 °C for 5 min, cooled on ice and spun down briefly.

Phos-tag acrylamide SDS gels were prepared the same day as they were used. Phos-tag component was prepared according to manufacturer guide: to reach a 5 mM solution, 2 mg Phos-tag were dissolved in 20 µl methanol, subsequently 640 µl ddH2O were added. The solution was stored at 4 °C in a tin foil covered tube, to protect Phos-tag compound from light. For TodK analysis an 8 % gel (acrylamide/bisacrylamid ratio 29:1, stock solution 30 %) resolving gel was prepared,

supplemented with 50 µM Phos-tag compound and 100 µM $MnCl_2$. For the stacking gel, a 4.5 % gel was prepared using the same acrylamide stock solution. No Phos-tag or $MnCl_2$ were added to the stacking gel. Per sample 10 µg protein was loaded to the gel and gels were run under constant current conditions at 25 mA per gel, until the 50 kDa band of the standard reached the lower end of the gel but was not run off. Semi dry blotting was applied for protein transfer from the Phos-tag acrylamide SDS gel to PVDF membrane. To remove excess $MnCl_2$ from the gel, the gel was soaked in cathode buffer supplemented with 1 mM EDTA and incubated for 5 min with shaking. This was repeated five more times. Afterwards the gel was soaked and incubated for 10 min each in regular cathode buffer to remove EDTA from the gel before the blotting procedure. The remaining immunoblotting procedure was performed according to the standard semi dry blotting protocol.

8.4.5. Antibody generation and affinity purification of α-TodK and α-Hpk30 polyclonal antibodies

All custom-made antibodies used in this study were generated in rabbits with the company Eurogentec (Belgium). Purified protein (2.6 mg) were supplied and used for immunization via the “speedy” program (28 days). Serum samples from pre-immunization as well as various stages of duration were obtained and tested for antigen detection in immunoblot assays. All antibodies used in this study were purified from rabbit sera obtained from final bleed according to the following protocol. Antigen (1 mg) was separated via a 15 % SDS-PAGE (without comb, merely a thin stacker gel) and blotted onto a PVDF membrane via the wet blot procedure (section 8.4.6.2, 2 h 50 V). The membrane was soaked in methanol, dried, rewetted in methanol and stained with Ponceau S to visualize protein. The protein band was cut out as thin as possible and destained with water. Strip was transferred into a 15 ml falcon tube. All wash steps were performed in 14 ml of the respective buffers, unless stated otherwise. Membrane was washed once with glycine buffer and soak in glycine buffer for 5 min to remove poorly bound proteins. The membrane was washed twice with TBS-T each and blocked in 3 % w/v BSA in TBS-T for 2 h at RT with rotation. Blocking solution was discarded and membrane was washed twice with TBS-T again. Antibody serum was added (2 ml sera in 8 ml TBS-T) and incubated over night at 4 °C over night. Supernatant was recovered and frozen at – 20 °C. Membrane was soaked in TBS-T for 2 min and washed twice with PBS for 5 min each. Prior to elution the membrane was briefly rinsed with 1 ml of glycine buffer, this buffer was discarded. Another 1 ml of glycine buffer was added and incubated for 10 min with vortexing every minute. The eluted antibodies were transferred to an Eppendorf tube containing 125 µl Tris (1 M, pH 8.0; the exact volume needed to neutralize 1 ml glycine buffer to pH 7.0 was determined experimentally prior to the purification). The elution step was repeated once and both eluates were finally pooled together. Sodium azide and BSA were added and antibodies were stored as 200 µl aliquots at – 20 °C until further use.

PonceauS

0.1 % (w/v) Ponceaus S
5 % glacial acedic acid

TBS-T

20 mM Tris pH 7.4
500 mM NaCl
0.05 % (v/v) Tween-20

Glycine buffer

100 mM glycine pH 2.5

PBS

8 mM Na_2HPO_4
2 mM KH_2PO_4 pH 7.4
135 mM NaCl
3.5 mM KCl

8.4.6. Immunoblot analysis

For specific protein of interest detection, immunoblot analysis were performed. The antibodies and conditions used in this study are listed below (Table 10).

Table 10: Antibodies used in this study and the respective conditions of incubation.

Protein	Molecular mass	SDS PAGE	Transfer	purification of 1st ab	Dilution of 1st ab	incubation
KapC	126 kDa	8 %	wet	yes	1:100	1 h RT
TodK	57 kDa	8 %	semi-dry	yes	1:100	overnight 4 °C
Hpk30	57 kDa	8 %	semi-dry	yes	1:100	overnight 4 °C
MrpC	27 kDa	11%	semi-dry	yes	1:500	1 h RT
RedF	14 kDa	15 %	-	-	-	-
Trx-tag	18 kDa	15 %	-	-	-	-

8.4.6.1 Semi-dry blot

Proteins were transferred from SDS-gels to PVDF membrane (Millipore) by semi-dry transfer. Two pieces of Whatman paper were soaked in anode buffer I and put to the anode of the blotting apparatus (PeqLab). One piece of Whatman paper was soaked in anode buffer II and laid on top. PVDF membrane was activated in 100 % methanol, washed in water and positioned on top of the Whatman papers. The SDS-gel was added and the sandwich was completed by three Whatman paper pieced which were pre-soaked in cathode buffer. Air bubbles were rolled out and the transfer chamber was closed. Transfer occurred at constant current of 100 mA per minigel for 75 min. Upon disassembly, the PVDF membrane was briefly incubated in 100 % methanol and either dried or directly blocked. For the blocking reaction, membrane was overlaid with blocking solution and incubated either 1 h at RT or overnight at 4 °C. Afterwards primary antibodies were added at desired dilution and incubated as noted in Table 10. Primary antibodies were recovered and stored at – 20 °C until further. Membranes were washed three times with blocking solution for 5-10 min each. secondary antibody was added (anti rabbit-HRP, 1:20000, Thermo Scientific) and incubated for 1 h at RT. Afterwards, secondary antibody was discarded and membranes were

washed three times with 1 x PBS for 5 – 10 min each. Membranes were probed with enhanced chemiluminescence substrate (Thermo Scientific) and signals were detected using autoradiography films (Thermo Scientific).

anode buffer I	anode buffer II	cathode buffer
300 mM Tris pH 10.4 10 % (v/v) methanol	25 mM Tris pH 10.4 10 % (v/v) methanol	25 mM Tris pH 9.4 40 mM glycine 10 % (v/v) methanol

Blocking solution	PBS(T)
1x PBS buffer 50 g dry milk powder 1 ml Tween per 1 l	8 mM Na_2HPO_4 2 mM KH_2PO_4 pH 7.4 135 mM NaCl 3.5 mM KCl (0.05 % (v/v) Tween-20)

8.4.6.2 Wet blot

SDS-gel was soaked in transfer buffer for 15 min at RT with shaking. Four pieced of Whatman paper as well as one piece of PVDF membrane (Millipore) were prepared per gel. PVDF membrane was prepared by soaking in 100 % methanol for 15 sec and was rinsed with water. Transfer-cassette was assembled as follows from anode to cathode to: foam – 2 pieces of Whatman paper – PVDF membrane – SDS-gel - 2 pieces of Whatman – foam. Bubbles were rolled out carefully and cassette was inserted into tank (Hoeffer), filled up with transfer buffer and closed. Transfer was performed at 4 °C with stirring overnight at constant voltage of 20 V. Upon disassembly, PVDF membrane was again rinsed in 100 % methanol and either dried or submerged in blocking solution as described above for semi-dry transfer.

Blotting buffer (Towbin buffer)

25 mM Tris
192 mM glycine
0.05 % (w/v) SDS
10 % Methanol

8.4.7. Pull-down assay

Vegetative cultures of DZ2 (50 ml each) were grown to mid logarithmic phase (OD_{550nm} 0.5-0.7) and harvested by centrifugation (4700 x g, 15 min, 4 °C). Cells were either used directly or frozen at – 20 °C until use. Cells were kept on ice from here on. To ensure that all batches consisted of a homogenous lysate, pools of cell lysate were prepared and separated at the time of incubation with bait protein. Per pull-down batch one cell pellet was resuspended in 10 ml lysis buffer supplemented with 1:100 SMPI. Cells were lysed using a French press and a debris spin was performed (15000 x g, 30 min, 4 °C). Parallel to this, RedF and Trx-tag (as negative control) was autophosphorylated using acetylphosphate as small phosphor donor as previously

described (Jagadeesan, 2008). The phosphorylation reaction was run for 30 min at 30 °C. During this incubation, agarose was prepared. Per batch 40 µl slurry Ni-NTA Agarose (Quiagen) was washed once with H_20 and twice with wash buffer A. Centrifugation was performed at 500 x g for 2 min at 4 °C. Of the prepared lysate 10 ml per batch were mixed with bait protein (either RedF~P or Trx-tag) and pre-incubate for 3 h at 4 °C with rotation (12 rpm). This solution was subsequently added to the prepared agarose aliquots and incubated for 60 min at 4 °C with rotation (12 rpm). Beads were washed with 14 ml wash buffer A and pelleted (500 x g, 2 min, 4 °C). Subsequent wash steps followed by centrifugation as above included 14 ml wash buffer B1 (containing 300 mM D-Galactose to elute sugar binding proteins) as well as wash steps with Wash buffer B2 and wash buffer C (both containing increasing NaCl concentrations). Agarose was resuspended in 1 ml wash buffer A and transferred to an Eppendorf tube. After pelleting down the beads, and removal of buffer, elution was performed one after the other in 80 µl elution buffers A, B and C, containing increasing concentrations of imidazole (incubation for 5 min on ice followed by centrifugation). In a pre-experiment, it was determined that Trx-His_6-RedF elutes from the Ni-NTA agarose beads between 50 and 300 mM imidazole. Hence, the wash buffers contained 20 mM imidazole and stringency during the wash steps was accomplished by increasing salt concentration instead of increasing imidazole concentration. The obtained elution supernatants were mixed with 2 x LSB each and boiled at 99 °C for 5 min.

Lysis / Wash buffer A

50 mM	HEPES pH 7.6
100 mM	NaCl
10 mM	Imidazole
0.1 % (w/v)	CHAPS

Wash buffer B1	Wash buffer B2	Wash buffer C
50 mM HEPES pH 7.6	50 mM HEPES pH 7.6	50 mM HEPES pH 7.6
100 mM NaCl	300 mM NaCl	500 mM NaCl
20 mM Imidazole	20 mM Imidazole	20 mM Imidazole
300 mM D-Galactose		

Elution buffer A	Elution buffer B	Elution buffer C
50 mM HEPES pH 7.6	50 mM HEPES pH 7.6	50 mM HEPES pH 7.6
100 mM NaCl	100 mM NaCl	100 mM NaCl
50 mM Imidazole	150 mM Imidazole	300 mM Imidazole

8.4.8. Radiolabeled *in vitro* autophosphorylation and chemical stability assays

For *in vitro* phosphorylation assays, 10 µM purified histidine kinase protein was added to phosphorylation reaction buffer. Phosphorylation reaction was initiated with 0.5 mM ATP and 1.7 µM [γ^{32}P]-ATP (222 TBq/mmol, Hartmann Analytic, Braunschweig) and reaction was run for 0 – 60 min at 32 °C. Per time point, 10 µl sample were removed from the reaction mix and quenched by mixing 1:2 with 2 x LSB. Samples were not heated and immediately frozen at – 20 °C. After all time points have been taken, samples were separated via SDS-PAGE (12 %). Gels were exposed to a storage phosphor screen (GE Healthcare) over night and analyzed using a Storm™ 800 imaging system (GE Healthcare). Afterwards, SDS-gels were stained with Coomassie blue as per standard protocol.

To test chemical stability of phosphor groups on Hpk30, autophosphorylation reaction was performed as above in a 5x batch size. Reaction was quenched with the appropriate amount of 2 x LSB and 20 µl were immediately frozen at – 20 °C. From the remaining pool of autophosphorylated Hpk30, 20 µl were each mixed with 4 µl of 1 M NaOH, 1 M HCl or H_2O and incubated for 1 h at 42 °C (Duclos *et al.*, 1991, Shi, 2008). 20 µl of each reaction were separated via SDS-PAGE and analyzed as above. Signals intensities were quantified using ImageJ 1.43U and evaluated using Excel. SDS-gels were eventually stained using Coomassie blue.

phosphorylation reaction buffer

storage buffer supplemented with

5 mM $MgCl_2$
50 mM KCl

9. Abbreviations

Si-Units were used in this thesis.

Amino acids were named using the standard three and one letter codes.

aa	amino acid(s)
APS	ammoniumperoxodisulfat
AR	autoradiogram
ATP	adenosine tri phosphate
BLASTp	basic local alignment search tool (proteins query mode)
bp	base pair(s)
°C	degree Celsius
CA	histidine kinase like ATPase domain
c-di-GMP	bis-(3´5´)-cyclic dimeric GMP
cDNA	complementary DNA
CF	clone fruiting
CFU	Colony forming units
ChiP-Seq	chromatin immunoprecipitation DNA-sequencing
CLSM	confocal laser scanning microscopy
CRP	cyclic AMP receptor protein
CS	Coomassie stain
Ct	cyclic threshold
CYE	casitone yeast extraxt
d, h, min, sec	day(s), hour(s), minute(s), second(s)
Da	dalton
DNA	desoxyribonucleic acid
DHp	dimerization and histidine phosphotransfer domain
EBP	enhancer-binding-protein
EDTA	ethylenediaminetetraacetic acid
EMSA	electrophoretic mobility shift assay
EPS	exopolysaccharide
eSTK	eukaryote-like serine/threonine kinase
eSTP	eukaryote-like serine/threonine phosphatase
FHA	fork head-associated
FITC-ConA	fluorescein-conjugated concavalin A
FPLC	Fast protein liquid chromatography
g	gram
gal	galactose
GFP	green fluorescent protein
HEPES	4-(2-hydroxyethyl)-1-piperazineethanesulfonic acid
His-Asp	histidine-aspartate
HPt	His-containing phosphotransfer proteins
(Hy)HPK	(hybrid) histidine protein kinase
IPTG	Isopropyl β-D-1-thiogalactopyranoside
Km	kanamycin

l	liter
LB	Luria Bertani
LSB	Laemmli sample buffer
M	molar
MiST	microbial signal transduction database
MOPS	3-(N-morpholino)propanesulfonic acid
n, µ, m, k, M	nano, micro, milli, kilo, mega
nm	nano meter
ΔNR	negative regulator deletion
OD	optical density
PAS	Per-ARNT-Sim
PCR	polymerase chain reaction
PIPES	piperazine-N,N′-bis(2-ethanesulfonic acid)
ppGpp	guanosine-3′,5′-bispyrophosphate
Pr	Promoter
qRT-PCR	quantitative real time PCR
REC	receiver domain
RNA	ribonucleic acid
rpm	rotations per minute
RR	response regulator
RT	room temperature
SDS-PAGE	sodium dodecyl sulfate polyacrylamide gel electrophoresis
SMART	simple modular architecture research tool
SMPI	sigma mammalian protease inhibitor cocktail
STPK	serine/threonine protein kinase
TCS	two component system
TEMED	N,N,N,N-tetramethylethyleneediamine
Tris	2-amino-2-hydroxymethyl-propane-1,3-diol
Trx-His_6	thioredoxin-hexa histidine-tag
UV	ultra violett
(v/v)	volume per volume
(w/v)	weight per volume
WT	wild type

10. References

Akiyama, T., Inouye, S. and Komano, T., (2003) Novel developmental genes, fruCD, of Myxococcus xanthus: involvement of a cell division protein in multicellular development. *J Bacteriol* **185**: 3317-3324.

Allen, J.J., Li, M., Brinkworth, C.S., Paulson, J.L., Wang, D., Hubner, A., Chou, W.H., Davis, R.J., Burlingame, A.L., Messing, R.O., Katayama, C.D., Hedrick, S.M. and Shokat, K.M., (2007) A semisynthetic epitope for kinase substrates. *Nat Methods* **4**: 511-516.

Alm, E., Huang, K. and Arkin, A., (2006) The evolution of two-component systems in bacteria reveals different strategies for niche adaptation. *PLoS Comput Biol* **2**: e143.

Altschul, S.F., Madden, T.L., Schaffer, A.A., Zhang, J., Zhang, Z., Miller, W. and Lipman, D.J., (1997) Gapped BLAST and PSI-BLAST: a new generation of protein database search programs. *Nucleic Acids Res* **25**: 3389-3402.

Appleby, J.L., Parkinson, J.S. and Bourret, R.B., (1996) Signal transduction via the multi-step phosphorelay: not necessarily a road less traveled. *Cell* **86**: 845-848.

Appleby, J.L. and Bourret, R.B., (1998) Proposed signal transduction role for conserved CheY residue Thr87, a member of the response regulator active-site quintet. *J Bacteriol* **180**: 3563-3569.

Av-Gay, Y. and Everett, M., (2000) The eukaryotic-like Ser/Thr protein kinases of Mycobacterium tuberculosis. *Trends Microbiol* **8**: 238-244.

Barak, R., Welch, M., Yanovsky, A., Oosawa, K. and Eisenbach, M., (1992) Acetyladenylate or its derivative acetylates the chemotaxis protein CheY in vitro and increases its activity at the flagellar switch. *Biochemistry* **31**: 10099-10107.

Barbieri, C.M. and Stock, A.M., (2008) Universally applicable methods for monitoring response regulator aspartate phosphorylation both in vitro and in vivo using Phos-tag-based reagents. *Anal Biochem* **376**: 73-82.

Beebe, J.M., (1941) The Morphology and Cytology of Myxococcus xanthus, N. Sp. *J Bacteriol* **42**: 193-223.

Berg, H.C. and Purcell, E.M., (1977) Physics of chemoreception. *Biophys J* **20**: 193-219.

Berleman, J.E., Vicente, J.J., Davis, A.E., Jiang, S.Y., Seo, Y.E. and Zusman, D.R., (2011) FrzS regulates social motility in Myxococcus xanthus by controlling exopolysaccharide production. *PLoS One* **6**: e23920.

Besant, P.G. and Attwood, P.V., (2009) Detection and analysis of protein histidine phosphorylation. *Mol Cell Biochem* **329**: 93-106.

Bhandari, P. and Gowrishankar, J., (1997) An Escherichia coli host strain useful for efficient overproduction of cloned gene products with NaCl as the inducer. *J Bacteriol* **179**: 4403-4406.

Bhardwaj, V., (2013) Characterization of the role of MrpC in Myxococcus xanthus developmental cell fate determination. In: Max-Planck-Institut für Terrestrische Mikrobiologie. Philipps-Universität Marburg, http://dx.doi.org/10.17192/z2013.0387.

Birnboim, H.C. and Doly, J., (1979) A rapid alkaline extraction procedure for screening recombinant plasmid DNA. *Nucleic Acids Res* **7**: 1513-1523.

Blethrow, J.D., Glavy, J.S., Morgan, D.O. and Shokat, K.M., (2008) Covalent capture of kinase-specific phosphopeptides reveals Cdk1-cyclin B substrates. *Proc Natl Acad Sci U S A* **105**: 1442-1447.

Blom, N., Gammeltoft, S. and Brunak, S., (1999) Sequence and structure-based prediction of eukaryotic protein phosphorylation sites. *J Mol Biol* **294**: 1351-1362.

Bourret, R.B., (2010) Receiver domain structure and function in response regulator proteins. *Curr Opin Microbiol* **13**: 142-149.

Bourret, R.B., Thomas, S.A., Page, S.C., Creager-Allen, R.L., Moore, A.M. and Silversmith, R.E., (2010) Measurement of response regulator autodephosphorylation rates spanning six orders of magnitude. *Methods Enzymol* **471**: 89-114.

Boynton, T.O., McMurry, J.L. and Shimkets, L.J., (2013) Characterization of Myxococcus xanthus MazF and implications for a new point of regulation. *Mol Microbiol* **87**: 1267-1276.

Bren, A. and Eisenbach, M., (1998) The N terminus of the flagellar switch protein, FliM, is the binding domain for the chemotactic response regulator, CheY. *J Mol Biol* **278**: 507-514.

Bretl, D.J. and Kirby, J.R., (2016) Molecular Mechanisms of Signaling in Myxococcus xanthus Development. *J Mol Biol* **428**: 3805-3830.

Burbulys, D., Trach, K.A. and Hoch, J.A., (1991) Initiation of sporulation in B. subtilis is controlled by a multicomponent phosphorelay. *Cell* **64**: 545-552.

Burchard, R.P. and Dworkin, M., (1966) A bacteriophage for Myxococcus xanthus: isolation, characterization and relation of infectivity to host morphogenesis. *J Bacteriol* **91**: 1305-1313.

Burger, L. and van Nimwegen, E., (2008) Accurate prediction of protein-protein interactions from sequence alignments using a Bayesian method. *Mol Syst Biol* **4**: 165.

Campbell, A., Viswanathan, P., Barrett, T., Son, B., Saha, S. and Kroos, L., (2015) Combinatorial regulation of the dev operon by MrpC2 and FruA during Myxococcus xanthus development. *J Bacteriol* **197**: 240-251.

Campos, J.M. and Zusman, D.R., (1975) Regulation of development in Myxococcus xanthus: effect of 3':5'-cyclic AMP, ADP, and nutrition. *Proc Natl Acad Sci U S A* **72**: 518-522.

Canova, M.J., Baronian, G., Brelle, S., Cohen-Gonsaud, M., Bischoff, M. and Molle, V., (2014) A novel mode of regulation of the Staphylococcus aureus Vancomycin-resistance-associated response regulator VraR mediated by Stk1 protein phosphorylation. *Biochem Biophys Res Commun* **447**: 165-171.

Cao, P., Dey, A., Vassallo, C.N. and Wall, D., (2015) How Myxobacteria Cooperate. *J Mol Biol* **427**: 3709-3721.

Carlson, H.K., Plate, L., Price, M.S., Allen, J.J., Shokat, K.M. and Marletta, M.A., (2010) Use of a semisynthetic epitope to probe histidine kinase activity and regulation. *Anal Biochem* **397**: 139-143.

Casino, P., Rubio, V. and Marina, A., (2009) Structural insight into partner specificity and phosphoryl transfer in two-component signal transduction. *Cell* **139**: 325-336.

Casino, P., Rubio, V. and Marina, A., (2010) The mechanism of signal transduction by two-component systems. *Curr Opin Struct Biol* **20**: 763-771.

Chao, J.D., Papavinasasundaram, K.G., Zheng, X., Chavez-Steenbock, A., Wang, X., Lee, G.Q. and Av-Gay, Y., (2010) Convergence of Ser/Thr and two-component signaling to coordinate expression of the dormancy regulon in Mycobacterium tuberculosis. *J Biol Chem* **285**: 29239-29246.

Chen, Y.E., Tsokos, C.G., Biondi, E.G., Perchuk, B.S. and Laub, M.T., (2009) Dynamics of two Phosphorelays controlling cell cycle progression in Caulobacter crescentus. *J Bacteriol* **191**: 7417-7429.

Cheung, J. and Hendrickson, W.A., (2010) Sensor domains of two-component regulatory systems. *Curr Opin Microbiol* **13**: 116-123.

Childers, W.S. and Shapiro, L., (2014) A pseudokinase couples signaling pathways to enable asymmetric cell division in a bacterium. *Microb Cell* **2**: 29-32.

Childers, W.S., Xu, Q., Mann, T.H., Mathews, II, Blair, J.A., Deacon, A.M. and Shapiro, L., (2014) Cell fate regulation governed by a repurposed bacterial histidine kinase. *PLoS Biol* **12**: e1001979.

Cho, K. and Zusman, D.R., (1999) Sporulation timing in Myxococcus xanthus is controlled by the espAB locus. *Mol Microbiol* **34**: 714-725.

Christen, M., Kulasekara, H.D., Christen, B., Kulasekara, B.R., Hoffman, L.R. and Miller, S.I., (2010) Asymmetrical distribution of the second messenger c-di-GMP upon bacterial cell division. *Science* **328**: 1295-1297.

Chung, C.T., Niemela, S.L. and Miller, R.H., (1989) One-step preparation of competent Escherichia coli: transformation and storage of bacterial cells in the same solution. *Proc Natl Acad Sci U S A* **86**: 2172-2175.

Claessen, D., Rozen, D.E., Kuipers, O.P., Sogaard-Andersen, L. and van Wezel, G.P., (2014) Bacterial solutions to multicellularity: a tale of biofilms, filaments and fruiting bodies. *Nat Rev Microbiol* **12**: 115-124.

Crosson, S., Rajagopal, S. and Moffat, K., (2003) The LOV domain family: photoresponsive signaling modules coupled to diverse output domains. *Biochemistry* **42**: 2-10.

Curtis, P.D., Taylor, R.G., Welch, R.D. and Shimkets, L.J., (2007) Spatial organization of Myxococcus xanthus during fruiting body formation. *J Bacteriol* **189**: 9126-9130.

Cusick, J.K., Hager, E. and Gill, R.E., (2002) Characterization of bcsA mutations that bypass two distinct signaling requirements for Myxococcus xanthus development. *J Bacteriol* **184**: 5141-5150.

Cusick, J.K., Hager, E. and Gill, R.E., (2015) Identification of a mutant locus that bypasses the BsgA protease requirement for social development in Myxococcus xanthus. *FEMS Microbiol Lett* **362**: 1-8.

Dahl, J.L., Ulrich, C.H. and Kroft, T.L., (2011) Role of phase variation in the resistance of Myxococcus xanthus fruiting bodies to Caenorhabditis elegans predation. *J Bacteriol* **193**: 5081-5089.

Diodati, M.E., Gill, R.E., Plamann, L. and Singer, M., (2008) Initiation and early developmental events. In: Myxobacteria: Multicellularity and Differentiation. Whitworth, D.E. (ed). Washington DC: ASM Press, pp. 43-76.

Dubnau, D. and Losick, R., (2006) Bistability in bacteria. *Mol Microbiol* **61**: 564-572.

Duclos, B., Marcandier, S. and Cozzone, A.J., (1991) Chemical properties and separation of phosphoamino acids by thin-layer chromatography and/or electrophoresis. *Methods Enzymol* **201**: 10-21.

Dunmire, V., Tatar, L.D. and Plamann, L., (1999) Genetic suppression analysis of an asgA missense mutation in Myxococcus xanthus. *Microbiology* **145 (Pt 6)**: 1299-1306.

Durocher, D., Taylor, I.A., Sarbassova, D., Haire, L.F., Westcott, S.L., Jackson, S.P., Smerdon, S.J. and Yaffe, M.B., (2000) The molecular basis of FHA domain:phosphopeptide binding specificity and implications for phospho-dependent signaling mechanisms. *Mol Cell* **6**: 1169-1182.

Dutta, R. and Inouye, M., (1996) Reverse phosphotransfer from OmpR to EnvZ in a kinase-/phosphatase+ mutant of EnvZ (EnvZ.N347D), a bifunctional signal transducer of Escherichia coli. *J Biol Chem* **271**: 1424-1429.

Dworkin, M., (1966) Biology of the myxobacteria. *Annu Rev Microbiol* **20**: 75-106.

Dworkin, M. and Sadler, W., (1966) Induction of cellular morphogenesis in Myxococcus xanthus. I. General description. *J Bacteriol* **91**: 1516-1519.

Dyer, C.M. and Dahlquist, F.W., (2006) Switched or not?: the structure of unphosphorylated CheY bound to the N terminus of FliM. *J Bacteriol* **188**: 7354-7363.

Ellehauge, E., Norregaard-Madsen, M. and Sogaard-Andersen, L., (1998) The FruA signal transduction protein provides a checkpoint for the temporal co-ordination of intercellular signals in *Myxococcus xanthus* development. *Mol Microbiol* **30**: 807-817.

Fritsch, F., Mauder, N., Williams, T., Weiser, J., Oberle, M. and Beier, D., (2011) The cell envelope stress response mediated by the LiaFSRLm three-component system of Listeria monocytogenes is controlled via the phosphatase activity of the bifunctional histidine kinase LiaSLm. *Microbiology* **157**: 373-386.

Furusawa, G., Dziewanowska, K., Stone, H., Settles, M. and Hartzell, P., (2011) Global analysis of phase variation in Myxococcus xanthus. *Mol Microbiol* **81**: 784-804.

Gajdiss, M., Turck, M. and Bierbaum, G., (2017) Bacterial Histidine Kinases: Overexpression, Purification, and Inhibitor Screen. *Methods Mol Biol* **1520**: 247-259.

Galperin, M.Y., (2005) A census of membrane-bound and intracellular signal transduction proteins in bacteria: bacterial IQ, extroverts and introverts. *BMC Microbiol* **5**: 35.

Galperin, M.Y., (2006) Structural classification of bacterial response regulators: diversity of output domains and domain combinations. *J Bacteriol* **188**: 4169-4182.

Galperin, M.Y., (2010) Diversity of structure and function of response regulator output domains. *Curr Opin Microbiol* **13**: 150-159.

Galperin, M.Y., Higdon, R. and Kolker, E., (2010) Interplay of heritage and habitat in the distribution of bacterial signal transduction systems. *Mol Biosyst* **6**: 721-728.

Gamble, R.L., Coonfield, M.L. and Schaller, G.E., (1998) Histidine kinase activity of the ETR1 ethylene receptor from Arabidopsis. *Proc Natl Acad Sci U S A* **95**: 7825-7829.

Gao, R. and Stock, A.M., (2009) Biological insights from structures of two-component proteins. *Annu Rev Microbiol* **63**: 133-154.

Gao, Z., Wen, C.K., Binder, B.M., Chen, Y.F., Chang, J., Chiang, Y.H., Kerris, R.J., 3rd, Chang, C. and Schaller, G.E., (2008) Heteromeric interactions among ethylene receptors mediate signaling in Arabidopsis. *J Biol Chem* **283**: 23801-23810.

Garcia-Hernandez, R., Moraleda-Munoz, A., Castaneda-Garcia, A., Perez, J. and Munoz-Dorado, J., (2009) Myxococcus xanthus Pph2 is a manganese-dependent protein phosphatase involved in energy metabolism. *J Biol Chem* **284**: 28720-28728.

Garre, S., Senevirathne, C. and Pflum, M.K., (2014) A comparative study of ATP analogs for phosphorylation-dependent kinase-substrate crosslinking. *Bioorg Med Chem* **22**: 1620-1625.

Gilbert, D.G., (1980) Dispersal of yeasts and bacteria by Drosophila in a temperate forest. *Oecologia* **46**: 135-137.

Goldman, B.S., Nierman, W.C., Kaiser, D., Slater, S.C., Durkin, A.S., Eisen, J.A., Ronning, C.M., Barbazuk, W.B., Blanchard, M., Field, C., Halling, C., Hinkle, G., Iartchuk, O., Kim, H.S., Mackenzie, C., Madupu, R., Miller, N., Shvartsbeyn, A., Sullivan, S.A., Vaudin, M., Wiegand, R. and Kaplan, H.B., (2006) Evolution of sensory complexity recorded in a myxobacterial genome. *Proc Natl Acad Sci U S A* **103**: 15200-15205.

Gomez-Santos, N., Treuner-Lange, A., Moraleda-Munoz, A., Garcia-Bravo, E., Garcia-Hernandez, R., Martinez-Cayuela, M., Perez, J., Sogaard-Andersen, L. and Munoz-Dorado, J., (2012) Comprehensive set of integrative plasmid vectors for copper-inducible gene expression in Myxococcus xanthus. *Appl Environ Microbiol* **78**: 2515-2521.

Gonzalez-Pastor, J.E., (2011) Cannibalism: a social behavior in sporulating Bacillus subtilis. *FEMS Microbiol Rev* **35**: 415-424.

Gooderham, W.J. and Hancock, R.E., (2009) Regulation of virulence and antibiotic resistance by two-component regulatory systems in Pseudomonas aeruginosa. *FEMS Microbiol Rev* **33**: 279-294.

Goodman, A.L., Merighi, M., Hyodo, M., Ventre, I., Filloux, A. and Lory, S., (2009) Direct interaction between sensor kinase proteins mediates acute and chronic disease phenotypes in a bacterial pathogen. *Genes Dev* **23**: 249-259.

Goulian, M., (2010) Two-component signaling circuit structure and properties. *Curr Opin Microbiol* **13**: 184-189.

Greenstein, A.E., Grundner, C., Echols, N., Gay, L.M., Lombana, T.N., Miecskowski, C.A., Pullen, K.E., Sung, P.Y. and Alber, T., (2005) Structure/function studies of Ser/Thr and Tyr protein phosphorylation in Mycobacterium tuberculosis. *J Mol Microbiol Biotechnol* **9**: 167-181.

Grefen, C., Stadele, K., Ruzicka, K., Obrdlik, P., Harter, K. and Horak, J., (2008) Subcellular localization and in vivo interactions of the Arabidopsis thaliana ethylene receptor family members. *Mol Plant* **1**: 308-320.

Gutu, A.D., Wayne, K.J., Sham, L.T. and Winkler, M.E., (2010) Kinetic characterization of the WalRKSpn (VicRK) two-component system of Streptococcus pneumoniae: dependence of WalKSpn (VicK) phosphatase activity on its PAS domain. *J Bacteriol* **192**: 2346-2358.

Hager, E., Tse, H. and Gill, R.E., (2001) Identification and characterization of spdR mutations that bypass the BsgA protease-dependent regulation of developmental gene expression in Myxococcus xanthus. *Mol Microbiol* **39**: 765-780.

Haldimann, A., Fisher, S.L., Daniels, L.L., Walsh, C.T. and Wanner, B.L., (1997) Transcriptional regulation of the Enterococcus faecium BM4147 vancomycin resistance gene cluster by the VanS-VanR two-component regulatory system in Escherichia coli K-12. *J Bacteriol* **179**: 5903-5913.

Hanks, S.K. and Hunter, T., (1995) Protein kinases 6. The eukaryotic protein kinase superfamily: kinase (catalytic) domain structure and classification. *FASEB J* **9**: 576-596.

Harris, B.Z., Kaiser, D. and Singer, M., (1998) The guanosine nucleotide (p)ppGpp initiates development and A-factor production in *Myxococcus xanthus*. *Genes Dev* **12**: 1022-1035.

Henry, J.T. and Crosson, S., (2011) Ligand-binding PAS domains in a genomic, cellular, and structural context. *Annu Rev Microbiol* **65**: 261-286.

Hidaka, Y., Park, H. and Inouye, M., (1997) Demonstration of dimer formation of the cytoplasmic domain of a transmembrane osmosensor protein, EnvZ, of Escherichia coli using Ni-histidine tag affinity chromatography. *FEBS Lett* **400**: 238-242.

Higgs, P.I., Cho, K., Whitworth, D.E., Evans, L.S. and Zusman, D.R., (2005) Four unusual two-component signal transduction homologs, RedC to RedF, are necessary for timely development in Myxococcus xanthus. *J Bacteriol* **187**: 8191-8195.

Higgs, P.I., Jagadeesan, S., Mann, P. and Zusman, D.R., (2008) EspA, an orphan hybrid histidine protein kinase, regulates the timing of expression of key developmental proteins of Myxococcus xanthus. *J Bacteriol* **190**: 4416-4426.

Higgs, P.I., P.L. Hartzell, C. Holkenbrink and E. Hoiczyk, (2014) *Myxococcus xanthus* vegetative and developmental cell heterogeneity. In: Myxobacteria: Genomics, Cellular and Molecular Biology. Higgs, Z.Y.a.P.I. (ed). pp. 51-77.

Hillesland, K.L., Velicer, G.J. and Lenski, R.E., (2009) Experimental evolution of a microbial predator's ability to find prey. *Proc Biol Sci* **276**: 459-467.

Hoch, J.A., (2000) Two-component and phosphorelay signal transduction. *Curr Opin Microbiol* **3**: 165-170.

Hoiczyk, E., Ring, M.W., McHugh, C.A., Schwar, G., Bode, E., Krug, D., Altmeyer, M.O., Lu, J.Z. and Bode, H.B., (2009) Lipid body formation plays a central role in cell fate determination during developmental differentiation of Myxococcus xanthus. *Mol Microbiol* **74**: 497-517.

Holkenbrink, C., Hoiczyk, E., Kahnt, J. and Higgs, P.I., (2014) Synthesis and assembly of a novel glycan layer in Myxococcus xanthus spores. *J Biol Chem* **289**: 32364-32378.

Horstmann, N., Saldana, M., Sahasrabhojane, P., Yao, H., Su, X., Thompson, E., Koller, A. and Shelburne, S.A., 3rd, (2014) Dual-site phosphorylation of the control of virulence regulator impacts group a streptococcal global gene expression and pathogenesis. *PLoS Pathog* **10**: e1004088.

Hsing, W. and Silhavy, T.J., (1997) Function of conserved histidine-243 in phosphatase activity of EnvZ, the sensor for porin osmoregulation in Escherichia coli. *J Bacteriol* **179**: 3729-3735.

Hsu, J.L., Chen, H.C., Peng, H.L. and Chang, H.Y., (2008) Characterization of the histidine-containing phosphotransfer protein B-mediated multistep phosphorelay system in Pseudomonas aeruginosa PAO1. *J Biol Chem* **283**: 9933-9944.

Hu, W., Lux, R. and Shi, W., (2013) Analysis of exopolysaccharides in Myxococcus xanthus using confocal laser scanning microscopy. *Methods Mol Biol* **966**: 121-131.

Huntley, S., Hamann, N., Wegener-Feldbrugge, S., Treuner-Lange, A., Kube, M., Reinhardt, R., Klages, S., Muller, R., Ronning, C.M., Nierman, W.C. and Sogaard-Andersen, L., (2011) Comparative genomic analysis of fruiting body formation in Myxococcales. *Mol Biol Evol* **28**: 1083-1097.

Huntley, S., Zhang, Y., Treuner-Lange, A., Kneip, S., Sensen, C.W. and Sogaard-Andersen, L., (2012) Complete genome sequence of the fruiting myxobacterium Corallococcus coralloides DSM 2259. *J Bacteriol* **194**: 3012-3013.

Huntley, S., Kneip, S., Treuner-Lange, A. and Sogaard-Andersen, L., (2013) Complete genome sequence of Myxococcus stipitatus strain DSM 14675, a fruiting myxobacterium. *Genome Announc* **1**: e0010013.

Huse, M. and Kuriyan, J., (2002) The conformational plasticity of protein kinases. *Cell* **109**: 275-282.

Hutchings, M.I., Hoskisson, P.A., Chandra, G. and Buttner, M.J., (2004) Sensing and responding to diverse extracellular signals? Analysis of the sensor kinases and response regulators of Streptomyces coelicolor A3(2). *Microbiology* **150**: 2795-2806.

Huynh, T.N., Noriega, C.E. and Stewart, V., (2010) Conserved mechanism for sensor phosphatase control of two-component signaling revealed in the nitrate sensor NarX. *Proc Natl Acad Sci U S A* **107**: 21140-21145.

Inclan, Y.F., Laurent, S. and Zusman, D.R., (2008) The receiver domain of FrzE, a CheA-CheY fusion protein, regulates the CheA histidine kinase activity and downstream signalling to the A- and S-motility systems of Myxococcus xanthus. *Mol Microbiol* **68**: 1328-1339.

Iniesta, A.A., Garcia-Heras, F., Abellon-Ruiz, J., Gallego-Garcia, A. and Elias-Arnanz, M., (2012) Two systems for conditional gene expression in Myxococcus xanthus inducible by isopropyl-beta-D-thiogalactopyranoside or vanillate. *J Bacteriol* **194**: 5875-5885.

Inoue, H., Nojima, H. and Okayama, H., (1990) High efficiency transformation of Escherichia coli with plasmids. *Gene* **96**: 23-28.

Inouye, S., Jain, R., Ueki, T., Nariya, H., Xu, C.Y., Hsu, M.Y., Fernandez-Luque, B.A., Munoz-Dorado, J., Farez-Vidal, E. and Inouye, M., (2000) A large family of eukaryotic-like protein Ser/Thr kinases of Myxococcus xanthus, a developmental bacterium. *Microb Comp Genomics* **5**: 103-120.

Inouye, S., Nariya, H. and Munoz-Dorado, J., (2008) Protein Ser/Thr Kinases and Phosphatases in Myxococcus xanthus. In: Myxobacteria - Multicellularity and Differentiation. Whitworth, D.E. (ed). Washington, DC: ASM Press, pp. 191-210.

Inouye, S. and Nariya, H., (2008) Dual regulation with Ser/Thr kinase cascade and a His/Asp TCS in Myxococcus xanthus. *Adv Exp Med Biol* **631**: 111-121.

Ivanova, N., Daum, C., Lang, E., Abt, B., Kopitz, M., Saunders, E., Lapidus, A., Lucas, S., Glavina Del Rio, T., Nolan, M., Tice, H., Copeland, A., Cheng, J.F., Chen, F., Bruce, D., Goodwin, L., Pitluck, S., Mavromatis, K., Pati, A., Mikhailova, N., Chen, A., Palaniappan, K., Land, M., Hauser, L., Chang, Y.J., Jeffries, C.D., Detter, J.C., Brettin, T., Rohde, M., Goker, M., Bristow, J., Markowitz, V., Eisen, J.A., Hugenholtz, P., Kyrpides, N.C. and Klenk, H.P., (2010) Complete genome sequence of Haliangium ochraceum type strain (SMP-2). *Stand Genomic Sci* **2**: 96-106.

Jagadeesan, S., (2008) The Myxococcus xanhus Red two-component signal transduction system: a novel “four-component” signaling mechanism. In: Max-Planck-Institut für Terrestrische Mikrobiologie. Philipps-Universität Marburg.

Jagadeesan, S., Mann, P., Schink, C.W. and Higgs, P.I., (2009) A novel "four-component" two-component signal transduction mechanism regulates developmental progression in Myxococcus xanthus. *J Biol Chem* **284**: 21435-21445.

Jenal, U. and Galperin, M.Y., (2009) Single domain response regulators: molecular switches with emerging roles in cell organization and dynamics. *Curr Opin Microbiol* **12**: 152-160.

Jiang, P., Atkinson, M.R., Srisawat, C., Sun, Q. and Ninfa, A.J., (2000) Functional dissection of the dimerization and enzymatic activities of Escherichia coli nitrogen regulator II and their regulation by the PII protein. *Biochemistry* **39**: 13433-13449.

Julien, B., Kaiser, A.D. and Garza, A., (2000) Spatial control of cell differentiation in *Myxococcus xanthus*. *Proc Natl Acad Sci U S A* **97**: 9098-9103.

Kaimer, C. and Zusman, D.R., (2013) Phosphorylation-dependent localization of the response regulator FrzZ signals cell reversals in Myxococcus xanthus. *Mol Microbiol* **88**: 740-753.

Kaiser, D., (2001) Building a multicellular organism. *Annu Rev Genet* **35**: 103-123.

Kaiser, D., (2004) Signaling in myxobacteria. *Annu Rev Microbiol* **58**: 75-98.

Keane, R. and Berleman, J., (2016) The predatory life cycle of Myxococcus xanthus. *Microbiology* **162**: 1-11.

Kelley, L.A., Mezulis, S., Yates, C.M., Wass, M.N. and Sternberg, M.J., (2015) The Phyre2 web portal for protein modeling, prediction and analysis. *Nat Protoc* **10**: 845-858.

Kenney, L.J., (2010) How important is the phosphatase activity of sensor kinases? *Curr Opin Microbiol* **13**: 168-176.

Kessin, R.H., Gundersen, G.G., Zaydfudim, V. and Grimson, M., (1996) How cellular slime molds evade nematodes. *Proc Natl Acad Sci U S A* **93**: 4857-4861.

Kim, S.K. and Kaiser, D., (1990a) C-factor: a cell-cell signaling protein required for fruiting body morphogenesis of M. xanthus. *Cell* **61**: 19-26.

Kim, S.K. and Kaiser, D., (1990b) Purification and properties of Myxococcus xanthus C-factor, an intercellular signaling protein. *Proc Natl Acad Sci U S A* **87**: 3635-3639.

Kim, S.K. and Kaiser, D., (1990c) Cell motility is required for the transmission of C-factor, an intercellular signal that coordinates fruiting body morphogenesis of Myxococcus xanthus. *Genes Dev* **4**: 896-904.

Kimura, Y., Mori, Y., Ina, Y. and Takegawa, K., (2011) Enzymatic and functional analysis of a protein phosphatase, Pph3, from Myxococcus xanthus. *J Bacteriol* **193**: 2657-2661.

Kinoshita-Kikuta, E., Kinoshita, E., Eguchi, Y. and Koike, T., (2016) Validation of Cis and Trans Modes in Multistep Phosphotransfer Signaling of Bacterial Tripartite Sensor Kinases by Using Phos-Tag SDS-PAGE. *PLoS One* **11**: e0148294.

Kinoshita, E., Kinoshita-Kikuta, E., Matsubara, M., Yamada, S., Nakamura, H., Shiro, Y., Aoki, Y., Okita, K. and Koike, T., (2008) Separation of phosphoprotein isotypes having the same number of phosphate groups using phosphate-affinity SDS-PAGE. *Proteomics* **8**: 2994-3003.

Kinoshita, E., Kinoshita-Kikuta, E., Shiba, A., Edahiro, K., Inoue, Y., Yamamoto, K., Yoshida, M. and Koike, T., (2014) Profiling of protein thiophosphorylation by Phos-tag affinity electrophoresis: evaluation of adenosine 5'-O-(3-thiotriphosphate) as a phosphoryl donor in protein kinase reactions. *Proteomics* **14**: 668-679.

Kirby, J.R. and Zusman, D.R., (2003) Chemosensory regulation of developmental gene expression in Myxococcus xanthus. *Proc Natl Acad Sci U S A* **100**: 2008-2013.

Klose, K.E., Weiss, D.S. and Kustu, S., (1993) Glutamate at the site of phosphorylation of nitrogen-regulatory protein NTRC mimics aspartyl-phosphate and activates the protein. *J Mol Biol* **232**: 67-78.

Koch, M.K., McHugh, C.A. and Hoiczyk, E., (2011) BacM, an N-terminally processed bactofilin of Myxococcus xanthus, is crucial for proper cell shape. *Mol Microbiol* **80**: 1031-1051.

Kornev, A.P. and Taylor, S.S., (2010) Defining the conserved internal architecture of a protein kinase. *Biochim Biophys Acta* **1804**: 440-444.

Kraemer, S.A., Toups, M.A. and Velicer, G.J., (2010) Natural variation in developmental life-history traits of the bacterium Myxococcus xanthus. *FEMS Microbiol Ecol* **73**: 226-233.

Kroos, L., (2017) Highly Signal-Responsive Gene Regulatory Network Governing Myxococcus Development. *Trends Genet* **33**: 3-15.

Laemmli, U.K., (1970) Cleavage of structural proteins during the assembly of the head of bacteriophage T4. *Nature* **227**: 680-685.

Lan, C.Y. and Igo, M.M., (1998) Differential expression of the OmpF and OmpC porin proteins in Escherichia coli K-12 depends upon the level of active OmpR. *J Bacteriol* **180**: 171-174.

Lasker, M., Bui, C.D., Besant, P.G., Sugawara, K., Thai, P., Medzihradszky, G. and Turck, C.W., (1999) Protein histidine phosphorylation: increased stability of thiophosphohistidine. *Protein Sci* **8**: 2177-2185.

Laub, M.T. and Goulian, M., (2007) Specificity in two-component signal transduction pathways. *Annu Rev Genet* **41**: 121-145.

Laue, B.E. and Gill, R.E., (1995) Using a phase-locked mutant of Myxococcus xanthus to study the role of phase variation in development. *J Bacteriol* **177**: 4089-4096.

Lee, B., Higgs, P.I., Zusman, D.R. and Cho, K., (2005) EspC is involved in controlling the timing of development in Myxococcus xanthus. *J Bacteriol* **187**: 5029-5031.

Lee, B., (2009) The role of negative regulators in coordination of the Myxococcus xanthus developmental program. In: Max-Planck-Institut für Terrestrische Mikrobiologie. Philipps-Universität Marburg.

Lee, B., Schramm, A., Jagadeesan, S. and Higgs, P.I., (2010) Two-component systems and regulation of developmental progression in Myxococcus xanthus. *Methods Enzymol* **471**: 253-278.

Lee, B., Mann, P., Grover, V., Treuner-Lange, A., Kahnt, J. and Higgs, P.I., (2011a) The *Myxococcus xanthus* spore cuticula protein C is a fragment of FibA, an extracellular metalloprotease produced exclusively in aggregated cells. *PLoS One* **6**: e28968.

Lee, B., Holkenbrink, C., Treuner-Lange, A. and Higgs, P.I., (2012) Myxococcus xanthus developmental cell fate production: heterogeneous accumulation of developmental regulatory proteins and reexamination of the role of MazF in developmental lysis. *J Bacteriol* **194**: 3058-3068.

Lee, J.S., Son, B., Viswanathan, P., Luethy, P.M. and Kroos, L., (2011b) Combinatorial regulation of fmgD by MrpC2 and FruA during Myxococcus xanthus development. *J Bacteriol* **193**: 1681-1689.

Leonardy, S., Freymark, G., Hebener, S., Ellehauge, E. and Sogaard-Andersen, L., (2007) Coupling of protein localization and cell movements by a dynamically localized response regulator in Myxococcus xanthus. *EMBO J* **26**: 4433-4444.

Letunic, I., Doerks, T. and Bork, P., (2015) SMART: recent updates, new developments and status in 2015. *Nucleic Acids Res* **43**: D257-260.

Lewis, K., (2007) Persister cells, dormancy and infectious disease. *Nat Rev Microbiol* **5**: 48-56.

Lewis, R.J., Brannigan, J.A., Muchova, K., Barak, I. and Wilkinson, A.J., (1999) Phosphorylated aspartate in the structure of a response regulator protein. *J Mol Biol* **294**: 9-15.

Li, S.G., Zhou, X.W., Li, P.F., Han, K., Li, W., Li, Z.F., Wu, Z.H. and Li, Y.Z., (2012) The existence and diversity of myxobacteria in lake mud - a previously unexplored myxobacteria habitat. *Environ Microbiol Rep* **4**: 587-595.

Li, Y., Sun, H., Ma, X., Lu, A., Lux, R., Zusman, D. and Shi, W., (2003) Extracellular polysaccharides mediate pilus retraction during social motility of Myxococcus xanthus. *Proc Natl Acad Sci U S A* **100**: 5443-5448.

Li, Z.F., Li, X., Liu, H., Liu, X., Han, K., Wu, Z.H., Hu, W., Li, F.F. and Li, Y.Z., (2011) Genome sequence of the halotolerant marine bacterium Myxococcus fulvus HW-1. *J Bacteriol* **193**: 5015-5016.

Libby, E.A., Goss, L.A. and Dworkin, J., (2015) The Eukaryotic-Like Ser/Thr Kinase PrkC Regulates the Essential WalRK Two-Component System in Bacillus subtilis. *PLoS Genet* **11**: e1005275.

Lin, W.J., Walthers, D., Connelly, J.E., Burnside, K., Jewell, K.A., Kenney, L.J. and Rajagopal, L., (2009) Threonine phosphorylation prevents promoter DNA binding of the Group B Streptococcus response regulator CovR. *Mol Microbiol* **71**: 1477-1495.

Lobedanz, S. and Sogaard-Andersen, L., (2003) Identification of the C-signal, a contact-dependent morphogen coordinating multiple developmental responses in Myxococcus xanthus. *Genes Dev* **17**: 2151-2161.

Lopez, D., Vlamakis, H., Losick, R. and Kolter, R., (2009a) Cannibalism enhances biofilm development in Bacillus subtilis. *Mol Microbiol* **74**: 609-618.

Lopez, D., Vlamakis, H. and Kolter, R., (2009b) Generation of multiple cell types in Bacillus subtilis. *FEMS Microbiol Rev* **33**: 152-163.

Lopez, D. and Kolter, R., (2010) Extracellular signals that define distinct and coexisting cell fates in Bacillus subtilis. *FEMS Microbiol Rev* **34**: 134-149.

Lux, R., Li, Y., Lu, A. and Shi, W., (2004) Detailed three-dimensional analysis of structural features of Myxococcus xanthus fruiting bodies using confocal laser scanning microscopy. *Biofilms* **1**: 293-303.

Madhusudan, Akamine, P., Xuong, N.H. and Taylor, S.S., (2002) Crystal structure of a transition state mimic of the catalytic subunit of cAMP-dependent protein kinase. *Nat Struct Biol* **9**: 273-277.

Mann, T.H., Seth Childers, W., Blair, J.A., Eckart, M.R. and Shapiro, L., (2016) A cell cycle kinase with tandem sensory PAS domains integrates cell fate cues. *Nat Commun* **7**: 11454.

Marina, A., Waldburger, C.D. and Hendrickson, W.A., (2005) Structure of the entire cytoplasmic portion of a sensor histidine-kinase protein. *EMBO J* **24**: 4247-4259.

Mascher, T., Helmann, J.D. and Unden, G., (2006) Stimulus perception in bacterial signal-transducing histidine kinases. *Microbiol Mol Biol Rev* **70**: 910-938.

Meiser, P., Bode, H.B. and Muller, R., (2006) The unique DKxanthene secondary metabolite family from the myxobacterium Myxococcus xanthus is required for developmental sporulation. *Proc Natl Acad Sci U S A* **103**: 19128-19133.

Mittal, S. and Kroos, L., (2009a) Combinatorial regulation by a novel arrangement of FruA and MrpC2 transcription factors during Myxococcus xanthus development. *J Bacteriol* **191**: 2753-2763.

Mittal, S. and Kroos, L., (2009b) A combination of unusual transcription factors binds cooperatively to control Myxococcus xanthus developmental gene expression. *Proc Natl Acad Sci U S A* **106**: 1965-1970.

Moglich, A., Ayers, R.A. and Moffat, K., (2009a) Design and signaling mechanism of light-regulated histidine kinases. *J Mol Biol* **385**: 1433-1444.

Moglich, A., Ayers, R.A. and Moffat, K., (2009b) Structure and signaling mechanism of Per-ARNT-Sim domains. *Structure* **17**: 1282-1294.

Moglich, A., Ayers, R.A. and Moffat, K., (2010) Addition at the molecular level: signal integration in designed Per-ARNT-Sim receptor proteins. *J Mol Biol* **400**: 477-486.

Moon, K. and Gottesman, S., (2009) A PhoQ/P-regulated small RNA regulates sensitivity of Escherichia coli to antimicrobial peptides. *Mol Microbiol* **74**: 1314-1330.

Moore, J.B., Shiau, S.P. and Reitzer, L.J., (1993) Alterations of highly conserved residues in the regulatory domain of nitrogen regulator I (NtrC) of Escherichia coli. *J Bacteriol* **175**: 2692-2701.

Muller, F.D., Treuner-Lange, A., Heider, J., Huntley, S.M. and Higgs, P.I., (2010) Global transcriptome analysis of spore formation in Myxococcus xanthus reveals a locus necessary for cell differentiation. *BMC Genomics* **11**: 264.

Muller, F.D., Schink, C.W., Hoiczyk, E., Cserti, E. and Higgs, P.I., (2012) Spore formation in Myxococcus xanthus is tied to cytoskeleton functions and polysaccharide spore coat deposition. *Mol Microbiol* **83**: 486-505.

Munoz-Dorado, J., Inouye, S. and Inouye, M., (1991) A gene encoding a protein serine/threonine kinase is required for normal development of M. xanthus, a gram-negative bacterium. *Cell* **67**: 995-1006.

Munoz-Dorado, J., Higgs, P.I. and Elias-Arnanz, M., (2014) Abundance and Complexity of Signalling Mechanisms in Myxobacteria. In: Myxobacteria: Genomics, Cellular and Molecular Biology. Yang, Z. and Higgs, P.I. (eds). Norfolk, UK: Caister Academic Press, pp. 127-150.

Munoz-Dorado, J., Marcos-Torres, F.J., Garcia-Bravo, E., Moraleda-Munoz, A. and Perez, J., (2016) Myxobacteria: Moving, Killing, Feeding, and Surviving Together. *Front Microbiol* **7**: 781.

Nakamura, Y., Gojobori, T. and Ikemura, T., (2000) Codon usage tabulated from international DNA sequence databases: status for the year 2000. *Nucleic Acids Res* **28**: 292.

Nan, B. and Zusman, D.R., (2011) Uncovering the mystery of gliding motility in the myxobacteria. *Annu Rev Genet* **45**: 21-39.

Nariya, H. and Inouye, S., (2002) Activation of 6-phosphofructokinase via phosphorylation by Pkn4, a protein Ser/Thr kinase of Myxococcus xanthus. *Mol Microbiol* **46**: 1353-1366.

Nariya, H. and Inouye, S., (2003) An effective sporulation of Myxococcus xanthus requires glycogen consumption via Pkn4-activated 6-phosphofructokinase. *Mol Microbiol* **49**: 517-528.

Nariya, H. and Inouye, S., (2005a) Modulating factors for the Pkn4 kinase cascade in regulating 6-phosphofructokinase in Myxococcus xanthus. *Mol Microbiol* **56**: 1314-1328.

Nariya, H. and Inouye, S., (2005b) Factors that modulate the Pkn4 kinase cascade in Myxococcus xanthus. *J Mol Microbiol Biotechnol* **9**: 147-153.

Nariya, H. and Inouye, S., (2005c) Identification of a protein Ser/Thr kinase cascade that regulates essential transcriptional activators in Myxococcus xanthus development. *Mol Microbiol* **58**: 367-379.

Nariya, H. and Inouye, S., (2006) A protein Ser/Thr kinase cascade negatively regulates the DNA-binding activity of MrpC, a smaller form of which may be necessary for the Myxococcus xanthus development. *Mol Microbiol* **60**: 1205-1217.

Nariya, H. and Inouye, M., (2008) MazF, an mRNA interferase, mediates programmed cell death during multicellular Myxococcus development. *Cell* **132**: 55-66.

Ninfa, A.J. and Magasanik, B., (1986) Covalent modification of the glnG product, NRI, by the glnL product, NRII, regulates the transcription of the glnALG operon in Escherichia coli. *Proc Natl Acad Sci U S A* **83**: 5909-5913.

Nolen, B., Taylor, S. and Ghosh, G., (2004) Regulation of protein kinases; controlling activity through activation segment conformation. *Mol Cell* **15**: 661-675.

O'Connor, K.A. and Zusman, D.R., (1991a) Development in *Myxococcus xanthus* involves differentiation into two cell types, peripheral rods and spores. *J Bacteriol* **173**: 3318-3333.

O'Connor, K.A. and Zusman, D.R., (1991b) Analysis of Myxococcus xanthus cell types by two-dimensional polyacrylamide gel electrophoresis. *J Bacteriol* **173**: 3334-3341.

O'Connor, K.A. and Zusman, D.R., (1991c) Behavior of peripheral rods and their role in the life cycle of Myxococcus xanthus. *J Bacteriol* **173**: 3342-3355.

Ortiz-Lombardia, M., Pompeo, F., Boitel, B. and Alzari, P.M., (2003) Crystal structure of the catalytic domain of the PknB serine/threonine kinase from Mycobacterium tuberculosis. *J Biol Chem* **278**: 13094-13100.

Pallen, M., Chaudhuri, R. and Khan, A., (2002) Bacterial FHA domains: neglected players in the phospho-threonine signalling game? *Trends Microbiol* **10**: 556-563.

Pathak, D.T., Wei, X. and Wall, D., (2012) Myxobacterial tools for social interactions. *Res Microbiol* **163**: 579-591.

Paul, R., Jaeger, T., Abel, S., Wiederkehr, I., Folcher, M., Biondi, E.G., Laub, M.T. and Jenal, U., (2008) Allosteric regulation of histidine kinases by their cognate response regulator determines cell fate. *Cell* **133**: 452-461.

Pereira, S.F., Goss, L. and Dworkin, J., (2011) Eukaryote-like serine/threonine kinases and phosphatases in bacteria. *Microbiol Mol Biol Rev* **75**: 192-212.

Perez, J., Castaneda-Garcia, A., Jenke-Kodama, H., Muller, R. and Munoz-Dorado, J., (2008) Eukaryotic-like protein kinases in the prokaryotes and the myxobacterial kinome. *Proc Natl Acad Sci U S A* **105**: 15950-15955.

Porter, S.L., Wadhams, G.H. and Armitage, J.P., (2008a) Rhodobacter sphaeroides: complexity in chemotactic signalling. *Trends Microbiol* **16**: 251-260.

Porter, S.L., Roberts, M.A., Manning, C.S. and Armitage, J.P., (2008b) A bifunctional kinase-phosphatase in bacterial chemotaxis. *Proc Natl Acad Sci U S A* **105**: 18531-18536.

Psakis, G., Mailliet, J., Lang, C., Teufel, L., Essen, L.O. and Hughes, J., (2011) Signaling kinetics of cyanobacterial phytochrome Cph1, a light regulated histidine kinase. *Biochemistry* **50**: 6178-6188.

Rajagopal, L., Vo, A., Silvestroni, A. and Rubens, C.E., (2006) Regulation of cytotoxin expression by converging eukaryotic-type and two-component signalling mechanisms in Streptococcus agalactiae. *Mol Microbiol* **62**: 941-957.

Rajagopalan, R. and Kroos, L., (2014) Nutrient-regulated proteolysis of MrpC halts expression of genes important for commitment to sporulation during Myxococcus xanthus development. *J Bacteriol* **196**: 2736-2747.

Rajagopalan, R. and Kroos, L., (2017) The dev Operon Regulates the Timing of Sporulation during Myxococcus xanthus Development. *J Bacteriol* **199**.

Rasmussen, A.A. and Sogaard-Andersen, L., (2003) TodK, a putative histidine protein kinase, regulates timing of fruiting body morphogenesis in Myxococcus xanthus. *J Bacteriol* **185**: 5452-5464.

Rasmussen, A.A., Porter, S.L., Armitage, J.P. and Sogaard-Andersen, L., (2005) Coupling of multicellular morphogenesis and cellular differentiation by an unusual hybrid histidine protein kinase in Myxococcus xanthus. *Mol Microbiol* **56**: 1358-1372.

Rasmussen, A.A., Wegener-Feldbrugge, S., Porter, S.L., Armitage, J.P. and Sogaard-Andersen, L., (2006) Four signalling domains in the hybrid histidine protein kinase RodK of Myxococcus xanthus are required for activity. *Mol Microbiol* **60**: 525-534.

Reichenbach, H., (1993) Biology of the Myxobacteria: Ecology and Taxonomy. In: Myxobacteria II. Dworkin, M. and Kaiser, A.D. (eds). Washington DC: American Society for Microbilology, pp. 13-62.

Reichenbach, H., (1999) The ecology of the myxobacteria. *Environ Microbiol* **1**: 15-21.

Rhie, H.G. and Shimkets, L.J., (1989) Developmental bypass suppression of Myxococcus xanthus csgA mutations. *J Bacteriol* **171**: 3268-3276.

Rhodenizer, D., Martin, I., Bhandari, P., Pletcher, S.D. and Grotewiel, M., (2008) Genetic and environmental factors impact age-related impairment of negative geotaxis in Drosophila by altering age-dependent climbing speed. *Exp Gerontol* **43**: 739-748.

Robinson, M., Son, B., Kroos, D. and Kroos, L., (2014) Transcription factor MrpC binds to promoter regions of hundreds of developmentally-regulated genes in Myxococcus xanthus. *BMC Genomics* **15**: 1123.

Roman, S.J., Meyers, M., Volz, K. and Matsumura, P., (1992) A chemotactic signaling surface on CheY defined by suppressors of flagellar switch mutations. *J Bacteriol* **174**: 6247-6255.

Romeralo, M., Skiba, A., Gonzalez-Voyer, A., Schilde, C., Lawal, H., Kedziora, S., Cavender, J.C., Glockner, G., Urushihara, H. and Schaap, P., (2013) Analysis of phenotypic evolution in Dictyostelia highlights developmental plasticity as a likely consequence of colonial multicellularity. *Proc Biol Sci* **280**: 20130976.

Rosenberg, E., Keller, K.H. and Dworkin, M., (1977) Cell density-dependent growth of Myxococcus xanthus on casein. *J Bacteriol* **129**: 770-777.

Russo, F.D. and Silhavy, T.J., (1991) EnvZ controls the concentration of phosphorylated OmpR to mediate osmoregulation of the porin genes. *J Mol Biol* **222**: 567-580.

Schaffer, A.A., Aravind, L., Madden, T.L., Shavirin, S., Spouge, J.L., Wolf, Y.I., Koonin, E.V. and Altschul, S.F., (2001) Improving the accuracy of PSI-BLAST protein database searches with composition-based statistics and other refinements. *Nucleic Acids Res* **29**: 2994-3005.

Schneiker, S., Martins dos Santos, V.A., Bartels, D., Bekel, T., Brecht, M., Buhrmester, J., Chernikova, T.N., Denaro, R., Ferrer, M., Gertler, C., Goesmann, A., Golyshina, O.V., Kaminski, F., Khachane, A.N., Lang, S., Linke, B., McHardy, A.C., Meyer, F., Nechitaylo, T., Puhler, A., Regenhardt, D., Rupp, O., Sabirova, J.S., Selbitschka, W., Yakimov, M.M., Timmis, K.N., Vorholter, F.J., Weidner, S., Kaiser, O. and Golyshin, P.N., (2006) Genome sequence of the ubiquitous hydrocarbon-degrading marine bacterium Alcanivorax borkumensis. *Nat Biotechnol* **24**: 997-1004.

Schneiker, S., Perlova, O., Kaiser, O., Gerth, K., Alici, A., Altmeyer, M.O., Bartels, D., Bekel, T., Beyer, S., Bode, E., Bode, H.B., Bolten, C.J., Choudhuri, J.V., Doss, S., Elnakady, Y.A., Frank, B., Gaigalat, L., Goesmann, A., Groeger, C., Gross, F., Jelsbak, L., Jelsbak, L., Kalinowski, J., Kegler, C., Knauber, T., Konietzny, S., Kopp, M., Krause, L., Krug, D., Linke, B., Mahmud, T., Martinez-Arias, R., McHardy, A.C., Merai, M., Meyer, F., Mormann, S., Munoz-Dorado, J., Perez, J., Pradella, S., Rachid, S., Raddatz, G., Rosenau, F., Ruckert, C., Sasse, F., Scharfe, M., Schuster, S.C., Suen, G., Treuner-Lange, A., Velicer, G.J., Vorholter, F.J., Weissman, K.J., Welch, R.D., Wenzel, S.C., Whitworth, D.E., Wilhelm, S., Wittmann, C., Blocker, H., Puhler, A. and Muller, R., (2007) Complete genome sequence of the myxobacterium Sorangium cellulosum. *Nat Biotechnol* **25**: 1281-1289.

Schramm, A., Lee, B. and Higgs, P.I., (2012) Intra- and interprotein phosphorylation between two-hybrid histidine kinases controls Myxococcus xanthus developmental progression. *J Biol Chem* **287**: 25060-25072.

Schreiber, M., Res, I. and Matter, A., (2009) Protein kinases as antibacterial targets. *Curr Opin Cell Biol* **21**: 325-330.

Schultz, J., Milpetz, F., Bork, P. and Ponting, C.P., (1998) SMART, a simple modular architecture research tool: identification of signaling domains. *Proc Natl Acad Sci U S A* **95**: 5857-5864.

Schumacher, D. and Sogaard-Andersen, L., (2017) Regulation of Cell Polarity in Motility and Cell Division in Myxococcus xanthus. *Annu Rev Microbiol* **71**: 61-78.

Segall, J.E., Manson, M.D. and Berg, H.C., (1982) Signal processing times in bacterial chemotaxis. *Nature* **296**: 855-857.

Seidman, C.E., Struhl, K., Sheen, J. and Jessen, T., (2001) Introduction of Plasmid DNA into Cells. *Current Protocols in Molecular Biology*: 37:II:31.38:31.38.31–31.38.10.

Senevirathne, C. and Pflum, M.K., (2013) Biotinylated phosphoproteins from kinase-catalyzed biotinylation are stable to phosphatases: implications for phosphoproteomics. *Chembiochem* **14**: 381-387.

Shank, E.A. and Kolter, R., (2011) Extracellular signaling and multicellularity in Bacillus subtilis. *Curr Opin Microbiol* **14**: 741-747.

Shapiro, J.A., (1988) Bacteria as Multicellular Organisms. *Scientific American* **258**: 82-89.

Shapiro, J.A., (1998) Thinking about bacterial populations as multicellular organisms. *Annu Rev Microbiol* **52**: 81-104.

Shi, X., (2008) An analysis of two-component regulatory systems in Myxococcus xanthus. In: Max-Planck-Institut für terrestrische Mikrobiologie. Philipps-Universität Marburg.

Shi, X., Wegener-Feldbrugge, S., Huntley, S., Hamann, N., Hedderich, R. and Sogaard-Andersen, L., (2008) Bioinformatics and experimental analysis of proteins of two-component systems in Myxococcus xanthus. *J Bacteriol* **190**: 613-624.

Shimkets, L., Reichenbach, H. and Dworkin, M., (2006) The Myxobacteria. . In: The Prokaryotes. Dworkin, M. (ed). New York: Springer, pp. 31-115.

Shimkets, L.J., (1990) Social and developmental biology of the myxobacteria. *Microbiol Rev* **54**: 473-501.

Shimkets, L.J., (1999) Intercellular signaling during fruiting-body development of Myxococcus xanthus. *Annu Rev Microbiol* **53**: 525-549.

Silversmith, R.E., Levin, M.D., Schilling, E. and Bourret, R.B., (2008) Kinetic characterization of catalysis by the chemotaxis phosphatase CheZ. Modulation of activity by the phosphorylated CheY substrate. *J Biol Chem* **283**: 756-765.

Singer, M. and Kaiser, D., (1995) Ectopic production of guanosine penta- and tetraphosphate can initiate early developmental gene expression in *Myxococcus xanthus*. *Genes Dev* **9**: 1633-1644.

Singh, B.N., (1947) Myxobacteria in soils and composts; their distribution, number and lytic action on bacteria. *J Gen Microbiol* **1**: 1-10.

Skerker, J.M. and Laub, M.T., (2004) Cell-cycle progression and the generation of asymmetry in Caulobacter crescentus. *Nat Rev Microbiol* **2**: 325-337.

Smaldone, G.T., Jin, Y., Whitfield, D.L., Mu, A.Y., Wong, E.C., Wuertz, S. and Singer, M., (2014) Growth of Myxococcus xanthus in continuous-flow-cell bioreactors as a method for studying development. *Appl Environ Microbiol* **80**: 2461-2467.

Smith, J., Queller, D.C. and Strassmann, J.E., (2014) Fruiting bodies of the social amoeba Dictyostelium discoideum increase spore transport by Drosophila. *BMC Evol Biol* **14**: 105.

Smith, J.G., Latiolais, J.A., Guanga, G.P., Pennington, J.D., Silversmith, R.E. and Bourret, R.B., (2004) A search for amino acid substitutions that universally activate response regulators. *Mol Microbiol* **51**: 887-901.

Sogaard-Andersen, L., (2004) Cell polarity, intercellular signalling and morphogenetic cell movements in Myxococcus xanthus. *Curr Opin Microbiol* **7**: 587-593.

Son, B., Liu, Y. and Kroos, L., (2011) Combinatorial regulation by MrpC2 and FruA involves three sites in the fmgE promoter region during Myxococcus xanthus development. *J Bacteriol* **193**: 2756-2766.

Stein, E.A., Cho, K., Higgs, P.I. and Zusman, D.R., (2006) Two Ser/Thr protein kinases essential for efficient aggregation and spore morphogenesis in Myxococcus xanthus. *Mol Microbiol* **60**: 1414-1431.

Stewart, R.C., (2010) Protein histidine kinases: assembly of active sites and their regulation in signaling pathways. *Curr Opin Microbiol* **13**: 133-141.

Stock, A.M., Robinson, V.L. and Goudreau, P.N., (2000) Two-component signal transduction. *Annu Rev Biochem* **69**: 183-215.

Stock, J. and Da Re, S., (2000) Signal transduction: response regulators on and off. *Curr Biol* **10**: R420-424.

Sudo, S.Z. and Dworkin, M., (1969) Resistance of vegetative cells and microcysts of Myxococcus xanthus. *J Bacteriol* **98**: 883-887.

Sun, H. and Shi, W., (2001a) Analyses of *mrp* genes during *Myxococcus xanthus* development. *J Bacteriol* **183**: 6733-6739.

Sun, H. and Shi, W., (2001b) Genetic studies of mrp, a locus essential for cellular aggregation and sporulation of Myxococcus xanthus. *J Bacteriol* **183**: 4786-4795.

Szurmant, H., Bunn, M.W., Cannistraro, V.J. and Ordal, G.W., (2003) Bacillus subtilis hydrolyzes CheY-P at the location of its action, the flagellar switch. *J Biol Chem* **278**: 48611-48616.

Szurmant, H. and Ordal, G.W., (2004) Diversity in chemotaxis mechanisms among the bacteria and archaea. *Microbiol Mol Biol Rev* **68**: 301-319.

Tan, C.H., Lee, K.W., Burmolle, M., Kjelleberg, S. and Rice, S.A., (2017) All together now: experimental multispecies biofilm model systems. *Environ Microbiol* **19**: 42-53.

Tan, I.S. and Ramamurthi, K.S., (2014) Spore formation in Bacillus subtilis. *Environ Microbiol Rep* **6**: 212-225.

Taylor, B.L. and Zhulin, I.B., (1999) PAS domains: internal sensors of oxygen, redox potential, and light. *Microbiol Mol Biol Rev* **63**: 479-506.

Taylor, S.S., Yang, J., Wu, J., Haste, N.M., Radzio-Andzelm, E. and Anand, G., (2004) PKA: a portrait of protein kinase dynamics. *Biochim Biophys Acta* **1697**: 259-269.

Thomas, S.A., Brewster, J.A. and Bourret, R.B., (2008a) Two variable active site residues modulate response regulator phosphoryl group stability. *Mol Microbiol* **69**: 453-465.

Thomas, S.H., Wagner, R.D., Arakaki, A.K., Skolnick, J., Kirby, J.R., Shimkets, L.J., Sanford, R.A. and Loffler, F.E., (2008b) The mosaic genome of Anaeromyxobacter dehalogenans strain 2CP-C suggests an aerobic common ancestor to the delta-proteobacteria. *PLoS One* **3**: e2103.

Thomasson, B., Link, J., Stassinopoulos, A.G., Burke, N., Plamann, L. and Hartzell, P.L., (2002) MglA, a small GTPase, interacts with a tyrosine kinase to control type IV pili-mediated motility and development of Myxococcus xanthus. *Mol Microbiol* **46**: 1399-1413.

Thony-Meyer, L. and Kaiser, D., (1993) devRS, an autoregulated and essential genetic locus for fruiting body development in Myxococcus xanthus. *J Bacteriol* **175**: 7450-7462.

Treuner-Lange, A., Ward, M.J. and Zusman, D.R., (2001) Pph1 from Myxococcus xanthus is a protein phosphatase involved in vegetative growth and development. *Mol Microbiol* **40**: 126-140.

Treuner-Lange, A., (2010) The phosphatomes of the multicellular myxobacteria Myxococcus xanthus and Sorangium cellulosum in comparison with other prokaryotic genomes. *PLoS One* **5**: e11164.

Tse, H. and Gill, R.E., (2002) Bypass of A- and B-signaling requirements for Myxococcus xanthus development by mutations in spdR. *J Bacteriol* **184**: 1455-1457.

Tzeng, L. and Singer, M., (2005) DNA replication during sporulation in Myxococcus xanthus fruiting bodies. *Proc Natl Acad Sci U S A* **102**: 14428-14433.

Tzeng, L., Ellis, T.N. and Singer, M., (2006) DNA replication during aggregation phase is essential for Myxococcus xanthus development. *J Bacteriol* **188**: 2774-2779.

Udo, H., Lam, C.K., Mori, S., Inouye, M. and Inouye, S., (2000) Identification of a substrate for Pkn2, a protein Ser/Thr kinase from Myxococcus xanthus by a novel method for substrate identification. *J Mol Microbiol Biotechnol* **2**: 557-563.

Ueki, T., Inouye, S. and Inouye, M., (1996) Positive-negative KG cassettes for construction of multi-gene deletions using a single drug marker. *Gene* **183**: 153-157.

Ueki, T. and Inouye, S., (2003) Identification of an activator protein required for the induction of *fruA*, a gene essential for fruiting body development in *Myxococcus xanthus*. *Proc Natl Acad Sci U S A* **100**: 8782-8787.

Uhl, M.A. and Miller, J.F., (1996) Integration of multiple domains in a two-component sensor protein: the Bordetella pertussis BvgAS phosphorelay. *EMBO J* **15**: 1028-1036.

Ulrich, L.E. and Zhulin, I.B., (2010) The MiST2 database: a comprehensive genomics resource on microbial signal transduction. *Nucleic Acids Res* **38**: D401-407.

van Gestel, J., Vlamakis, H. and Kolter, R., (2015) Division of Labor in Biofilms: the Ecology of Cell Differentiation. *Microbiol Spectr* **3**: MB-0002-2014.

Velicer, G.J., Kroos, L. and Lenski, R.E., (1998) Loss of social behaviors by myxococcus xanthus during evolution in an unstructured habitat. *Proc Natl Acad Sci U S A* **95**: 12376-12380.

Velicer, G.J. and Stredwick, K.L., (2002) Experimental social evolution with Myxococcus xanthus. *Antonie Van Leeuwenhoek* **81**: 155-164.

Velicer, G.J., Lenski, R.E. and Kroos, L., (2002) Rescue of social motility lost during evolution of Myxococcus xanthus in an asocial environment. *J Bacteriol* **184**: 2719-2727.

Velicer, G.J. and Hillesland, K.L., (2008) Why Cooperate? The Ecology and Evolution of Myxobacteria. In: Myxobacteria - Multicellularity and Differentiation. Withworth, D.E. (ed). Washington, D.C.: ASM Press, pp. 17-40.

Velicer, G.J. and Vos, M., (2009) Sociobiology of the myxobacteria. *Annu Rev Microbiol* **63**: 599-623.

Velicer, G.J., Mendes-Soares, H. and Wielgoss, S., (2014) Whence Comes Social Diversity? Ecological and Evolutionary Analysis of the Myxobacteria. In: Myxobacteria - Genomics, Cellular and Molecular Biology. Yang, Z. and Higgs, P.I. (eds). Norfolk, UK: Caister Academic Press, pp. 1-29.

Vlamakis, H., Chai, Y., Beauregard, P., Losick, R. and Kolter, R., (2013) Sticking together: building a biofilm the Bacillus subtilis way. *Nat Rev Microbiol* **11**: 157-168.

Vos, M. and Velicer, G.J., (2006) Genetic population structure of the soil bacterium Myxococcus xanthus at the centimeter scale. *Appl Environ Microbiol* **72**: 3615-3625.

Vos, M. and Velicer, G.J., (2008) Natural variation of gliding motility in a centimetre-scale population of Myxococcus xanthus. *FEMS Microbiol Ecol* **64**: 343-350.

Wadhams, G.H. and Armitage, J.P., (2004) Making sense of it all: bacterial chemotaxis. *Nat Rev Mol Cell Biol* **5**: 1024-1037.

Wegener-Feldbrugge, S. and Sogaard-Andersen, L., (2009) The atypical hybrid histidine protein kinase RodK in Myxococcus xanthus: spatial proximity supersedes kinetic preference in phosphotransfer reactions. *J Bacteriol* **191**: 1765-1776.

Weiss, V., Kramer, G., Dunnebier, T. and Flotho, A., (2002) Mechanism of regulation of the bifunctional histidine kinase NtrB in Escherichia coli. *J Mol Microbiol Biotechnol* **4**: 229-233.

Welch, M., Oosawa, K., Aizawa, S. and Eisenbach, M., (1993) Phosphorylation-dependent binding of a signal molecule to the flagellar switch of bacteria. *Proc Natl Acad Sci U S A* **90**: 8787-8791.

Welch, M., Oosawa, K., Aizawa, S.I. and Eisenbach, M., (1994) Effects of phosphorylation, Mg2+, and conformation of the chemotaxis protein CheY on its binding to the flagellar switch protein FliM. *Biochemistry* **33**: 10470-10476.

West, A.H. and Stock, A.M., (2001) Histidine kinases and response regulator proteins in two-component signaling systems. *Trends Biochem Sci* **26**: 369-376.

West, S.A., Diggle, S.P., Buckling, A., Gardner, A. and Griffin, A.S., (2007) The Social Lives of Microbes. *Annual Review of Ecology, Evolution and Sysstematics* **38**: 53-77.

Whitworth, D.E. and Cock, P.J., (2008) Two-component systems of the myxobacteria: structure, diversity and evolutionary relationships. *Microbiology* **154**: 360-372.

Wilke, K.E., Francis, S. and Carlson, E.E., (2012) Activity-based probe for histidine kinase signaling. *J Am Chem Soc* **134**: 9150-9153.

Willett, J.W. and Kirby, J.R., (2012) Genetic and biochemical dissection of a HisKA domain identifies residues required exclusively for kinase and phosphatase activities. *PLoS Genet* **8**: e1003084.

Wireman, J.W. and Dworkin, M., (1977) Developmentally induced autolysis during fruiting body formation by *Myxococcus xanthus*. *J Bacteriol* **129**: 798-802.

Wolanin, P.M., Thomason, P.A. and Stock, J.B., (2002) Histidine protein kinases: key signal transducers outside the animal kingdom. *Genome Biol* **3**: REVIEWS3013.

Wu, S.S. and Kaiser, D., (1995) Genetic and functional evidence that Type IV pili are required for social gliding motility in Myxococcus xanthus. *Mol Microbiol* **18**: 547-558.

Wu, S.S. and Kaiser, D., (1997) Regulation of expression of the pilA gene in Myxococcus xanthus. *J Bacteriol* **179**: 7748-7758.

Wuichet, K., Cantwell, B.J. and Zhulin, I.B., (2010) Evolution and phyletic distribution of two-component signal transduction systems. *Curr Opin Microbiol* **13**: 219-225.

Xie, C., Zhang, H., Shimkets, L.J. and Igoshin, O.A., (2011) Statistical image analysis reveals features affecting fates of Myxococcus xanthus developmental aggregates. *Proc Natl Acad Sci U S A* **108**: 5915-5920.

Yamada, S., Nakamura, H., Kinoshita, E., Kinoshita-Kikuta, E., Koike, T. and Shiro, Y., (2007) Separation of a phosphorylated histidine protein using phosphate affinity polyacrylamide gel electrophoresis. *Anal Biochem* **360**: 160-162.

Young, T.A., Delagoutte, B., Endrizzi, J.A., Falick, A.M. and Alber, T., (2003) Structure of Mycobacterium tuberculosis PknB supports a universal activation mechanism for Ser/Thr protein kinases. *Nat Struct Biol* **10**: 168-174.

Zhou, L., Lei, X.H., Bochner, B.R. and Wanner, B.L., (2003) Phenotype microarray analysis of Escherichia coli K-12 mutants with deletions of all two-component systems. *J Bacteriol* **185**: 4956-4972.

Zhu, Y., Qin, L., Yoshida, T. and Inouye, M., (2000) Phosphatase activity of histidine kinase EnvZ without kinase catalytic domain. *Proc Natl Acad Sci U S A* **97**: 7808-7813.

Zusman, D.R., Scott, A.E., Yang, Z. and Kirby, J.R., (2007) Chemosensory pathways, motility and development in Myxococcus xanthus. *Nat Rev Microbiol* **5**: 862-872.

11. Acknowledgment / Danksagung

The current page (Acknowledgment / Danksagung) contains personal data, hence it is not part of the electronically published version of the thesis.

Diese Seite (Acknowledgment / Danksagung) enthält persönliche Daten, daher ist sie nicht Bestandteil der Online-Veröffentlichung dieser Dissertation.

12. CV

The current page (CV) contains personal data, hence it is not part of the electronically published version of the thesis.

Diese Seite (CV) enthält persönliche Daten, daher ist sie nicht Bestandteil der Online-Veröffentlichung dieser Dissertation.

13. Versicherung

Hiermit versichere ich, dass ich die vorliegende Dissertation mit dem Titel

“Signal transduction systems

in the *Myxococcus xanthus* developmental program”

selbstständig verfasst, keine anderen als die im Text angegebenen Hilfsmittel verwendet und sämtliche Stellen, die dem Wortlaut oder dem Sinn nach aus anderen Werken entnommen sind, mit Quellenangabe kenntlich gemacht habe. Die Dissertation wurde in der jetzigen oder einer ähnlichen Form noch bei keiner anderen Hochschule eingereicht und hat noch keinem anderen Prüfungszweck gedient.

Marburg, den_____._____._____ _____

Maike M. Glaser

14. Einverständniserklärung

Hiermit erkläre ich mich einverstanden, dass die vorliegende Dissertation mit dem Titel

“Signal transduction systems in the *Myxococcus xanthus* developmental program”

in Bibliotheken zugänglich gemacht wird.

Dazu gehört, dass sie

- von der Bibliothek der Einrichtung, in der meine Dissertation angefertigt wurde, zur Benutzung in ihren Räumen bereitgehalten wird;
- in konventionellen und maschinenlesbaren Katalogen, Verzeichnissen und Datenbanken verzeichnet wird;
- im Rahmen der urheberrechtlichen Bestimmungen für Kopierzwecke benutzt werden kann.

Marburg, den _____._____._____ _____

Maike M. Glaser

Marburg, den _____._____._____ _____

Penelope I. Higgs